THE IMMUNOMETABOLISM OF NOD PROTEIN SIGNALING

THE METABOLIC AND INFLAMMATORY EFFECTS OF NUCLEOTIDE OLIGOMERIZATION DOMAIN (NOD) PROTEIN SIGNALING DURING OBESITY AND BACTERIAL STRESS

By

JOSEPH F. CAVALLARI, B.Sc.

A Thesis Submitted to the School of Graduate Studies in Partial Fulfilment of the Requirements for the Degree Doctor of Philosophy

DESCRIPTIVE NOTE

McMaster University DOCTOR OF PHILOSOPHY (2017) Hamilton, Ontario (Biochemistry and Biomedical Sciences)

TITLE: The metabolic and inflammatory effects of nucleotide oligomerization domain (NOD) protein signaling during obesity and bacterial stress

AUTHOR: Joseph F. Cavallari, B.Sc. (McMaster University)

SUPERVISOR: Dr. Jonathan D. Schertzer

NUMBER OF PAGES: xvii, 220

LAY ABSTRACT

Obesity is associated with insulin resistance, which is the primary predictor of type 2 diabetes. This research aims to understand the relationship between obesity, insulin, and diabetes by investigating the immune system. Inflammation contributes to insulin resistance during obesity. Inflammation is controlled by the immune system, which normally protects the body against disease. Good bacteria living inside the gut are beneficial because they aid digestion and increase nutrient absorption. Studying how bacteria interact with the immune system is important because microbes activate inflammatory responses. Therefore, different bacteria might be critical in preventing or promoting insulin resistance and diabetes during obesity. This research investigates the therapeutic effects of small compounds found in certain types of bacteria that interact with the immune system. These compounds activate specific immune responses and might be used as a new type of drug based on a "probiotic" health strategy. Bacterial compounds may reduce the amount of inflammation during obesity, thereby reducing the rates of type 2 diabetes.

ABSTRACT

Intestinal dysbiosis contributes to obesity and insulin resistance, but intervening with antibiotics, prebiotics, or probiotics can be limited by specificity or sustained changes in microbial composition. Postbiotics include bacterial components such as lipopolysaccharides, which have been shown to promote insulin resistance during metabolic endotoxemia. The data presented in this thesis demonstrates that bacterial cell wall-derived muramyl dipeptide (MDP) is an insulin-sensitizing postbiotic that requires the nucleotide oligomerization domain 2 (NOD2) protein. Injecting MDP lowered adipose inflammation and reduced glucose intolerance in obese mice without causing weight loss. MDP reduced hepatic insulin resistance during obesity and low-level endotoxemia. NOD1-activating peptidoglycan worsened glucose tolerance. The transcription factor interferon regulatory factor 4 (IRF4) distinguished opposing glycemic responses to different types of peptidoglycan. IRF4 was dispensable for exacerbated glucose intolerance via NOD1, but was required for MDP/NOD2-induced insulin sensitization and lower metabolic tissue inflammation during obesity and endotoxemia.

ACKNOWLEDGEMENTS

I would like to thank my supervisor, Dr. Jonathan Schertzer, for his ambitious scientific energy and leadership. His relentlessly positive outlook made grad school not only bearable, but enjoyable. I am grateful to him for taking a chance on me, and for giving me the best possible start for the next stage of my career. Thank you for cultivating a fantastic learning environment.

I would also like to thank my committee members, Dr. Deborah Sloboda and Dr. Gregory Steinberg, for their sound scientific guidance and helpful suggestions over the years. I am also grateful to them for placing their trust in me to lead TA activities for the undergraduate nutrition & metabolism course for multiple years.

My former undergraduate thesis supervisor, Dr. Lori Burrows, introduced me to the wonderful world of academic science. Thank you for giving me a solid foundation (and providing the push) to pursue graduate studies.

To all members of the Schertzer lab, past and present, thank you for providing a fun and comfortable work environment. Your scientific support and friendship over the years enhanced the grad school experience. Being with the lab from the beginning and watching it grow and succeed has been an amazing opportunity.

To the Biochemistry and Biomedical Sciences staff, especially Lisa Kush, thank you for helping me navigate the many departmental and scholarship guidelines. Thanks to CIHR for providing scholarship funding throughout this project.

I would like to thank my entire family for their love and support throughout my entire life. I am eternally grateful to my parents, who raised me to be the person I am today. Thank you for putting up with my extended absences over the past few years and for encouraging me when things were tough. Chris, Mike, Jake, and Hailey – thank you for being a great source of stress-relief and laughter.

To Jessica – for keeping me sane, day and night – I love you and I thank you. This endeavour would have been much more trying without your patience, support, and insight. I am unsure what life will have in store for us, but I cannot wait to find out with you.

TABLE OF CONTENTS

LIST OF FIGURES

LIST OF ABBREVIATIONS

2DG	2-[1,2-^{3}H (N)]-Deoxy-D-glucose (2DG)
AS160	Akt substrate of 160 kDa
β	beta
CARD	caspase-activation and recruitment domain
CCL2	C-C motif chemokine ligand 2
CT	computed tomography
DAG	diacylglycerol
DM	diabetes mellitus
DNA	deoxyribonucleic acid
ELISA	enzyme-linked immunosorbent assay
FOXO1	forkhead box protein O1
GDR	glucose disposal rate
GINF	glucose infusion rate
GLUT#	glucose transporter #
GSK3	glycogen synthase kinase 3
GTT	glucose tolerance test
HFD	high-fat diet
HGO/HGP	hepatic glucose output/production
HOMA-IR	homeostatic model assessment of insulin resistance
IL#	interleukin #
IMCL	intramuscular lipid
IRF4	interferon regulatory factor 4
IRS	insulin receptor substrate
ITT	insulin tolerance test
JNK	c-Jun N-terminal kinase
LAL	limulus amebocyte lysate
LPS	lipopolysaccharide
LRR	leucine-rich repeat
MCP-1	monocyte chemoattractant protein 1
meso-DAP	meso-diaminopimelic acid
MAPK	mitogen-activated protein kinase
MDP	muramyl dipeptide
NAFLD	non-alcoholic fatty liver disease
NEFA	non-esterified fatty acid
NF-κB	nuclear factor kappa-B
NLR	nucleotide oligomerization domain-like receptor
NLRP3	nucleotide oligomerization domain-like receptor, pyrin domain-containing 3
NOD1	nucleotide oligomerization domain 1
NOD2	nucleotide oligomerization domain 2
PCR	polymerase chain reaction

PI3K	phosphatidylinositol 3-kinase
PKB	protein kinase B
PKC	protein kinase C
PRR	pattern recognition receptor
PTT	pyruvate tolerance test
RIPK2	receptor-interacting serine/threonine-protein kinase 2
RNA	ribonucleic acid
ROS	reactive oxygen species
SCFA	short chain fatty acid
TAG	triacylglycerol
T1D	type 1 diabetes
T2D	type 2 diabetes
Th1	T helper type 1
Th1	T helper type 2
Th17	T helper type 17
TLR	toll-like receptor
TNF	tumor necrosis factor
WT	wild type

DECLARATION OF ACADEMIC ACHIEVMENT

The first-author peer-reviewed papers listed below comprise the majority of content presented in this thesis. The results described in section 3.1.1 were from Denou et al. and experiments were performed with members from the Schertzer laboratory. The results from Denou et al. were important in developing the hypothesis and direction of this thesis.

First-author peer-reviewed contributions

Cavallari JF, Schertzer JD. Intestinal Microbiota Contributes to Energy Balance, Metabolic Inflammation, and Insulin Resistance in Obesity. J Obes Metab Syndr. 2017 Sep 30;26(3):161–71.

Cavallari JF, Fullerton MD, Duggan BM, Foley KP, Denou E, Smith BK, et al. Muramyl Dipeptide-Based Postbiotics Mitigate Obesity-Induced Insulin Resistance via IRF4. Cell Metab. 2017 May 2;25(5):1063–1074.e3.

Cavallari JF, Denou E, Foley KP, Khan WI, Schertzer JD. Different Th17 immunity in gut, liver, and adipose tissues during obesity: the role of diet, genetics, and microbes. Gut Microbes. 2016;7(1):82–9.

Co-author peer-reviewed contributions

Denou E, Lolmède K, Garidou L, Pomie C, Chabo C, Lau TC, et al. Defective NOD2 peptidoglycan sensing promotes diet-induced inflammation, dysbiosis, and insulin resistance. EMBO Mol Med. 2015 Mar 1;7(3):259–74.

Henriksbo BD, Lau TC, Cavallari JF, Denou E, Chi W, Lally JS, et al. Fluvastatin causes NLRP3 inflammasome-mediated adipose insulin resistance. Diabetes. 2014 Nov;63(11):3742–7.

Chi W, Dao D, Lau TC, Henriksbo BD, Cavallari JF, Foley KP, et al. Bacterial peptidoglycan stimulates adipocyte lipolysis via NOD1. PLoS One. 2014 May 14;9(5):e97675.

CHAPTER ONE: Introduction

1.1 Obesity and metabolic disease

Obesity is a worldwide health concern, with nearly one-third of the global population defined as overweight (body mass index between 25.0 to < 30 body weight/height^2) or obese (body mass index ≥ 30.0) (1). Obesity rates are projected to increase (2) and obesity status or even being overweight is a significant risk factor for all-cause mortality (3). Beyond reducing the quality of life and average life expectancy for affected individuals, the healthcare-associated monetary impacts of obesity are increasingly burdensome (4). Therefore, the rising prevalence of obesity has prompted intense research into limiting the disease and its detrimental complications.

1.1.1 Etiology and health consequences of obesity

Although genetic components are known to contribute to obesity (5,6), environmental factors such as those linked to industrialization also influence the prevalence of obesity. Food availability, variety, and increased palatability can influence weight gain (7). Foods are now commonly engineered with additional fat and sugar to make them more palatable, a practice that takes advantage of neuronal reward circuits to encourage these eating habits (8). Aside from energy intake, sedentary lifestyles also contribute to obesity by reducing energy expenditure. For example, modern improvements to manufacturing, technology, and automation have seen the

requirement for physical human labour diminish. These high-energy output jobs have been largely replaced by low-activity work (9,10). The increased energy content of modern human dietary habits combined with decreased energy expenditure ultimately tip the energy balance scales towards excess energy storage, and eventually obesity.

Beyond energy balance, other factors contribute to the rising occurrence of obesity. Maternal nutrient excess during pregnancy is associated with long-term health impacts on offspring, including increased risk of obesity and metabolic complications (11–13). The gut microbiota is another factor with considerable impacts on energy utilization. While this concept is discussed in more detail below, recent advances in our understanding of how obesity status impacts gut bacterial communities (and the inverse) reveal a unique symbiotic relationship with important implications for metabolic health (14). Thus, the incidence of obesity can be influenced by host genetics, individual behavior, inherited multigenerational factors, and specific communities of commensal microorganisms.

Obesity is now recognized as a disease (15). The most important health consequence of obesity is the increased risk of developing diseases such as sleep apnea/breathing complications, non-alcoholic fatty liver disease, cardiovascular diseases (such as stroke, heart attack, and hypertension), type 2 diabetes, and some obesity-related cancers (1). Thus, obesity is a major contributor to the leading causes of mortality worldwide.

The findings presented in this thesis will focus on the relationship between obesity and the development of type 2 diabetes.

1.2 Type 2 diabetes

Diabetes mellitus (DM) is a disease characterized by chronically elevated blood glucose levels and an insufficiency in insulin production by the beta (β)-cells of the pancreas. The two main types of DM are described as insulin-dependent (type 1 diabetes (T1D)) and noninsulin-dependent (type 2 diabetes (T2D)). T1D occurs when the pancreas cannot produce insulin due to autoimmune-mediated destruction of pancreatic β-cells, and patients rely on exogenous insulin to control blood glucose. T1D is more likely to occur in genetically predisposed individuals exposed to as of yet uncharacterized environmental triggers (16). T2D develops as the cells and tissues of the body become increasingly resistant to the actions of insulin. The pancreas is able to compensate for this resistance by increasing insulin production, but β-cells eventually become exhausted and fail. Environmental factors such as diet and lifestyle are major contributors to the development of T2D. For example, diet and exercise alter insulin sensitivity, though a role for genetics in T2D has been described (17). T2D is the more common form of DM, and occurrence of this disease is concomitant with the rise in obesity worldwide (18).

Consequences of chronically elevated blood glucose levels include nerve, kidney, retina, and blood vessel/cardiovascular damage, as well as increased susceptibility to infection (19). As a result of these complications, there are approximately 1.5 million deaths from DM every year (20). Given that T2D is a large contributor to DM-associated mortality, it is important to understand how obesity influences the development of insulin resistance that precedes T2D.

1.2.1 Insulin

Canine pancreatic extracts were the first effective treatment of DM in humans (21). The hormone insulin has since been characterized as the molecule responsible for mediating the body's energy supply and macronutrient balance after feeding (22). Insulin promotes the uptake of glucose from blood into tissue and also initiates the synthesis and storage of glucose as glycogen (glycogenesis) within the liver and muscle, as well as smaller amounts in other tissues. Endogenous production of glucose in the liver from gluconeogenic substrates (hepatic gluconeogenesis) and from the release of glucose from stored glycogen (glycogenolysis) is inhibited by insulin.

The anabolic effects of insulin are not limited to the control of glucose/glycogen. Lipid metabolism is also regulated by the hormone, via inhibition of lipolysis and stimulation of lipogenesis. Insulin activates

lipoprotein lipase in adipocytes and inhibits the enzyme in muscle, with the cumulative effect of these actions favouring triglyceride storage in adipose tissue and preventing oxidation of fatty acids in skeletal muscle (23). Genes involved in production of fatty acid synthase, which plays a key role in *de novo* lipogenesis by converting excess carbohydrate into fatty acids for lipid storage, are regulated by insulin (24–27). Insulin also inhibits hormone-sensitive lipase responsible for releasing fatty acids from triglycerides stored in adipose tissue (28). In muscle, insulin promotes protein synthesis (29,30).

The primary endogenous mechanism driving insulin secretion involves the detection of elevated blood glucose through glucose uptake via glucose transporters on β-cells (31–33). This uptake triggers a biphasic release of insulin-containing vesicles from pancreatic β-cells. Following the initial rapid (approximately 10 minutes) secretion, there is a slower and steady release of the hormone that lasts for hours (34,35). Interestingly, loss of the initial phase of insulin secretion is a common precursor to DM (36,37). Other nutrients have been identified as triggers for insulin release, such as fatty acids and amino acids (38,39). Hormones produced by the body such as melatonin, estrogen, leptin, and glucagon-like peptide-1 (among others) also control insulin secretion (40–45). Some classes of drugs function as insulin secretagogues and are used for the treatment of T2D. As they

increase insulin secretion, these drugs carry a risk of inducing hypoglycemia (46).

1.2.2 Insulin signaling and clearance

Insulin achieves its effects by an intricate signal transduction cascade that can be simplified into three main “nodes”: insulin receptor substrate (IRS), phosphatidylinositol 3-kinase (PI3K), and Akt/protein kinase B (PKB) (47). Binding of insulin to the insulin receptor causes dimerization of the receptor and autophosphorylation of tyrosine residues. The phosphorylated receptor recruits and phosphorylates many proteins, of which IRS proteins activate PI3K. Phosphorylated PI3K mediates several phosphorylation events that ultimately result in phosphorylated (activated) Akt/PKB (48,49). Tissue-specific glucose actions of insulin involve divergent signaling events downstream of the IRS/PI3K/Akt pathway. In adipose and muscle, activated Akt/PKB phosphorylates Akt substrate of 160 kDa (AS160/TBC1D4) to mediate release of glucose transporter 4 (GLUT4)-containing vesicles to the cell surface, thus initiating insulin-stimulated glucose uptake (50). In liver, activated Akt/PKB phosphorylates glycogen synthase kinase 3 (GSK3) resulting in the activation of glycogen synthase, concomitantly stimulating glycogen production (47). Finally, phosphorylation of the transcription factor forkhead box protein O1

(FOXO1) by Akt/PKB causes the exclusion of this protein from the nucleus, thereby inhibiting gluconeogenic gene transcription in the liver (51,52).

Following initiation of the insulin signaling cascade there is a requirement to mitigate the pathway in order to prevent aberrant metabolic events such as hypoglycemia from prolonged insulin signaling. A key mechanism that the body uses to regulate blood glucose and prevent hypoglycemia is clearance of insulin (53). While all insulin-sensitive cells are capable of removing and degrading the hormone, this role is largely mediated by the liver, followed by the kidneys and muscle (53–55). Degradation of insulin is achieved by insulin-degrading enzyme after internalization of the hormone/insulin receptor complex within a cell (56,57). Interestingly, insulin clearance rate is inversely associated with insulin resistance and hepatic insulin clearance is impaired in obesity, illustrating the importance of this mechanism to the development of T2D (58–60).

1.2.3 Insulin resistance

As briefly discussed above, the onset of T2D is preceded by period of insensitivity to insulin where metabolic tissues such as adipose, liver, and muscle require increasing amounts of the hormone to maintain glucose homeostasis (61,62). This insulin resistance can last for many years in humans, which is often coincident with compensatory hyperinsulinemia. In fact, hyperinsulinemia contributes to obesity and insulin resistance during

prediabetes progression (63,64), but ultimately elevated blood glucose to a level deemed to be T2D can develop based on insulin insufficiency relative to sensitivity (65). There are many causes of insulin resistance and the condition is a field of intense research, chiefly because it represents a therapeutic window where the progression to T2D can be halted or reversed.

The regulation of insulin signaling is a delicate balance that is tightly controlled. Another key inhibitory mechanism that the body uses to regulate blood glucose after insulin signaling is via serine/threonine phosphorylation of proteins such as the insulin receptor, IRS, and Akt/PKB (among others) within the insulin signaling pathway (48,66,67). For example, serine phosphorylation of IRS1 attenuates tyrosine phosphorylation of IRS1 and mitigates signal propagation required for the metabolic and anabolic actions of insulin (68). Known mediators of serine/threonine phosphorylation of insulin signaling components include fatty acids, hyperglycemia, mitochondrial dysfunction, endoplasmic reticulum stress, and inflammation that activate serine/threonine kinases such as c-Jun N-terminal kinases (JNK) (69–75). These stress responses can sufficiently disrupt insulin signaling leading to tissue insulin resistance and whole body dysglycemia. For example, serine/threonine phosphorylation of the insulin receptor has been observed in insulin resistant rats and humans (76–79). Serine phosphorylation of IRS is increased in obese and diabetic mice, thus linking

alternative phosphorylation of insulin signaling molecules with obesity that is associated with insulin resistance (80–82).

Genetics can also predispose individuals to insulin resistance. For example, mutations of the insulin receptor leading to reduced insulin binding/signal transduction are established genetic causes of insulin resistance (83,84). Similar associations have been made for proteins in the insulin signaling pathway, such as IRS-1, PI3K, and Akt/PKB (85–87). Loss of β-cell function also varies between individuals and is an inherited characteristic, with some individuals able to compensate with sufficient amounts of insulin and never progress to T2D (65,88). Although there is a role for genetics in the progression to T2D, environmental factors are the predominant cause of insulin resistance.

1.3 Obesity and inflammation alter tissues involved in glucose control

Obesity induces several physiological and molecular changes, including chronic low-level inflammation that can influence insulin sensitivity. This section will discuss the origins of inflammation during obesity and how different tissues are impacted. Understanding the links between immune and metabolic systems is an important consideration to combat obesity-driven disease development.

1.3.1 Obesity, inflammation, and insulin resistance

The etiology of insulin resistance is multifaceted and incompletely understood. It is known that fat-laden diets and obesity cause chronic, low-grade inflammation, which is a key component that can promote glucose intolerance and insulin resistance (89–93). For example, obesity is associated with excess circulating fatty acids, immunogenic bacterial molecules, and endogenous host damage signals such as reactive oxygen species (ROS), among other molecules, that can engage pathways that increase inflammatory cytokine production (94–97). As discussed above, inflammatory cytokines can decrease insulin sensitivity by engaging serine/threonine kinases that alter phosphorylation status of key proteins in the insulin signal transduction pathway (47,81,98–101).

An example of one key inflammatory factor involved in insulin resistance is highlighted by the fact that neutralization of tumor necrosis factor (TNF) alleviates insulin resistance during high-fat diet (HFD)-induced obesity in rodent models. There are still many ill-defined aspects of immunometabolism during obesity and insulin resistance. It is not yet clear if TNF neutralization strategies alter insulin action or glucose homeostasis in humans (102,103). The links between inflammatory cytokines and insulin resistance is unclear and remains a complex and important area of research. For example, cytokines such as interleukin (IL)6 are increased during obesity and can also stimulate insulin resistance upon acute

administration in mice (104–107). Conversely, IL6 has also been shown to have anti-inflammatory and insulin-sensitizing actions during obesity (108–111). Thus, there remains an incomplete understanding of how the immune system regulates inflammation during an obese state. One key concept appears to be compartmentalized immune and metabolic response, which is discussed below.

1.3.2 Obesity and circulating factors

The systemic circulation is often the route between distant tissues and cells that can mediate molecular crosstalk. Obesity is a source of increased circulating fatty acids, which can have detrimental inflammatory effects via ectopic accumulation in metabolic tissues (discussed below). The state of insulin resistance often coincides with elevated blood glucose and even clinical hyperglycemia. Elevated blood glucose is associated with oxidative stress that can precipitate inflammation (112). Hyperglycemia can also induce insulin resistance independently of oxidative stress, via advanced glycation end products that promote serine phosphorylation of IRS (113). Additionally, high-fat feeding leads to acute increases in circulating endotoxin that engage innate immune signaling pathways that lead to metabolic inflammation (discussed below) (114).

The circulation also carries endocrine factors that have importance during obesity. For example, leptin is a hormone produced by adipose tissue

that mediates a satiety signal to regulate feeding (115). Adiposity status is linked with higher circulating leptin, and mutations in the leptin receptor and resultant leptin insensitivity have been associated with obesity (116,117). These concepts suggest that resistance to leptin may be a factor in obesity. Leptin is a known mediator of pro-inflammatory responses during obesity that contribute to the chronic condition (118).

Although chronic, low-level, circulating inflammation is a hallmark of obesity, the amount of inflammation is small compared to overt infection or sepsis (which also promotes insulin resistance/hyperglycemia (119–121)). Also, the relative inflammatory contribution of each metabolic tissue during obesity is poorly represented by a snapshot analysis of low-level circulating inflammation. An emerging concept is that of compartmentalized immune responses during obesity (122,123). Metabolic tissues are the sites of insulin action and resistance that have whole-body impacts on glucose homeostasis. Therefore, scrutiny of individual tissues for their specific inflammatory status during obesity may be a more useful strategy in understanding the etiology and possible targeted treatment of metabolic disease.

1.3.3 Obesity and adipose

Adipose tissue is a key site for energy storage. The tissue is a mixture of adipocytes, immune cells, and vasculature that provides access

to the rest of the body and delivers nutrients via circulation (124). The anabolic effects of insulin on adipose tissue include stimulation of glucose uptake and lipogenesis, and inhibition of lipolysis.

As a storage depot for excess energy and fat that expands during obesity, adipose tissue is an obvious source of metabolic inflammation (125). Adipocyte hypertrophy due to excessive energy storage raises fatty acid concentrations in the circulation, priming the body for ectopic lipid deposition in other metabolic tissues (94,126). Similarly, endoplasmic reticulum stress, a source of chronic cellular inflammation, is increased in adipose tissue during obesity and has been shown to augment lipolysis, further contributing to elevated blood lipids (127,128).

Expansion of adipose tissue during obesity is associated with macrophage infiltration and upregulation of pro-inflammatory genes that parallels the development of insulin resistance (129–131). Immune cells recruited to adipose tissue during obesity can become polarized, shifting the inflammatory tone of the tissue to a pro-inflammatory state (132). Indeed, obese adipose tissue in experimental rodent models and humans is characterized by an increased secretion of pro-inflammatory cytokines such as TNF that activates JNK (and others) to mediate alternative phosphorylation of components within the insulin signaling pathway (80,132–134). Other key inflammatory proteins produced by adipose tissue that contribute to insulin resistance during obesity include IL1β, IL6, and C-

C motif chemokine ligand 2/monocyte chemoattractant protein-1 (CCL2/MCP1; involved in immune cell recruitment) (135–140).

The pro-inflammatory state of obese adipose tissue, combined with the recruitment of immune cells in response to an inflammatory stimulus, sets the stage for an inflammatory cycle that exacerbates metabolic deficiencies. The key consequences for impaired insulin action in adipose tissue during obesity include impaired glucose uptake that contributes to hyperglycemia, and enhanced lipolysis that contributes to ectopic lipid accumulation. The importance of adipose to energy homeostasis highlights the need to understand how inflammation contributes to metabolic impairments in this tissue during obesity.

1.3.4 Obesity and muscle

Skeletal muscle is the largest site of glucose deposition in the body, accounting for approximately 80% of insulin-stimulated glucose uptake (141,142). This tissue is also an important site for free fatty acid utilization, which sustains energy needs during fasting (143). Insulin normally functions to augment glucose uptake, oxidation, and glycogen synthesis, and suppress fatty acid oxidation in muscle, in addition to promoting protein synthesis (30,144).

During obesity, impaired lipogenesis and increased lipolysis contributes to increased circulating fatty acids. In muscle, this increased

lipid content accumulates and leads to enlargement of intramuscular lipid (IMCL) stores that correlates with insulin sensitivity (145,146). While increased IMCL is associated with obesity and insulin resistance, trained athletes also contain an elevated muscular lipid content. However, their tissues are more insulin sensitive and have a higher lipid oxidation capacity (147,148). Therefore, IMCL can be a marker of insulin resistance during obesity, but the metabolic capability of muscle must also be considered (149).

A particularly important characteristic of IMCL during obesity is as a source of lipid metabolites that interfere with insulin signaling. Elevated lipids equate with higher amounts of fatty acid intermediates (for example, lipids that have not been oxidized or stored as triacylglycerol (TAG)) (73). These lipid species include diacylglycerol (DAG) and ceramide that contribute to insulin resistance in humans and animals (126,150). DAGs can activate (among other kinases) protein kinase C (PKC) that inhibits tyrosine phosphorylation of IRS proteins (73,150,151). Ceramide-activated protein phosphatase inhibits Akt/PKB to interfere with insulin signaling (152–155).

The precise role of cytokine-driven muscle inflammation on insulin sensitivity is unclear. Inflammatory cytokines may promote oxidative stress which correlates with insulin insensitivity (156). Consequences of high-fat feeding and obesity are known to include macrophage infiltration in muscle and subsequent cytokine production (157,158). The origin of macrophage

inflammation (e.g. bacterial versus dietary lipid) may be an important factor that determines the effect on insulin sensitivity in muscle cells (159). In addition, the role of some inflammatory cytokines within muscle and their contribution to insulin resistance during obesity remains unsolved (160,161). For example, acute administration of both TNF and IL6 mechanistically induce insulin resistance in muscle cell models and in skeletal muscle in humans, and IL6 is elevated in adipose tissue, liver, and circulation during obesity (105,162–166). But IL6 signaling also suppresses hepatic and systemic inflammation and insulin resistance during obesity (109–111). Combined with the fact that exercise is associated with skeletal muscle release of IL6 illustrates that context is important (167,168). This apparent disparity can be viewed as an example of the compartmentalization of immune responses in different tissues during obesity.

1.3.5 Obesity and liver

The liver is a key regulator of glucose metabolism, and maintains a large supply of glucose as glycogen for use throughout the body. The metabolic cell of the liver is the hepatocyte, which responds to insulin by suppressing glucose production via inhibition of gluconeogenesis and glycogenolysis. This insulin-dependent effect is an important determinant of glycemia status in the body.

The resident immune cell population of the liver is the Kupffer cell, or hepatic macrophage, that can rapidly polarize depending on the local metabolic and inflammatory status of the liver (169). Interestingly, activated (inflammatory) Kupffer cells inhibit insulin sensitivity in obese mice, but ablation of Kupffer cells during diet-induced obesity worsens insulin signaling (170,171). Thus, there appears to be an immunoregulatory or protective role mediated by resident hepatic macrophages, in response to the progression of liver inflammation during obesity. Indeed, alternative activation of Kupffer cells during obesity reduces insulin resistance (172).

Dysregulated lipid handling and ectopic lipids from expanding adipose during obesity can promote non-alcoholic fatty liver disease (NAFLD) (173). Aside from causing inflammation and exacerbating insulin desensitization, excess lipid stores promote the accumulation of lipid intermediates such as DAGs and ceramide that interfere with hepatic insulin signaling (126,174–177). Inhibition of PKC (activated by DAGs) can prevent hepatic insulin resistance during NAFLD (178).

The liver is uniquely positioned, in that it is connected with the intestinal system via the hepatic portal circulation. Thus, the liver, a key metabolic tissue, directly interfaces with bacterial and nutrient content from the gut. A recent appreciation for this relationship between the gut and metabolic tissues has given rise to an expansive amount of research with

important implications for our understanding of obesity and its associated metabolic defects.

1.3.6 Obesity and the gastrointestinal tract

The gastrointestinal tract represents one of the largest mucosal barrier systems in the body and processes ingested nutrients. The gut is exposed to components of the external environment and maintains a barrier between these external environmental components and the internal organs of the host. This barrier is essential to protect the internal environment from penetration by pathogenic bacteria. Gastrointestinal immunity, such as T helper 17 (Th17) responses, mediates antimicrobial defences that are important for maintaining a suitably or nearly sterile internal environment compared to the plethora of microbes in the external environment (179–181).

Obesity is associated with elevated splenic and systemic Th17 immunity (182,183). In the ileum, HFD-feeding has been shown to impair Th17 immunity in mice (123,184). Obesity may therefore promote a permissive gut immune barrier environment that promotes other factors (such as specific bacteria or nutrients) to contribute to metabolic tissue inflammation and insulin resistance (implications discussed below). In line with this concept, HFD-feeding in mice depletes resident intestinal eosinophils that promote epithelial repair and barrier maintenance (185).

Intestinal permeability is increased during obesity in mice (186–188), and bacterial taxa associated with HFD-feeding promote intestinal inflammation that precedes and correlates with obesity and insulin resistance (189,190). Treatment of mice with gut anti-inflammatory agents reduces obesity-related insulin resistance (191).

Another consequence of obesity and altered diets is perturbations to the composition of symbiotic gut microbial communities. As discussed in the upcoming sections, specific gut bacteria (and their immunogenic components) can have significant and potentially exploitable characteristics for host metabolic health.

1.4 Bacteria and obesity

1.4.1 Metabolic implications of gut bacterial colonization

Recent advances in measuring the composition and predicted function of the intestinal microbiota have provided evidence for commensal microbes as a new environmental factor involved in metabolic disease. Trillions of bacteria make up the diverse microbial communities in different anatomical locations in humans. The intestine harbours most of these bacteria, and recent estimates place the number of bacteria at a 1-to-1 ratio with host cells in humans (192). These commensal bacteria are often symbionts that influence the metabolism of the host though macro- and micronutrient processing and the production of metabolites that cannot be

made by the host. Bacterial colonization has long been known to be critical for the education and development of the immune system (193). Therefore, the role of the gut microbiota, and bacterial components and metabolites in immunometabolism during metabolic disease should be assessed.

Germ-free animals have been used to characterize and test relationships between obesity-related dysbiosis (for example, deleterious changes in the composition of the gut microbiota) and host energy balance. Initial experiments that compared germ-free mice to conventional counterparts, and later colonization of mice born germ-free showed that bacteria regulate energy extraction that is sufficient to change body mass, body composition, and insulin sensitivity. These changes occurred in spite of decreased food intake in germ-free mice and it was found that host extraction and retention of dietary components and energy content is a key mechanism by which bacteria influence energy balance (194). Further experiments demonstrated that mice lacking colonizing bacteria are resistant to HFD-induced obesity and insulin resistance, and exhibit increased fat metabolism and excretion that ultimately prevents weight gain (195,196). It was also found that the change in the composition of the gut microbiota during obesity was sufficient to increase energy extraction from food (197). Interestingly, leanness, adiposity, and aspects of metabolic dysfunction are transmissible via the microbiota (198,199). Thus, dysbiosis

during obesity is a strong factor regulating body composition and glucose metabolism.

1.4.2 Antibiotics and host metabolic consequences

If diet and obesity-induced changes to gut microbiota composition have significant effects on the host, can intentional and directed changes to gut bacterial communities also have effects on host metabolism? Indeed, drugs that are designed to target microbes and disrupt microbial communities, such as antibiotics, have been reported to alter host energy balance and metabolism (200). For example, it has been known for a long time that low-dose antibiotics promote growth in farm animals (201). It was hypothesized that antibiotics reduced energy requirements of constantly providing immune tolerance to colonizing bacteria, but it was not clear why antibiotics were effective in promoting growth when only given during a therapeutic window in early life. Cho et al. (202) have reported that low-dose antibiotics given early in life caused increased obesity and lipid storage later in life in mice. Sub-therapeutic antibiotic treatment given to mice in early life increased adiposity, gut short chain fatty acid (SCFA) production (resulting in increased acetate, butyrate, and propionate), and hepatic expression of genes related to lipogenesis and triglyceride synthesis. The antibiotic treatment combined with HFD-feeding in mice caused additional weight gain and adiposity, increased hallmarks of non-alcoholic fatty liver disease,

and also adversely affected glucose metabolism (203). Studies in humans have not yet generated results that are as clear. While it has been demonstrated that acute antibiotic use in adult humans reduces gut microbial diversity and impacts metabolite production, significant changes in host insulin sensitivity or markers of inflammation were unremarkable (204,205). Thus, while antibiotic use can affect human gut microbiota composition, physiology, and bacterial metabolism in the short term, it is not yet possible to ascertain the host changes in metabolism relevant to metabolic disease. Further, it is not clear if widespread antibiotic-induced changes in the microbiota can be tailored to combat metabolic disease. The long-term impact to host metabolism after discontinuing antibiotic use is also unclear. Broad-spectrum antibiotics are therefore not positioned as an ideal candidate treatment to limit metabolic disease.

1.4.3 Pre- and probiotics

The fact that antibiotic-dependent and independent changes to gut microbial communities can potentiate metabolic changes in mice, albeit temporarily, demonstrates that components of the gut microbiota are at least tangentially interacting with host metabolism. Therefore, it is worthwhile to explore the concept of bacterial-host metabolic interactions further. Indeed, there is evidence to support the notion that specific bacteria or bacterial components can add to the drug repertoire to combat metabolic

disease. Two examples of this concept include “probiotics” (specific known strains of live bacteria that are associated with intestinal health in the host) and “prebiotics” (digestible compounds that encourage the growth of certain bacterial species).

Probiotics containing a single strain of *Lactobacillus rhamnosus*, *Bifidobacterium animalis*, or *Propionibacterium freudenreichii* have been reported to possess anti-inflammatory activity when administered to normal healthy adults (206). These effects are often bacterial strain specific. Similar work has demonstrated that probiotic supplementation with a cocktail containing multiple *Lactobacillus*, *Streptococcus*, and *Bifidobacterium* species opposed increases in body and fat mass in humans when challenged with a HFD (207). Similarly, *Lactobacillus casei* has also been shown to prevent high-fat overfeeding-induced insulin resistance (208). Mechanistically, some probiotic species such as *Lactobacillus reuteri* may function to improve incretin and insulin secretion, allowing for possible improvements in glucose homeostasis in insulin-resistant individuals (209).

The bacterial species *Akkermansia muciniphila* has been continuously implicated in beneficial metabolic profiles. The presence of intestinal or fecal *Akkermansia muciniphila* is inversely associated with fasting glucose, adipocyte size, body fat distribution, and microbiome gene richness following dietary intervention in humans (210). In mice, the administration of *Akkermansia muciniphila* has been shown to mitigate

metabolic inflammation, insulin resistance, and preserve gut barrier integrity during diet-induced obesity (211). Bacteria that may help to combat metabolic disease, such as *Akkermansia muciniphila*, appear to be modifiable with prebiotics/dietary constituents such as oligofructose (211–215) or grape polyphenols that concomitantly reduce aspects of HFD-induced metabolic syndrome (216). Interestingly, non-bacterial microorganisms can also have similar “prebiotic” effects on gut microbiota composition and improvements in host metabolism. An extract of the fungal species *Ganoderma lucidum* prevented obesity, reduced liver and adipose tissue inflammation, and increased the Bacteroidetes to Firmicutes ratio in mice fed a HFD (217).

1.4.4 Postbiotics

Pre- and probiotics aim to modify the composition of gut bacterial communities as their primary intended mechanism. It may be difficult to maintain these changes, as the gut bacteria is rapidly changed with diet (218). This finding is supported by long-term studies in humans (219). Additionally, oral probiotics must survive ingestion and transit within the upper gastrointestinal tract for several hours to have any meaningful effect on the host (220,221). Prebiotics are limited by specificity and the difficulty in shaping the microbial community in a tailored way that provides a net benefit to host metabolism (222). Indeed, it is a daunting task to understand

how a change in the composition of trillions of resident bacteria relates to obesity-related inflammation and insulin resistance.

Conversely, a simple concept is that components of bacteria are positioned to alter host metabolism. In fact, live bacteria are not always required to induce host responses. Unique endogenous or secreted factors from bacteria warrant investigation in metabolic disease. For example, the bacterial protein Amuc_1100 from *Akkermansia muciniphila*, has been identified as a factor that is sufficient to improve aspects of obesity-related metabolic disease (223,224). Therefore, an alternate approach to combatting metabolic disease may be to test the secreted factors, cellular components, and metabolites of bacteria that, upon delivery to a host, can have biological effects on it. We and others define these molecules as "postbiotics" (225,226).

Examples of metabolite-postbiotics such as microbial-derived SCFAs or flavonoids can directly influence host feeding behaviour, energy metabolism, insulin secretion, and insulin sensitivity (227–230). The mechanisms driving the metabolic effects of these bacterial-derived molecules are diverse. For example, microbial-derived metabolites can be epigenetic factors that induce host responses relevant to the susceptibility to metabolic disease (231,232). It has been demonstrated that bacterial colonization of mice regulates epigenetic programming in host tissues, and that a Western-style diet, high in fat and sugar, affects histone modifications

in liver, colon, and adipose tissues (233). Interestingly, a Western-style diet reduced production of the SCFAs acetate, propionate, and butyrate in the murine gut, and supplementing these SCFAs had similar effects on the epigenetic state of mouse tissues to that of bacterial colonization. This raises an important concept, since bacterial derived metabolites (such as SCFAs) have now been found to alter epigenetic control of host metabolism. Microbial-sourced SCFAs in the gut have been shown to suppress insulin signaling in adipose tissue in mice, consequently preventing fat accumulation during HFD-feeding (228). Additionally, acetate produced by bacteria links the microbiota, brain, and pancreatic β-cells to promote metabolic syndrome during obesity by driving increased appetite and insulin secretion in the host (229).

Another source of postbiotics that can propagate metabolic effects, such as inflammation and insulin resistance, is microbial components from live or dead bacteria (234). Host detection of bacterial cell wall fragments is sufficient to promote innate and adaptive immune responses and promote metabolic inflammation, lipolysis, and insulin resistance (235–238). But microbiota-derived factors can also protect against insulin resistance. For example, “immunization” with proximal gut microbiota-derived extracts from HFD-diabetic mice promotes immunological tolerance and decreases HFD-induced insulin resistance in mice (239). However, the identity of the microbial factor responsible for tolerization and reduced insulin resistance

is not known. In fact, very little is known about specific bacterial components that can elicit insulin-sensitizing or anti-inflammatory effects in metabolic tissues. Therefore, the identification and characterization of novel bacterial postbiotic molecules from bacteria represents an underutilized avenue of potential drug alternatives to combat obesity-associated metabolic disease. A greater understanding of the mechanisms involved and how bacterial components interact with host immune and metabolic systems is required.

1.5 Immunometabolism: bacteria-host interactions

1.5.1 Host immunity and metabolic disease

An “obese” microbiota skews certain aspects of intestinal immunity to a more inflammatory state that may impact metabolic tissues and precipitate aspects of metabolic disease such as insulin resistance (189). Conversely, diet-induced obesity and/or the related dysbiosis can also compromise other aspects of immunity in the gut important for maintaining mucosal barrier integrity. For example, Th17 immune responses are *decreased* in the ileum and colon but *increased* in the liver during obesity, which represents a key example of compartmentalized immunity during obesity (123,184). Thus, obesity allows for a permissive gut environment whereby bacteria, their metabolites, or their components can evade detection and may be able to penetrate into metabolic tissues and promote microbial inflammation-related insulin resistance (95,187,188,240,241).

To limit damage to host tissues from invading pathogens, pattern recognition receptors (PRRs) of the innate immune system serve as one of the first lines of detection and defense. PRRs respond to a variety of conserved molecular structures unique to non-host cells, referred to as pathogen-associated molecular patterns, in order to mount a rapid response to threats. It has been established that pathogen-sensing systems contribute to inflammation that can precipitate metabolic defects such as insulin resistance during obesity. For example, feeding mice a diet containing excessive lipids can produce a chronic, low-level increase in circulating bacterial lipopolysaccharide (LPS), which can promote toll-like receptor (TLR)4/CD14-mediated inflammation and insulin resistance (95,242,243). *Tlr4* expression is elevated during obesity (244,245). Interestingly, dietary components such as fatty acids can engage TLR4-linked responses to initiate inflammation and insulin resistance (244,246–250).

PRRs can also be engaged by endogenous host molecules. Low levels of damage-associated molecular patterns (DAMPs) are indicators of dead cells or injured tissue and initiate TLR signaling cascades to initiate repair (251). During obesity there is an increased quantity of DAMPs, such as ROS (96). Excessive DAMPs can cause chronic inflammation and can interfere with insulin signaling.

Despite the known role of PRRs in contributing to and exacerbating inflammation and metabolic perturbations during obesity (252), immunoregulatory systems exist to control and limit inflammatory responses. The potential for PRRs to provide *protection* from metabolic disease characteristics has been poorly described.

1.5.2 NOD1 and NOD2

The nucleotide oligomerization domain- or NOD-like receptors (NLRs) are another family of PRRs that respond to a variety of bacterial molecules and endogenous danger signals (253). Two key members of this family are the intracellular NOD proteins, which are composed of an N-terminal single- (NOD1) or dual- (NOD2) caspase-activation and recruitment domain (CARD), a central NOD, and a C-terminal leucine-rich repeat (LRR) domain that is critical for ligand recognition and binding (Figure 1.1) (254–258). NOD1 and NOD2 proteins initiate inflammatory responses after recognizing bacterial cell wall (peptidoglycan) fragments consisting of sugars and amino acids (259). NOD1 recognizes meso-diaminopimelic acid (meso-DAP)-containing muropeptides, found more often in Gram-negative strains (Figure 1.2) (260–263). NOD2 detects muramyl dipeptide (MDP)-containing peptidoglycan found in all bacteria (Figure 1.2) (263), but is more abundant in Gram-positive strains that possess a 2- to 10-fold thicker cell wall, thus positioning NOD2 as a general

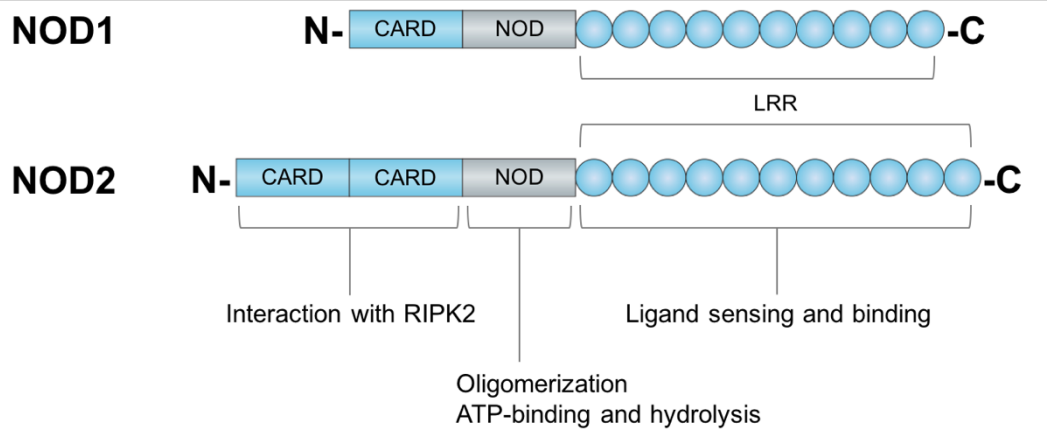

Figure 1.1 Domain structures of NOD1 and NOD2.

NOD1 contains a single N-terminal caspase-activation and recruitment domain (CARD) domain, while NOD2 contains dual-CARD domains that are important for interaction with RIPK2. The central domain of both proteins is important for nucleotide (ATP) binding and protein self-oligomerization. The C-terminal leucine-rich repeat (LRR) region mediates ligand binding. Adapted from Philpott et al. 2014 (256).

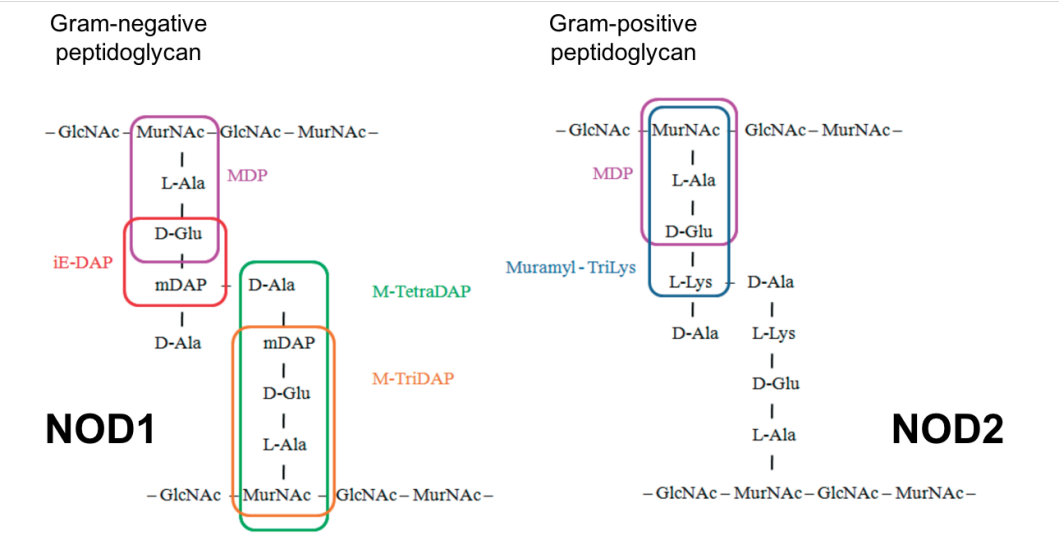

Figure 1.2 Peptidoglycan motifs recognized by NOD1 and NOD2.

Chemical structures of Gram-negative and Gram-positive peptidoglycan. NOD1 recognizes meso-DAP-containing peptidoglycan. NOD2 recognizes MDP-containing peptidoglycan. Adapted from Antosz et al. 2013 (263).

sensor of peptidoglycan (260,264,265). Upon activation of either protein, NOD1 or NOD2 self-oligomerize and interact with receptor-interacting serine/threonine-protein kinase 2 (RIPK2) which propagates the signal and ultimately activates nuclear factor kappa-B (NF-κB) and mitogen-activated protein kinase (MAPK) pathways (Figure 1.3) (266–270). The resultant inflammatory response involves the production of cytokines, chemokines, and antimicrobial peptides to mediate host defense (271). Mutations in either the *Nod1* or *Nod2* genes are associated with aberrant innate immune responses and consequences for infection and inflammatory disease susceptibility, highlighting the importance of these proteins in health (272,273).

1.5.3 NOD1 in inflammatory and metabolic diseases

Detection of bacterial peptidoglycan by NOD1 primes the innate immune system and enhances neutrophil-mediated bacterial killing during infection (274–277). NOD1 has been linked with intestinal mucosal adherence and translocation of commensal bacteria in the early stages of type 2 diabetes (278). NOD1-null mice were found to have reduced bacterial translocation to metabolic tissues and improved protection from HFD-induced insulin resistance. There is evidence showing increased NOD1 (but not NOD2) inflammatory activity in subcutaneous adipose depots in humans with metabolic syndrome (279). Activation of NOD1 *in vivo* worsens diet-

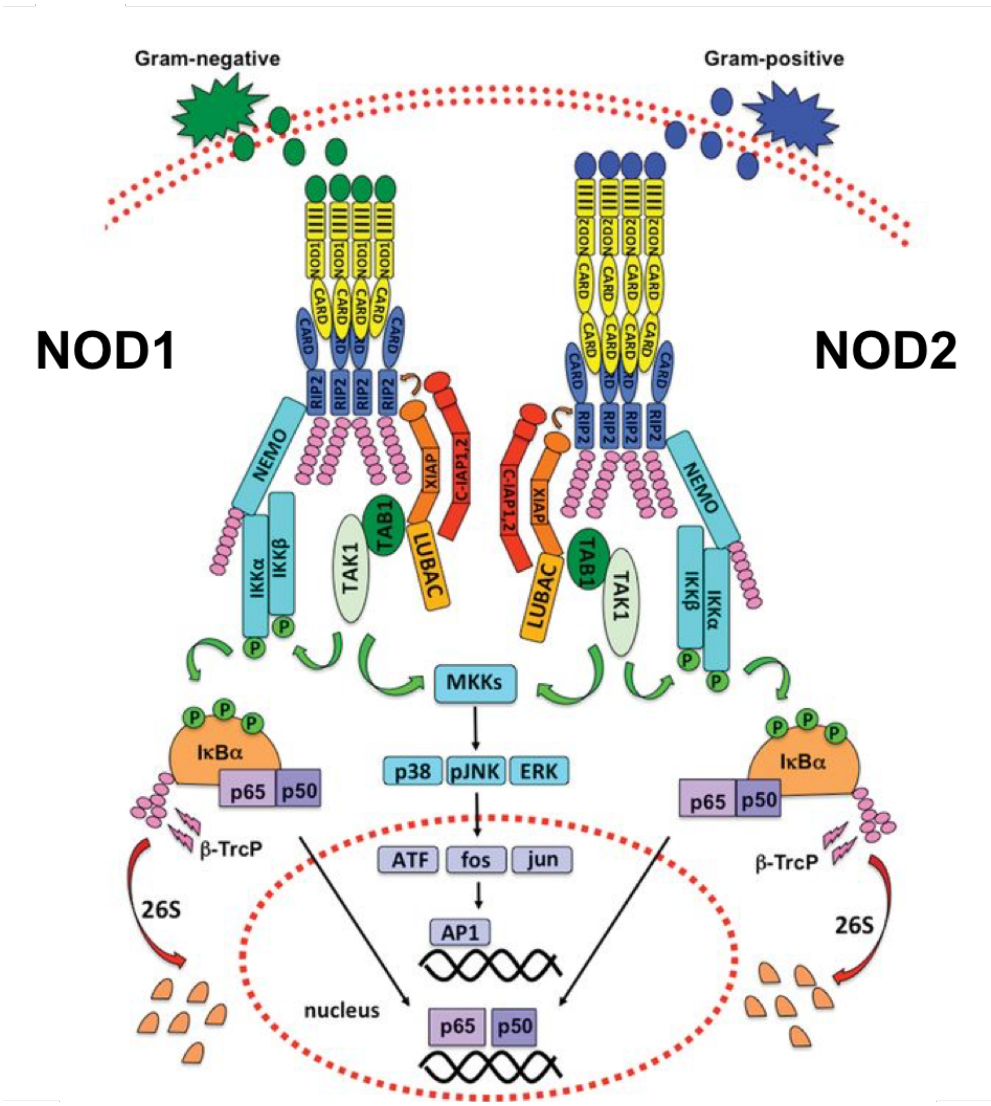

Figure 1.3 NOD signaling pathway.

Upon binding their respective peptidoglycan motifs, NOD1 and NOD2 self-oligomerize, bind to RIPK2, and initiate a signaling cascade that results in the activation of inflammatory pathways to mediate host defence against pathogens. Adapted from Correa et al 2012 (270).

induced inflammation and insulin resistance (237), and induces vascular inflammation and accelerates the development of atherosclerosis in a mouse model of the disease (280,281). In addition, we and others have shown that NOD1 activation induces lipolysis, suppresses adipocyte differentiation, and augments adipose inflammation (235,237,282). Inhibition of NOD1 limits NF-κB activation (283). Thus, NOD1 signaling is associated with pro-inflammatory activity and susceptibility to a worsened metabolic state during obesity.

1.5.4 NOD2 in inflammatory disease

Similar to NOD1, NOD2 plays a major role in regulating innate and adaptive immunity in mice, as well as controlling gut bacterial composition, proliferation, and pathogenicity (269,284–288). *Nod2* expression is increased in the ileum and colon of patients with Crohn's disease (289). It is not clear if this association represents a protective response to the inflammatory environment during Crohn's disease. This is possible since *Nod2* mutations that result in a defective NOD2 protein, and mutations that result in defective downstream actions in the NOD2-signaling pathway, have been identified as a major genetic contributor to an increased risk of Crohn's disease in humans, or susceptibility to experimental colitis in mice (290–293). The origin of inflammation instigated by defective NOD2 signaling is not fully known, but augmented inflammation can be linked to

defects in NOD2-mediated gut bacterial control and cellular immunity. For example, mutations in the *Nod2* gene are associated with increased gut permeability in mice and affect the composition of the microbiota (294). Additionally, functional NOD2 signaling can negatively regulate TLR-mediated pro-inflammatory T helper type 1 (Th1) immune responses that typify Crohn's disease patients with mutated NOD2 (295,296), and positively regulate immunomodulatory T helper type 2 (Th2) immune responses (297,298). Suppression of TLR inflammation via NOD2 signaling has been linked with protection from colitis-associated colorectal tumorigenesis in mice (299,300). Thus, these studies implicate NOD2 as a key regulator of innate immunity responsible for both preventing increased gut bacteria translocation and also preventing excessive microbial-driven inflammation and disease.

It is paradoxical that NOD2, an activator of immunity, can have anti-inflammatory effects in certain disease states. It is possible that NOD2 helps to control a specific community of intestinal bacteria that provides protection from deleterious host responses, but there is limited evidence for this to date. In addition to antibacterial or initial immune responses induced by NOD2, this PRR may help to limit inflammation during or after the mounting of an immune response, which would be positioned to mitigate chronic inflammation and damage to host tissues (301). This is an attractive feature of NOD2 signalling because it may be particularly relevant to chronic

inflammation of low magnitude indicative of obesity, where NOD2 may dampen repeated, excessive, but low-level inflammatory stressors. For example, NOD2 pre-activation of macrophages decreases the production of pro-inflammatory cytokines upon subsequent challenge with TLR ligands (302). This immune tolerance mechanism appears to require NOD2-mediated secretion of anti-inflammatory mediators (303,304). Thus, there seems to be an anti-inflammatory component of chronic NOD2 signaling that can potentially be used to treat inflammatory diseases *in vivo*. Indeed, activation of NOD2 with its peptidoglycan ligand MDP elicits protective anti-inflammatory effects in mouse models of colitis (305,306). MDP treatment also prevented the loss of body mass and preserved colonic crypt architecture in this model of inflammatory bowel disease (305,306).

It was reported that NOD2 mediates its protective effects during experimental colitis via interferon regulatory factor 4 (IRF4) (305,306). Specifically, NOD2 was reported to downregulate colonic inflammation via IRF4-mediated inhibition of NF-κB signaling. IRF4 is a transcription factor that supresses inflammation induced from multiple TLRs (307–309). With respect to metabolism, *Irf4* deletion within mouse adipose tissue macrophages promotes metabolic inflammation during obesity (310), and *Irf4* deletion within adipocytes dysregulates lipid handling and causes increased adiposity during HFD-feeding in mice (311). This transcription factor can also bind directly to the promoters of *il4* and *il10* (312,313), which

are Th2 cytokines with anti-inflammatory and insulin-sensitizing properties (314,315). Thus, IRF4 appears to be a potential key link between NOD2 immunity and metabolism.

1.5.5 NODs in immunometabolism

The immunometabolic contribution of the peptidoglycan-sensing NOD proteins in obesity and metabolic disease is not fully known. Acute activation of NOD1 causes whole-body and hepatic insulin resistance (237) and deletion of *Nod1* can protect against diet-induced insulin resistance in mice (278). This is consistent with the fact that microbiota-derived muropeptides acting on NOD1, but not NOD2, augment systemic immunity (276,277). In contrast, NOD2 activation attenuates inflammation induced by other bacterial products and protects against inflammatory colitis (302,305). Deletion of *Nod2* in mice worsens insulin resistance during obesity (316,317). The mechanisms by which both NOD1 and NOD2 elicit their differential effects on inflammation and glucose metabolism are not known.

1.6 Objectives and hypothesis

Our lab recently discovered that deletion of *Nod2* exacerbated metabolic tissue inflammation and insulin resistance when mice were fed an obesity-causing HFD (316). These findings demonstrate that intact NOD2 signaling is beneficial during metabolic stress. This data, combined

with the protective role of NOD2 activation during chronic inflammatory states such as experimental colitis, positions NOD2 as an attractive therapeutic postbiotic target for mitigating metabolic inflammatory disorders. The recent discoveries that activation of an immunity protein (such as NOD2) can be protective during chronic inflammation represent an additional layer of complexity in understanding how immune responses interact with endocrine control of metabolism during metabolic diseases such as obesity.

We hypothesized that NOD2 activation would result in anti-inflammatory and insulin-sensitizing effects directly in metabolic tissues in mice fed an obesity-causing HFD. We also hypothesized that the protective inflammatory and metabolic effects of NOD2 activation would require the transcription factor IRF4. The objective of this thesis is to characterize the inflammatory and metabolic effects of NOD2 signaling in animal models of obesity and bacterial inflammation.

CHAPTER TWO: Materials and methods

2.1 Mice

All animal procedures for this study were approved by the McMaster University Animal Research Ethics Board in accordance with the guidelines of the Canadian Council of Animal Care. For all studies, mice were 8-10 weeks old before dietary intervention or experiment initiation. Animals were maintained on a 12-hour light/dark cycle, and experiments were performed on multiple cohorts of mice born from different parents at different times of the year. Except where indicated, male mice were used for experiments. Wild type (WT) C57BL/6J mice were obtained from The Jackson Laboratory (strain 000664) or from our in-house colony established from C57BL/6J mice received from The Jackson Laboratory. The majority of experiments were conducted on C57BL/6J mice born under specific-pathogen-free conditions at McMaster University. For certain experiments, where indicated, results were confirmed in C57BL/6J mice ordered from The Jackson Laboratory. Leptin-deficient *ob/ob* mice (B6.Cg-Lep^{ob}/J; strain 000632), TLR4-mutant mice (C3H/HeJ; strain 000659), CD45.1-expressing C57BL/6 mice (B6.SJL-*Ptprc*^{a} *Pepc*^{b}/BoyJ; strain 002014), and albumin-cre transgenic mice (B6.Cg-Tg(Alb-cre)21Mgn/J; strain 003574) were obtained from The Jackson Laboratory. *Nod1*$^{-/-}$, *Nod2*$^{-/-}$, and *Nlrp3*$^{-/-}$ mice have each been backcrossed to C57BL/6J to at least the 12th generation as described in our lab's previous publications (237,316,318). *Irf4*$^{-/-}$ mice, derived from 129J mice and backcrossed to C57BL/6, were kindly provided by Dr. Tak

Mak (University Health Network) (319). *Nod2*$^{loxP/loxP}$ mice were kindly provided Dr. Philip Rosenstiel (University of Kiel) and were backcrossed to the C57BL/6J background for at least 10 generations by Dr. Dana Philpott (University of Toronto) who also kindly provided the mice for these experiments. Age-matched mice were used for all *in vivo* experiments.

2.2 Hematopoietic knockout mice

C57BL/6J CD45.1-expressing mice (B6.SJL-*Ptprc*^{a} *Pepc*^{b}/BoyJ) were treated with sulfamethoxazole and trimethoprim antibiotics in drinking water for 10 days before being subjected to lethal irradiation with 1100 Gy, delivered in 2 doses of 550 Gy, separated by 3 hours using a Gammacell 3000 irradiator. Immune cell progenitors were isolated from the bone marrow of CD45.2-expressing C57BL/6J WT or *Nod2*$^{-/-}$ mice and subjected to T-cell depletion. Briefly, bone marrow was treated with anti-CD4 (GK1.5; Bio X Cell), anti-CD8 (2.43; Bio X Cell), anti-Thy1.2 (30-H12; BD Biosciences), and low-tox guinea pig complement (Cedarlane) as described (320). Bone marrow treatments were performed by Dr. Nicole Barra and Dr. Amanda Lee. Donor cells (10 million cells per recipient mouse) were then injected into the tail vein of irradiated C57BL/6J WT CD45.1-expressing mice to reconstitute hematopoietic systems. Donor cell injections were performed by Dr. Nicole Barra. After 8 weeks of recovery, reconstitution of immune cell populations was confirmed via flow cytometry on

submandibular blood samples obtained from recipient mice. Flow cytometry was performed by Dr. Nicole Barra and Dr. Amanda Lee. Briefly, CD45.1 versus CD45.2 cell populations were quantified using cell surface detection with PE-Cy7 anti-mouse CD45.1 antibody and APC anti-mouse CD45.2 antibody (Figure 3.4; figure order was dictated by results section) as described (320).

2.3 Hepatocyte knockout mice

Hepatocyte-specific *Nod2*$^{-/-}$ animals (*Nod2*$^{-/-HKO}$) were created by crossing albumin-cre transgenic mice (B6.Cg-Tg(Alb-cre)21Mgn/J) (321,322) with *Nod2*$^{loxP/loxP}$ mice to create the knockout alb-cre^{positive}/*Nod2*$^{loxP/loxP}$ (*Nod2*$^{-/-HKO}$) and alb-cre^{negative}/*Nod2*$^{loxP/loxP}$ (WT) mice (Figure 3.8; figure order was dictated by results section).

Hepatocyte *Nod2* deletion was confirmed by tail deoxyribonucleic acid (DNA) genotyping. Mouse tail clippings were digested in 500 µl of tail lysis buffer (100 mM Tris-HCl, 5 mM Ethylenediaminetetraacetic acid, 200 mM NaCl, 0.2% w/v SDS) containing 1.5 units of proteinase K at 37 ºC overnight. The next morning, tubes containing digested tails were mixed by inverting several times, and centrifuged at 15 871 x g for 20 minutes at room temperature. Supernatant was added to 500 µl of isopropanol, mixed by inversion, incubated for 20 minutes at room temperature, and centrifuged at

15 871 x g for 10 minutes at room temperature. Precipitated DNA pellets were washed twice with a 75% ethanol:ultrapure water solution, and suspended in ultrapure water.

The presence of the albumin-cre transgene was confirmed by polymerase chain reaction (PCR) amplification of isolated DNA. Primers for the albumin-cre transgene (5' primer ATG AAA TGC GAG GTA AGT ATG G, 3' primer CGC CGC ATA ACC AGT GAA AC; amplifies only when albumin-cre is present) and a PCR internal control amplification band (5' primer CAA ATG TTG CTT GTC TGG TG, 3' primer GTC AGT CGA GTG CAC AGT TT; amplifies for all reactions) were used in a single reaction. The denaturing step was performed for 1 minute at 94 ºC, the annealing step was performed for 30 seconds at 60 ºC, and the extension step was performed for 1 minute at 72 ºC.

The presence of *loxP*-flanked *Nod2* was also confirmed by PCR amplification of isolated DNA (5' primer CGG TTG GTG GGA TTT CCT GTG C, 3' primer GCA GCC AGG GGT GAT GAT AAC AGG). The denaturing step was performed for 30 seconds at 94 ºC, the annealing step was performed for 30 seconds at 65 ºC, and the extension step was performed for 1 minute at 72 ºC. All PCR steps were performed using a SimpliAmp thermal cycler (Thermo Fisher Scientific). A standard genotyping

result for these mice is provided in (Figure 3.9; figure order was dictated by results section).

2.4 Dietary and inflammatory mouse models

For all studies, mice were 8-10 weeks old prior to dietary intervention or experiment initiation. Animals were fed a control diet (17% kcal from fat, 29% kcal from protein, 54% kcal from carbohydrate; cat# 8640 Teklad 22/5, Envigo) or one of two obesity-promoting HFD models, described below.

For chronic NOD2 activation experiments (HFD model #1 using a "prevention" approach), multiple, separate cohorts of male mice born from different parents were switched from a control diet to a HFD (60% kcal from fat, 20% kcal from protein, 20% kcal from carbohydrate; cat# D12492, Research Diets) when mice were 8-10 weeks old. HFD-fed mice were fed *ad libitum* for 5 weeks and NOD2 ligands were administered intraperitoneally 4 days/week during the 5-week period.

For "intervention" style experiments in mice with diet-induced obesity (HFD model #2), multiple, separate cohorts of male mice 8-10 weeks old were fed HFD (45% kcal from fat, 20% kcal from protein, 35% kcal from carbohydrate; cat# D12451, Research Diets) for 10-12 weeks and then

these obese mice were injected once per day with NOD1 or NOD2 ligands intraperitoneally for 3 days prior to experimentation.

For acute endotoxemia experiments, ultrapure LPS from *Escherichia coli O111:B4* (Cat# tlrl-3pelps, InvivoGen) was injected intraperitoneally at a dose of 0.1-0.2 mg/kg 2-6 hours prior to experiments in control diet-fed mice.

For NOD2 activation experiments, MDP (Cat# tlrl-mdp, InvivoGen) was used at 100 µg/injection and mifamurtide (Cat# SML0195, Sigma-Aldrich) was used at 50 µg/injection, except for dose-response experiments. For NOD1 activation experiments, iE-DAP (Cat# tlrl-dap, InvivoGen) was used at 100 µg/injection and FK565 was used at 10 µg/injection (Astellas Pharma). All ligands used for intraperitoneal injection were diluted in saline and frozen at -20 ºC. The volume used for all NOD ligand injections was 200 µL; control mice received equal volumes of saline as a vehicle.

2.5 Glucose, insulin, and pyruvate tolerance tests

Intraperitoneal glucose tolerance tests (GTTs) and insulin tolerance tests (ITTs; a measure of insulin activity/response) were performed in 6-hour fasted, conscious mice. The dose of D-glucose (Sigma-Aldrich) and insulin aspart (NovoRapid, Novo Nordisk) used is indicated in each figure caption.

Intraperitoneal pyruvate tolerance tests (PTTs) were performed in 16-hour fasted, conscious mice with 2 g/kg sodium pyruvate (Sigma-Aldrich). Blood glucose was determined by tail vein blood sampling using a handheld glucometer (Roche Accu-Check Performa). Area under the curve of blood glucose versus time (with baseline Y set to 0) for each experiment was calculated using GraphPad Prism 6 software.

2.6 Hyperinsulinemic-euglycemic Clamps

Control diet-fed and 60% kcal HFD-fed C57BL/6J mice were acclimated to the experimental environment, restrainer, and handling for 3 weeks prior to clamp experiment. Mice were anesthetized with isoflurane and an indwelling catheter was inserted into the right jugular vein 5–7 days before the clamp experiment by Dr. Morgan Fullerton. MDP injections prior to clamp experiments were performed intraperitoneally in isoflurane-anesthetized mice. For clamp experiments (performed with Dr. Morgan Fullerton), 5-hour fasted animals were placed into restrainers and basal tracer containing D-[3-^{3}H]glucose was infused at a rate of 7.5 μCi/h to determine the basal rate of glucose turnover. After 1 hour elapsed, blood glucose was measured and “basal” blood samples were collected. Insulin solution (containing 7.5 μCi/h D-[3-^{3}H]glucose) was then infused at a rate of 10 mU/kg/minute. Blood glucose was monitored via tail vein sampling, and non-radioactive glucose was infused at a variable rate to maintain

euglycemia (5-7 mmol/L). Upon achieving euglycemia, “clamped” blood samples were collected to determine the insulin-stimulated rate of glucose turnover. Collected blood samples were subjected to deproteinization with 0.3 N each of $Ba(OH)_2$ and $ZnSO_4$, and analyzed for radioactivity via liquid scintillation counting to determine the glucose disposal rate (GDR) and hepatic glucose production rate (HGP) for each animal. These parameters were calculated using the following equations (323):

GDR = clamp [^{3}H]-glucose infusion rate / specific activity of glucose

HGP = GDR – glucose infusion rate

2.7 2DG uptake

In some experiments, 2-[1,2-^{3}H (N)]-Deoxy-D-glucose (2DG) uptake was determined in mice that did not undergo hyperinsulinemic-euglycemic clamps. These experiments were focused on assessing adipose tissue insulin sensitivity, which was determined in mice that were fasted 5 hours and administered insulin (2 IU/kg i.p. for HFD-fed animals, 4 IU/kg for *ob/ob* animals) and 5 minutes later injected via tail vein with 2DG. Dr. Brennan Smith assisted in these experiments. Blood samples were taken at 5, 10, and 15 minutes post-2DG injection, subjected to deproteinization with 0.3 N each of $Ba(OH)_2$ and $ZnSO_4$, and analyzed for 2DG radioactivity via liquid scintillation counting. Tissue-specific glucose uptake was calculated by determining 2DG radioactivity in weighed gonadal white adipose tissue

samples and dividing this value by a function of blood 2DG radioactivity and blood glucose values over the duration of the assay.

2.8 MDP localization

In vivo localization of 100 µg intraperitoneally-injected MDP-rhodamine (Cat# tlrl-rmdp, InvivoGen) in isoflurane-anaesthetized mice was determined using the IVIS Spectrum *in vivo* imaging system (PerkinElmer) at an excitation wavelength of 535 nm and an emission wavelength of 580 nm.

2.9 CT imaging

Adiposity was determined via computed tomography (CT) scanning using the X-SPECT System (Gamma Medica) in isoflurane-anaesthetized mice at the McMaster Centre for Pre-Clinical and Translational Imaging. The voxel volume of adipose tissue for each mouse was calculated from the sum of all CT images using AMIRA v5.6 software with display/masking intensity of -450 to -125 Hounsfield units (radiodensity range for adipose tissue) (324).

2.10 NF-κB activity

For determination of NF-κB activity, previously liquid nitrogen flash-frozen mouse liver and gonadal white adipose tissue were removed from -

80 ºC storage and mechanically homogenized at 4.5 meters/second for 30 seconds using a FastPrep-24 tissue homogenizer (MP Biomedicals) and ceramic beads. Tissue lysates were quantified using BCA protein assay (Thermo Fisher Scientific). Samples were standardized to 40 µg total protein. Liver and white adipose tissue NF-κB p65 activity was quantified according to kit manufacturer's protocols (Cat# 40096, Active Motif). This kit allows for the assessment of relative levels of NF-κB p65 activity via enzyme-linked immunosorbent assay (ELISA)-based detection of transcription factor binding to immobilized oligonucleotide sequences containing an NF-κB consensus site.

2.11 Gene expression analyses

Total ribonucleic acid (RNA) was obtained from approximately 50 mg of indicated mouse tissues via mechanical homogenization in TRIzol reagent (Cat# 15596018, Thermo Fisher Scientific) at 4.5 meters/second for 30 seconds using a FastPrep-24 tissue homogenizer (MP Biomedicals) and glass beads, followed by phenol-chloroform extraction. Homogenate was centrifuged at 12 000 x g for 10 minutes at 4 ºC, the supernatant was added to a new tube containing chloroform at half the volume of supernatant, and the solution was mixed and centrifuged at 12 000 x g for 10 minutes at 4 ºC. The aqueous upper phase was then added to an equal volume of isopropanol, mixed, incubated at room temperature for 20

minutes, and centrifuged at 12 000 x g for 10 minutes at 4 ºC. Precipitated RNA pellets were washed twice with a 75% ethanol/ultrapure water solution. RNA pellets were suspended in ultrapure water and incubated at 55 ºC for 15 minutes.

Subsequently, cDNA was prepared using 1000 ng total RNA. Briefly, RNA was treated with DNAse I (Cat# 18068015, Thermo Fisher Scientific) and incubated at room temperature for 15 minutes. Random hexamer primers and dNTPs were added to RNA. Solutions were incubated at 95 ºC for 10 minutes to inactivate DNAse, followed by incubation at 55 ºC for 10 minutes to allow primers to anneal RNA strands. cDNA was prepared by adding SuperScript III Reverse Transcriptase (Cat# 18080044, Thermo Fisher Scientific) to RNA-primer solutions, followed by incubation at 55 ºC for 50 minutes, and 70 ºC for 15 minutes. cDNA was diluted 1/25 with ultrapure water.

Transcript expression was measured using TaqMan Gene Expression Assays (Thermo Fisher Scientific) with AmpliTaq Gold DNA polymerase (Cat# 4311818, Thermo Fisher Scientific). Briefly, cDNA was incubated with polymerase and TaqMan assays and placed in a Rotor-Gene Q real-time PCR cycler (QIAGEN). Samples completed 45 cycles of: incubation at 95

ºC for 5 seconds, and incubation at 58 ºC for 10 seconds. Target genes were compared to *Rplp0* housekeeping gene using the $\Delta\Delta C_T$ method.

2.12 Cytokine quantification

Mouse serum cytokines were quantified using a Bio-Plex Pro mouse cytokine 23-plex assay kit (Cat# M60009RDPD, Bio-Rad Laboratories) according to manufacturer's protocols. Briefly, magnetic beads coupled with cytokine-specific capture antibodies were added to a 96-well microplate. Mouse serum samples obtained from terminal cardiac blood were diluted to a final volume of 50 µL (1/4 dilution) with kit sample diluent. Prepared standards, blanks, and samples were then added to the assay plate. Unbound protein was washed from the plate, and biotinylated detection antibodies were added. Bound protein/bead/antibody "sandwiches" were detected using a streptavidin-phycoerythrin fluorescent reporter and measured with a BioPlex-200 instrument (Bio-Rad Laboratories). Cytokines were quantified based on a standard curve generated from prepared standards.

2.13 Endotoxin quantification

Mouse serum endotoxin levels were quantified using a Pierce Limulus Amebocyte Lysate (LAL) Chromogenic Endotoxin Quantitation Kit (Cat# 88282, Thermo Fisher Scientific) according to manufacturer's

protocols. This kit takes advantage of the reactivity of horseshoe crab blood cell lysate (i.e. LAL) to bacterial endotoxin, thus allowing for the quantification of LPS in biological samples. Briefly, mouse serum samples obtained from terminal cardiac blood were diluted to a final volume of 50 µL (1/80 dilution) with endotoxin-free water and heat-shocked at 70 ºC for 15 minutes. Prepared standards, blanks, and samples were vigorously mixed and added to a 96-well assay plate maintained at 37 ºC. LAL was added to each well, followed by chromogenic substrate solution, and stop solution with 37 ºC incubations between all reagent additions. Absorbance was measured with a Synergy H4 Hybrid reader (BioTek Instruments) and quantification of endotoxin in samples was calculated via interpolation from an endotoxin standard curve generated using the provided LPS sourced from *Escherichia coli* O111:B4.

2.14 NEFA quantification

Mouse serum non-esterified fatty acids (NEFA) were quantified using a NEFA-HR(2) kit (Cat# 999-34691; Cat# 995-34791; Cat# 991-34891; Cat# 993-35191, Wako Diagnostics) according to manufacturer's protocols. Triglycerides were measured by quantification of glycerol using the free glycerol reagent calibrated with glycerol standard solution (Sigma-Aldrich) and measured with a Synergy H4 Hybrid reader (BioTek Instruments).

Quantification of samples was calculated via interpolation from a glycerol standard curve.

2.15 Serum insulin quantification and HOMA-IR calculation

For determination of serum insulin after glucose injection, mice were fasted for 6 hours and injected intraperitoneally with 2 g/kg glucose. Tail blood samples (50 µL) were obtained at 0 (basal), 5, and 20 minutes post-injection. To quantify insulin, mouse serum was used with a rat/mouse insulin ELISA kit (Cat# EZRMI-13K, EMD Millipore) according to manufacturer's protocols and measured with a Synergy H4 Hybrid reader (BioTek Instruments). The homeostatic model assessment of insulin resistance (HOMA-IR) was calculated by multiplying blood glucose values determined in 6-hour fasted mice via tail vein blood sampling using a handheld glucometer (in mmol/L), by insulin values (in µU/mL), and dividing this value by 22.5 (325).

2.16 Tissue lipid analysis

Mouse skeletal muscle and liver that were previously liquid nitrogen flash-frozen were removed from -80 ºC storage and lipids were extracted using a Bligh and Dyer chloroform/methanol extraction method. Approximately 50 mg of tissue was weighed and mechanically homogenized at 4.5 meters/second for 30 seconds using a FastPrep-24

tissue homogenizer (MP Biomedicals) and ceramic beads. Homogenate was vigorously mixed with a 1:2 mixture of chloroform:methanol, followed by addition of chloroform and deionized water, with more vigorous mixing. Samples were centrifuged and the bottom chloroform phase was transferred to a fresh tube and freeze dried overnight. Samples were resuspended in a 5:95 mixture of 85% KOH:95% EtOH, heated at 60 ºC for 1 hour, mixed with 0.15M $MgSO_4$, and centrifuged to pellet debris. Triglycerides were measured by quantification of glycerol using the free glycerol reagent calibrated with glycerol standard solution (Sigma-Aldrich) and measured with a Synergy H4 Hybrid reader (BioTek Instruments). Quantification of samples was calculated via interpolation from a glycerol standard curve.

2.17 Quantification and statistical analysis

Values presented in figures are mean ± SEM. Data was assessed for normal distribution using the D'Agostino-Pearson normality test. For normally distributed data sets, statistical significance was determined by unpaired two-tailed *t*-test, one-way ANOVA with Tukey post hoc multiple comparison analyses, or two-way ANOVA with Sidak post hoc multiple comparison analyses. For non-normally distributed data sets, statistical significance was determined by Mann-Whitney *U* test or Kruskal-Wallis test. $P < 0.05$ was considered statistically significant. Statistical analyses and the

values of n for each experiment are reported in the figures and figure legends. Statistical analyses were calculated using GraphPad Prism 6 software.

CHAPTER THREE: Results

3.1 *Nod2* deletion in mice and obesity

3.1.1 Deletion of whole-body *Nod2* worsens glucose and insulin tolerance during diet-induced obesity

Defective NOD2 is associated with chronic inflammation and inflammatory diseases (269,291,326). Our lab sought to characterize the role of NOD2 during dietary stress and its contribution to obesity and metabolic disease in mice. In Denou et al., WT (*Nod2*$^{+/+}$*)* and *Nod2*$^{-/-}$ mice were fed an obesity-causing HFD for 16 weeks (316). While there was no difference in body mass (Figure 3.1A), *Nod2*$^{-/-}$ mice were insulin intolerant compared to WT mice (Figure 3.1B). Hyperinsulinemic-euglycemic clamps revealed that functional NOD2 is required to preserve whole-body insulin sensitivity during obesity. Specifically, *Nod2*$^{-/-}$ mice required a lower glucose infusion rate (GINF) to maintain euglycemia during a hyperinsulinemic state (Figure 3.1C). The clamp also revealed that *Nod2*$^{-/-}$ mice had significantly worsened liver insulin resistance, as insulin was less effective at suppressing hepatic glucose output (HGO) compared to WT mice (Figure 3.1D). *Nod2*$^{-/-}$ mice also experienced increased pyruvate intolerance, further suggesting that hepatic glucose control is impaired in these mice during obesity (Figure 3.1E). In addition, liver (Figure 3.2A) and adipose (Figure 3.2B) inflammatory transcripts were higher in obese *Nod2*$^{-/-}$ mice compared to obese WT mice. Together the results from Denou et al. demonstrate that

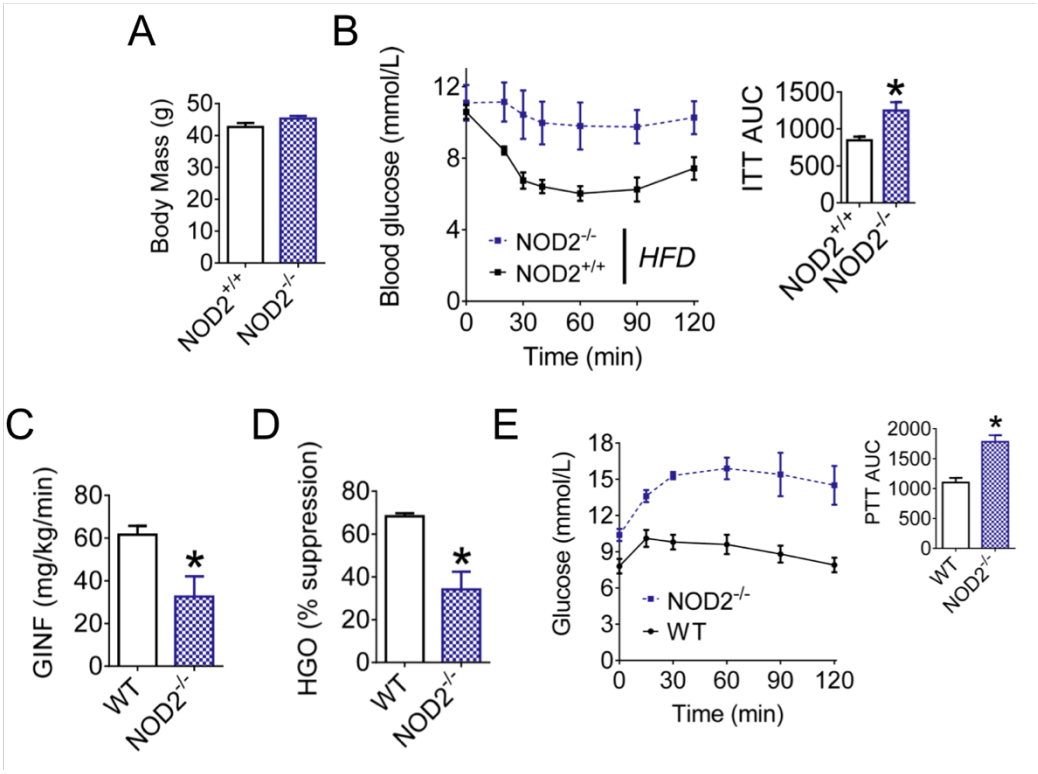

Figure 3.1 *Nod2* deletion in mice exacerbates diet-induced insulin resistance and impairs insulin action in the liver.

Body mass (A), insulin tolerance test (1 IU/kg; B), glucose infusion rate (GINF; C), suppression of hepatic glucose output (HGO; D), and pyruvate tolerance test (2 g/kg; E) of HFD-fed WT/NOD2$^{+/+}$ and NOD2$^{-/-}$ mice. Adapted from Denou et al 2015 (316).

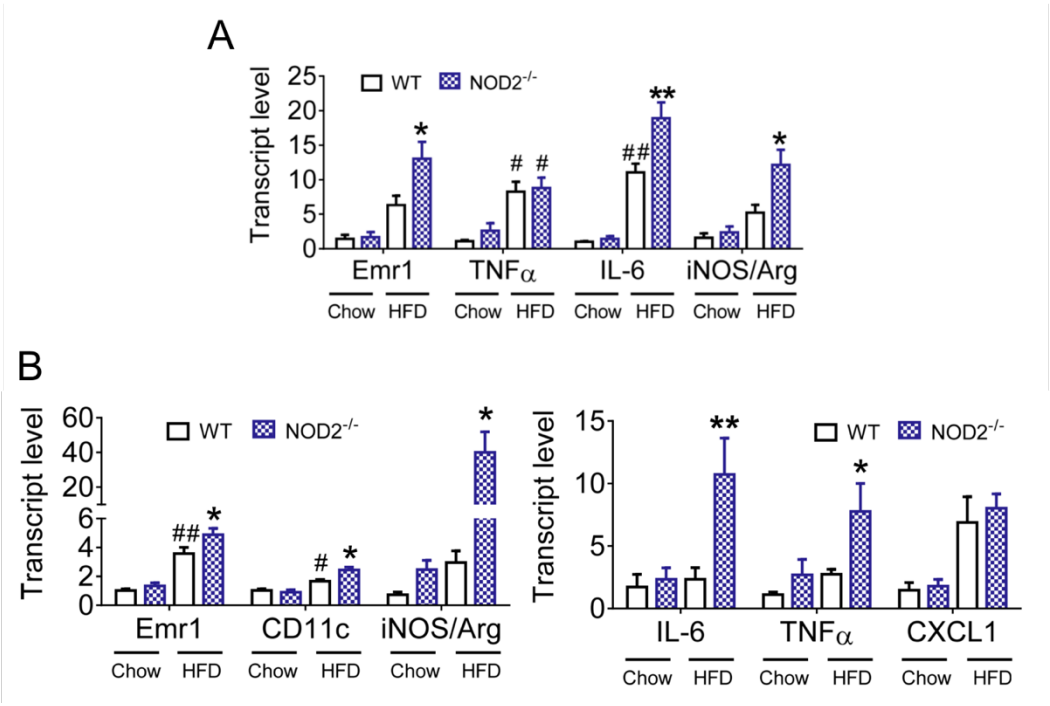

Figure 3.2 *Nod2* deletion promotes diet-induced metabolic tissue inflammation.

Liver (A) and adipose (B) inflammatory gene expression of control-diet and HFD-fed WT and NOD2$^{-/-}$ mice. Adapted from Denou et al 2015 (316).

whole-body deletion of *Nod2* results in increased metabolic tissue inflammation and insulin resistance during diet-induced obesity (316).

3.1.2 Deletion of hematopoietic cell *Nod2* does not alter glucose tolerance during HFD-induced obesity

Nod2 is highly expressed in immune cells, and its binding to the minimally bioactive peptidoglycan motif MDP prompts an innate immune response (255). The potential immunometabolism mechanisms underpinning dysglycemia during obesity-associated metabolic disease can involve many different cell types. Therefore, it was important for this thesis to build on our lab's discovery of increased insulin resistance in whole-body NOD2 knockout mice that were fed a HFD. Hence, it was determined if the contribution of NOD2 signaling within immune cells during HFD-induced obesity altered glucose control. Chimeric mice lacking immune cell NOD2 ($Nod2^{-/-BMT}$) as well as an isogenic control strain (WT^{BMT}) were generated using lethal irradiation of CD45.1-expressing C57BL/6J WT mice (Figure 3.3). After irradiation and recovery, the depletion of CD45.1-expressing cells and adoption of donor CD45.2-expressing cells in recipient mice was confirmed (Figure 3.4) (the experiment in Figure 3.4 was performed by Dr. Nicole Barra and Dr. Amanda Lee). WT^{BMT} and $Nod2^{-/-BMT}$ animals were fed an obesity-causing HFD (Figure 3.5). Baseline metabolic parameters were established using an i.p. GTT in animals fed a control diet (Figure 3.6).

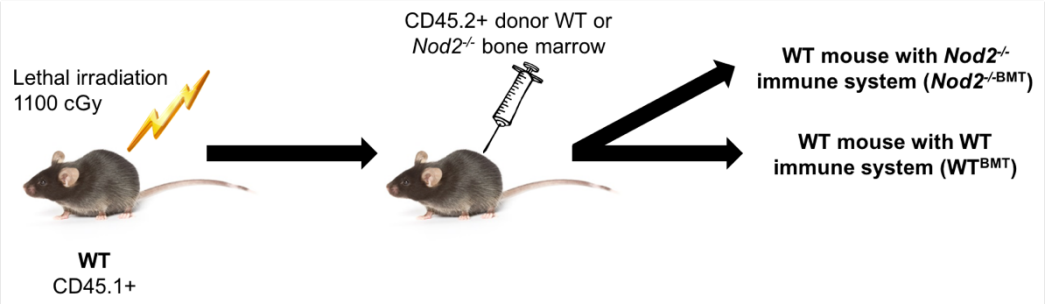

Figure 3.3 Generation schematic for hematopoietic-*Nod2*$^{-/-}$ mice.

Mice deficient in immune cell NOD2 were created by lethal irradiation of WT recipient mice, followed by reconstitution with immune cell progenitors from donor mice.

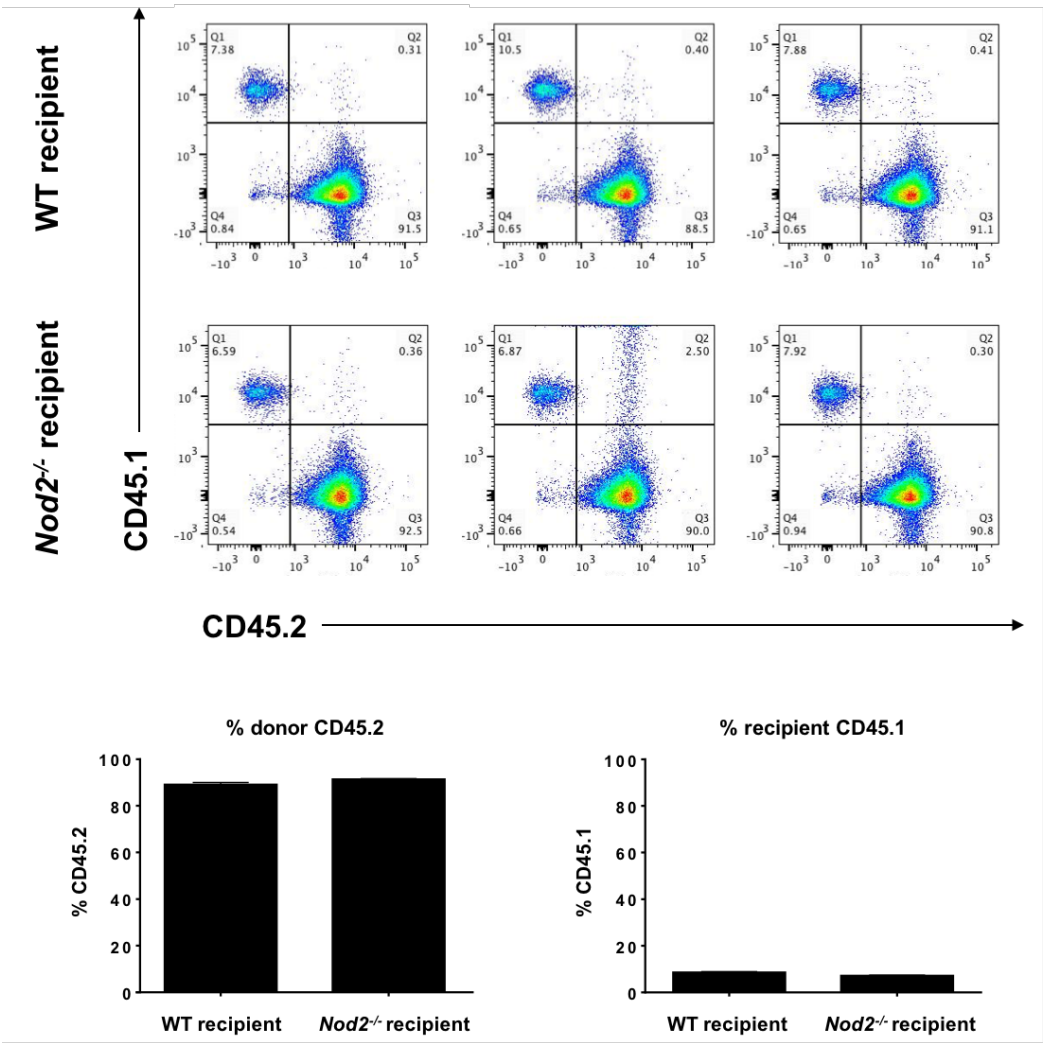

Figure 3.4 Confirmation of hematopoietic-*Nod2*$^{-/-}$ mice.

Following recovery from lethal irradiation, blood from recipient mice (originally CD45.1+) was assessed for CD45.1+ vs CD45.2+ cell populations. Adoption of donor cell genotype was confirmed as the major immune cell populations of WT- and NOD2-recipient mice were CD45.2+. This experiment was performed by Dr. Nicole Barra and Dr. Amanda Lee.

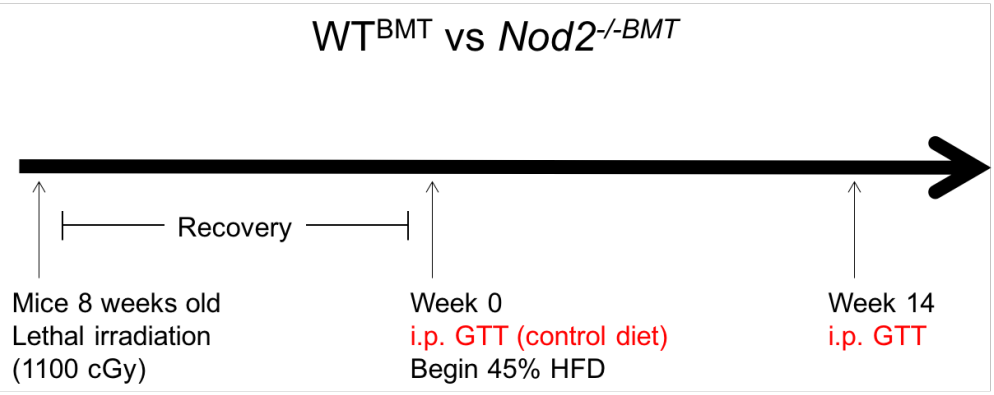

Figure 3.5 Experimental strategy for hematopoietic-Nod2-/- mice.

WT^{BMT} and *Nod2*$^{-/-BMT}$ mice fed a control diet were subjected to a GTT after recovery. Mice were then fed an obesity-causing HFD and glucose tolerance was assessed after 14 weeks.

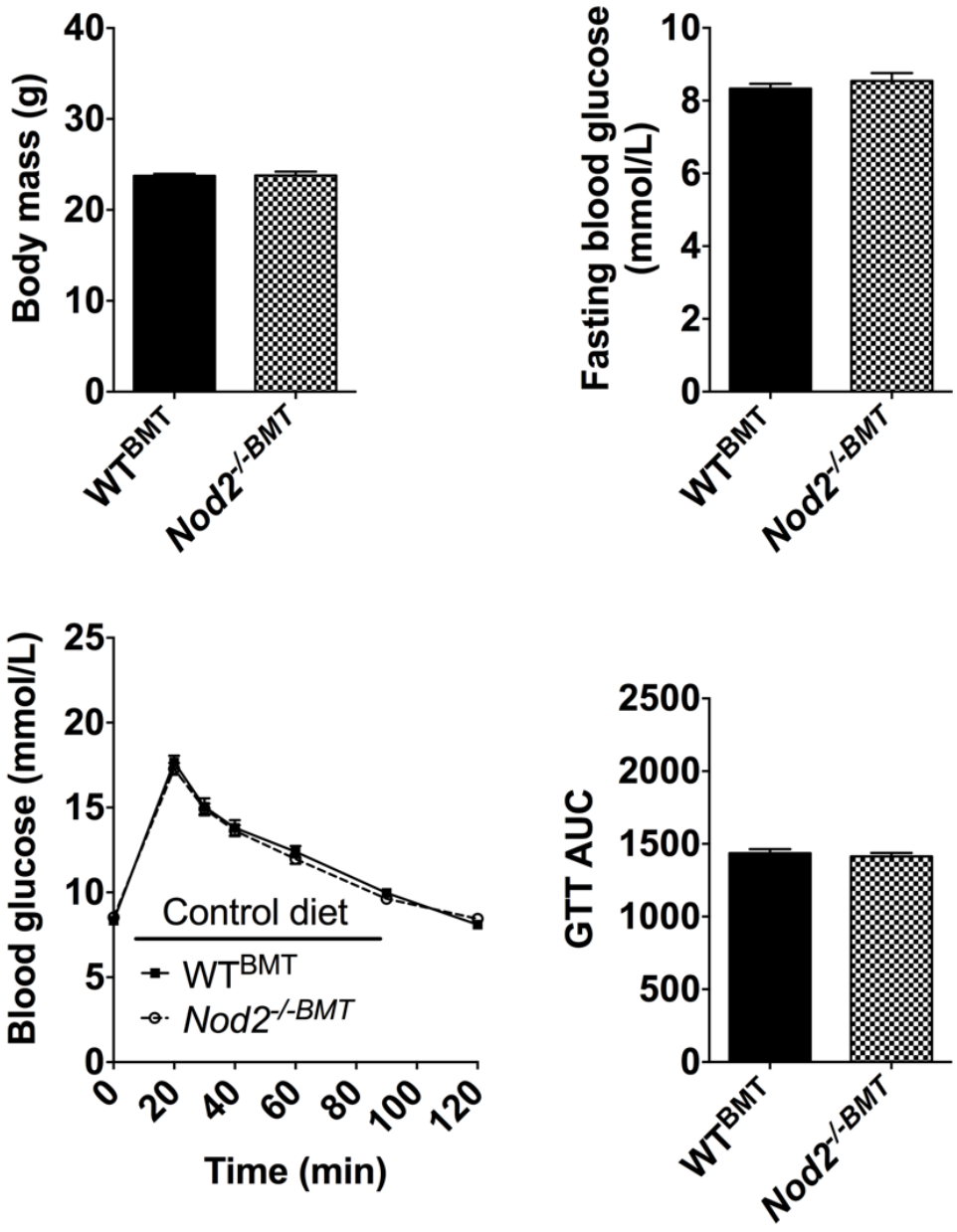

Figure 3.6 Pre-diet glucose tolerance assessment of hematopoietic-*Nod2*$^{-/-}$ mice.

Body mass, fasting blood glucose, and glucose tolerance test (2 g/kg) of control diet-fed WT^{BMT} and *Nod2*$^{-/-BMT}$ mice. n = 24-30 mice for each group. Values are mean ± SEM.

Following 14 weeks of HFD-feeding, these animals were subjected to a GTT and no significant differences in glucose tolerance were observed between WT^{BMT} and $Nod2^{-/-BMT}$ animals (Figure 3.7). This result, combined with our previous findings that whole-body $Nod2^{-/-}$ animals are metabolically impaired during obesity (316), indicates that hematopoietic NOD2 is not required for metabolic protection during HFD-induced obesity.

3.1.3 Deletion of hepatocyte *Nod2* does not alter glucose tolerance during HFD-induced obesity

We previously found that whole-body deletion of *Nod2* in mice increased inflammation and impaired insulin action in the liver during obesity-causing HFD feeding, and that *Nod2* expression was significantly increased in hepatocytes compared to non-hepatocytes during HFD-feeding (316). Therefore, we next sought to directly test the protective effects of intact NOD2 signaling within hepatocytes. Mice lacking hepatocyte NOD2 ($Nod2^{-/-HKO}$) as well as an isogenic control strain (WT^{loxP}) were generated by crossing albumin-cre transgenic mice with mice that had their *Nod2* genes flanked by *loxP* sequences ($Nod2^{loxP/loxP}$) (Figure 3.8). Following a standard breeding approach for tissue specific deletion in mice involving breeding for 3 generations, suitable cohorts of mice were established and the presence or absence of the albumin-cre transgene in $Nod2^{loxP/loxP}$ mice was confirmed (Figure 3.9).

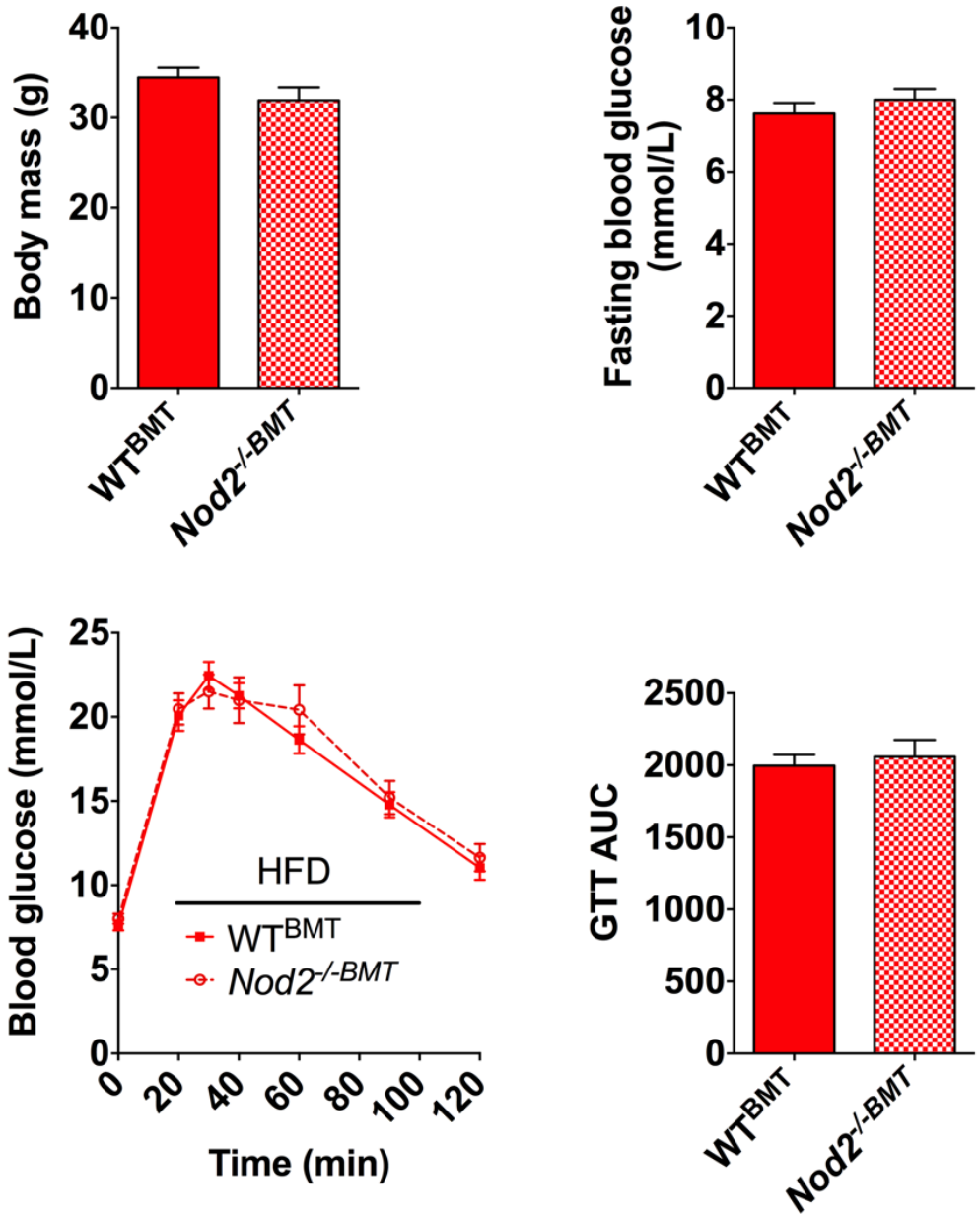

Figure 3.7 Post-diet glucose tolerance assessment of hematopoietic-*Nod2*$^{-/-}$ mice.

Body mass, fasting blood glucose, and glucose tolerance test (1.75 g/kg) of HFD-fed WT^{BMT} and *Nod2*$^{-/-BMT}$ mice. n = 12-15 mice for each group. Values are mean ± SEM.

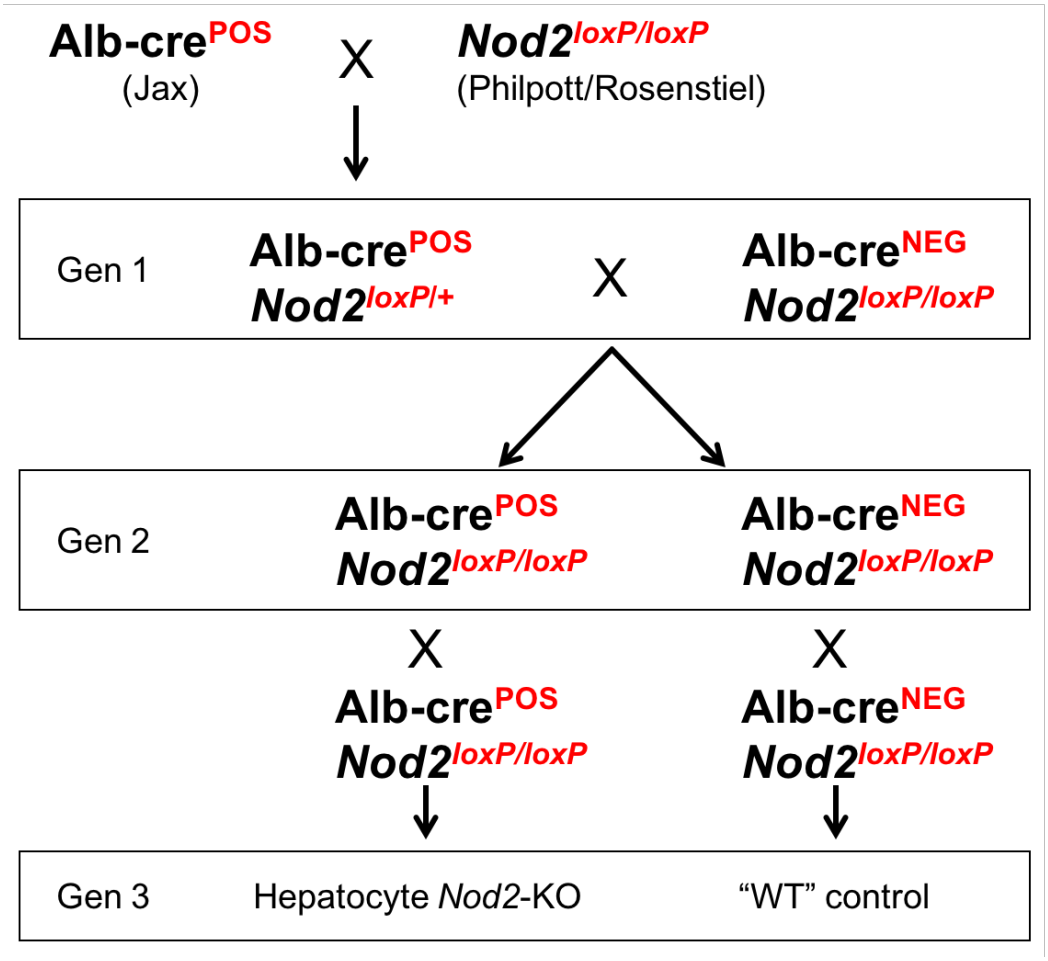

Figure 3.8 Breeding strategy for creation of hepatocyte-*Nod2*$^{-/-}$ mice.

Mice deficient in hepatocyte NOD2 were created by crossing albumin-cre transgenic mice with mice containing a *Nod2* gene flanked by *loxP* sequences. Excision of *Nod2* was achieved by genotyping and directed breeding for multiple generations.

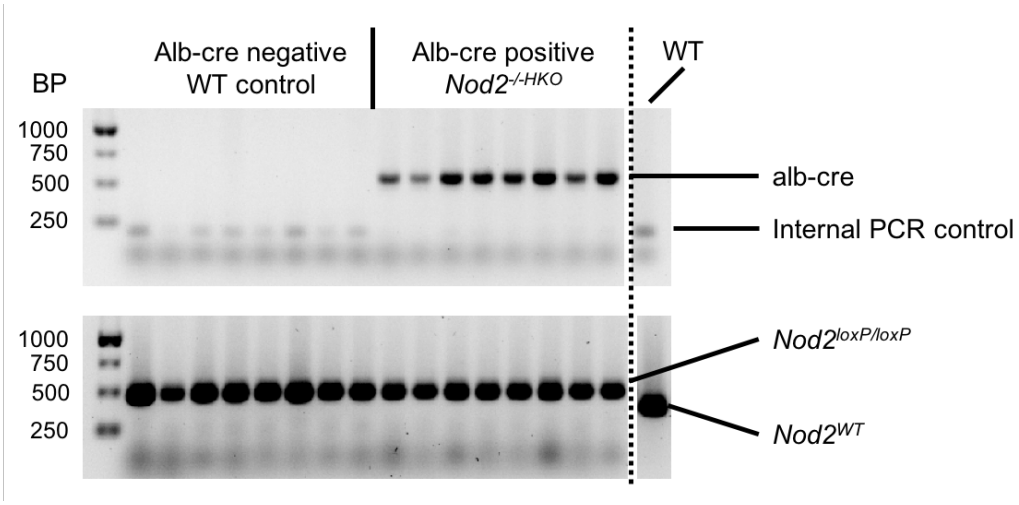

Figure 3.9 Genotyping result for hepatocyte-*Nod2*$^{-/-}$ mice.

Mice deficient in hepatocyte NOD2 (*Nod2*$^{-/-HKO}$) and isogenic control mice (WT^{loxP}) were genetically confirmed by tail DNA genotyping via PCR amplification of albumin-cre and *Nod2* sequences. Mice containing both the albumin-cre transgene and *loxP*-flanked *Nod2* were identified as hepatocyte NOD2$^{-/-}$ (*Nod2*$^{-/-HKO}$). Mice containing *loxP*-flanked *Nod2* but no albumin-cre transgene were identified as isogenic controls (WT^{loxP}).

We sought to directly test the role of hepatocyte NOD2 in obesity-associated metabolic disease. Hence, WT^{loxP} and $Nod2^{-/-HKO}$ animals were fed an obesity-causing HFD (Figure 3.10). Baseline metabolic parameters were established using an i.p. GTT in animals fed a control diet (Figure 3.11). Following 8 weeks of HFD-feeding, these animals were subjected to a GTT and no significant differences in glucose tolerance were observed between WT^{loxP} and $Nod2^{-/-HKO}$ animals (Figure 3.12). This result, combined with our previous findings that whole-body $Nod2^{-/-}$ animals are metabolically impaired during obesity (316), indicates that hepatocyte NOD2 is not required for metabolic protection during HFD-induced obesity.

3.1.4 Summary

Although the results in this thesis do not solve which cell type is responsible for mediating protection via NOD2 during obesity, they reveal that hematopoietic cells (i.e. the majority of immune cells) and hepatocytes (key metabolic cell in liver) are not responsible for cell-autonomous NOD2-mediated responses that mitigate dysglycemia during obesity. This dissertation did not attempt to solve the cell type responsible for worsened dysglycemia upon deletion of *Nod2*. Rather, these results and mouse models informed analysis and direction of future experiments regarding the mechanisms of action after NOD2 activation. For example, if NOD2 stimulation with MDP caused adipose tissue-specific effects, a plausible

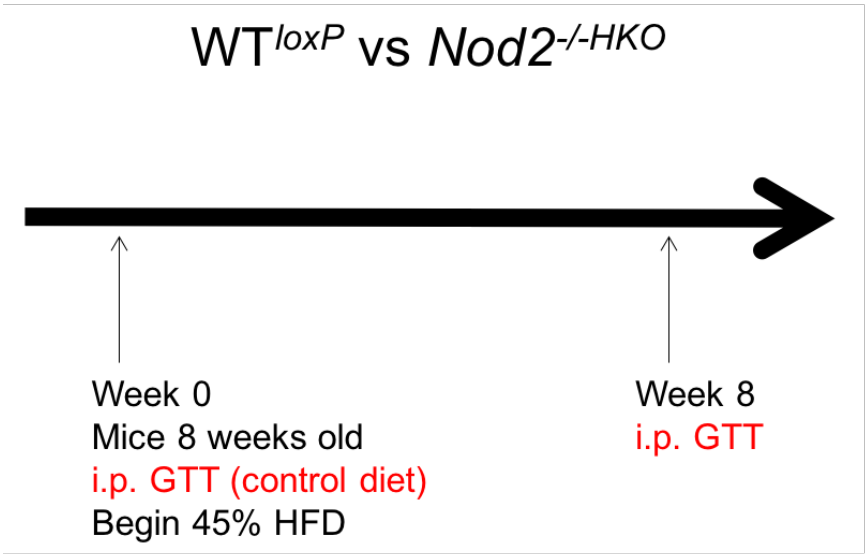

Figure 3.10 Experimental strategy for hepatocyte-*Nod2*$^{-/-}$ mice.

WT^{loxP} and *Nod2*$^{-/-HKO}$ mice fed a control diet were subjected to a GTT. Mice were then fed an obesity-causing HFD and glucose tolerance was tested after 8 weeks.

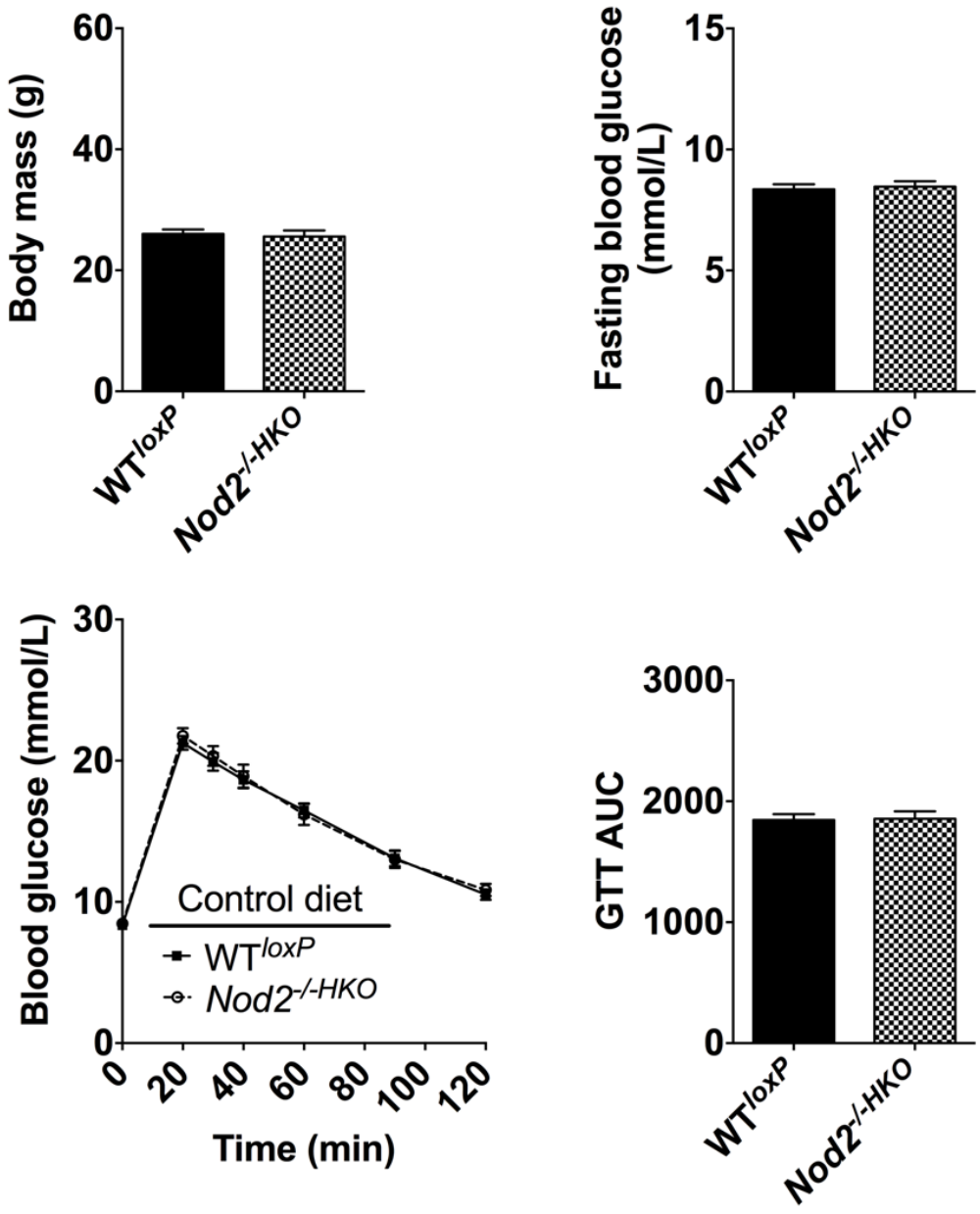

Figure 3.11 Pre-diet glucose tolerance assessment of hepatocyte-*Nod2*$^{-/-}$ mice.

Body mass, fasting blood glucose, and glucose tolerance test (2 g/kg) of control diet-fed WT^{loxP} and *Nod2*$^{-/-HKO}$ mice. n = 14-15 mice for each group. Values are mean ± SEM.

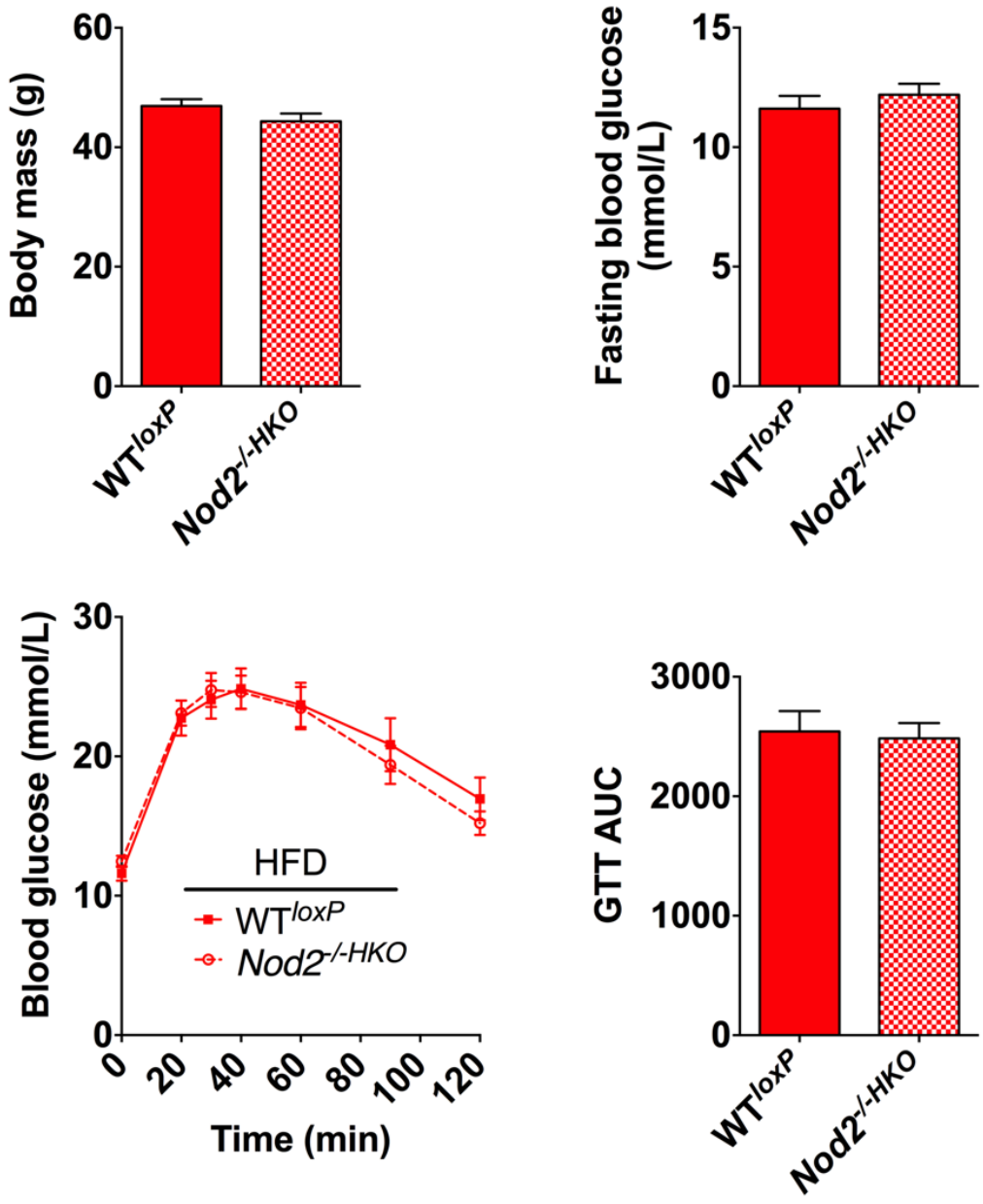

Figure 3.12 Post-diet glucose tolerance assessment of hepatocyte-*Nod2*$^{-/-}$ mice.

Body mass, fasting blood glucose, and glucose tolerance test (1 g/kg) of HFD-fed WT^{loxP} and *Nod2*$^{-/-HKO}$ mice. n = 10-14 mice for each group. Values are mean ± SEM.

conclusion would be that the effects were primarily adipocyte driven (versus adipose tissue macrophage). Thus, these studies were important for designing subsequent experiments to test if and how NOD2 activation could potentially improve glucose metabolism and limit metabolic inflammation during obesity.

3.2 NOD2 activation in mice and obesity status

3.2.1 Chronic NOD2 activation does not alter indices of obesity during HFD feeding in mice

We first determined the biological retention time and any possible tissue localization properties of NOD2 ligands. Rhodamine-labelled MDP was i.p. injected into anaesthetized mice and animals were visualized using a fluorescence imaging platform. The rhodamine-labelled MDP molecule did not accumulate in a specific organ, but rather quickly dispersed systemically throughout mice, and was undetectable 2 hours after injection (Figure 3.13).

The NOD2-activating ligand MDP can attenuate experimental colitis in mice (305), but the effects of MDP on obesity and insulin resistance, to this date, were not known. To investigate the physiological effects of NOD2 activation with MDP during developing metabolic disease, a “prevention-style” *in vivo* experimental HFD model was established where 100 μg MDP was administered via i.p. injection into mice 4 days per week for 5 weeks

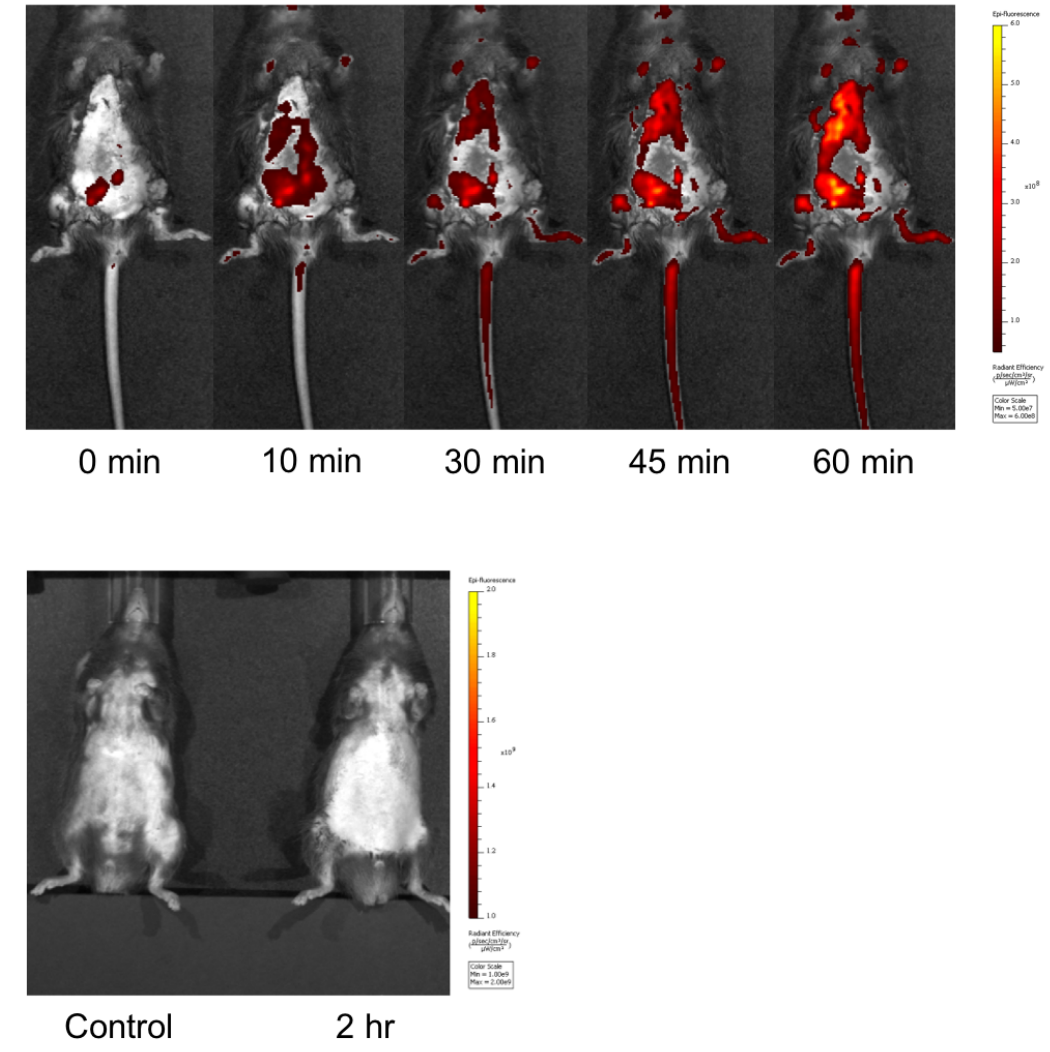

Figure 3.13 Localization of MDP-rhodamine *in vivo*.

Fluorescence of intraperitoneally injected rhodamine-labelled MDP in anaesthetized WT mice.

(Figure 3.14). Results were confirmed in multiple cohorts of mice from different parents. Body mass for WT mice that received saline or MDP was assessed in both diet groups (Figure 3.15). MDP treatment did not affect whole-body adipose tissue volume as determined by CT scanning of anaesthetized mice (Figure 3.16). Quantities of hepatic and muscle triglycerides, masses of various metabolic tissues and spleen, and circulating levels of bacterial endotoxin were unaffected by this MDP treatment regime (Figures 3.17-3.19).

3.2.2 Chronic NOD2 activation improves indices of glucose metabolism during HFD-induced obesity

To investigate the metabolic effects of NOD2 activation with MDP during the onset of diet-induced metabolic disease, the “prevention-style” *in vivo* experimental HFD model was used (Figure 3.14). In control diet-fed animals, NOD2 activation with MDP (100 µg/day, 4 days per week for 4-5 weeks) did not alter glucose tolerance (Figure 3.20). In HFD-fed animals, this MDP treatment protocol improved glucose and insulin tolerance (Figures 3.21-3.22).

Subsequently, tissue-specific responses that could explain the insulin-sensitizing effects of MDP were tested using several *in vivo* experimental approaches. In order to model the response to a bolus of

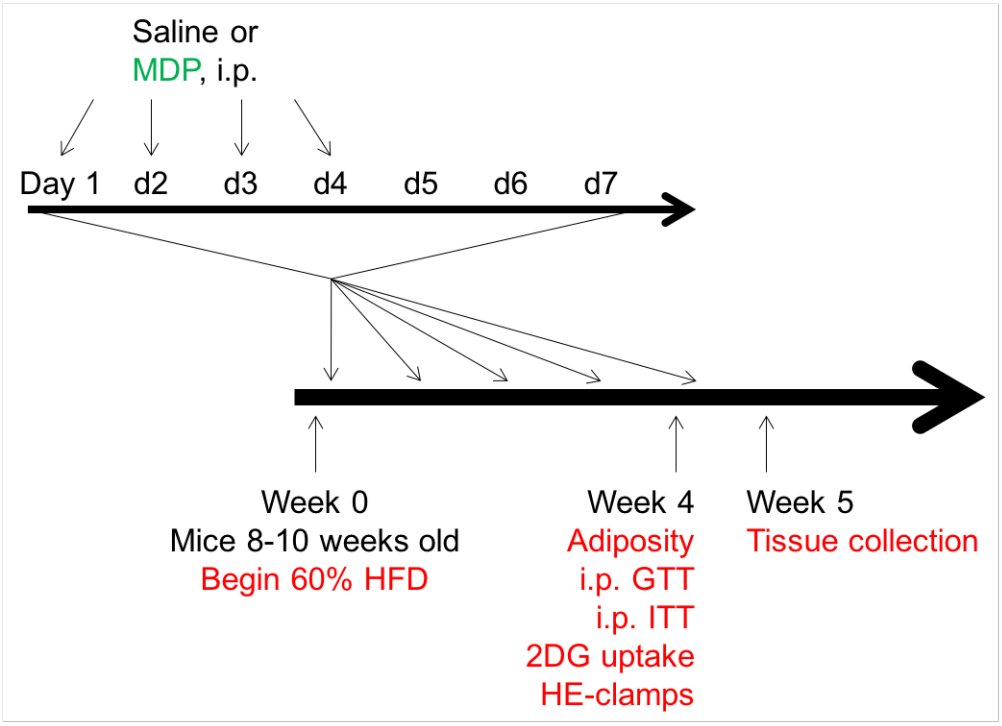

Figure 3.14 Experimental design for chronic MDP administration at the inception of HFD.

Mice were fed an obesity-causing HFD and received saline or 100 µg MDP i.p. 4 days/week, for a total of 5 weeks.

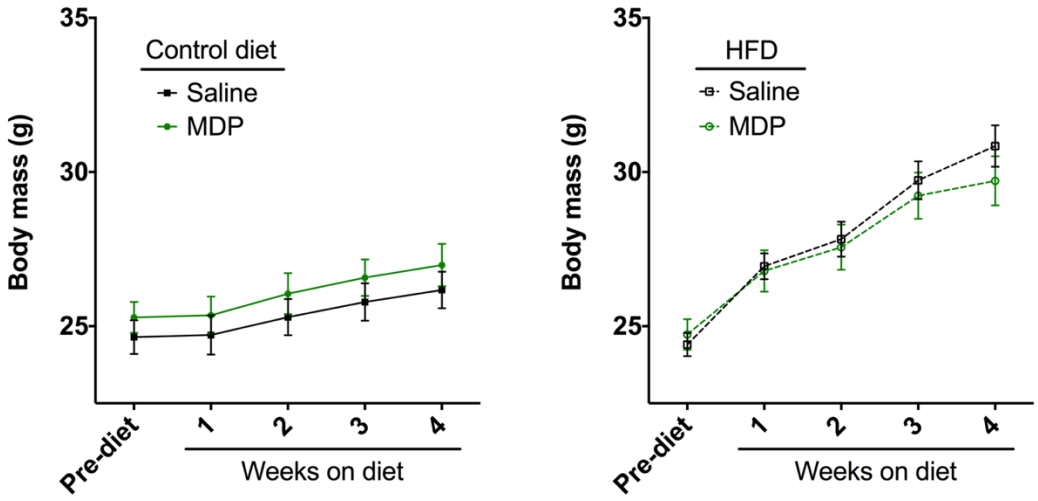

Figure 3.15 Body mass of WT mice chronically treated with MDP.

Body mass over time of control diet- or HFD-fed WT mice that received saline or MDP for 4 weeks. n = 10 mice for each group. Values are mean ± SEM.

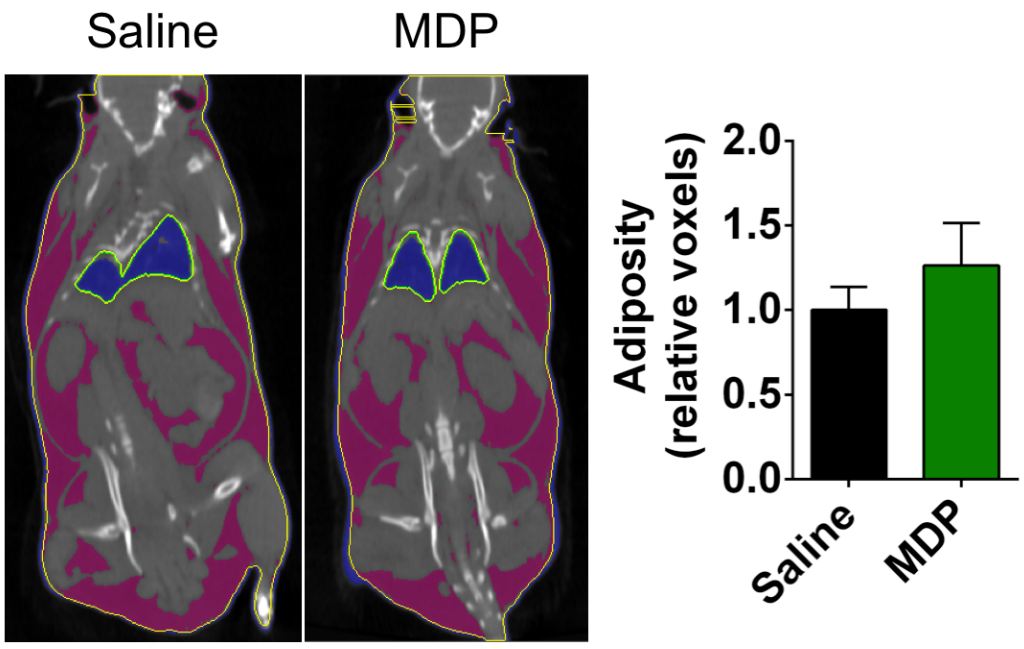

Figure 3.16 Adiposity of WT mice chronically treated with MDP.

Computed tomography representative images and quantified adiposity of HFD-fed WT mice that received saline or MDP for 4 weeks. n = 6 mice for each group. Values are mean ± SEM.

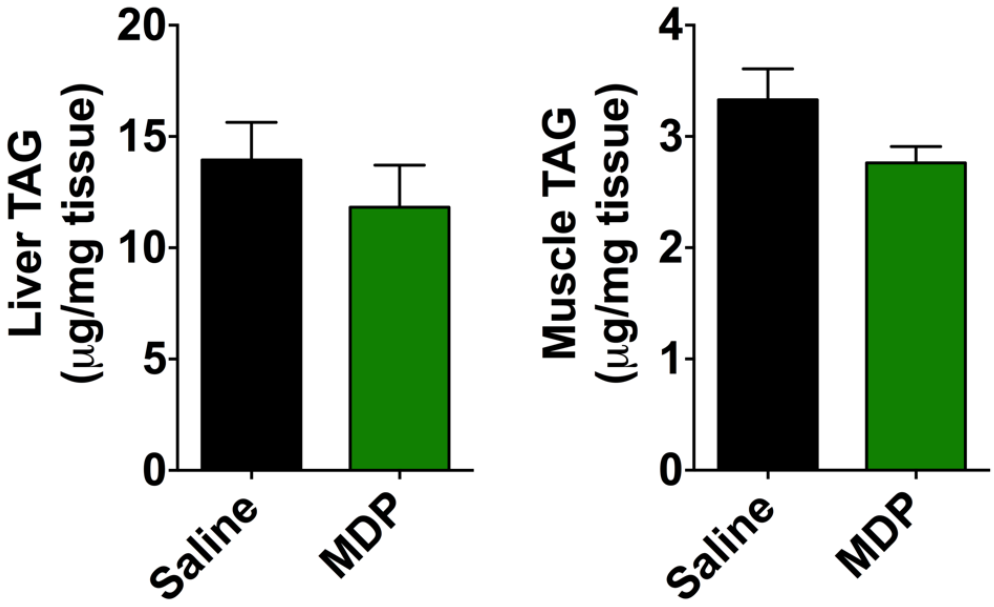

Figure 3.17 Tissue lipid content of WT mice chronically treated with MDP.

Liver and muscle triglyceride content of HFD-fed WT mice that received saline or MDP for 5 weeks. n = 8-10 mice for each group. Values are mean ± SEM.

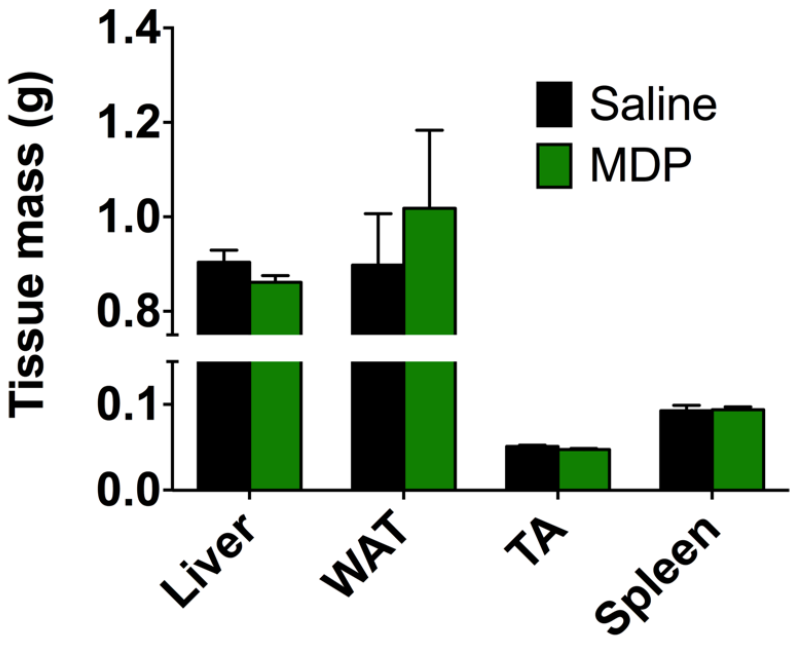

Figure 3.18 Tissue mass of WT mice chronically treated with MDP.

Liver, white adipose, tibialis anterior, and spleen masses of HFD-fed WT mice that received saline or MDP for 5 weeks. n = 5-6 mice for each group. Values are mean ± SEM.

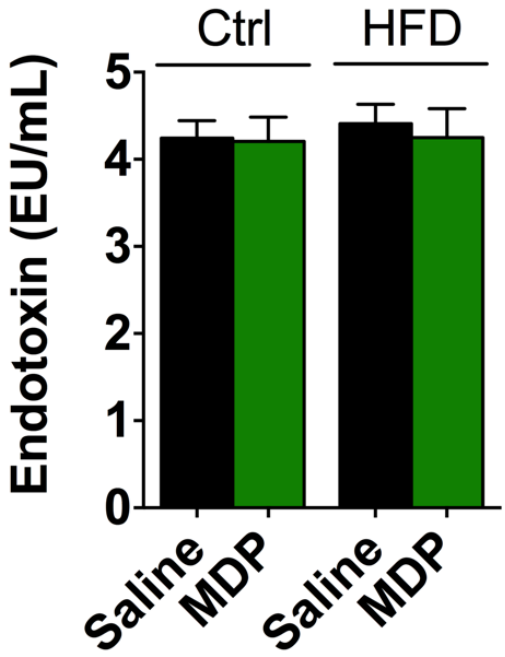

Figure 3.19 Endotoxemia of WT mice chronically treated with MDP.

Serum endotoxin content of control diet- or HFD-fed WT mice that received saline or MDP for 5 weeks. n = 10 mice for each group. Values are mean ± SEM.

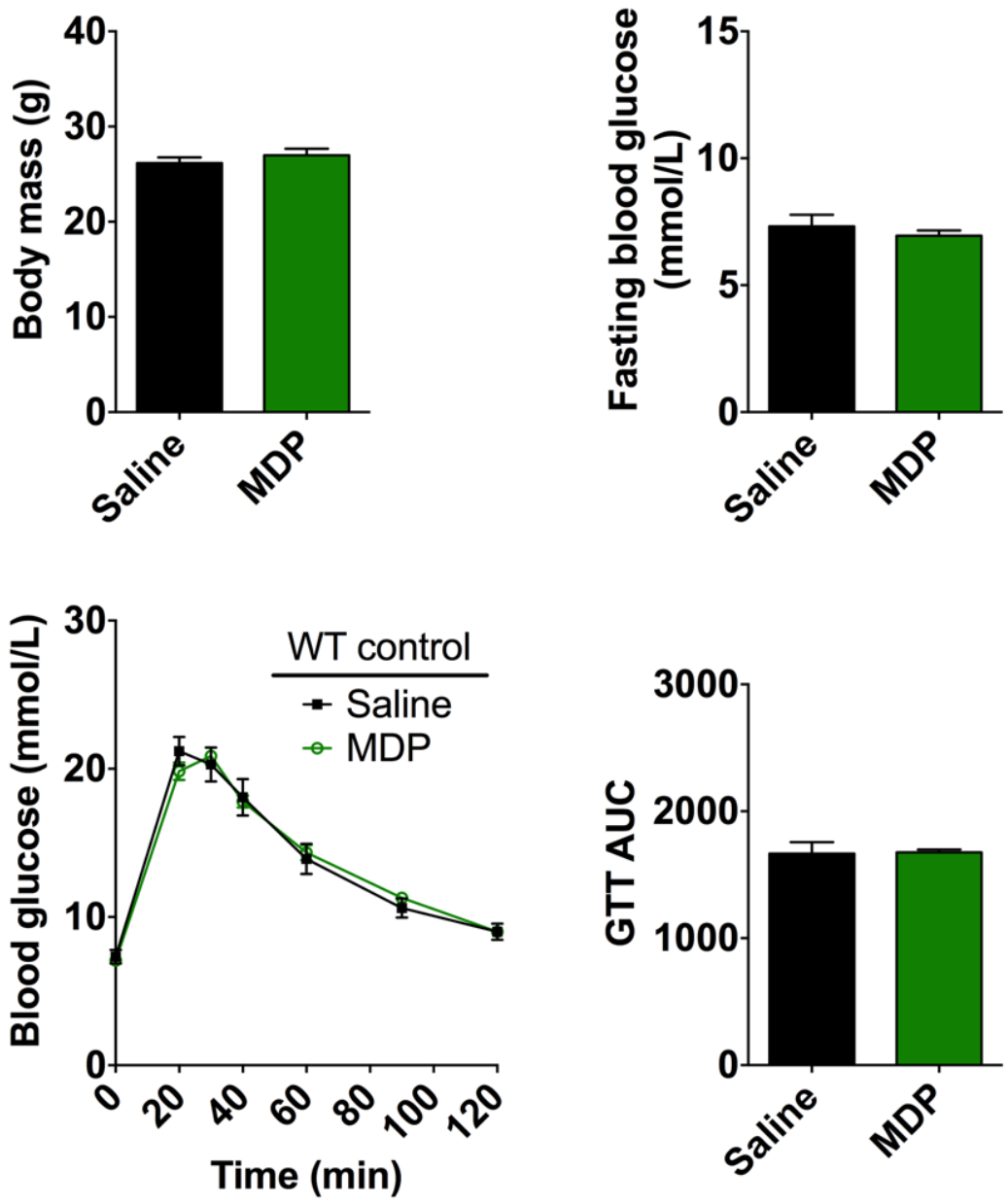

Figure 3.20 Glucose metabolism of WT mice chronically treated with MDP.

Body mass, fasting blood glucose, and glucose tolerance test (2 g/kg) of control diet-fed WT mice that received saline or MDP for 4 weeks. n = 9-10 mice for each group. Values are mean ± SEM.

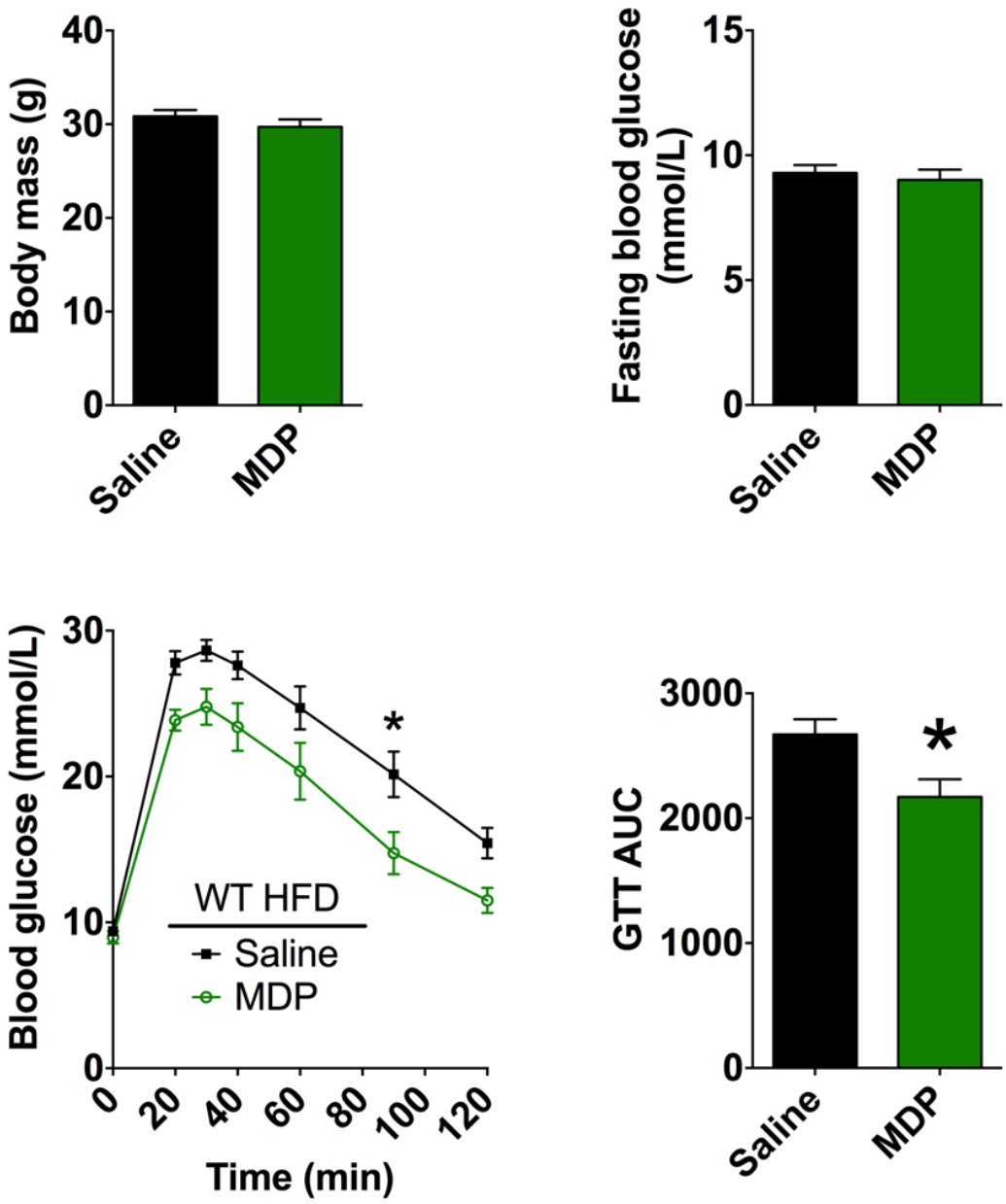

Figure 3.21 Glucose metabolism of WT mice chronically treated with MDP.

Body mass, fasting blood glucose, and glucose tolerance test (2 g/kg) of HFD-fed WT mice that received saline or MDP for 4 weeks. n = 8-9 mice for each group. Values are mean ± SEM. * indicates a significant difference between groups, as determined by two-way ANOVA (line graph) or unpaired two-tailed *t*-test (AUC graph) on normally distributed data.

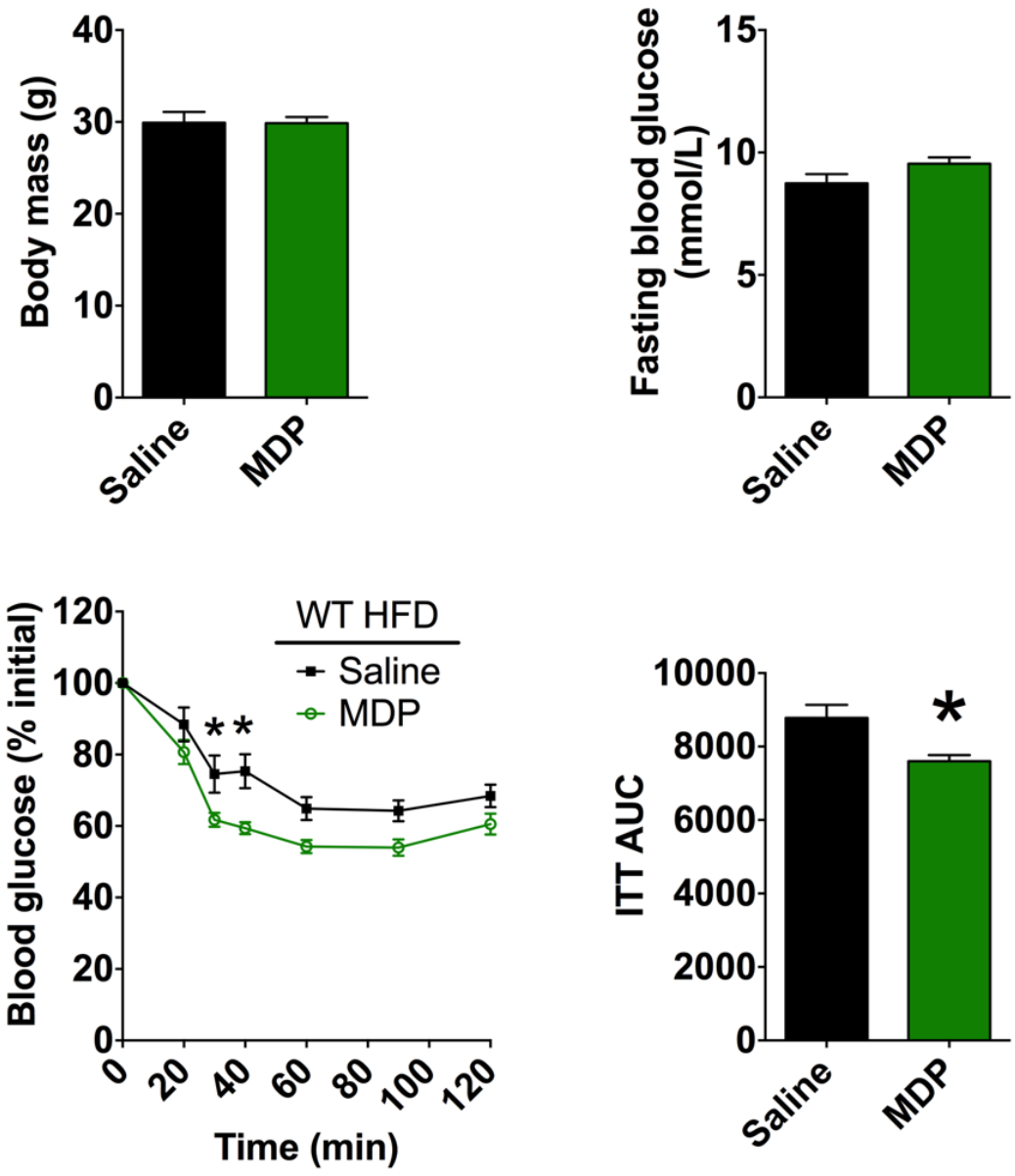

Figure 3.22 Insulin tolerance of WT mice chronically treated with MDP.

Body mass, fasting blood glucose, and insulin tolerance test (1 IU/kg) of HFD-fed WT mice that received saline or MDP for 4 weeks. n = 9-10 mice for each group. Values are mean ± SEM. * indicates a significant difference between groups, as determined by two-way ANOVA (line graph) or unpaired two-tailed *t*-test (AUC graph) on normally distributed data.

elevated insulin, 2 IU/kg of insulin was injected and uptake of 2DG in gonadal white adipose tissue 20 minutes after insulin injection was tested. MDP treatment did not alter insulin-stimulated 2DG uptake during HFD-feeding in WT mice (Figure 3.23). Hyperinsulinemic-euglycemic clamps revealed that MDP treatment during HFD-feeding improved liver insulin sensitivity as demonstrated by the increased insulin-suppression of HGP in MDP-treated WT mice (Figure 3.24). The glucose infusion rate required to maintain euglycemia during a hyperinsulinemic state (GINF), the GDR into peripheral tissues, and fasted and clamped serum levels of NEFA were not significantly altered by MDP treatment (Figure 3.24).

To probe the pathway specificity of MDP treatment, multiple knockout mouse strains were treated according to the “prevention-style” HFD-feeding model (Figure 3.14). In both *Nod2*$^{-/-}$ and *Ripk2*$^{-/-}$ animals, MDP treatment did not alter glucose tolerance (Figures 3.25-3.26). MDP did not improve glucose tolerance in mice with a mutant form of the TLR4 LPS receptor. In fact, these C3H/HeJ mice treated with MDP had increased fasting blood glucose and glucose intolerance (Figure 3.27). This result prompted us to test the relationship between MDP and LPS in later sections of this thesis.

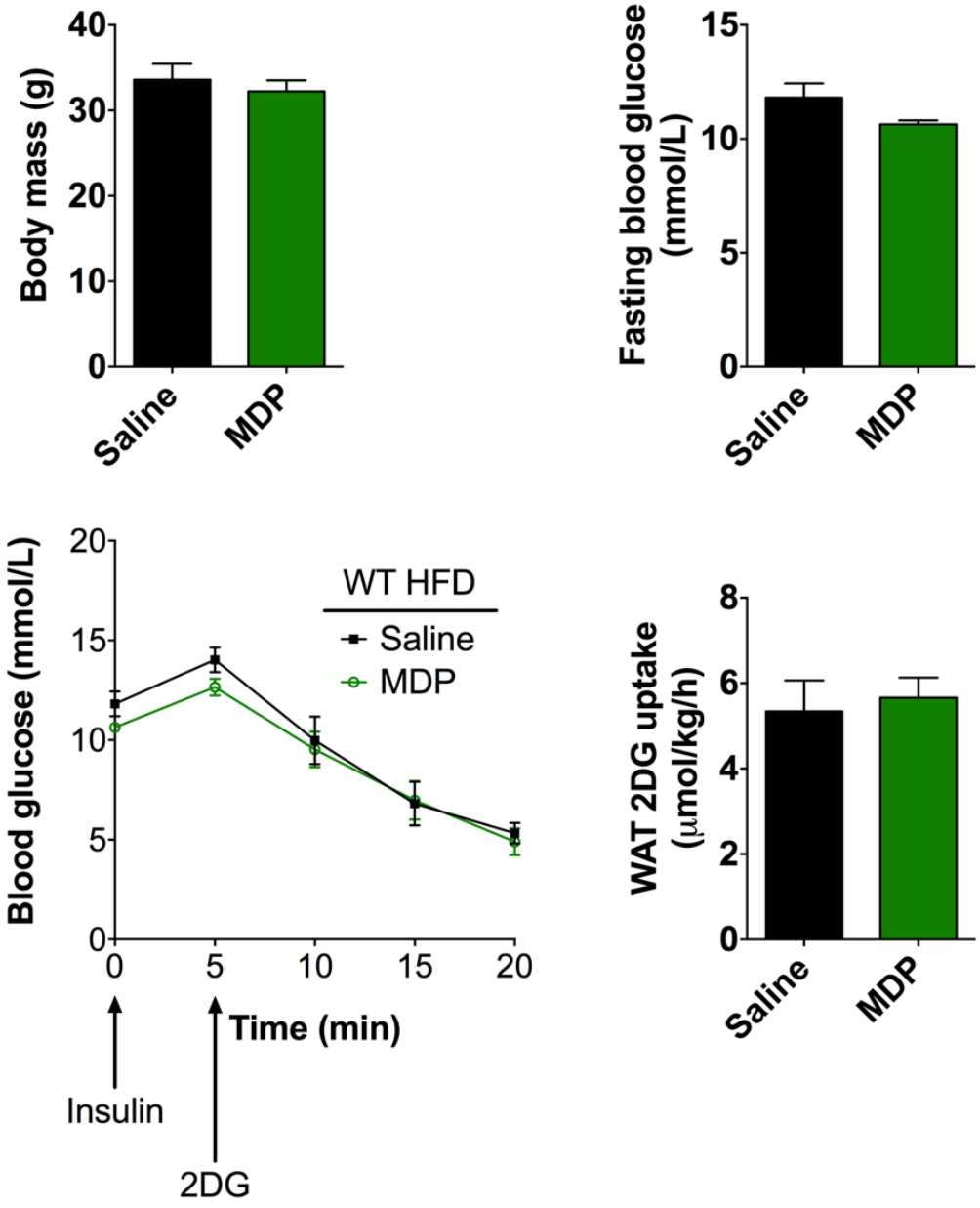

Figure 3.23 Adipose tissue insulin sensitivity in WT mice chronically treated with MDP.

Body mass, fasting blood glucose, insulin tolerance (2 IU/kg) and 2-[1,2-^{3}H (N)]-Deoxy-D-glucose (2DG) uptake in white adipose tissue of HFD-fed WT mice that received saline or MDP for 4 weeks. n = 7-8 mice for each group. Values are mean ± SEM.

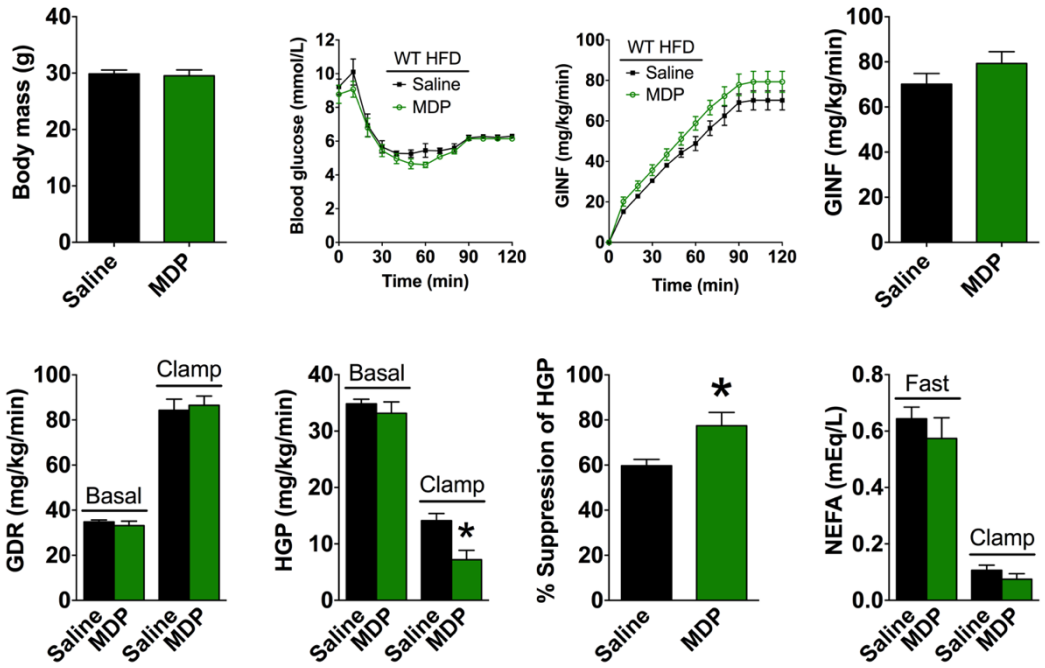

Figure 3.24 Whole-body and liver insulin sensitivity in WT mice chronically treated with MDP.

Body mass, blood glucose, glucose infusion rate (GINF), glucose disposal rate (GDR), hepatic glucose production (HGP), insulin-mediated suppression of HGP, and serum non-esterified fatty acids (NEFA) during the hyperinsulinemic-euglycemic clamp experiment of HFD-fed WT mice that received saline or MDP for 4 weeks. n = 5 mice for each group. Values are mean ± SEM. * indicates a significant difference between groups, as determined by Mann-Whitney U test on non-normally distributed data.

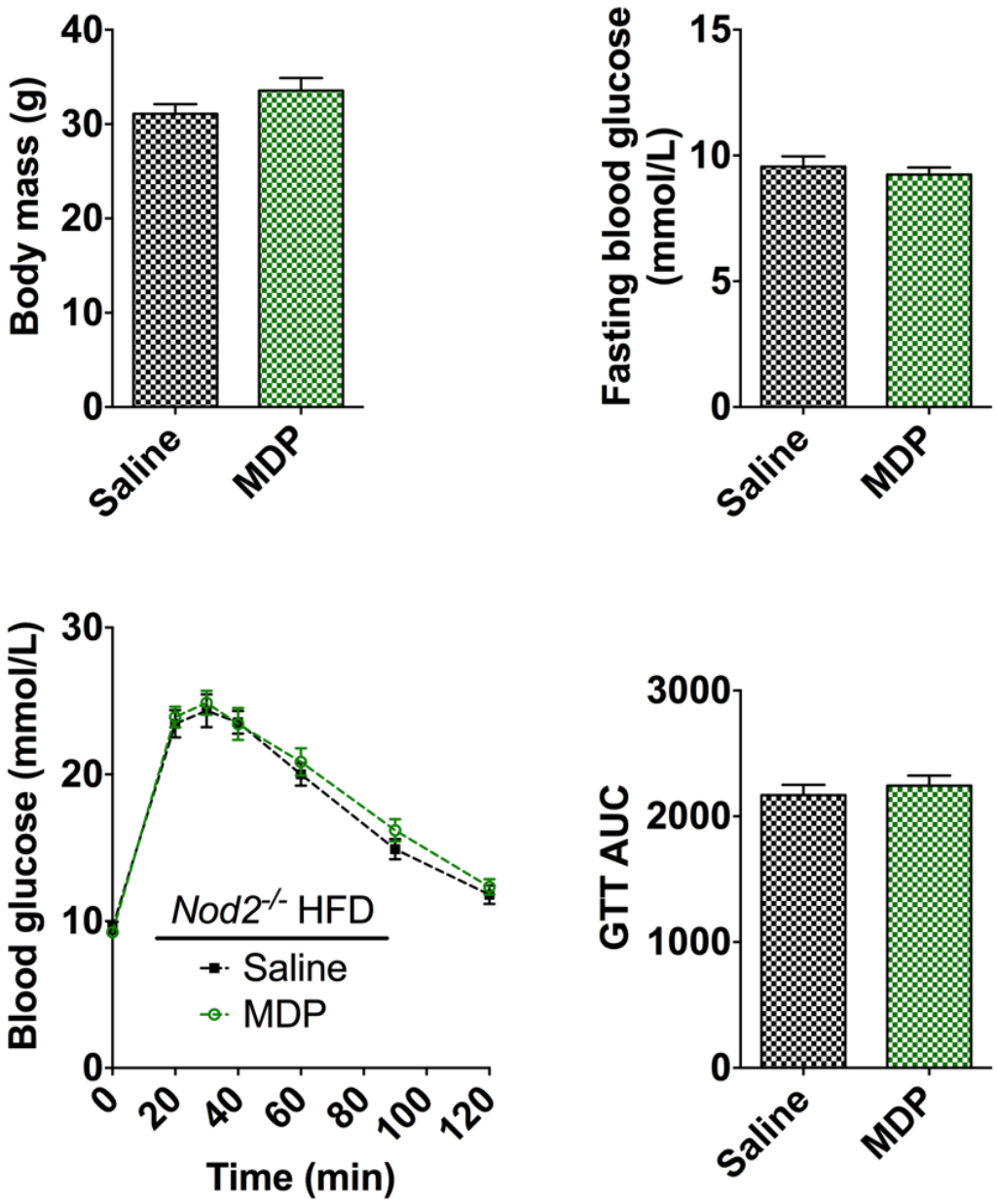

Figure 3.25 Glucose metabolism of *Nod2*$^{-/-}$ mice chronically treated with MDP.

Body mass, fasting blood glucose, and glucose tolerance test (2 g/kg) of HFD-fed *Nod2*$^{-/-}$ mice that received saline or MDP for 4 weeks. n = 7-9 mice for each group. Values are mean ± SEM.

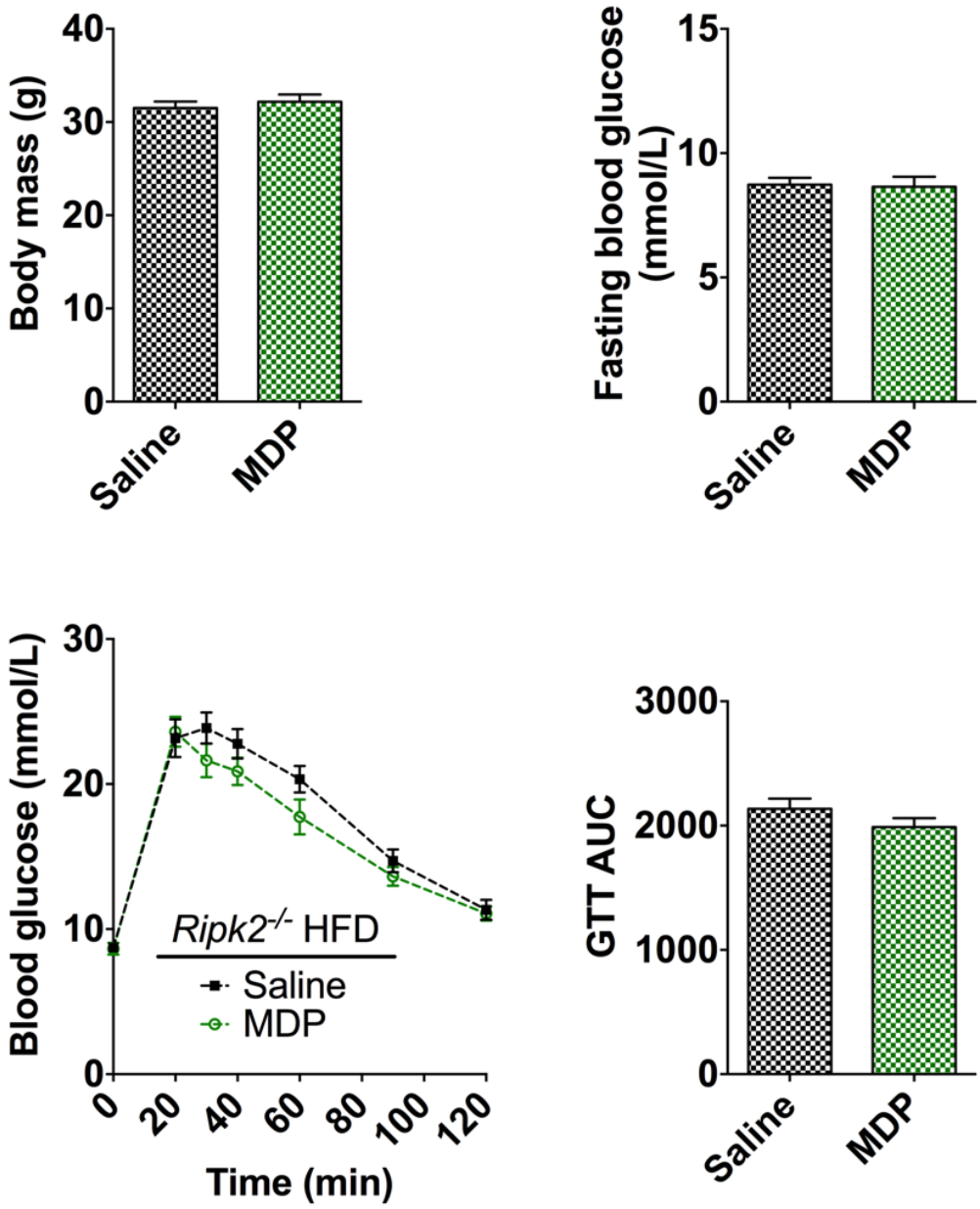

Figure 3.26 Glucose metabolism of *Ripk2*$^{-/-}$ mice chronically treated with MDP.

Body mass, fasting blood glucose, and glucose tolerance test (2 g/kg) of HFD-fed *Ripk2*$^{-/-}$ mice that received saline or MDP for 4 weeks. n = 10-11 mice for each group. Values are mean ± SEM.

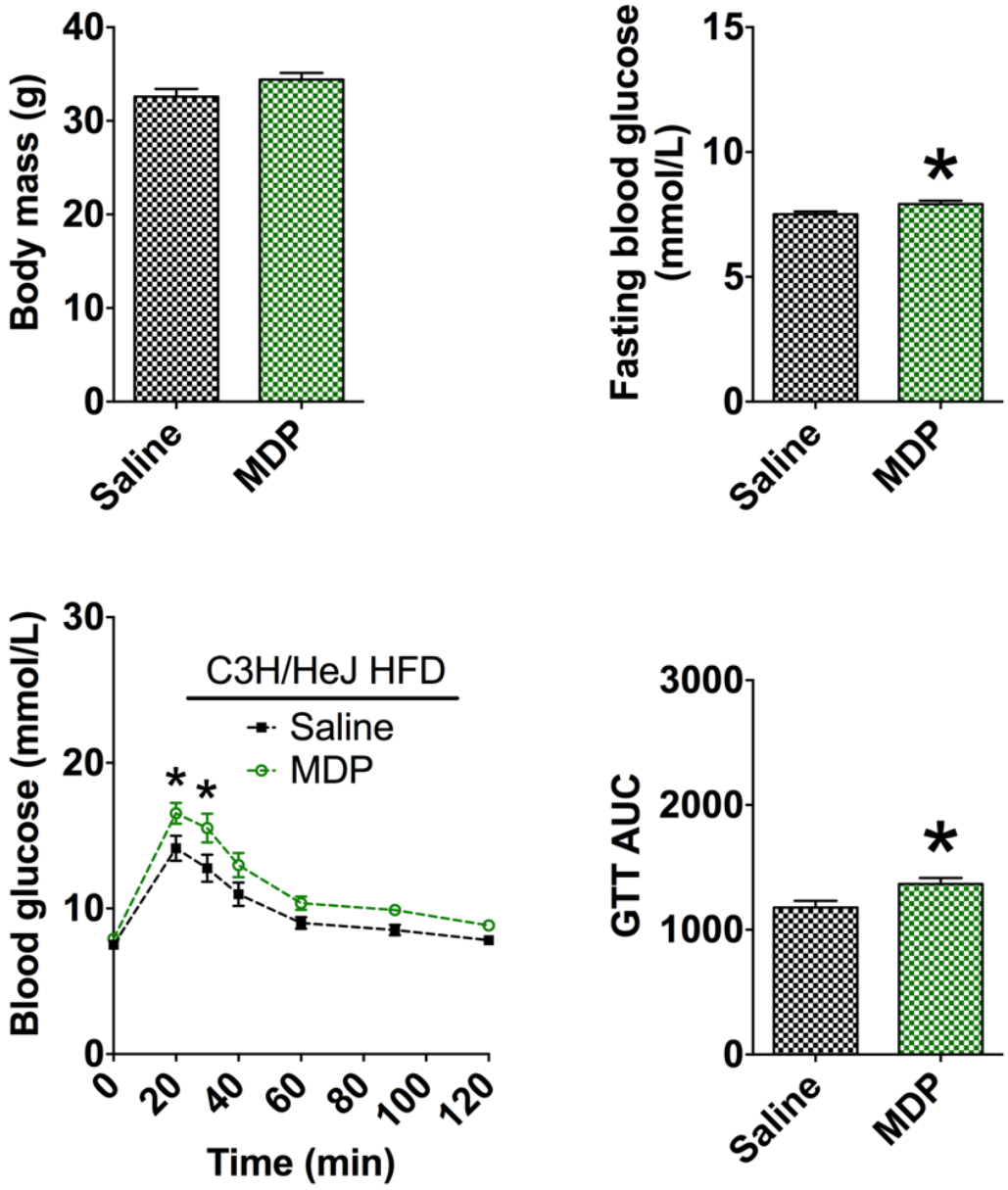

Figure 3.27 Glucose metabolism of C3H/HeJ mice chronically treated with MDP.

Body mass, fasting blood glucose, and glucose tolerance test (2 g/kg) of HFD-fed C3H/HeJ (LPS-receptor mutant) mice that received saline or MDP for 4 weeks. n = 12-13 mice for each group. Values are mean ± SEM. * indicates a significant difference between groups, as determined by two-way ANOVA (line graph) or unpaired two-tailed *t*-test (fasting blood glucose and AUC graphs) on normally distributed data.

3.2.3 Chronic NOD2 activation lowers liver and adipose tissue inflammation, but increases muscle inflammation during HFD-induced obesity

NOD2 is an innate immune protein that contributes to inflammatory responses upon activation. Acute stimulation of NOD2 activates the transcription factor NF-κB, which transports to the cell nucleus to mediate the upregulation of pro-inflammatory genes (327). In contrast, chronic activation of NOD2 *prior* to another inflammatory insult is known to dampen the magnitude of the subsequent inflammatory response (302,305,328). The dampened second immune response is often referred to as immune tolerance. The opposite of “immune tolerance” is immune synergy, where simultaneous or combined stimulation of immune signaling pathways and receptors results in an enhanced inflammatory response (329,330). To further investigate the role of NOD2 as an immunomodulator, the tolerance versus synergistic aspects of MDP treatment were tested during the additional stress of diet-induced obesity (or low-level endotoxin in later sections of this thesis). It was not known how NOD2 activation would interact with chronic low-level inflammation during diet-induced obesity, but our previous work supported the hypothesis that NOD2 would have a protective role (316). Our data shows that chronic NOD2 activation with MDP injections during the development diet-induced obesity in mice (a source of additional inflammation) (Figure 3.14) promoted immune

tolerance primarily in the adipose tissue. NF-κB activity in MDP treated mice was unchanged in liver, but significantly lower in gonadal white adipose tissue of HFD-fed mice (Figure 3.28). We next evaluated the downstream effects of chronic NOD2 activation beyond NF-κB-mediated inflammation.

In the livers of HFD-fed mice, chronic MDP treatment decreased the expression of genes classically categorized as pro-inflammatory such as *Ccl2* (coding for monocyte chemoattractant protein 1), *Cxcl10*, *Nos2*, and *Tnf*, while genes classically categorized as anti-inflammatory were not affected (Figure 3.29). Hepatic expression of immune cell markers was largely unchanged by chronic NOD2 activation, except for an increased expression of the monocyte marker *Itgam* (coding integrin alpha M; important in immune cell migration and adhesion factor (331)) (Figure 3.30, top). Hepatic expression of the gene encoding the pattern recognition receptor TLR4 was significantly increased by NOD2 activation (Figure 3.30, bottom-left). Chronic MDP treatment during obesity did not alter hepatic expression of selected metabolic transcripts (Figure 3.30, bottom-right).

In gonadal white adipose tissue, chronic MDP treatment decreased the expression of pro-inflammatory genes such as *Ccl2*, *Cxcl9*, *Cxcl10*, *Il1b*, and *Tnf*, (Figure 3.31). Anti-inflammatory genes, such as *Arg1*, *Il4*, and *Il10*, were also decreased by chronic NOD2 activation (Figure 3.31). The expression of several genes coding for immune cell markers was decreased in adipose tissue after chronic MDP treatment, including *Ccr7*, *Cd3e*, *Cd4*,

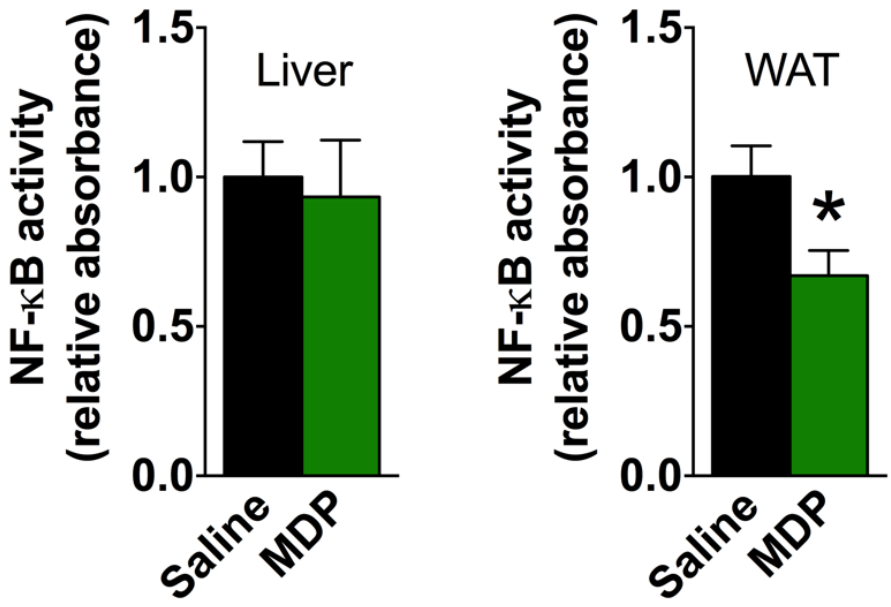

Figure 3.28 Tissue NF-κB activity of WT mice chronically treated with MDP.

Liver and white adipose NF-κB activity of HFD-fed WT mice that received saline or MDP for 5 weeks. n = 9-10 mice for each group. Values are mean ± SEM. * indicates a significant difference between groups, as determined by unpaired two-tailed *t*-test on normally distributed data.

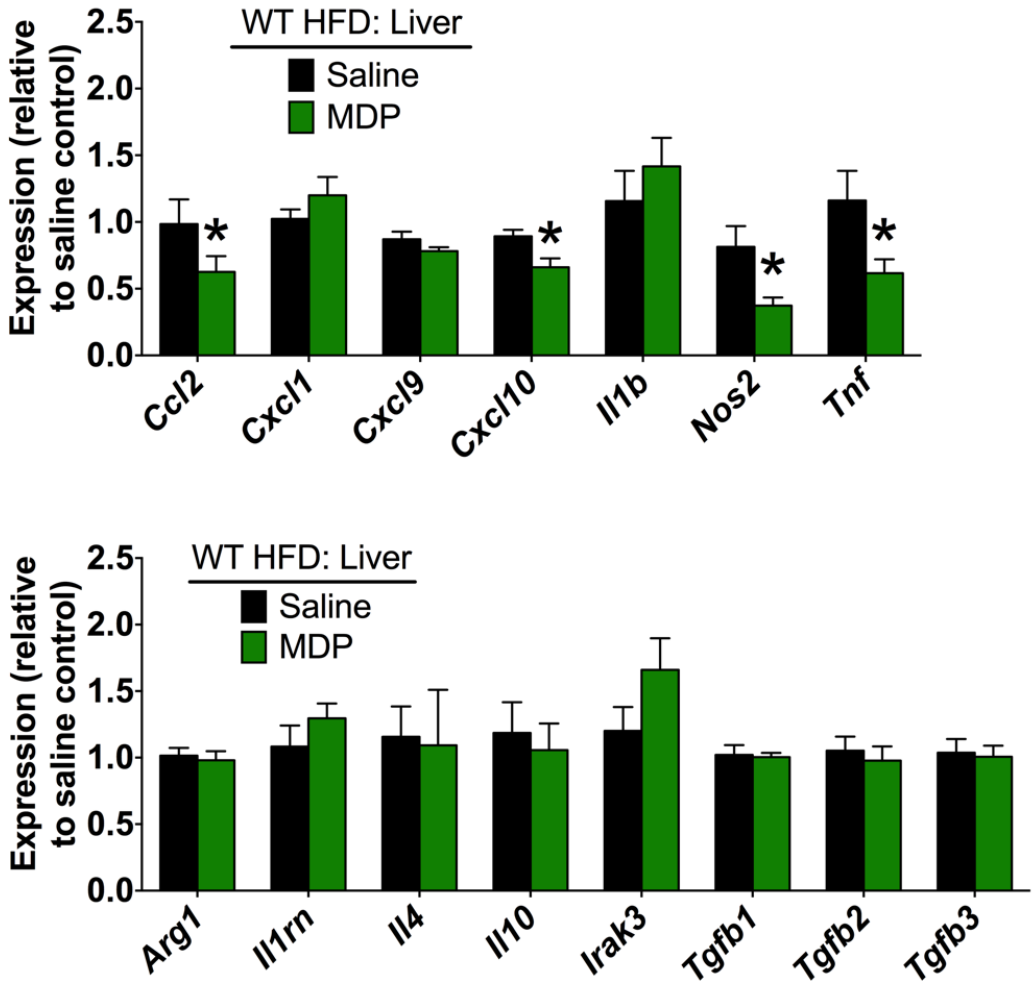

Figure 3.29 Liver inflammation of WT mice chronically treated with MDP.

Liver inflammatory gene expression of HFD-fed WT mice that received saline or MDP for 5 weeks. n = 9-10 mice for each group. Values are mean ± SEM. * indicates a significant difference between groups, as determined by unpaired two-tailed *t*-test on normally distributed data or by Mann-Whitney *U* test on non-normally distributed data.

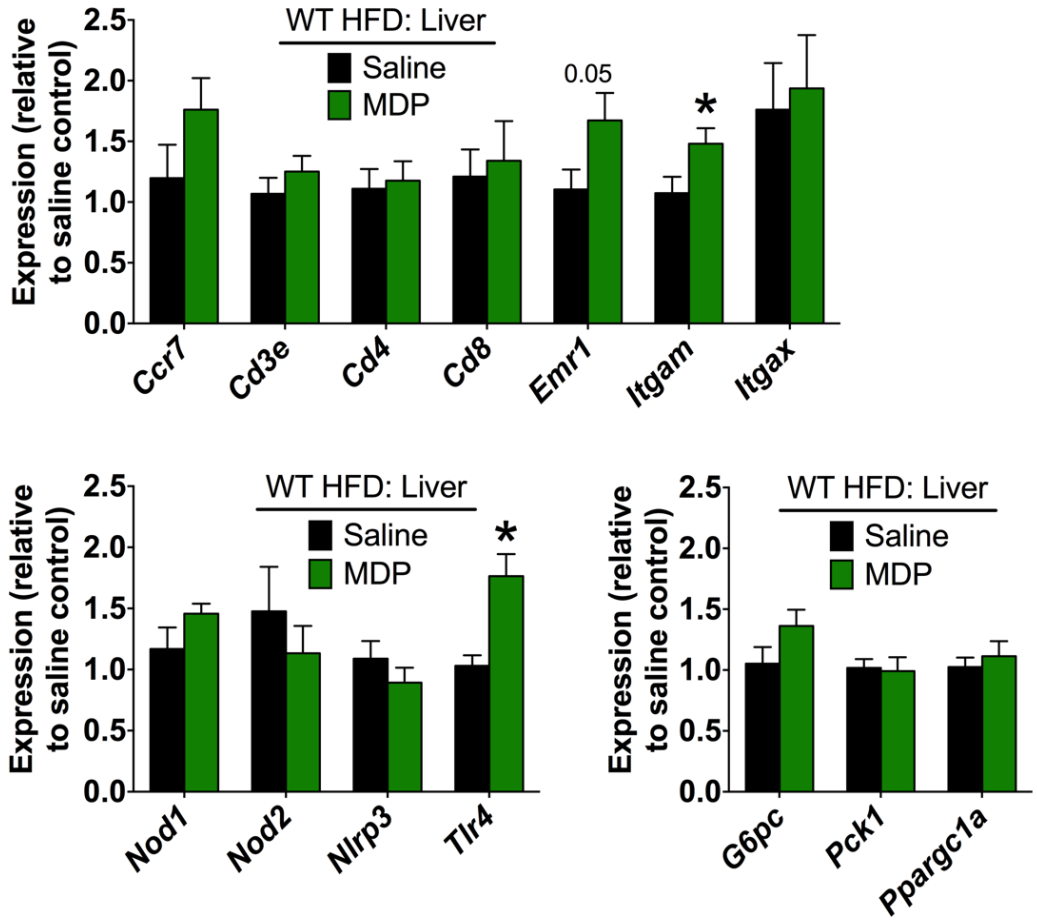

Figure 3.30 Liver inflammation of WT mice chronically treated with MDP.

Liver inflammatory and select metabolic gene expression of HFD-fed WT mice that received saline or MDP for 5 weeks. n = 9-10 mice for each group. Values are mean ± SEM. * indicates a significant difference between groups, as determined by unpaired two-tailed *t*-test on normally distributed data.

Cd8, and *Emr1* (Figure 3.32, top). In addition, genes coding for pattern recognition receptors NOD1, nucleotide oligomerization domain-like receptor, pyrin domain-containing 3 (NLRP3), and TLR4 were significantly decreased in adipose tissue by NOD2 activation (Figure 3.32, bottom-left). Chronic MDP treatment during obesity did not alter gonadal white adipose tissue expression of selected metabolic transcripts (Figure 3.32, bottom-right).

In contrast to effects in liver and fat, chronic MDP treatment increased muscle expression of pro-inflammatory genes such as *Ccl2*, *Cxcl9*, and *Cxcl10* (Figure 3.33, top). The expression of several genes coding for immune cell markers was also increased in response to chronic MDP treatment, including *Ccr7*, *Cd4*, *Cd8*, and *Emr1* (Figure 3.33, bottom). In addition, *Nod2* expression was significantly increased by NOD2 activation (Figure 3.33, bottom). These results are consistent with previous findings from our previous publications showing that MDP-induced muscle cell-autonomous inflammatory responses (332).

To determine if chronic MDP treatment had significant effects beyond metabolic tissues, mouse spleens were assessed for changes in inflammatory gene expression. Only minor decreases in gene expression were observed, where MDP-treated mice had lower levels of splenic *Cxcl1* and *Il1b* (Figure 3.34). As a further control to quantify the systemic effects of NOD2 activation, mouse serum was analyzed for the presence of

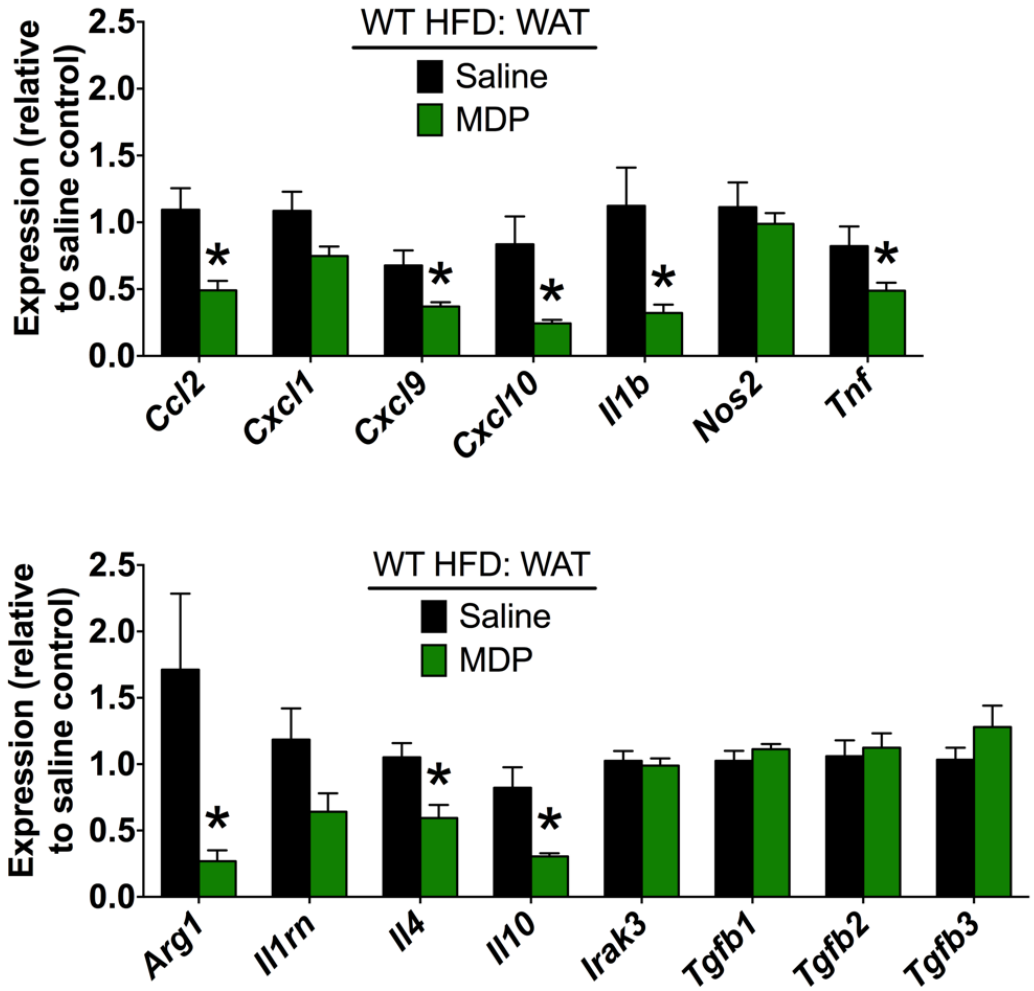

Figure 3.31 Adipose inflammation of WT mice chronically treated with MDP.

White adipose inflammatory gene expression of HFD-fed WT mice that received saline or MDP for 5 weeks. n = 9-10 mice for each group. Values are mean ± SEM. * indicates a significant difference between groups, as determined by unpaired two-tailed *t*-test on normally distributed data or by Mann-Whitney *U* test on non-normally distributed data.

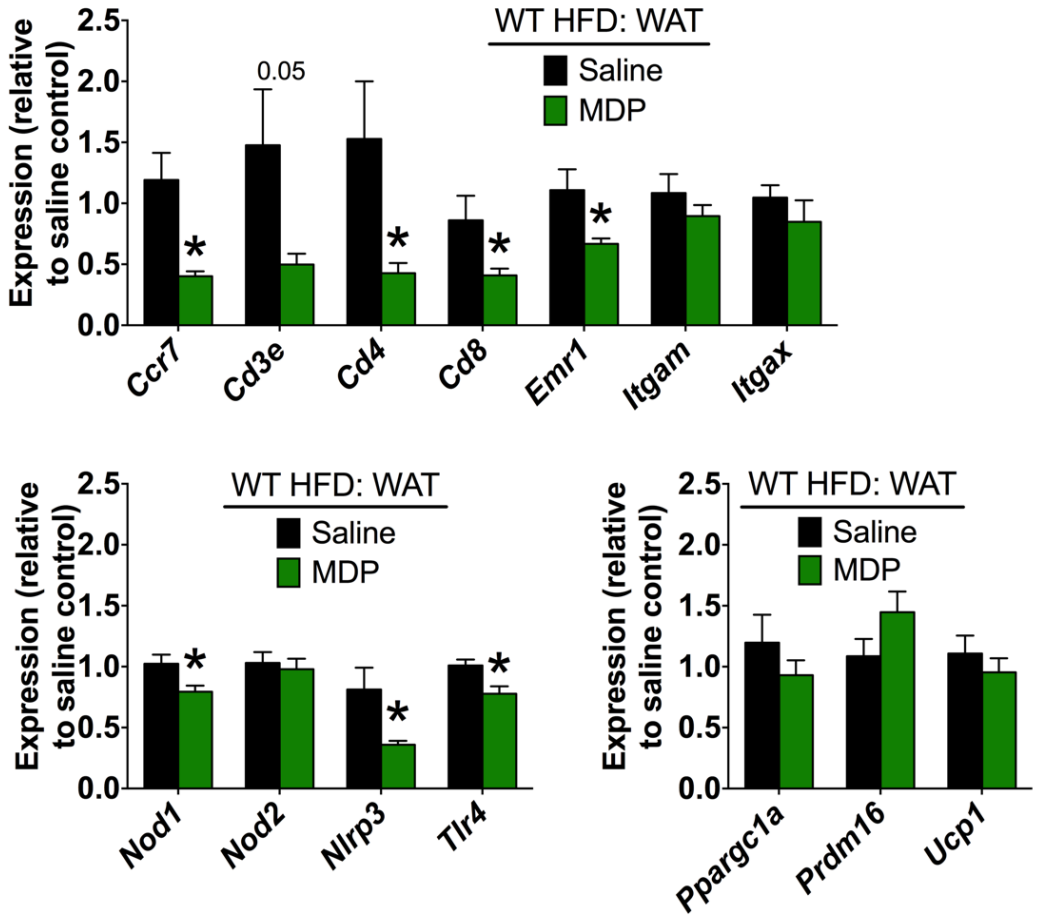

Figure 3.32 Adipose inflammation of WT mice chronically treated with MDP.

White adipose inflammatory and select metabolic gene expression of HFD-fed WT mice that received saline or MDP for 5 weeks. n = 9-10 mice for each group. Values are mean ± SEM. * indicates a significant difference between groups, as determined by unpaired two-tailed *t*-test on normally distributed data.

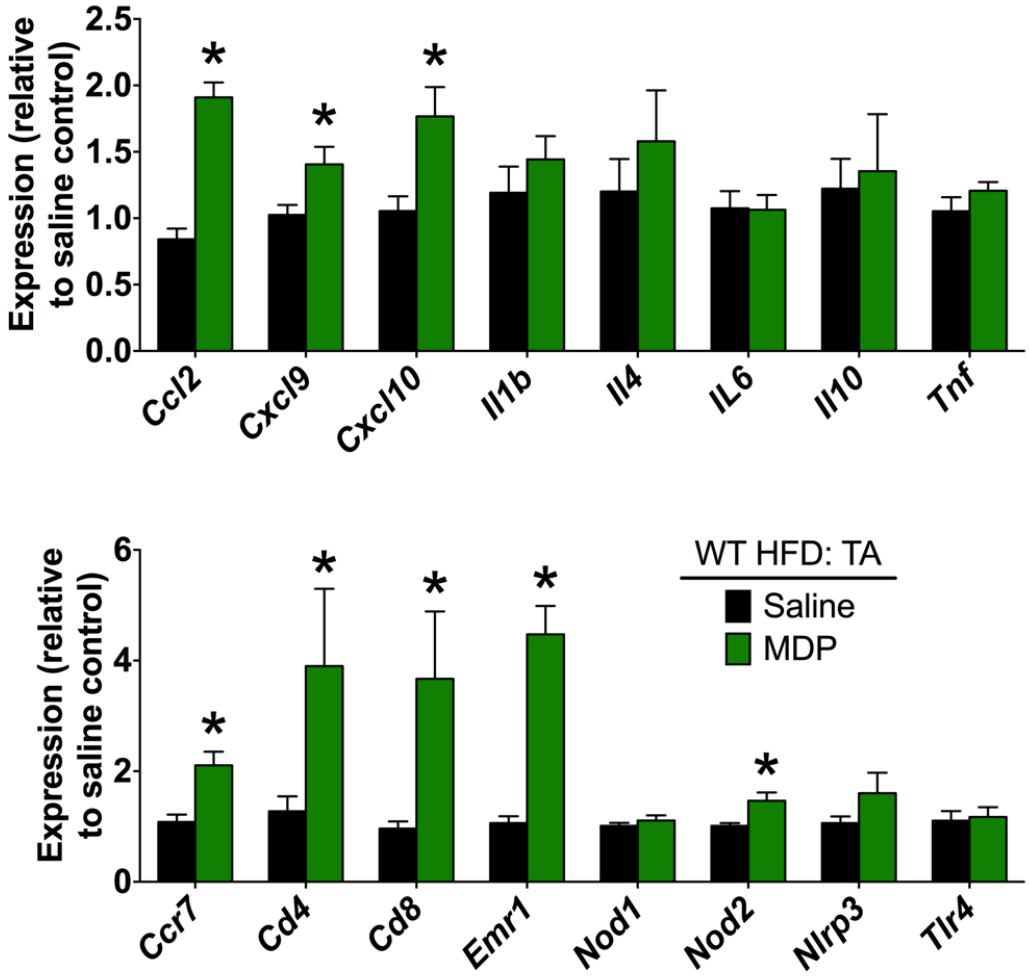

Figure 3.33 Muscle inflammation of WT mice chronically treated with MDP.

Tibialis anterior inflammatory gene expression of HFD-fed WT mice that received saline or MDP for 5 weeks. n = 8-10 mice for each group. Values are mean ± SEM. * indicates a significant difference between groups, as determined by unpaired two-tailed *t*-test on normally distributed data or by Mann-Whitney *U* test on non-normally distributed data.

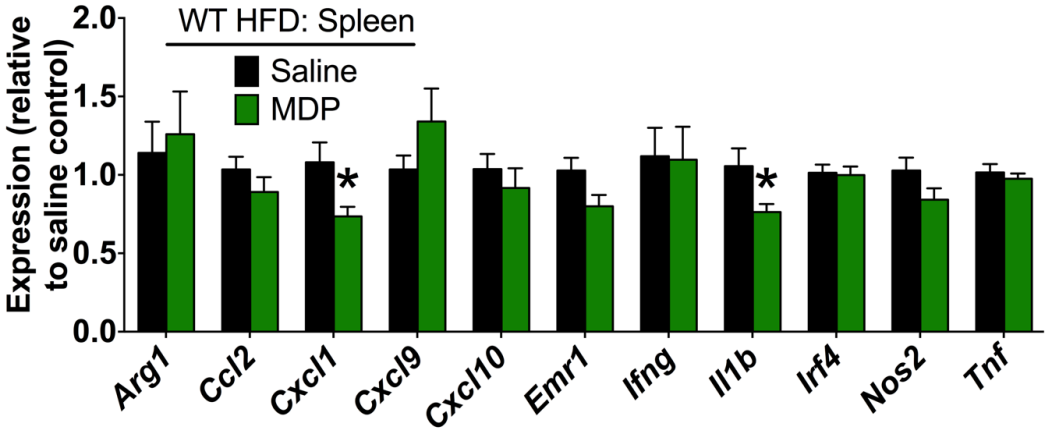

Figure 3.34 Spleen inflammation of WT mice chronically treated with MDP.

Spleen inflammatory gene expression of HFD-fed WT mice that received saline or MDP for 5 weeks. n = 9-10 mice for each group. Values are mean ± SEM. * indicates a significant difference between groups, as determined by unpaired two-tailed *t*-test on normally distributed data.

circulating cytokines and no significant changes between control and treated animals were observed (Figure 3.35).

3.2.4 Chronic NOD2 activation improves glucose metabolism in genetic obesity

To determine whether the insulin-sensitizing effects of NOD2 activation were dependent on dietary fat content or some other effect related to HFD-feeding, hyperphagic leptin-deficient (*ob/ob*) mice were fed a control-diet and treated with a similar “prevention-style” MDP model (Figure 3.36). After 2 weeks of MDP treatment (8 total injections), NOD2-activation in *ob/ob* mice resulted in improved glucose tolerance compared to vehicle-injected (control) *ob/ob* animals (Figure 3.37). Insulin (4 IU/kg)-stimulated uptake of 2DG in gonadal white adipose tissue was not affected by MDP treatment in *ob/ob* mice (Figure 3.38). These data demonstrating improved glucose tolerance in hyperphagic *ob/ob* mice, along with similar results in HFD-fed WT mice, but not control diet-fed WT mice, suggest that chronic MDP treatment improves glucose homeostasis in mice during obesity, regardless of the source (diet or genetic) of obesity.

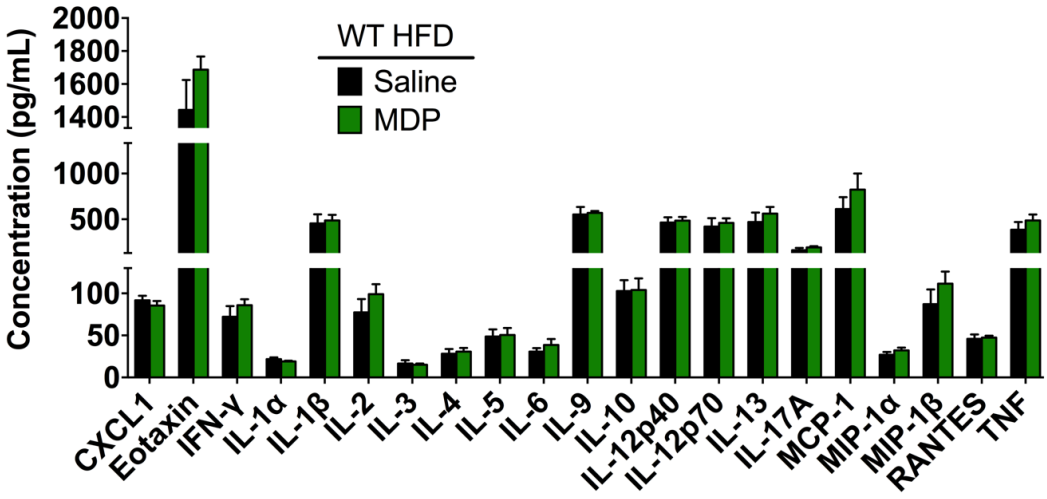

Figure 3.35 Systemic inflammation of WT mice chronically treated with MDP.

Serum cytokines of HFD-fed WT mice that received saline or MDP for 5 weeks. n = 8-10 mice for each group. Values are mean ± SEM.

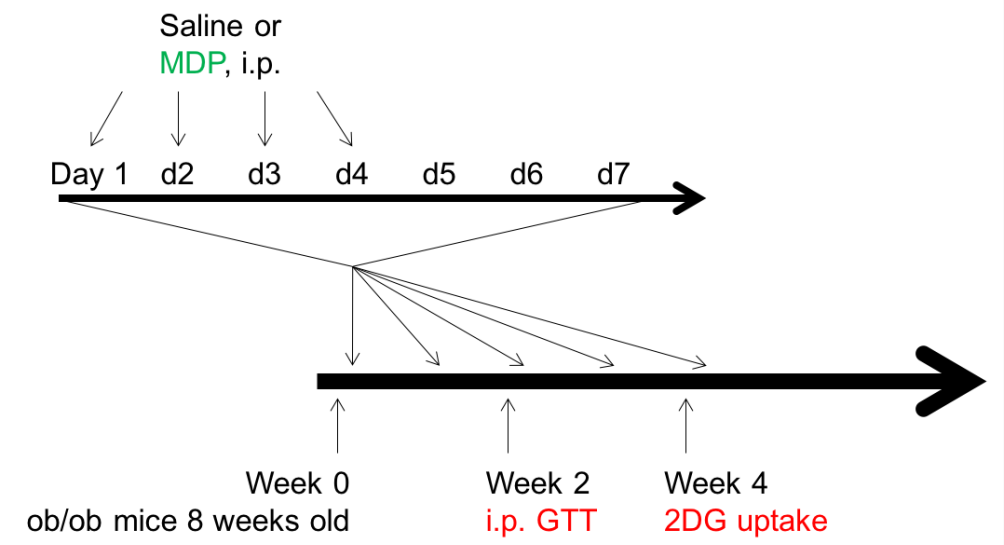

Figure 3.36 Experimental design for MDP administration in genetically obese (*ob/ob*) mice.

Leptin-deficient *ob/ob* mice were fed a control-diet and received saline or 100 µg MDP i.p. 4 days/week, for a total of 4 weeks.

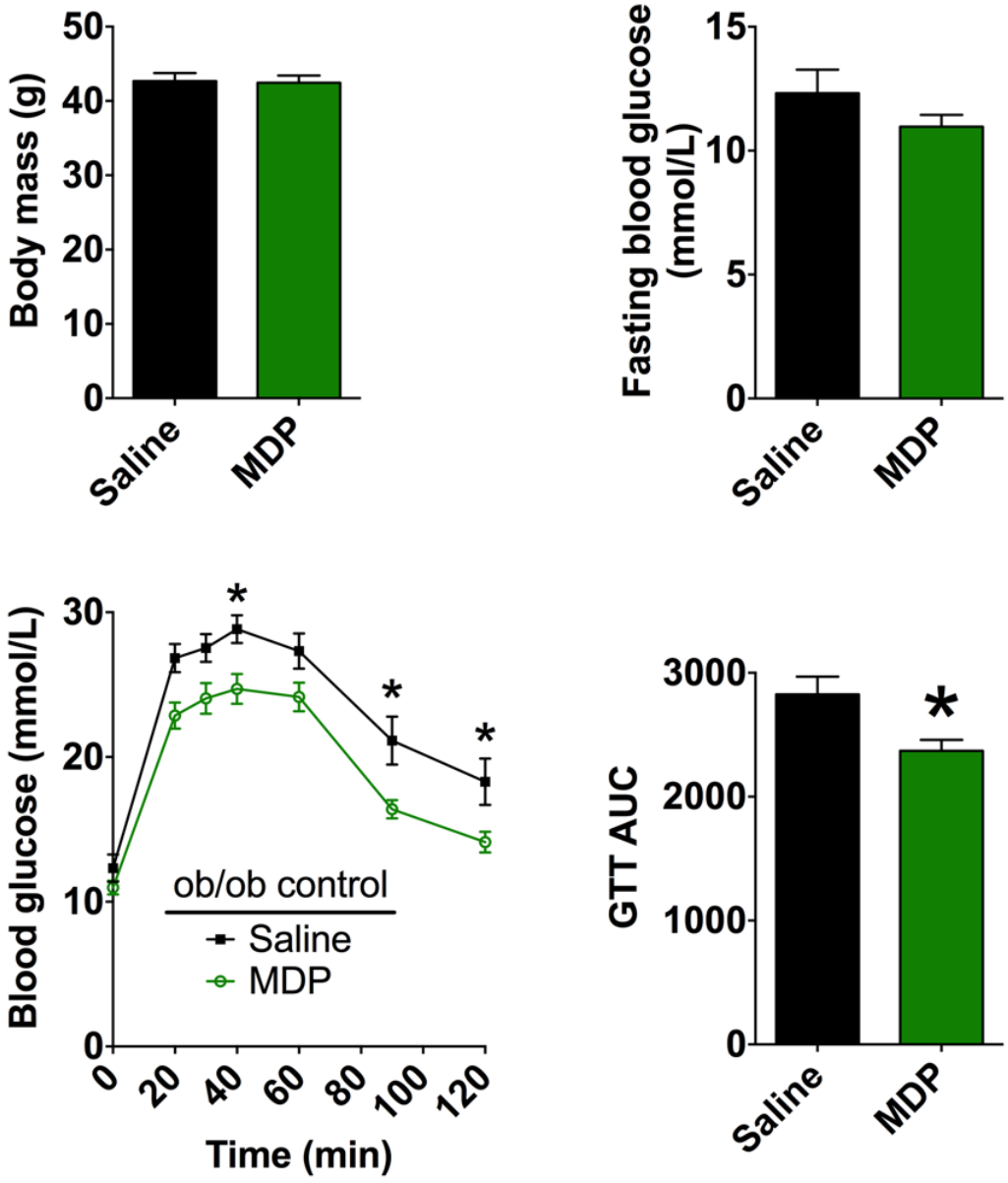

Figure 3.37 Glucose metabolism of genetically obese (*ob/ob*) mice chronically treated with MDP.

Body mass, fasting blood glucose, and glucose tolerance test (0.75 g/kg) of control diet-fed leptin-deficient *ob/ob* mice that received saline or MDP for 2 weeks. n = 10-11 mice for each group. Values are mean ± SEM. * indicates a significant difference between groups, as determined by two-way ANOVA (line graph) or unpaired two-tailed *t*-test (AUC graph) on normally distributed data.

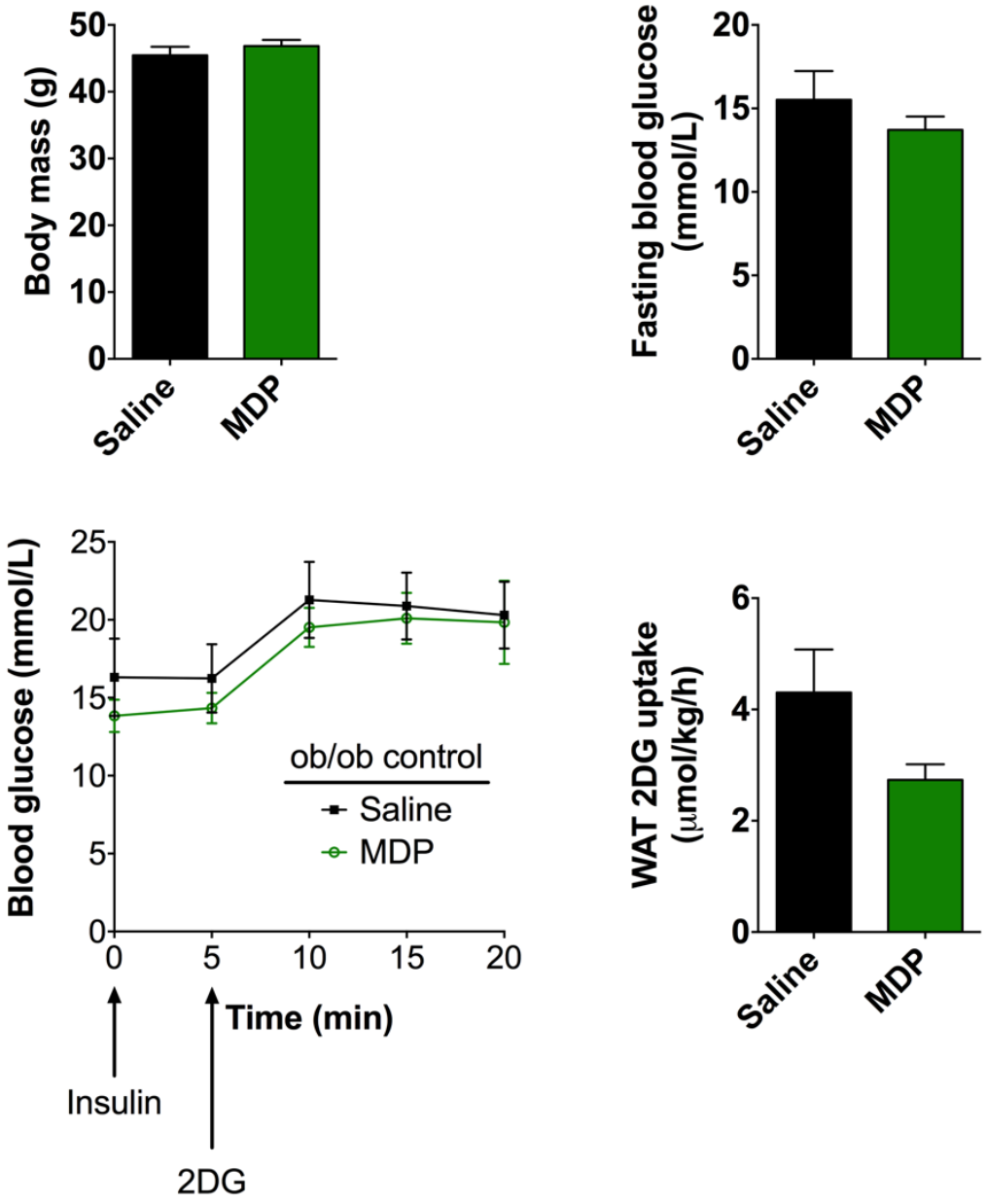

Figure 3.38 Adipose tissue insulin sensitivity in genetically obese (*ob/ob*) mice chronically treated with MDP.

Body mass, fasting blood glucose, insulin tolerance (4 IU/kg) and 2-[1,2-^{3}H (N)]-Deoxy-D-glucose (2DG) uptake in white adipose tissue of control diet-fed leptin-deficient *ob/ob* mice that received saline or MDP for 2 weeks. n = 7-8 mice for each group. Values are mean ± SEM.

3.2.5 Acute "intervention-style" activation of NOD2, but not NOD1, improves glucose tolerance during HFD-induced obesity

The data gathered from "prevention-style" studies of NOD2 activation demonstrated that chronic MDP treatment can improve glucose metabolism during the onset or early stages of metabolic disease in mice. We next tested if acute MDP treatment could alter glycemia after obesity had been established for an extended duration of time. To determine whether the effects of NOD2 activation extend to an acute setting during metabolic disease, we developed an "intervention-style" animal model where mice were fed a HFD for 10 weeks, then acutely injected with MDP (i.p.) for 3 days (Figure 3.39). In this model, both WT mice and mice lacking NOD2 in hepatocytes (*Nod2*$^{-/-HKO}$) that received MDP were more glucose tolerant than control-treated mice (Figures 3.40-3.41) (the experiment in Figure 3.40 was performed by Dr. Emmanuel Denou). Equimolar treatment with the minimal peptidoglycan motif that activates NOD1, iE-DAP, had no effect on glucose tolerance in this HFD model (Figure 3.42). These data suggest that the beneficial effects of NOD2 activation on glucose tolerance also occur in an acute manner, after obesity has been established for an extended duration of time.

Figure 3.39 Experimental design for acute MDP administration after long-term HFD-feeding.

Mice received saline or 100 µg MDP i.p. for 3 days after 10 weeks of HFD-feeding.

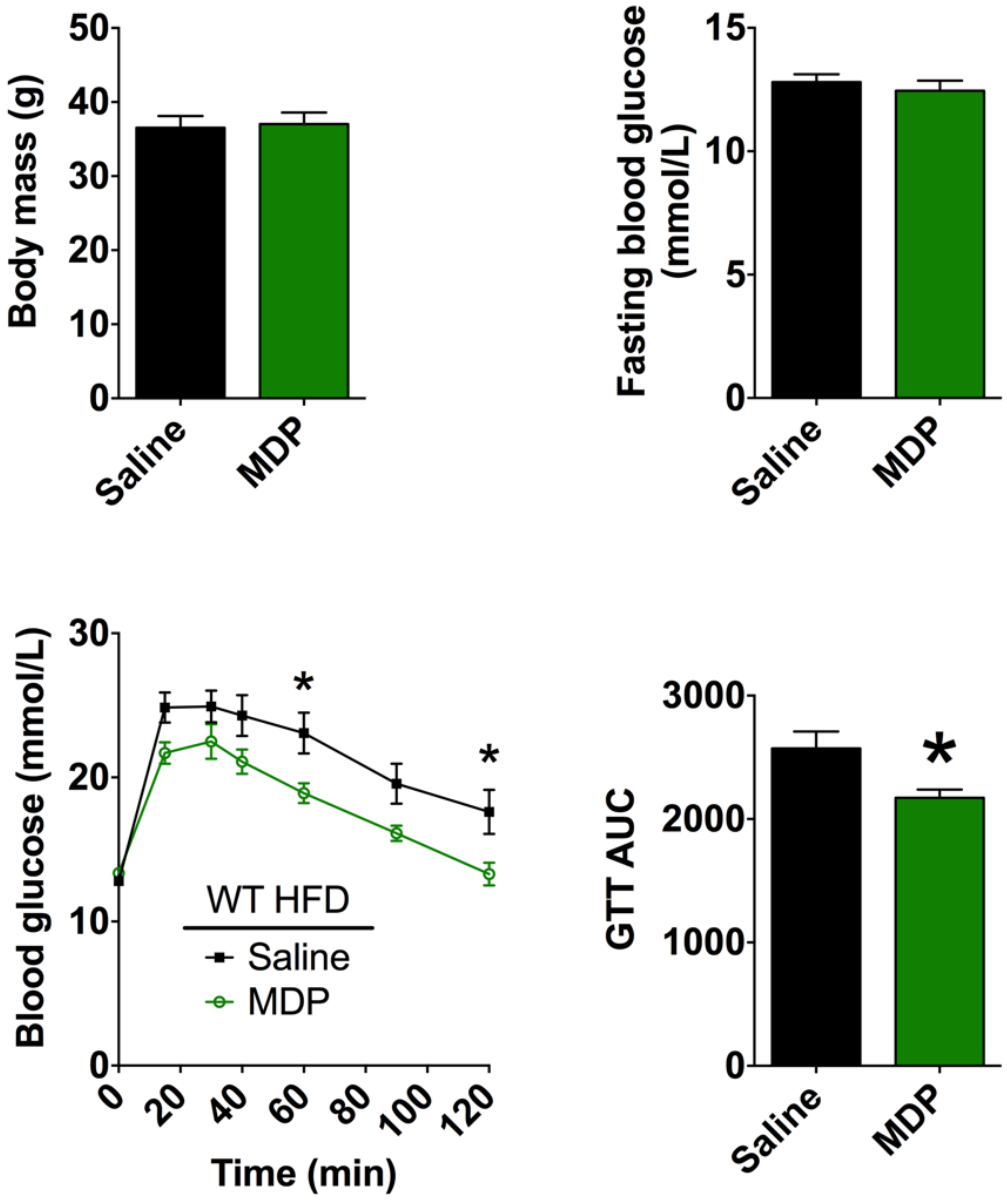

Figure 3.40 Glucose metabolism of WT mice acutely treated with MDP.

Body mass, fasting blood glucose, and glucose tolerance test (1 g/kg) of HFD-fed WT mice that received saline or MDP for 3 days. n = 8 mice for each group. Values are mean ± SEM. * indicates a significant difference between groups, as determined by two-way ANOVA (line graph) or unpaired two-tailed *t*-test (AUC graph) on normally distributed data. This experiment was performed by Dr. Emmanuel Denou.

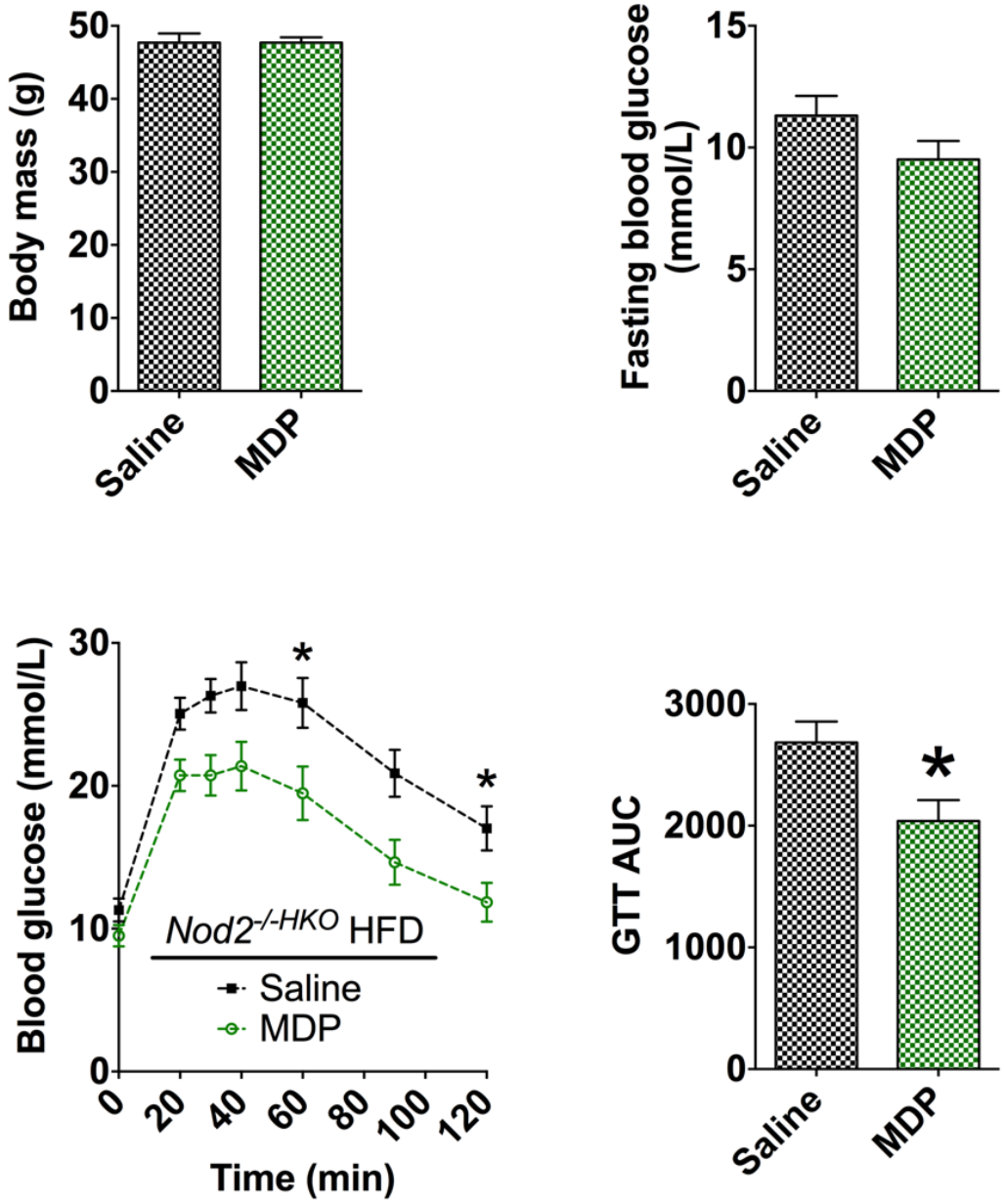

Figure 3.41 Glucose metabolism of hepatocyte-*Nod2*$^{-/-}$ mice acutely treated with MDP.

Body mass, fasting blood glucose, and glucose tolerance test (1 g/kg) of HFD-fed WT mice that received saline or MDP for 3 days. n = 7 mice for each group. Values are mean ± SEM. * indicates a significant difference between groups, as determined by two-way ANOVA (line graph) or Mann-Whitney *U* test (AUC graph) on non-normally distributed data.

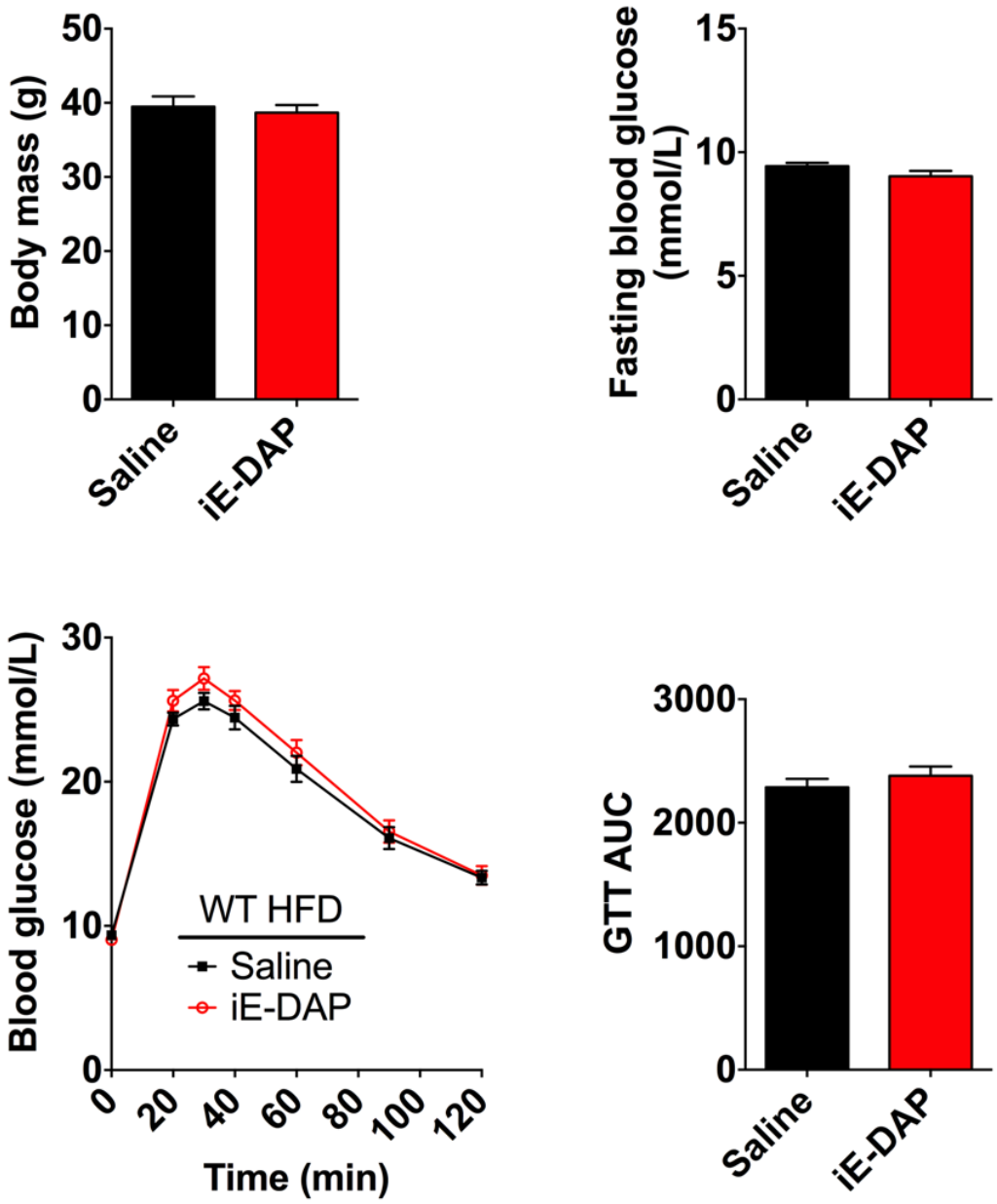

Figure 3.42 Glucose metabolism of WT mice acutely treated with iE-DAP.

Body mass, fasting blood glucose, and glucose tolerance test (1.75 g/kg) of HFD-fed WT mice that received saline or iE-DAP for 3 days. n = 11-13 mice for each group. Values are mean ± SEM.

3.3 NOD activation in mice and endotoxemia

3.3.1 NOD2 activation improves glucose metabolism during acute endotoxemia

The origins of metabolic and inflammatory outcomes during obesity are complex, and we wanted to assess potential mechanisms underpinning NOD2-mediated effects on glucose metabolism. Obesity is associated with an increased circulating level of bacterial LPS, and this metabolic endotoxemia is sufficient to promote inflammation and insulin resistance (95). Obesity also upregulates TLR signaling in mice (333). Chronic NOD2 stimulation reduces additional TLR-induced inflammation (302,305,306). In our characterization of the specificity of NOD2 activation effects during developing obesity, we observed that mice defective in functional LPS-sensing (i.e. TLR4 mutant mice) treated with MDP did not demonstrate improved glucose tolerance (Figure 3.27). This data suggests that the suppression of TLR4-mediated inflammation during obesity is at least one mechanism of the anti-inflammatory and insulin-sensitizing effects of MDP during obesity. We therefore next used a reductionist approach and assessed the metabolic and inflammatory effects of NOD2 activation during acute low-level endotoxemia in control diet-fed mice.

To investigate the metabolic effects of NOD2 activation during acute low-level endotoxemia, an “endotoxin-stress” *in vivo* experimental model was established. In this model, MDP was injected i.p. into mice for 3 days,

followed 18 hours later by a low-dose of LPS (Figure 3.43). An ultra-pure preparation of LPS was used for these experiments because it was a specific TLR4 agonist (i.e. not contaminated with other TLR-activating ligands) and thus limited variables within our experimental design. As a control, 3 injections of MDP alone (in the absence of LPS) had no effect on glucose tolerance (Figure 3.44). Three injections of MDP prior to LPS challenge increased glucose tolerance in male and female mice (Figures 3.45-3.46), and MDP-injected mice secreted less insulin in response to glucose (Figure 3.47). Acute LPS treatment, like severe sepsis, causes hypoglycemia and reduces fasting blood glucose (334,335), therefore, insulin tolerance tests were not feasible in this model. MDP treatment prior to LPS also reduced the HOMA-IR index (Figure 3.48) (325).

To more closely examine the relationship between NOD2 activation and glucose metabolism during acute low-level endotoxemia, MDP-treated mice were subjected to a pyruvate tolerance test (an indicator of hepatic gluconeogenesis). Following a 16-hour fast (to deplete liver glycogen) and 6-hour challenge with LPS, MDP-treated animals experienced lower glucose levels during the pyruvate challenge (Figure 3.49). To further assess NOD2 activation effects on liver glucose metabolism, hyperinsulinemic-euglycemic clamps were performed in animals subjected to the “endotoxin-stress” *in vivo* experimental model (Figure 3.43). The clamp experiment revealed that MDP treatment during endotoxemia

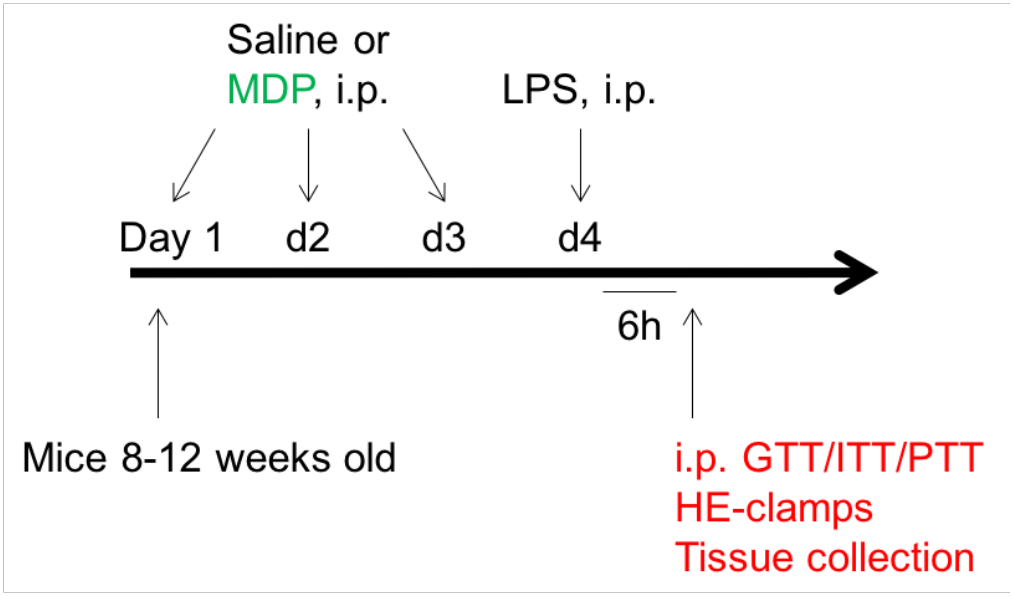

Figure 3.43 Experimental design for MDP administration prior to acute endotoxemia.

Control diet-fed mice received saline or 100 µg MDP i.p. for 3 days prior to induced acute endotoxemia.

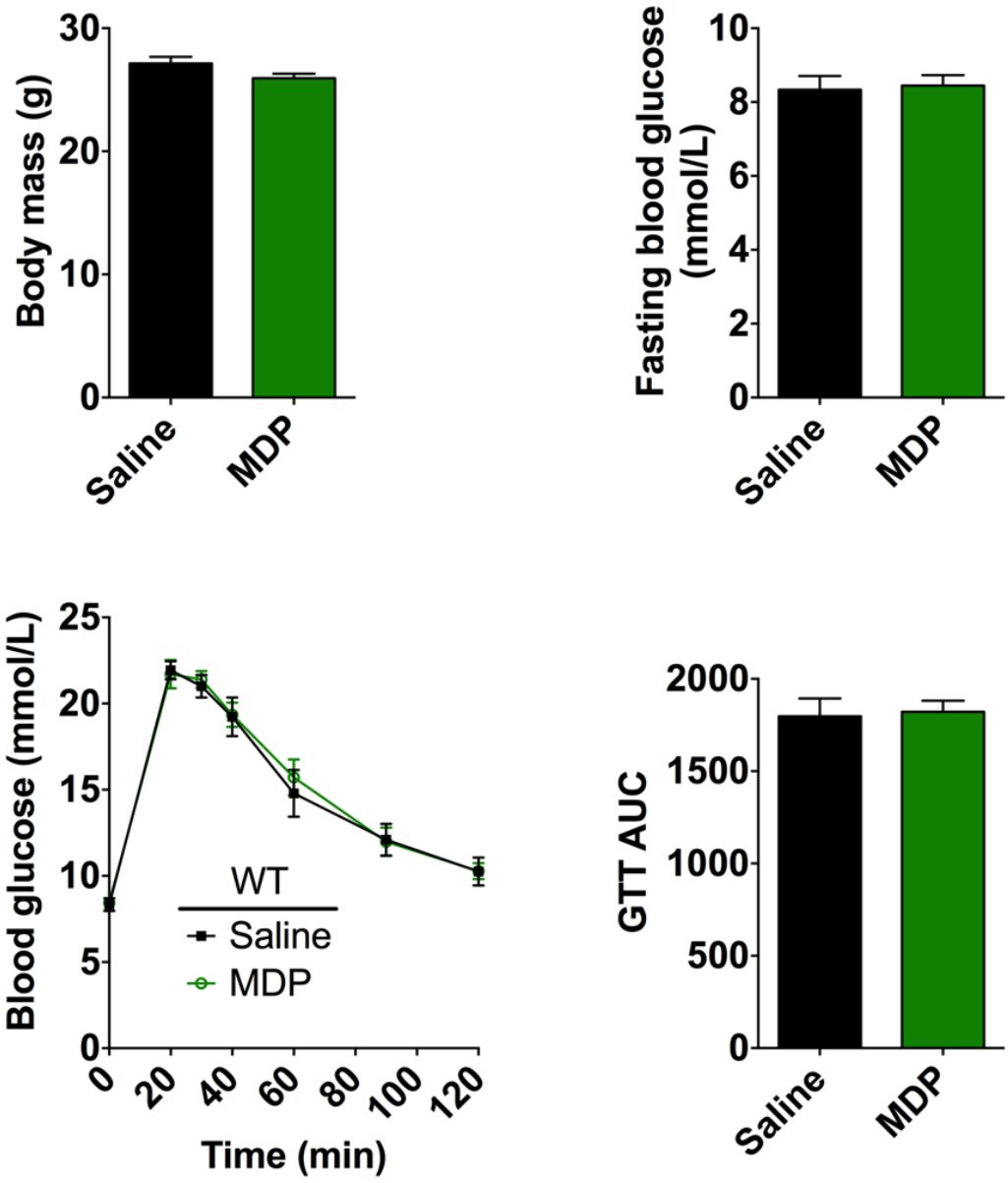

Figure 3.44 Glucose metabolism of WT mice treated with MDP.

Body mass, fasting blood glucose, and glucose tolerance test (2 g/kg) of control diet-fed WT mice that received saline or MDP for 3 days. n = 8 mice for each group. Values are mean ± SEM.

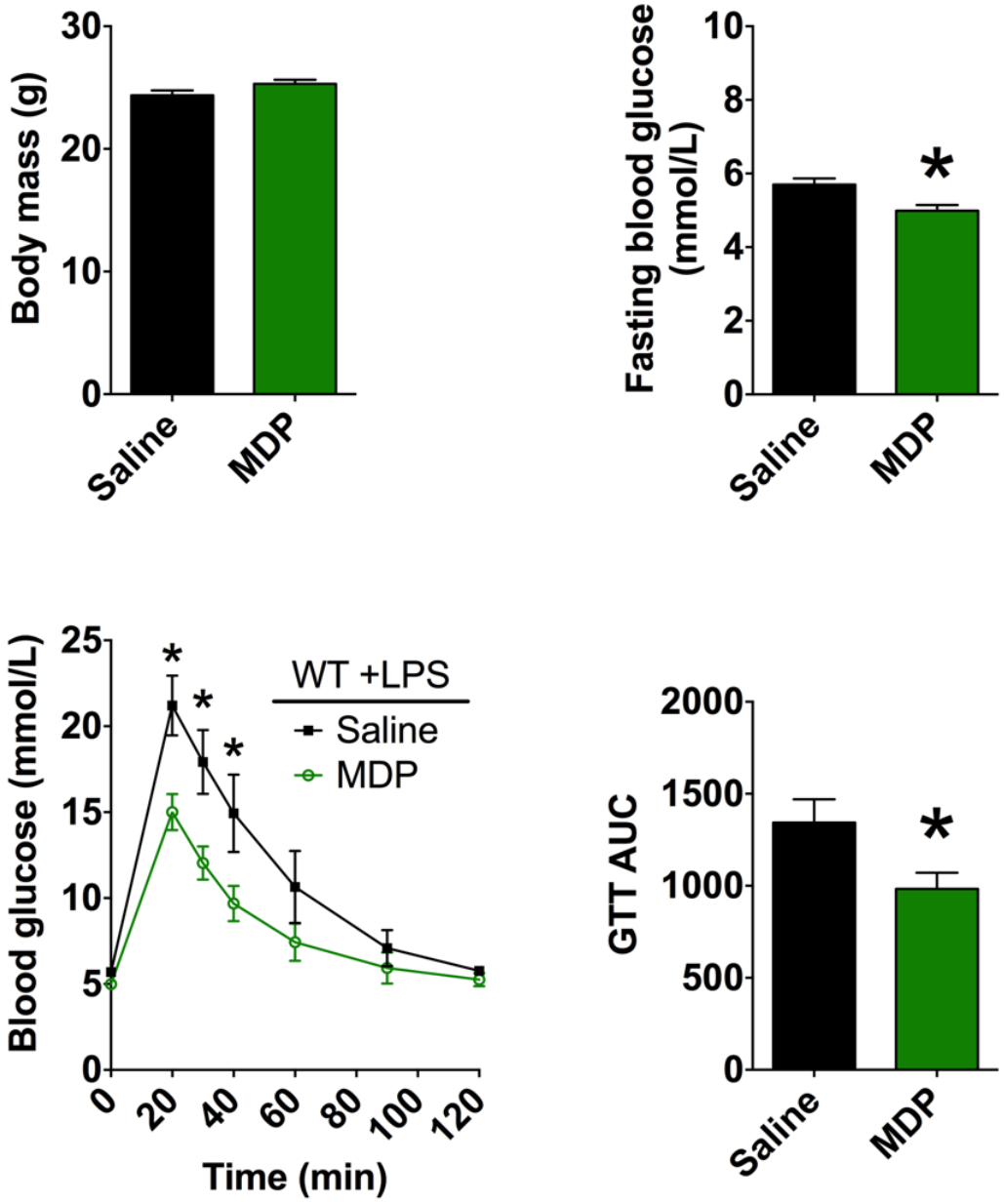

Figure 3.45 Glucose metabolism of WT mice treated with MDP prior to acute endotoxemia.

Body mass, fasting blood glucose, and glucose tolerance test (2 g/kg) of control diet-fed WT mice that received saline or MDP for 3 days prior to acute endotoxemia. n = 8-11 mice for each group. Values are mean ± SEM. * indicates a significant difference between groups, as determined by two-way ANOVA (line graph) or Mann-Whitney *U* test (fasting blood glucose and AUC graphs) on non-normally distributed data.

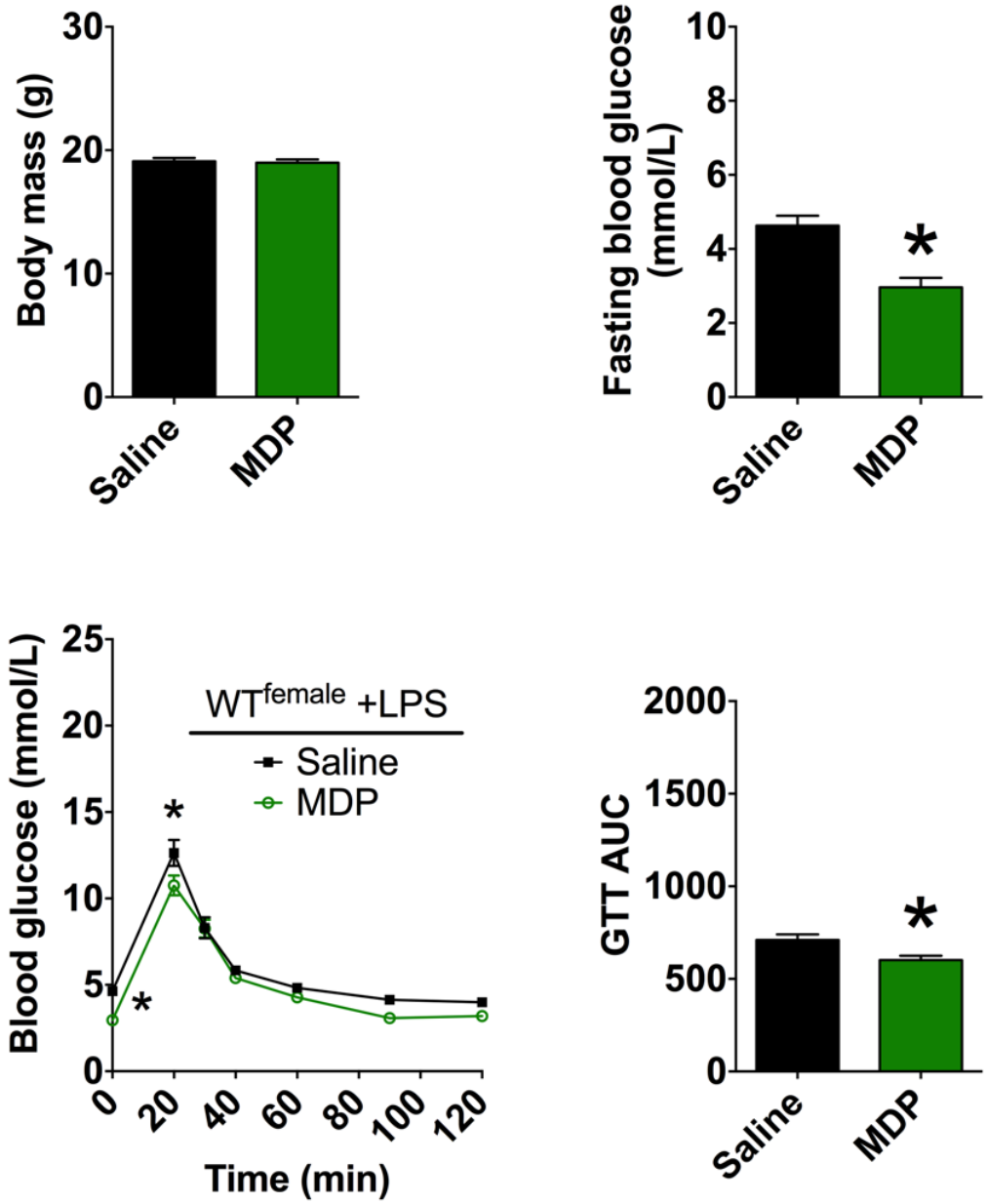

Figure 3.46 Glucose metabolism of female WT mice treated with MDP prior to acute endotoxemia.

Body mass, fasting blood glucose, and glucose tolerance test (2 g/kg) of control diet-fed female WT mice that received saline or MDP for 3 days prior to acute endotoxemia. n = 8-9 mice for each group. Values are mean ± SEM. * indicates a significant difference between groups, as determined by two-way ANOVA (line graph) or Mann-Whitney *U* test (fasting blood glucose and AUC graphs) on non-normally distributed data.

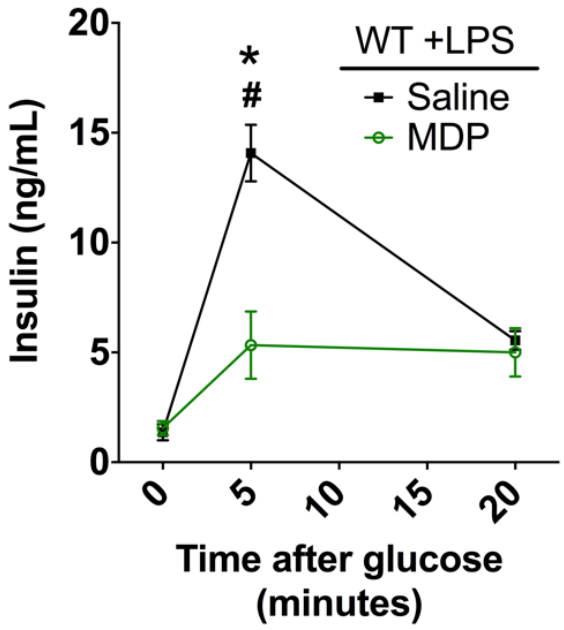

Figure 3.47 Insulin secretion of glucose-challenged WT mice treated with MDP prior to acute endotoxemia.

Serum insulin following glucose administration (2 g/kg) in control diet-fed WT mice that received saline or MDP for 3 days prior to acute endotoxemia. n = 9 mice for each group. Values are mean ± SEM. * indicates a significant difference between groups, as determined by two-way ANOVA. # indicates a significant difference compared to the zero-minute time point (saline), as determined by two-way ANOVA.

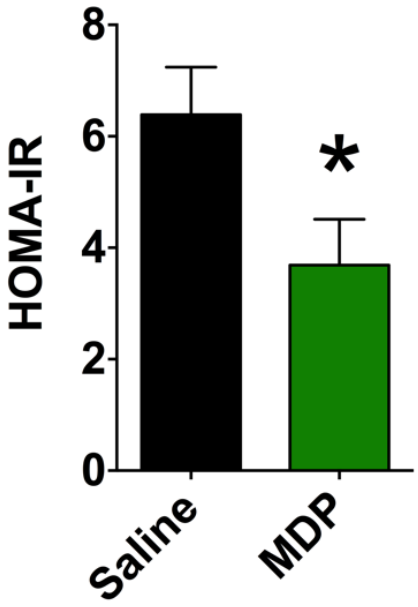

Figure 3.48 Insulin resistance index of WT mice treated with MDP prior to acute endotoxemia.

Homeostatic model assessment of insulin resistance (HOMA-IR) of control diet-fed WT mice that received saline or MDP for 3 days prior to acute endotoxemia. n = 8-9 mice for each group. Values are mean ± SEM. * indicates a significant difference between groups, as determined by unpaired two-tailed *t*-test on normally distributed data.

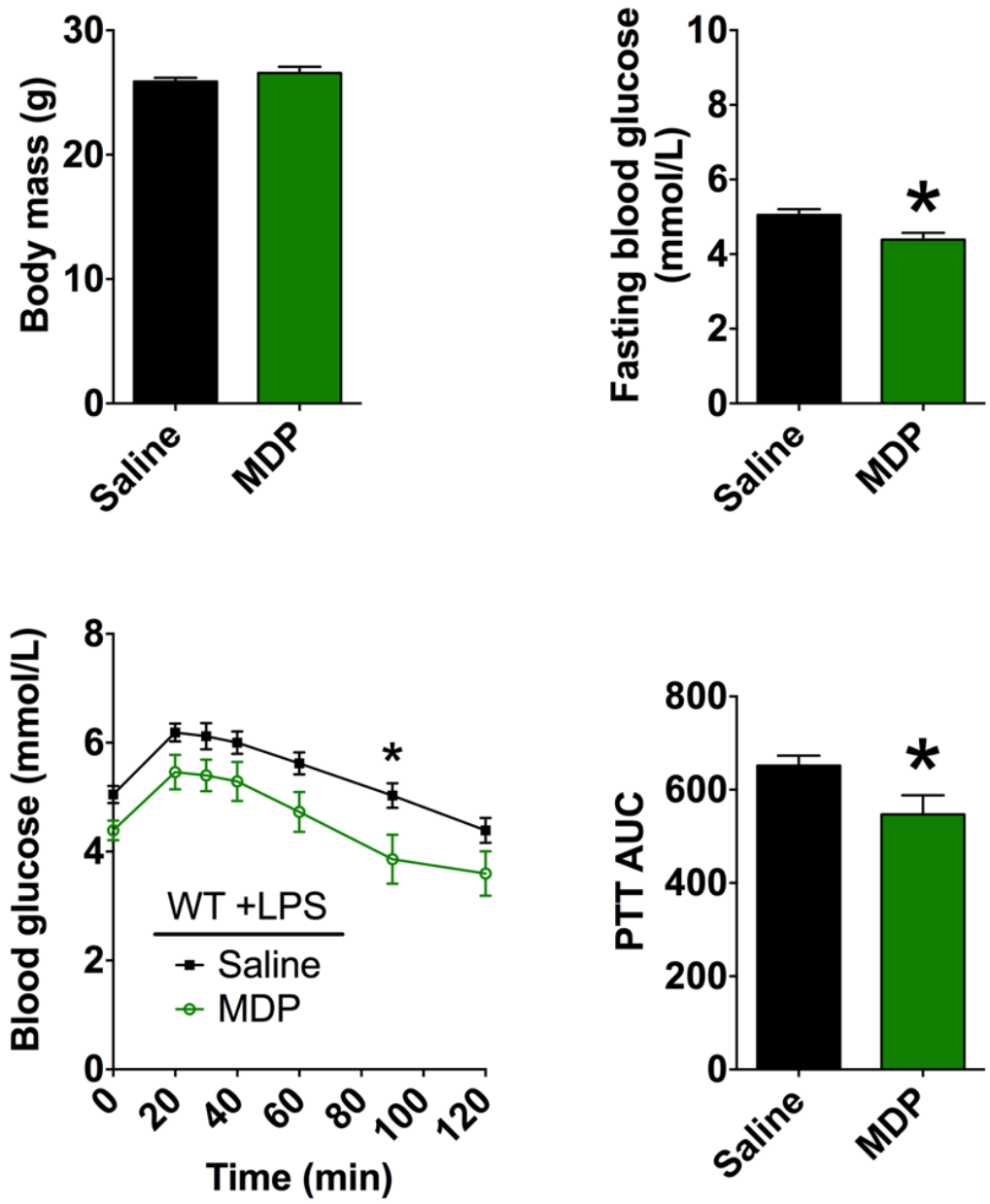

Figure 3.49 Pyruvate metabolism of WT mice treated with MDP prior to acute endotoxemia.

Body mass, fasting blood glucose, and pyruvate tolerance test (2 g/kg) of control diet-fed WT mice that received saline or MDP for 3 days prior to acute endotoxemia. n = 10 mice for each group. Values are mean ± SEM. * indicates a significant difference between groups, as determined by two-way ANOVA (line graph) or unpaired two-tailed *t*-test (fasting blood glucose and AUC graphs) on normally distributed data.

improved liver insulin sensitivity as demonstrated by the increased insulin-suppression of HGP in MDP-treated animals (Figure 3.50). To determine if the liver-centric metabolic outcomes of MDP were due to direct effects within hepatocytes, mice lacking hepatocyte NOD2 (*Nod2*$^{-/-HKO}$) were treated with MDP and LPS and assessed for glucose tolerance. MDP-treated animals had improved glucose tolerance similar to WT animals (Figure 3.51), suggesting that NOD2 activation improves hepatic glucose metabolism during low-level endotoxemia in a hepatocyte-independent manner.

To probe the pathway specificity of MDP treatment, multiple knockout mouse strains were also treated according to the "endotoxin-stress" *in vivo* experimental model (Figure 3.43). In whole-body *Nod2*$^{-/-}$ and *Ripk2*$^{-/-}$ mice, MDP treatment had no effect on glucose tolerance during the endotoxin stress after LPS injection (Figures 3.52-3.53). However, *Nod2*$^{-/-BMT}$ and *Nlrp3*$^{-/-}$ mice responded to MDP and these mice were more glucose tolerant during endotoxin stress (Figures 3.54-3.55). These data suggest that NOD2 signaling within immune cells, and NLRP3, are not involved in mediating the insulin-sensitizing effects of MDP during acute low-level endotoxemia.

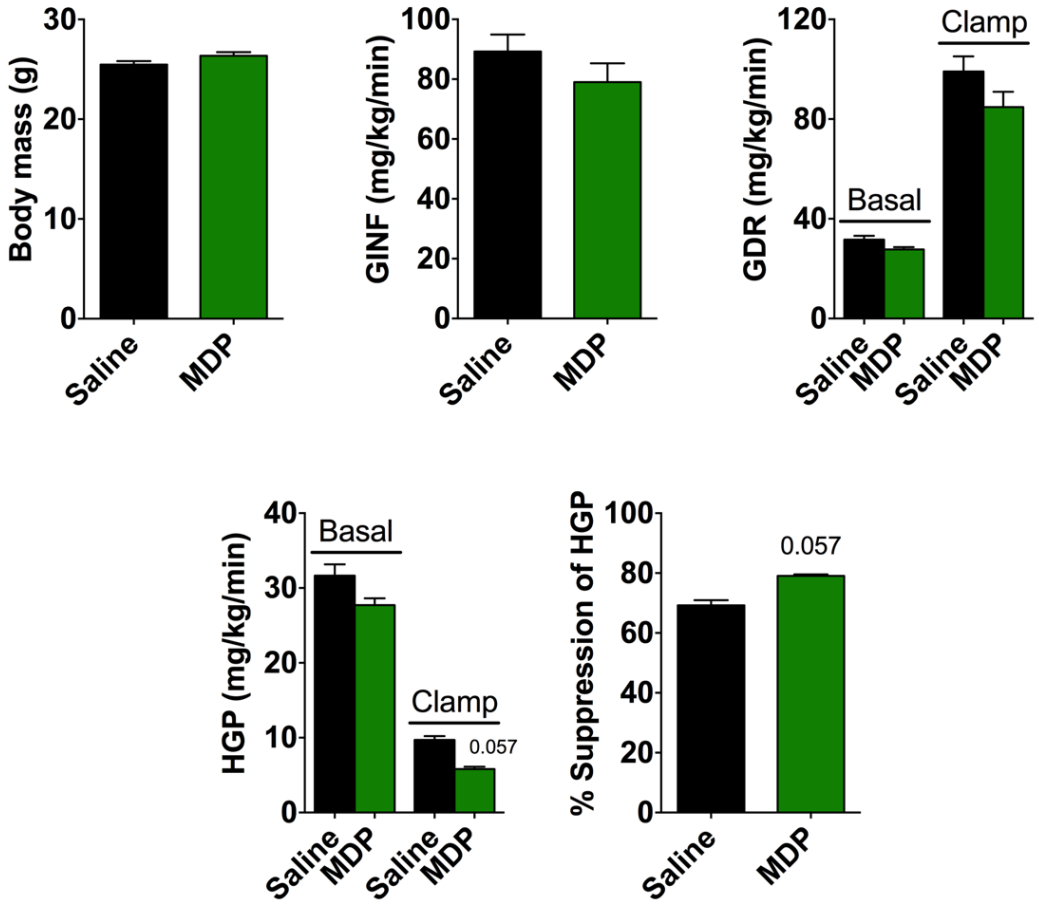

Figure 3.50 Whole-body and liver insulin sensitivity WT mice treated with MDP prior to acute endotoxemia.

Body mass, glucose infusion rate (GINF), glucose disposal rate (GDR), hepatic glucose production (HGP), and insulin-mediated suppression of HGP during the hyperinsulinemic-euglycemic clamp experiment of control diet-fed WT mice that received saline or MDP for 3 days prior to acute endotoxemia. n = 3-4 mice for each group. Values are mean ± SEM.

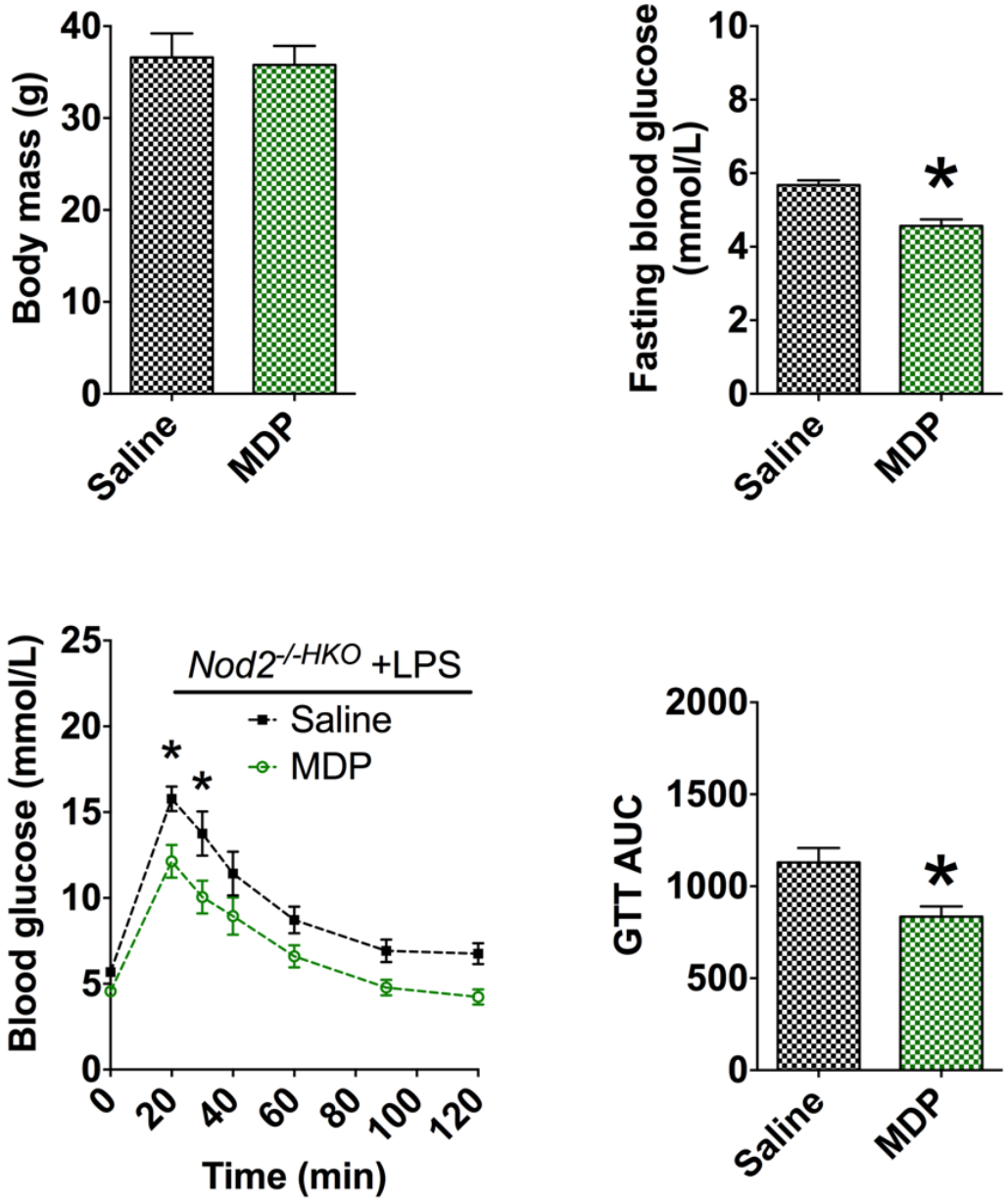

Figure 3.51 Glucose metabolism of hepatocyte-*Nod2*$^{-/-}$ mice treated with MDP prior to acute endotoxemia.

Body mass, fasting blood glucose, and glucose tolerance test (2 g/kg) of control diet-fed hepatocyte-*Nod2*$^{-/-}$ mice that received saline or MDP for 3 days prior to acute endotoxemia. n = 5-6 mice for each group. Values are mean ± SEM. * indicates a significant difference between groups, as determined by two-way ANOVA (line graph) or Mann-Whitney *U* test (fasting blood glucose and AUC graphs) on non-normally distributed data.

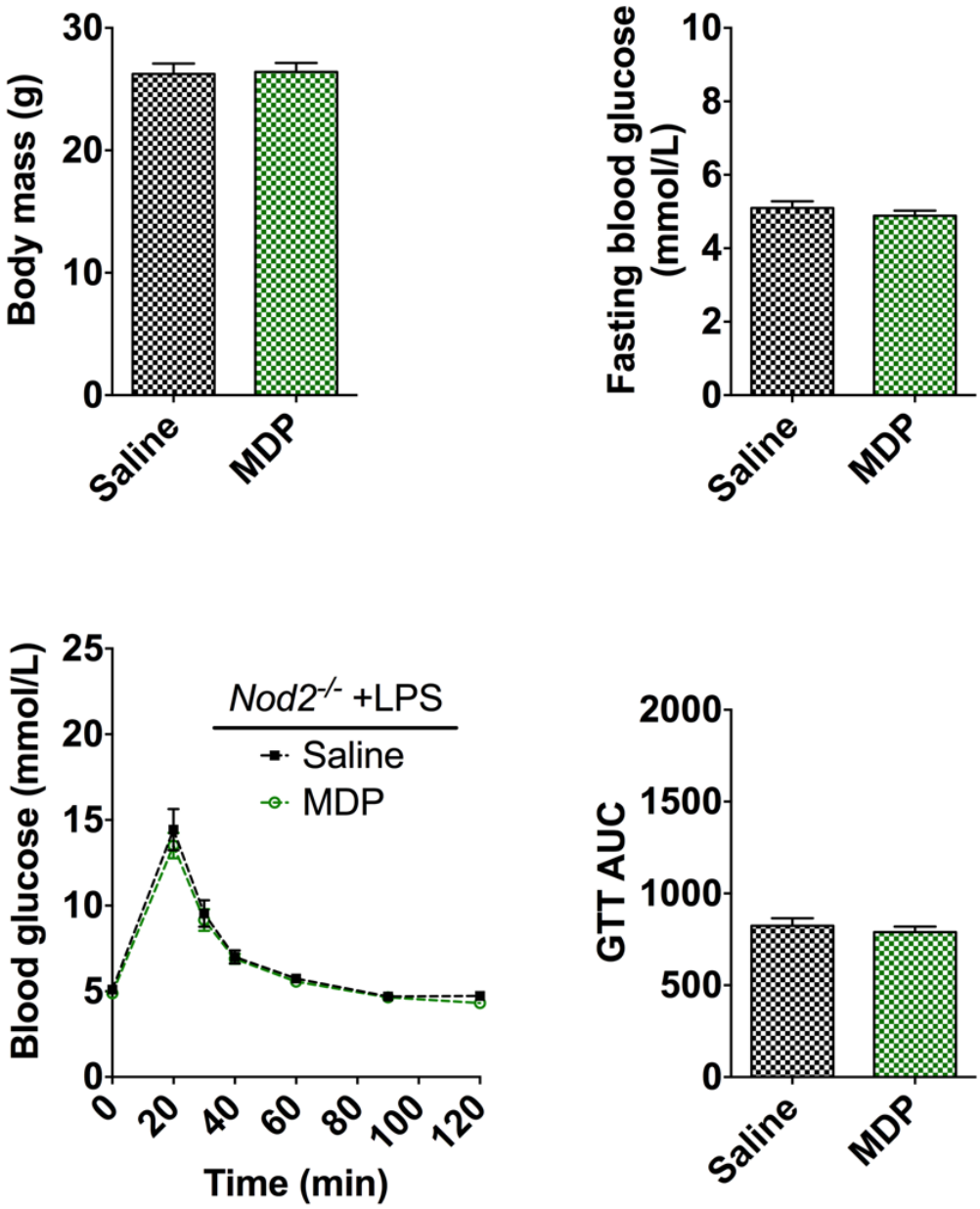

Figure 3.52 Glucose metabolism of *Nod2*$^{-/-}$ mice treated with MDP prior to acute endotoxemia.

Body mass, fasting blood glucose, and glucose tolerance test (2 g/kg) of control diet-fed *Nod2*$^{-/-}$ mice that received saline or MDP for 3 days prior to acute endotoxemia. n = 9-11 mice for each group. Values are mean ± SEM.

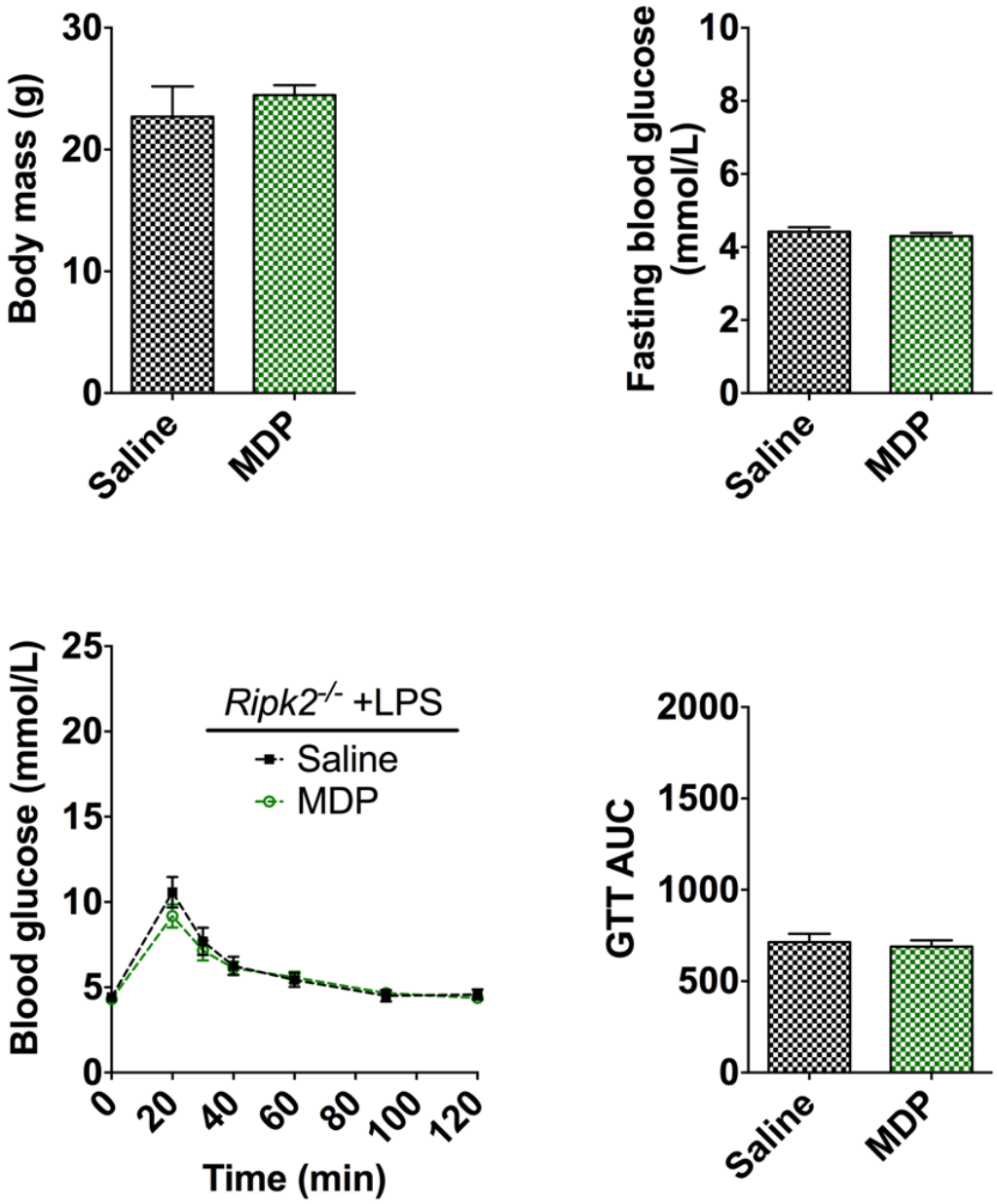

Figure 3.53 Glucose metabolism of *Ripk2*$^{-/-}$ mice treated with MDP prior to acute endotoxemia.

Body mass, fasting blood glucose, and glucose tolerance test (2 g/kg) of control diet-fed *Ripk2*$^{-/-}$ mice that received saline or MDP for 3 days prior to acute endotoxemia. n = 9 mice for each group. Values are mean ± SEM.

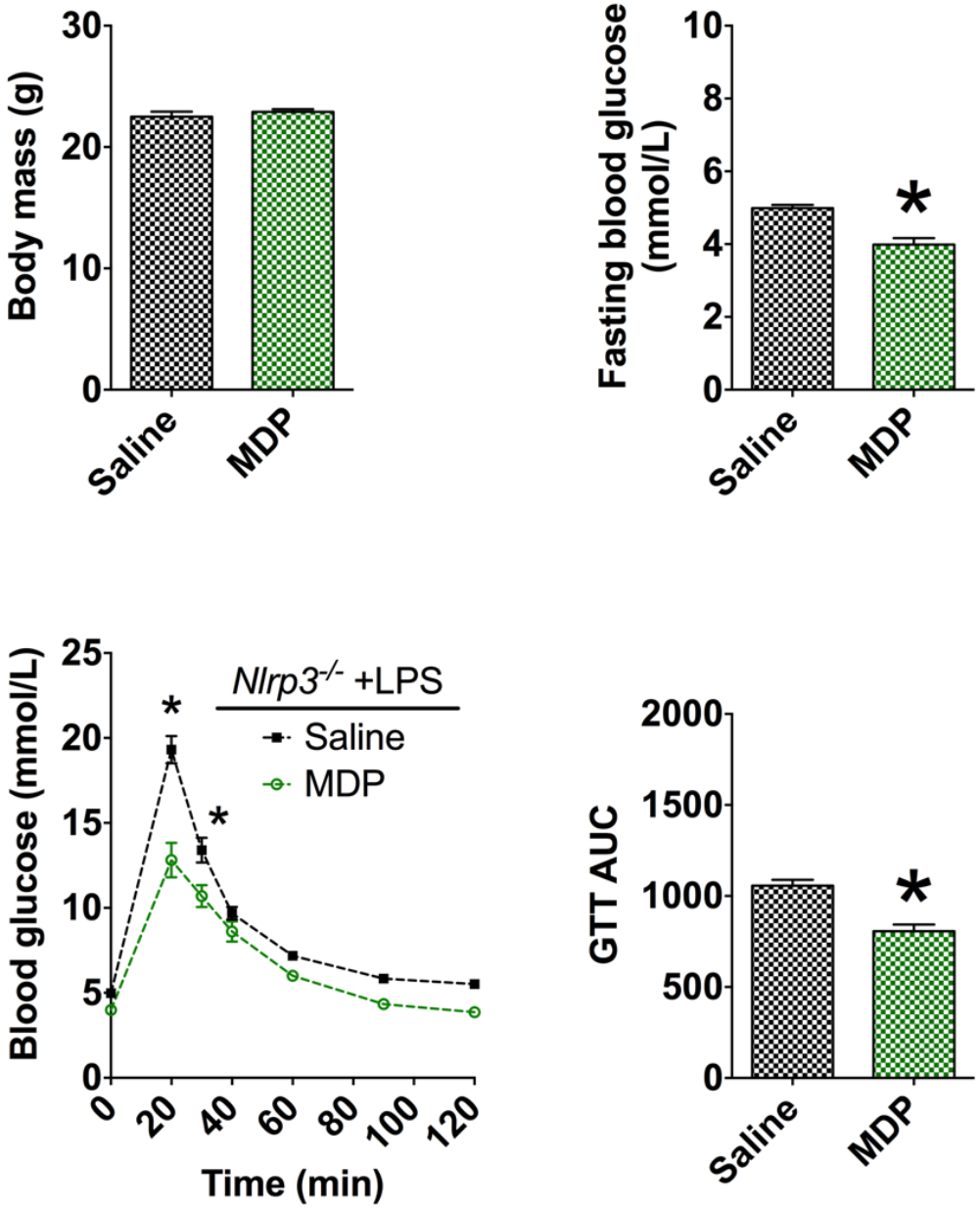

Figure 3.54 Glucose metabolism of *Nlrp3*$^{-/-}$ mice treated with MDP prior to acute endotoxemia.

Body mass, fasting blood glucose, and glucose tolerance test (2 g/kg) of control diet-fed *Nlrp3*$^{-/-}$ mice that received saline or MDP for 3 days prior to acute endotoxemia. n = 8-9 mice for each group. Values are mean ± SEM. * indicates a significant difference between groups, as determined by two-way ANOVA (line graph) or unpaired two-tailed *t*-test (fasting blood glucose and AUC graphs) on normally distributed data.

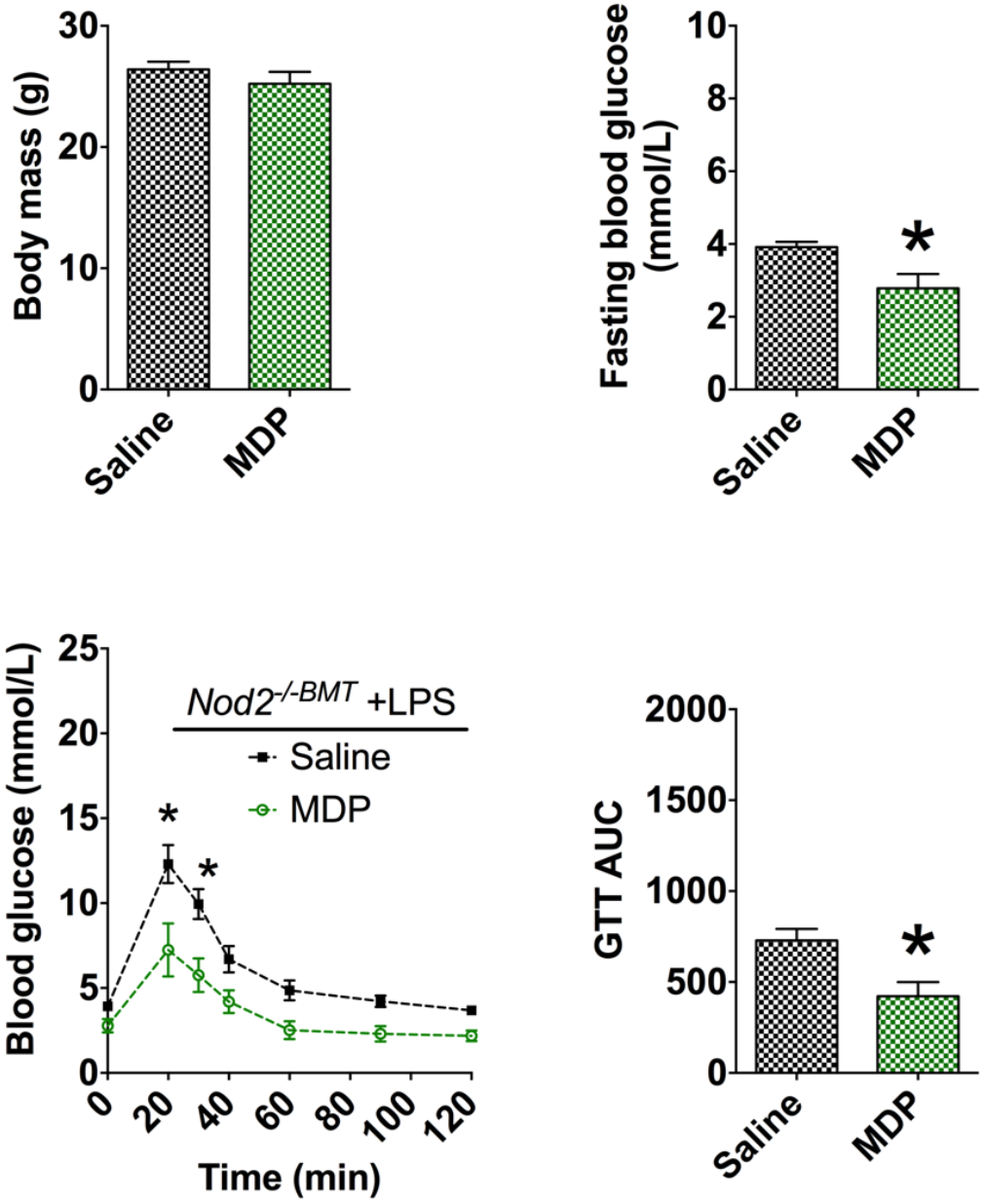

Figure 3.55 Glucose metabolism of hematopoietic-*Nod2*$^{-/-}$ mice treated with MDP prior to acute endotoxemia.

Body mass, fasting blood glucose, and glucose tolerance test (2 g/kg) of control diet-fed hematopoietic-*Nod2*$^{-/-}$ mice that received saline or MDP for 3 days prior to acute endotoxemia. n = 5-6 mice for each group. Values are mean ± SEM. * indicates a significant difference between groups, as determined by two-way ANOVA (line graph) or Mann-Whitney *U* test (fasting blood glucose and AUC graphs) on non-normally distributed data.

3.3.2 NOD1 activation worsens glucose metabolism during acute endotoxemia

To determine if the beneficial metabolic effects of MDP were unique to NOD2, we also investigated the metabolic phenotype imparted by NOD1 activation during acute low-level endotoxemia using a modified "endotoxin-stress" *in vivo* experimental model (Figure 3.56). Three injections of the NOD1-activating ligand FK565 (heptanoyl-γ-d-Glu-meso-DAP-Ala) prior to LPS challenge increased glucose intolerance (Figure 3.57), in stark contrast to the effects of MDP (Figure 3.45). Both *Nod1*$^{-/-}$ and *Ripk2*$^{-/-}$ mice were insensitive to FK565 (Figures 3.58-3.59), where glucose tolerance was not altered by FK565 injection. Collectively, these results confirmed ligand specificity for the NOD1/RIPK2 signaling pathway related to glucose control.

3.4 Role of IRF4 in NOD-mediated metabolic and inflammatory changes during HFD-induced obesity and acute endotoxemia

3.4.1 NOD2-mediated improvements in glucose metabolism and adipose tissue inflammation during HFD-induced obesity require IRF4

The protective effect of MDP on inflammatory colitis is known to be dependent on NOD2 and IRF4, with the key mechanism being a NOD2-IRF4-driven inhibition of NF-κB signaling (305,306). *Irf4* deletion promotes metabolic inflammation during obesity (310,311), thus positioning IRF4 as

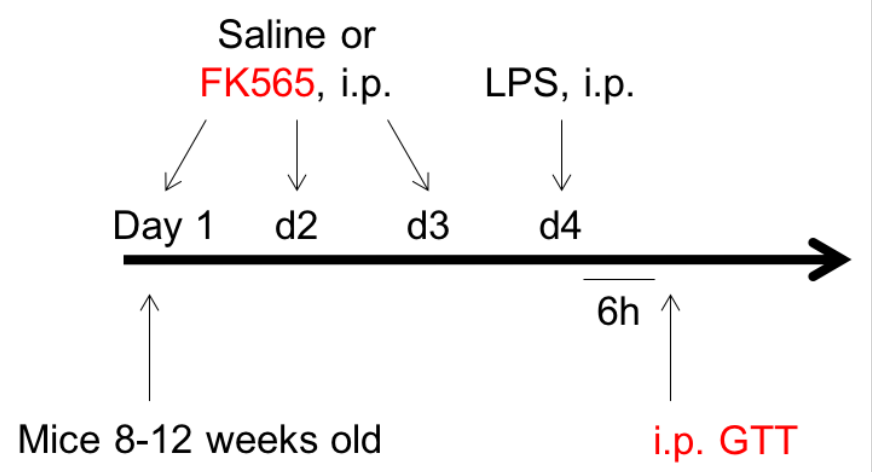

Figure 3.56 Experimental design for FK565 administration prior to acute endotoxemia.

Control diet-fed mice received saline or 10 µg FK565 i.p. for 3 days prior to induced acute endotoxemia.

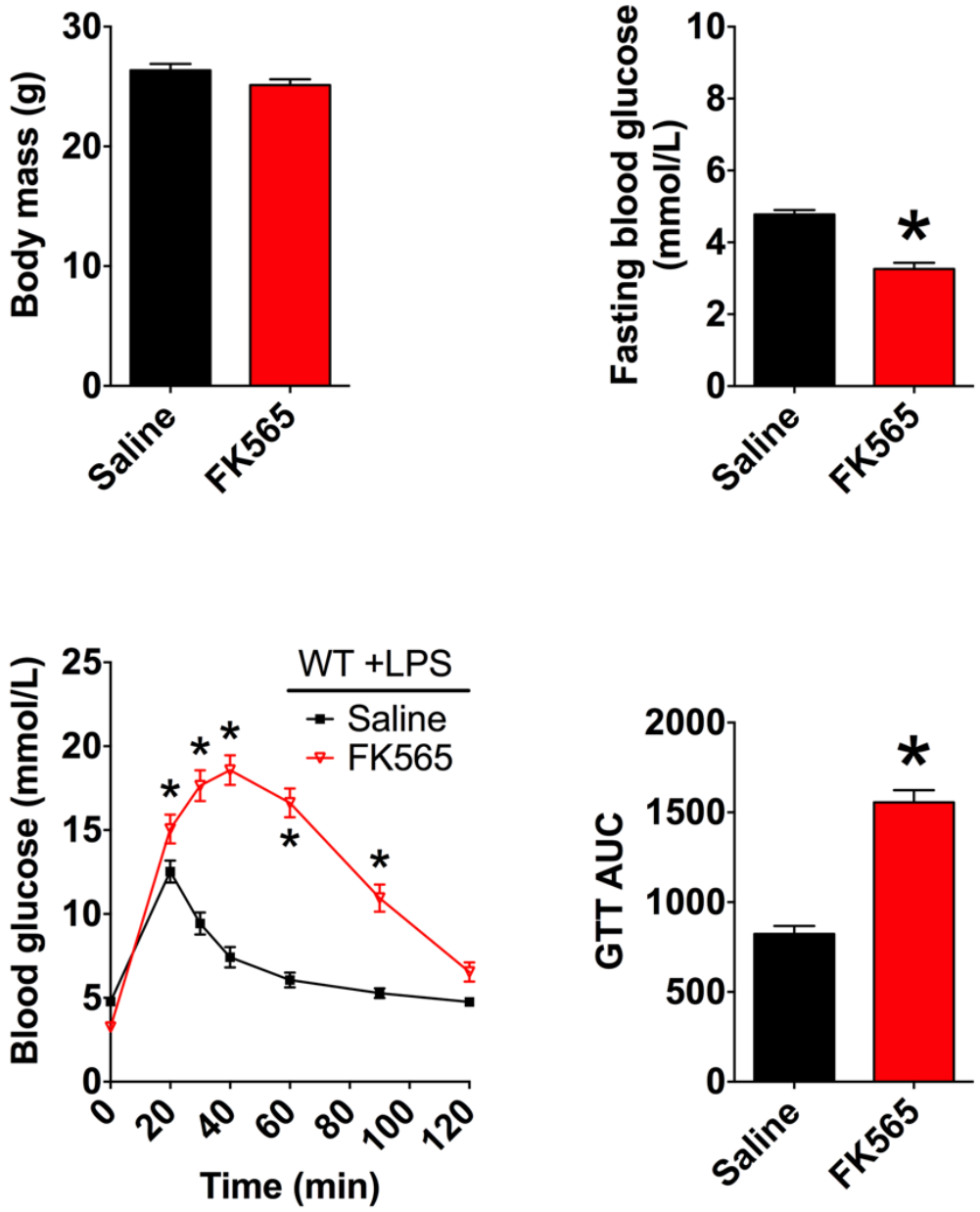

Figure 3.57 Glucose metabolism of WT mice treated with FK565 prior to acute endotoxemia.

Body mass, fasting blood glucose, and glucose tolerance test (2 g/kg) of control diet-fed WT mice that received saline or FK565 for 3 days prior to acute endotoxemia. n = 9-10 mice for each group. Values are mean ± SEM. * indicates a significant difference between groups, as determined by two-way ANOVA (line graph) or Mann-Whitney *U* test (fasting blood glucose and AUC graphs) on non-normally distributed data.

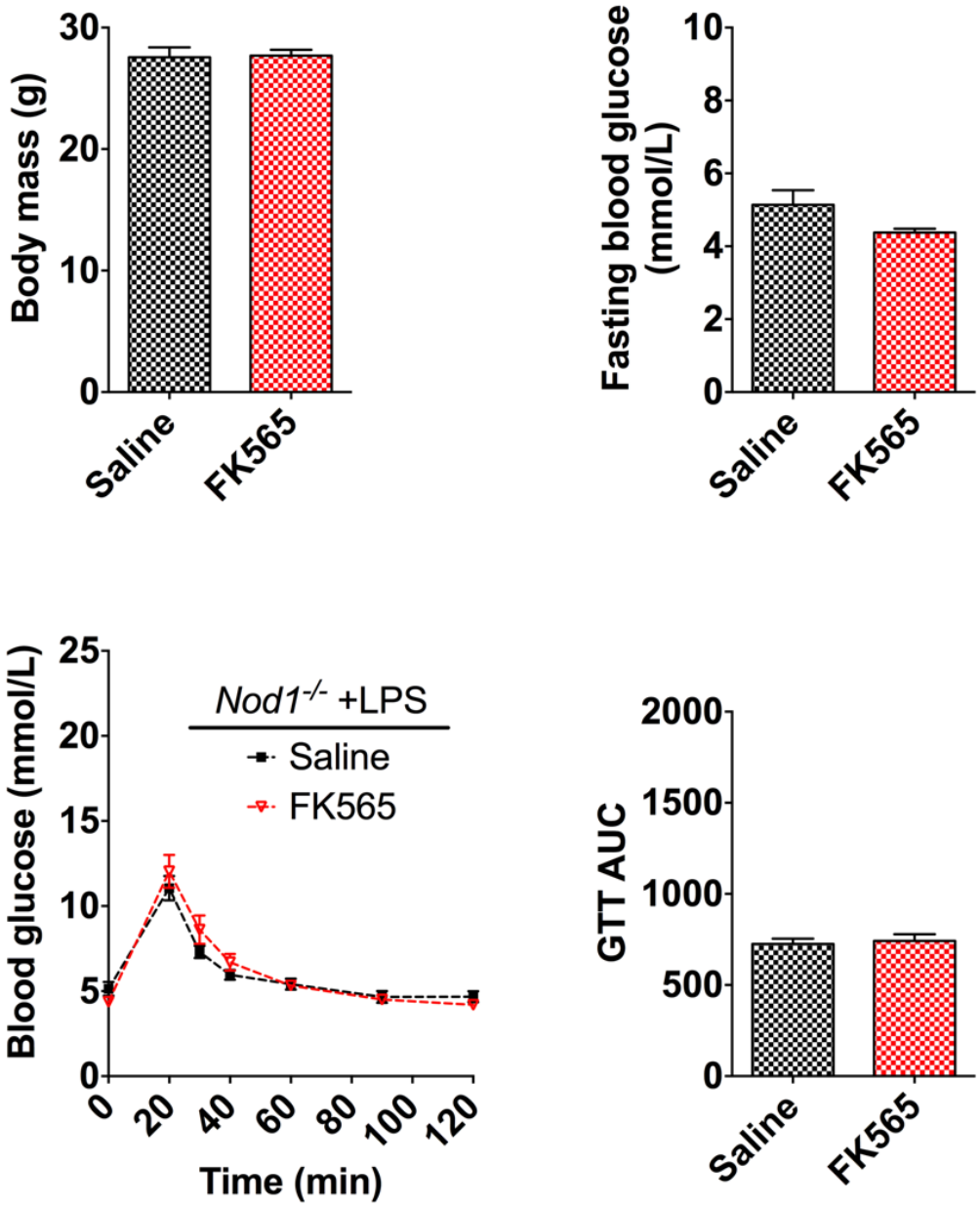

Figure 3.58 Glucose metabolism of *Nod1*$^{-/-}$ mice treated with FK565 prior to acute endotoxemia.

Body mass, fasting blood glucose, and glucose tolerance test (2 g/kg) of control diet-fed *Nod1*$^{-/-}$ mice that received saline or FK565 for 3 days prior to acute endotoxemia. n = 8 mice for each group. Values are mean ± SEM.

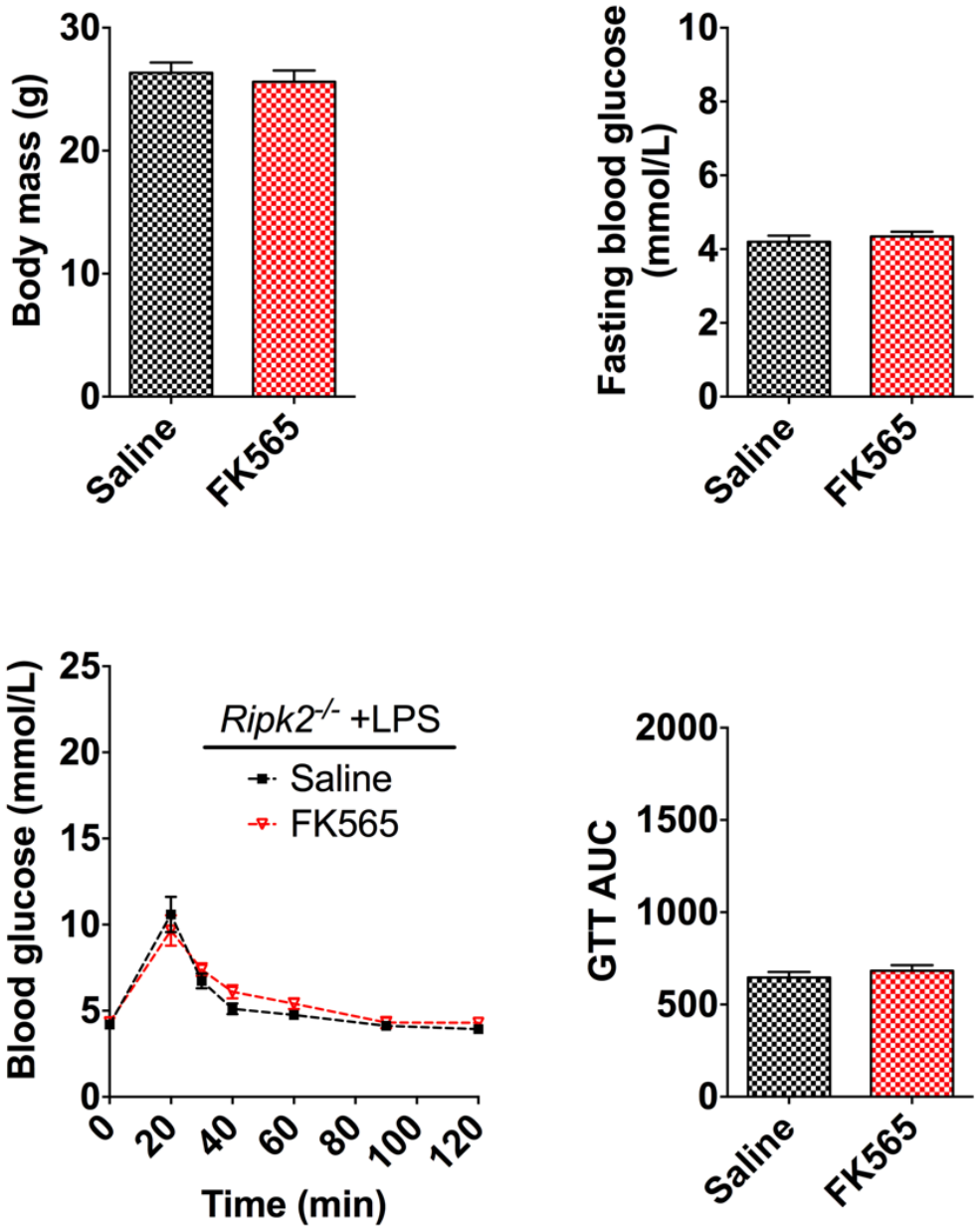

Figure 3.59 Glucose metabolism of *Ripk2*$^{-/-}$ mice treated with FK565 prior to acute endotoxemia.

Body mass, fasting blood glucose, and glucose tolerance test (2 g/kg) of control diet-fed *Ripk2*$^{-/-}$ mice that received saline or FK565 for 3 days prior to acute endotoxemia. n = 7-8 mice for each group. Values are mean ± SEM.

a possible mediator of the effects of MDP on insulin sensitivity and inflammation in our diet-induced obesity model. IRF4 may also explain the divergent effects of NOD1 versus NOD2 activation on glucose metabolism during acute low-level endotoxemia.

We first assessed metabolic tissues for altered *Irf4* expression. Chronic MDP treatment increased adipose and liver *Irf4* expression in C57BL6/J WT, but not *Nod2*$^{-/-}$ mice (Figure 3.60). MDP did not alter *Irf4* expression levels in spleen (non-metabolic tissue) (Figure 3.34). In contrast to the insulin sensitizing effects of MDP in HFD-fed C57BL/6J WT mice (Figures 3.21 and 3.28), MDP did not alter glucose tolerance in *Irf4*$^{-/-}$ mice fed an obesity-causing HFD (Figure 3.61). Furthermore, MDP did not decrease gonadal adipose NF-κB activity in *Irf4*$^{-/-}$ mice (Figure 3.62). Chronic MDP treatment in *Irf4*$^{-/-}$ mice decreased hepatic gene expression of *Cxcl10* and *Nos2* (Figure 3.63), similar to the changes observed in WT animals (Figure 3.29). The widespread decrease in inflammatory markers in adipose induced by chronic MDP treatment in WT mice did not occur in the adipose tissue of MDP-treated *Irf4*$^{-/-}$ mice (Figures 3.31-3.32, and 3.64). Analysis of *Irf4*$^{-/-}$ muscle gene expressions revealed similar changes as WT mice (Figures 3.33 and 3.65). These results suggest that adipose tissue is the key site of anti-inflammatory action of MDP via IRF4.

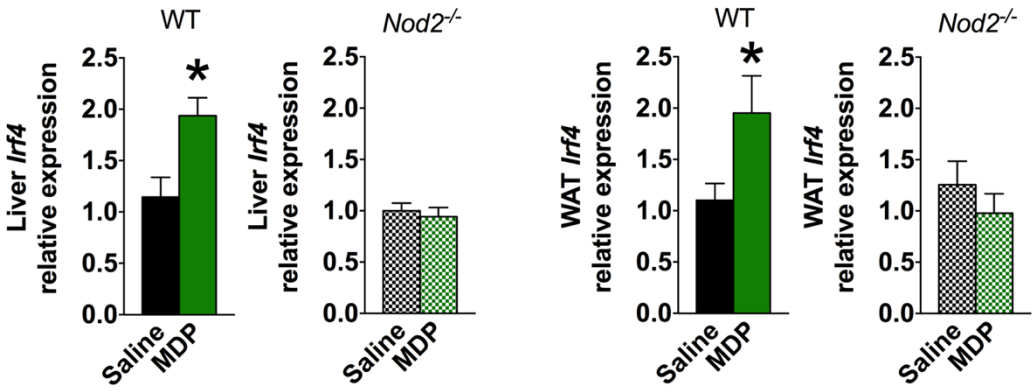

Figure 3.60 Tissue *Irf4* expression of WT and *Nod2*$^{-/-}$ mice chronically treated with MDP.

Liver and white adipose *Irf4* gene expression of HFD-fed WT mice that received saline or MDP for 5 weeks. n = 9-10 mice for each group. Values are mean ± SEM. * indicates a significant difference between groups, as determined by unpaired two-tailed *t*-test on normally distributed data or by Mann-Whitney *U* test on non-normally distributed data.

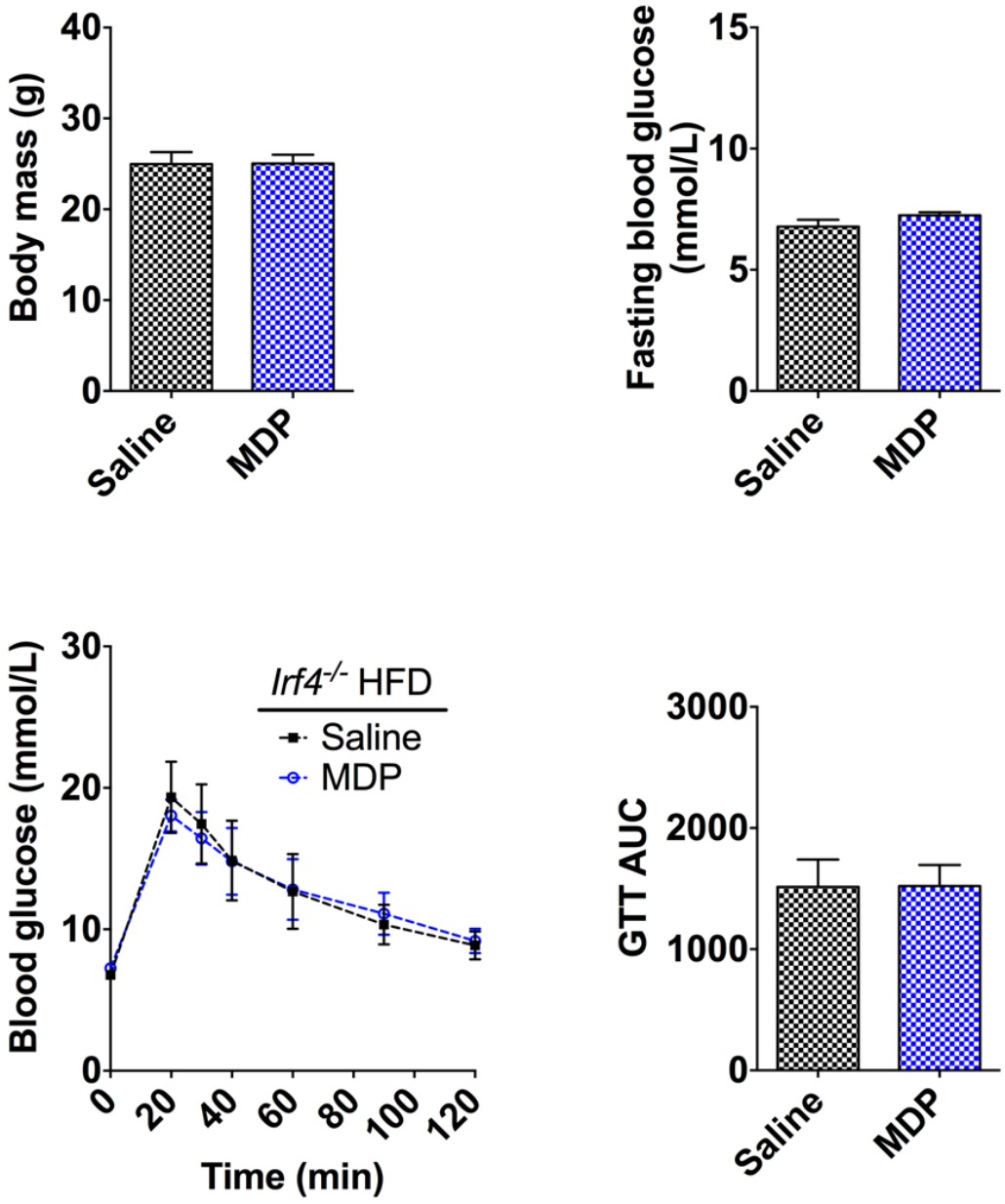

Figure 3.61 Glucose metabolism of *Irf4*$^{-/-}$ mice chronically treated with MDP.

Body mass, fasting blood glucose, and glucose tolerance test (2 g/kg) of HFD-fed *Irf4*$^{-/-}$ mice that received saline or MDP for 4 weeks. n = 6 mice for each group. Values are mean ± SEM.

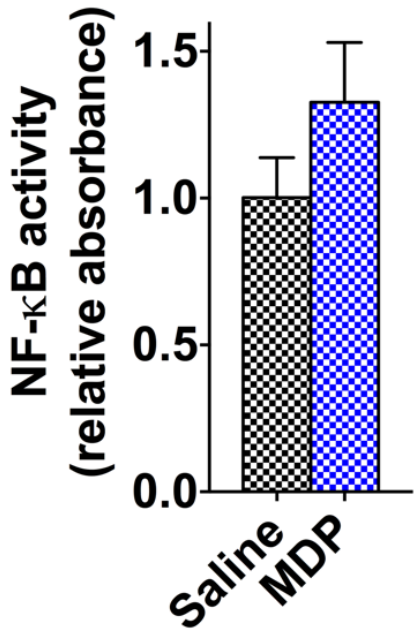

Figure 3.62 Tissue NF-κB activity of *Irf4*$^{-/-}$ mice chronically treated with MDP.

White adipose NF-κB activity of HFD-fed *Irf4*$^{-/-}$ mice that received saline or MDP for 5 weeks. n = 6 mice for each group. Values are mean ± SEM.

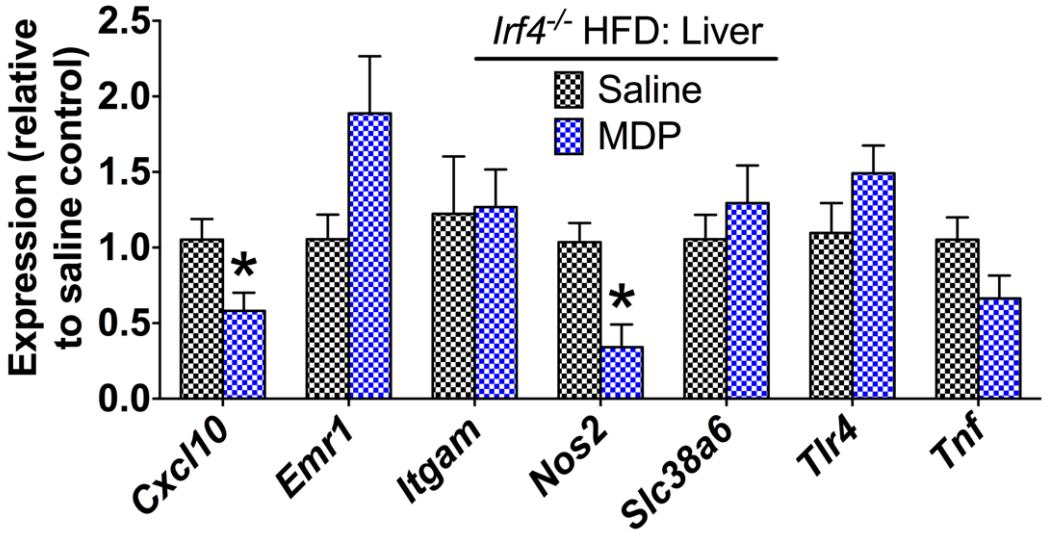

Figure 3.63 Liver inflammation of *Irf4*$^{-/-}$ mice chronically treated with MDP.

Liver inflammatory gene expression of HFD-fed *Irf4*$^{-/-}$ mice that received saline or MDP for 5 weeks. n = 6 mice for each group. Values are mean ± SEM. * indicates a significant difference between groups, as determined by Mann-Whitney *U* test on non-normally distributed data.

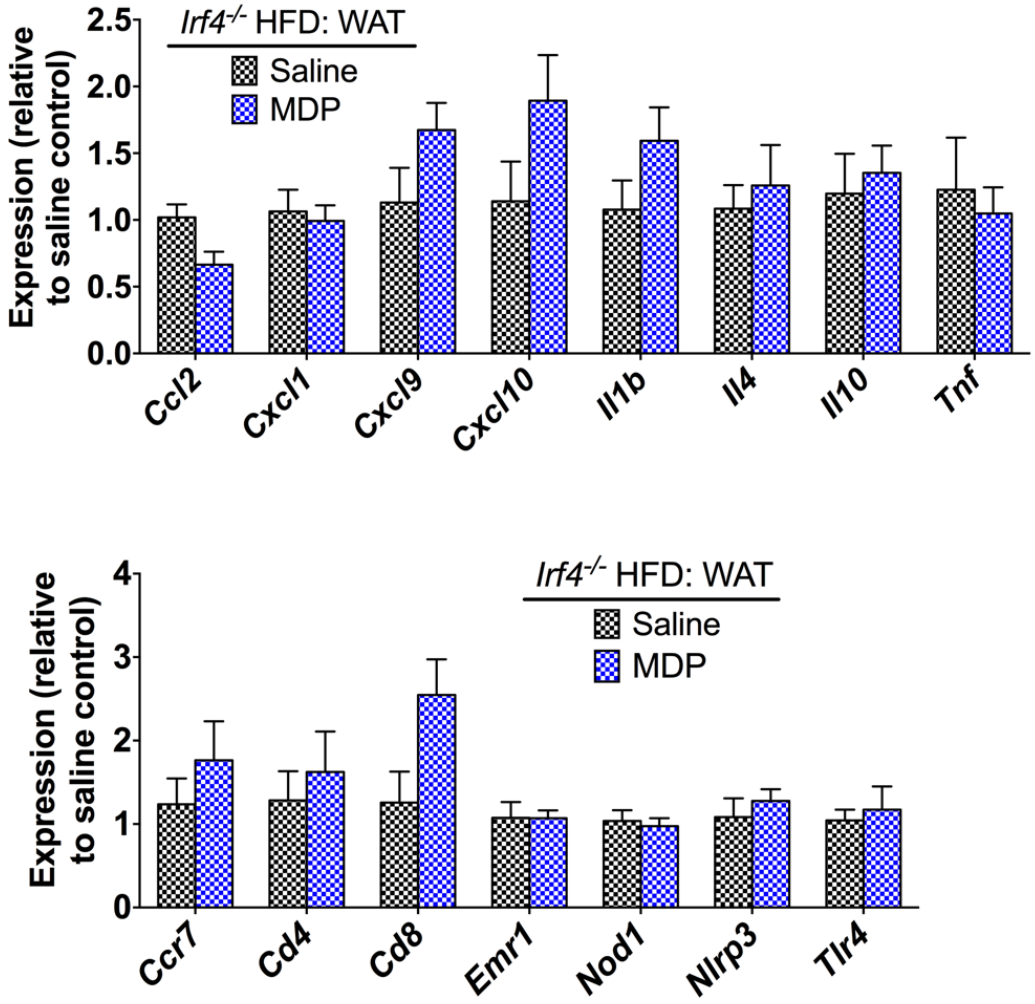

Figure 3.64 Adipose inflammation of *Irf4*$^{-/-}$ mice chronically treated with MDP.

White adipose tissue inflammatory gene expression of HFD-fed *Irf4*$^{-/-}$ mice that received saline or MDP for 5 weeks. n = 6 mice for each group. Values are mean ± SEM.

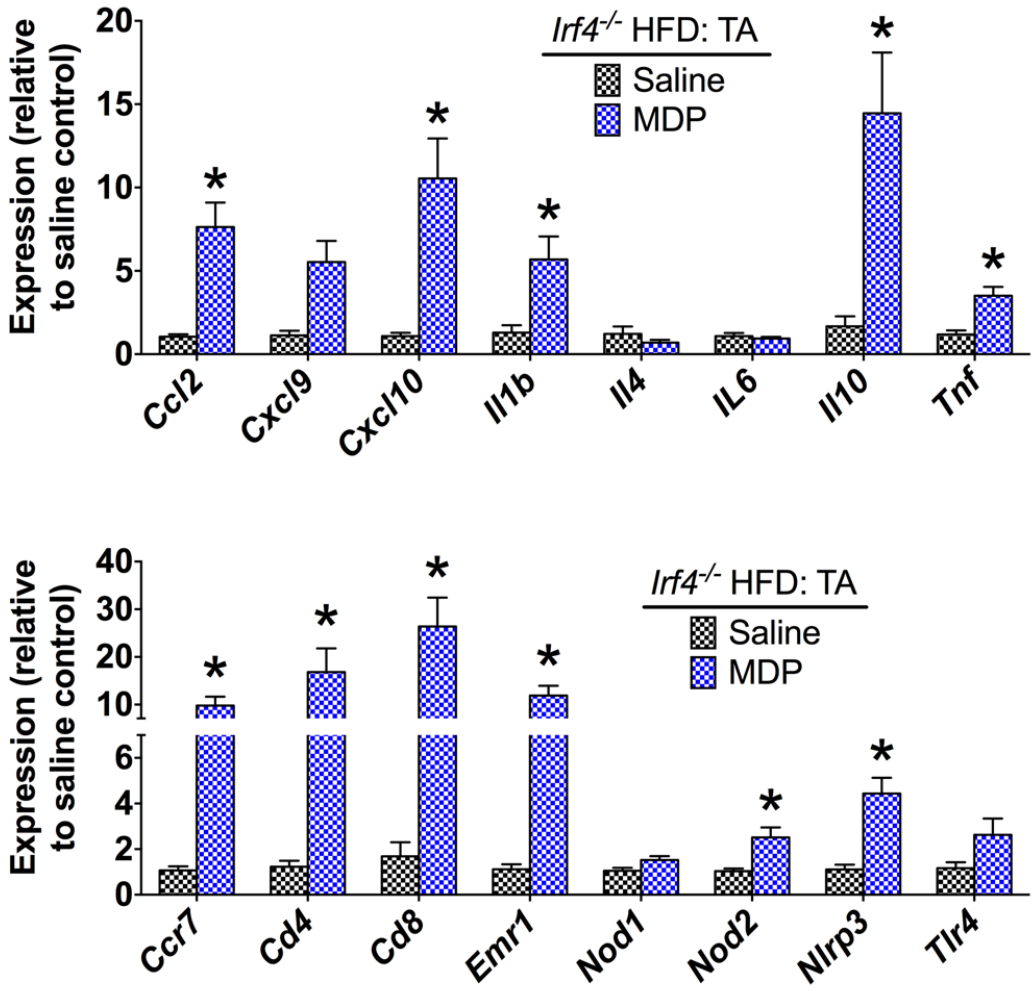

Figure 3.65 Muscle inflammation of *Irf4*$^{-/-}$ mice chronically treated with MDP.

Tibialis anterior inflammatory gene expression of HFD-fed *Irf4*$^{-/-}$ mice that received saline or MDP for 5 weeks. n = 6 mice for each group. Values are mean ± SEM. * indicates a significant difference between groups, as determined by Mann-Whitney *U* test on non-normally distributed data.

3.4.2 NOD2-mediated changes in glucose metabolism and inflammation during acute endotoxemia require IRF4

To establish if activating NOD2 also engages IRF4 in the "endotoxin-stress" *in vivo* experimental model (Figure 3.43), we first assessed metabolic tissues for altered *Irf4* expression. Three days of MDP treatment (without LPS) increased liver and adipose *Irf4* expression in WT mice (Figure 3.66). *Irf4* expression was higher in liver of MDP-treated animals at 2 and 6 hours after LPS injection in WT mice. Adipose tissue *Irf4* expression was lower at 2 and 6 hours post LPS injection irrespective of MDP treatment (Figure 3.66). In contrast to improved glucose tolerance in WT mice when MDP treatment preceded endotoxin challenge (Figures 3.45 and 3.48), *Irf4*$^{-/-}$ mice treated for 3 days with MDP and acutely challenged with endotoxin experienced no improvement in glucose tolerance (Figure 3.67) or changes in the HOMA-IR index (Figure 3.68) (the experiment in Figure 3.68 was performed by Dr. Kevin Foley). Intriguingly, treating mice with the NOD1-activating ligand FK565 in this endotoxin model increased glucose intolerance in both *Irf4*$^{-/-}$ mice (Figure 3.69) and WT mice (Figure 3.57). This result suggests that IRF4 specifically mediates NOD2-induced, but not NOD1-induced effects on glucose metabolism during acute endotoxemia.

Given the role of IRF4 in governing transcription, we assessed the contribution of this transcription factor on gene expression in metabolic tissues. In the liver, *Il10* was higher at both 2 and 6 hours post-endotoxin

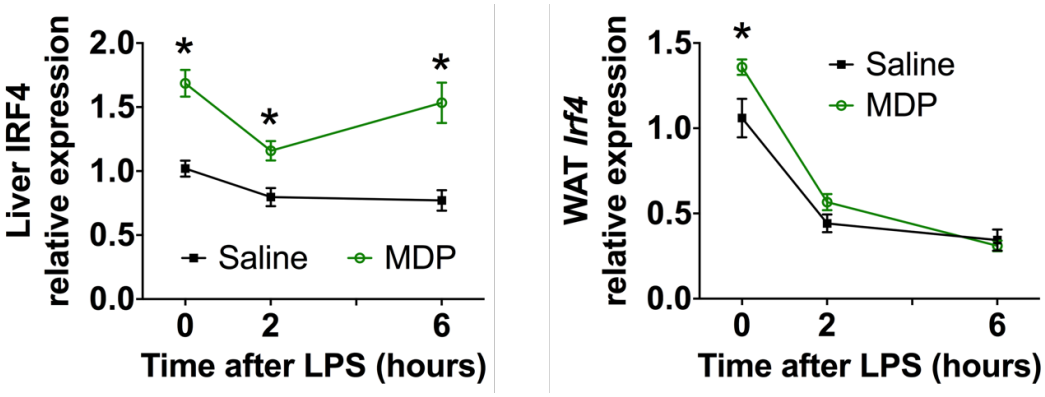

Figure 3.66 Tissue *Irf4* expression of WT mice treated with MDP prior to acute endotoxemia.

Liver and white adipose *Irf4* gene expression of control diet-fed WT mice that received saline or MDP for 3 days prior to acute endotoxemia. n = 9-10 mice for each group. Values are mean ± SEM. * indicates a significant difference between groups, as determined by two-way ANOVA.

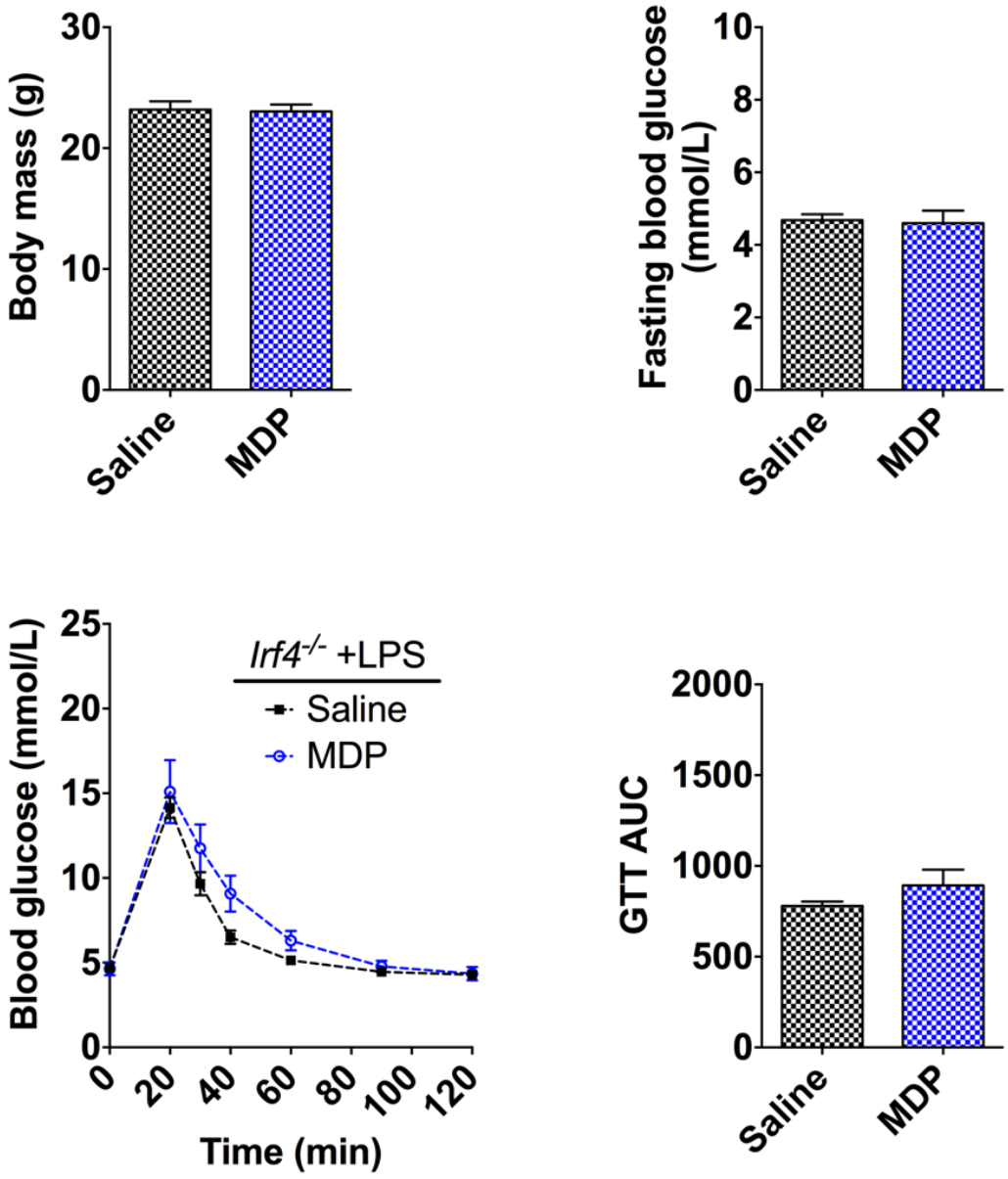

Figure 3.67 Glucose metabolism of *Irf4*$^{-/-}$ mice treated with MDP prior to acute endotoxemia.

Body mass, fasting blood glucose, and glucose tolerance test (2 g/kg) of control diet-fed *Irf4*$^{-/-}$ mice that received saline or MDP for 3 days prior to acute endotoxemia. n = 12-16 mice for each group. Values are mean ± SEM.

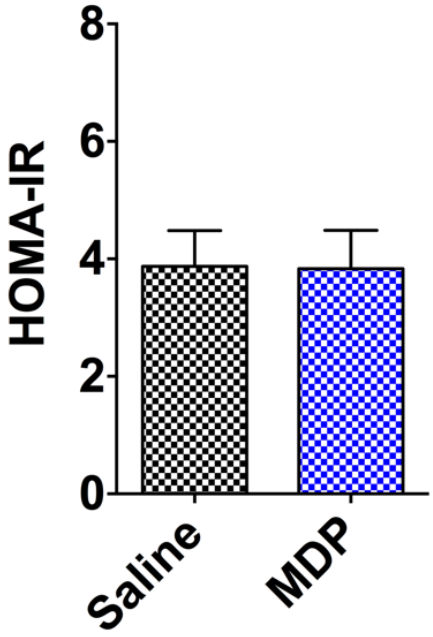

Figure 3.68 Insulin resistance index of *Irf4*$^{-/-}$ mice treated with MDP prior to acute endotoxemia.

Homeostatic model assessment of insulin resistance (HOMA-IR) of control diet-fed WT mice that received saline or MDP for 3 days prior to acute endotoxemia. n = 10-11 mice for each group. Values are mean ± SEM. This experiment was performed by Dr. Kevin Foley.

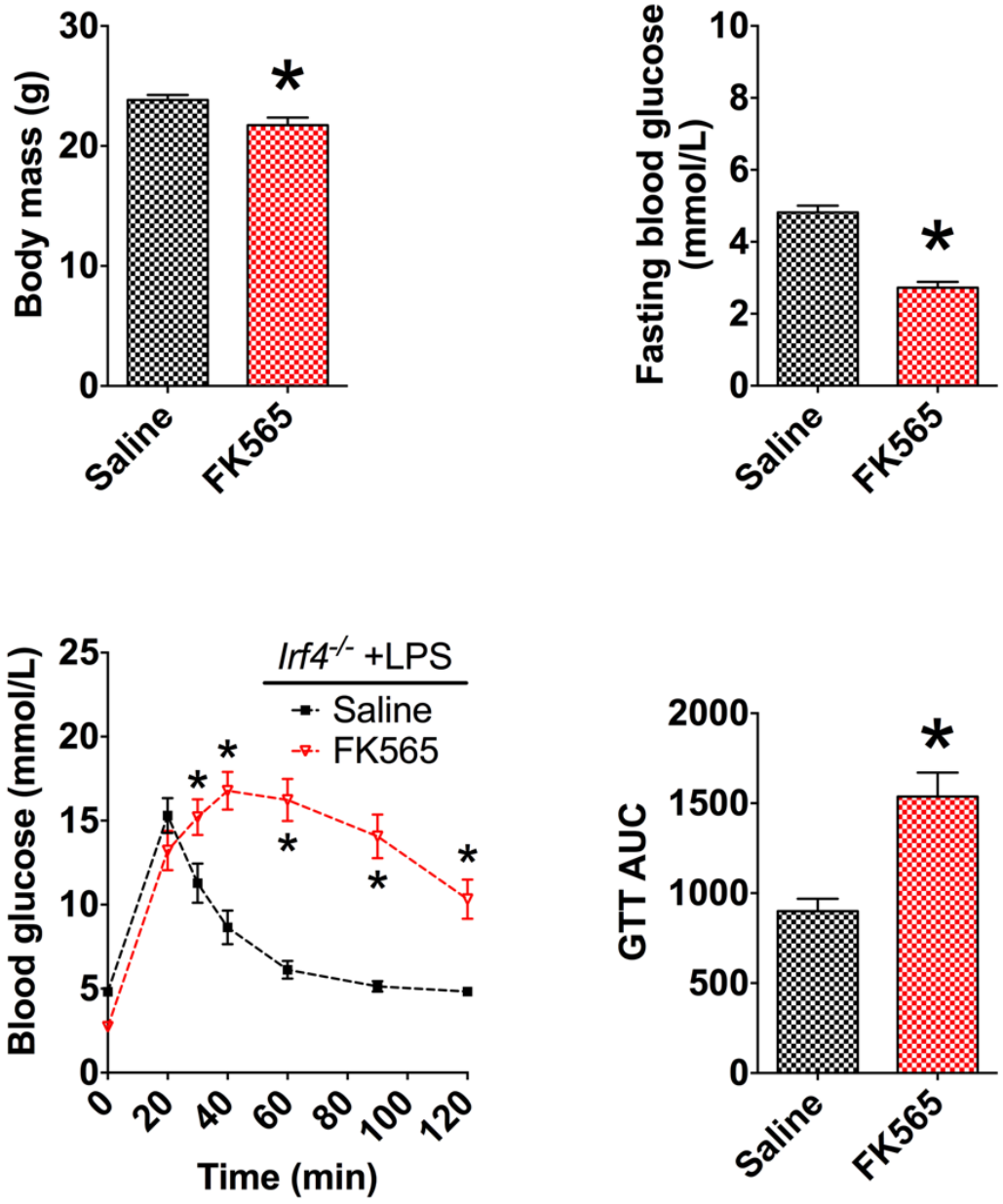

Figure 3.69 Glucose metabolism of *Irf4*$^{-/-}$ mice treated with FK565 prior to acute endotoxemia.

Body mass, fasting blood glucose, and glucose tolerance test (2 g/kg) of control diet-fed *Irf4*$^{-/-}$ mice that received saline or FK565 for 3 days prior to acute endotoxemia. n = 14-15 mice for each group. Values are mean ± SEM. * indicates a significant difference between groups, as determined by two-way ANOVA (line graph) or Mann-Whitney *U* test (body mass, fasting blood glucose, and AUC graphs) on non-normally distributed data.

challenge in MDP-treated WT mice compared to *Irf4*$^{-/-}$ mice (Figure 3.70). This finding is consistent with the fact that IRF4 binds to the promoter of *Il10* to regulate expression of this anti-inflammatory cytokine (312). Hepatic *Il1b* expression was significantly lower at 2 hours post-LPS in WT mice treated with MDP compared to *Irf4*$^{-/-}$ mice (Figure 3.70), further suggesting that MDP treatment contributes to IRF4-dependent suppression of certain inflammatory responses in the liver during acute endotoxin challenge. However, injecting MDP prior to LPS resulted in higher liver expression of some pro-inflammatory cytokines such as *Tnf* and *Il6* in WT compared to *Irf4*$^{-/-}$ mice (Figure 3.70). These data suggest that IRF4 controls an MDP-induced inflammatory gene program in the liver. MDP did not have widespread effects on inflammatory markers in adipose tissue during acute endotoxemia (Figure 3.71).

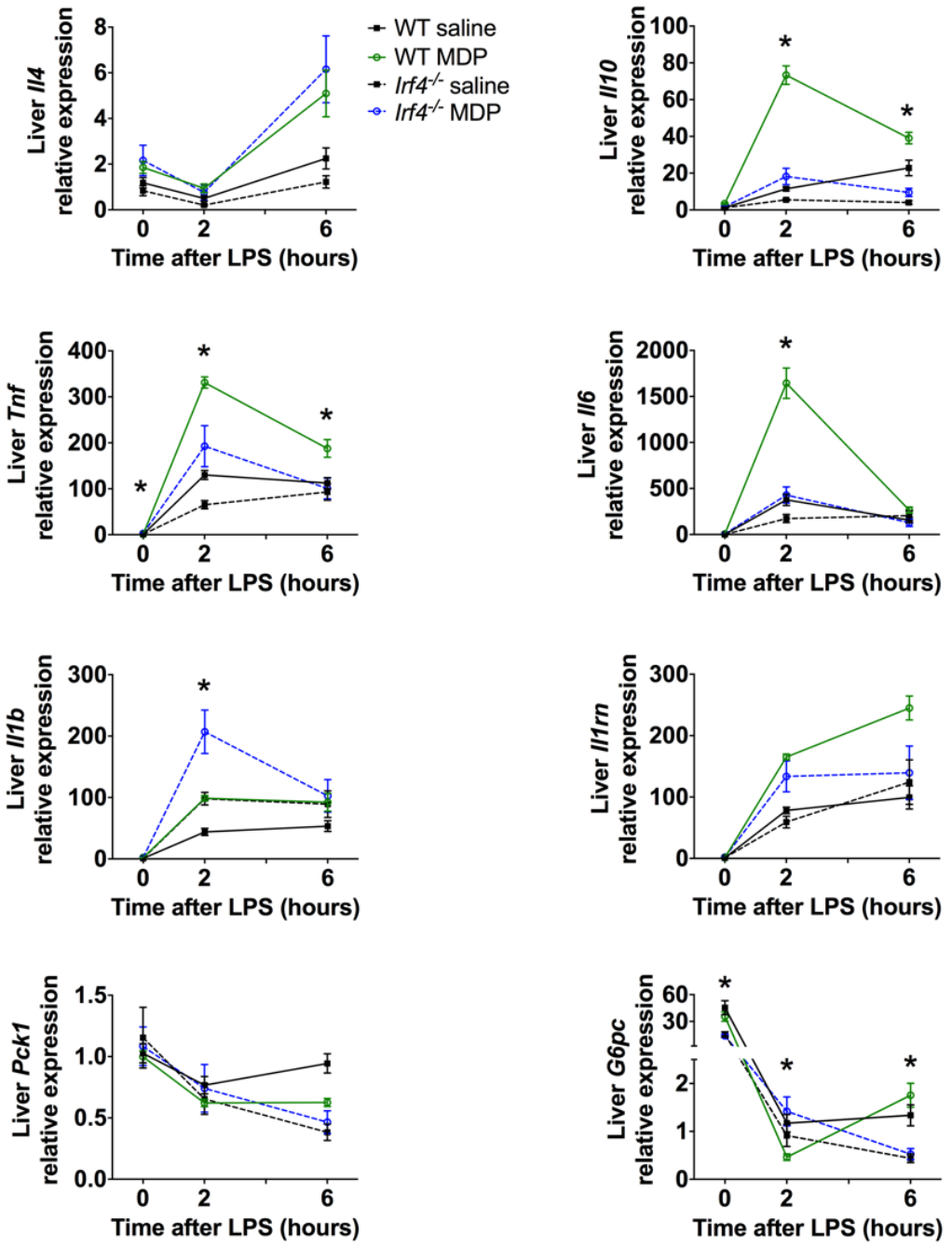

Figure 3.70 Liver inflammation of WT and *Irf4*$^{-/-}$ mice treated with MDP prior to acute endotoxemia.

Liver inflammatory gene expression of control diet-fed WT and *Irf4*$^{-/-}$ mice that received saline or MDP for 3 days prior to acute endotoxemia. n = 6-10 mice for each group. Values are mean ± SEM. * indicates a significant difference between groups, as determined by one-way ANOVA.

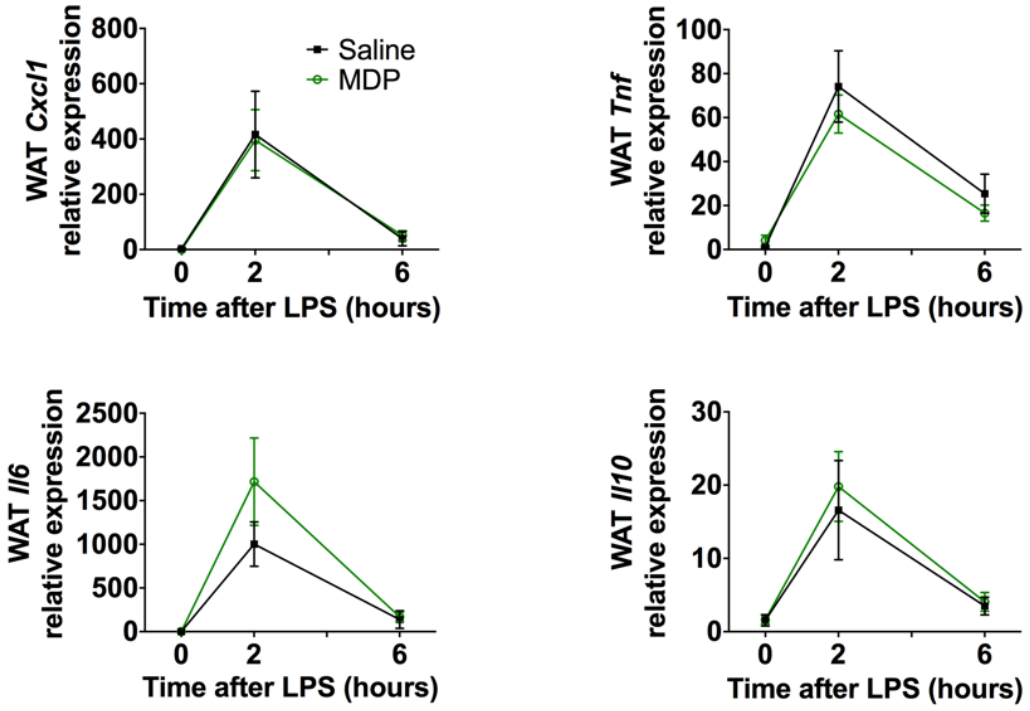

Figure 3.71 Adipose inflammation of WT mice treated with MDP prior to acute endotoxemia.

White adipose inflammatory gene expression of control diet-fed WT mice that received saline or MDP for 3 days prior to acute endotoxemia. n = 5-6 mice for each group. Values are mean ± SEM.

CHAPTER FOUR: Discussion and future directions

4.1 Introduction

The prevalence of obesity is increasing worldwide. Obesity is a risk factor for developing type 2 diabetes, which is often preceded by insulin resistance. Obesity is also associated with increased chronic inflammation that can contribute to insulin resistance in metabolic tissues. The burgeoning field of immunometabolism explores the link between immunity and metabolism and is relevant to many aspects of metabolic disease. Bacterial-sensing systems of the innate immune system are a potential link between host metabolism and immunity. It is known that the intracellular innate immune bacterial peptidoglycan-sensing NOD proteins contribute to metabolic inflammation and insulin resistance. The objective of this thesis is to characterize the immunometabolic effects of NOD signaling during obesity and metabolic disease, and the potential physiological relevance to blood glucose control and cellular mechanisms underpinning immune responses compartmentalized in metabolic tissues.

4.2 Deletion of *Nod2* and HFD-induced obesity

4.2.1 Whole-body NOD2 is required for maintenance of insulin sensitivity during diet-induced obesity

The contribution of innate immune system components to specific aspects of metabolic disease have recently been described. Many pattern recognition receptors of the innate immune system have been linked to

changes in glucose control. For example, a role for TLRs, including TLR2, 4, 5 and 9, in altering insulin sensitivity and blood glucose control has been described (243,333,336–342). In addition, NOD proteins have been implicated as a link between innate immunity and insulin sensitivity. Deletion of *Nod1* protected mice from glucose intolerance during diabetogenic diet-feeding (278). Furthermore, deletion of both *Nod1* and *Nod2* in HFD-fed, obese mice reduced insulin intolerance and inflammation, and acute *activation* of NOD1 exacerbated metabolic tissue inflammation and insulin resistance (237). Thus, NOD1 appeared to be deleterious during metabolic disease. A clearly defined role for NOD2 was not identified in these studies. The abundance of studies on the role of NOD2 in inflammatory diseases describe this bacterial-sensing protein as a dampener of chronic inflammation (295,302–306,343–347). In Denou et al., we expanded on this knowledge gap and found that whole body deletion of *Nod2* exacerbated insulin resistance in obese mice (316). Thus, we found that NOD2 is a critical protective immune response that helps to maintain insulin sensitivity and limits metabolic tissue inflammation during HFD-induced obesity in mice. The findings from this thesis highlighted a key role for NOD2 in adipose, liver, and intestinal tissues. However, conclusions drawn from whole-body deletion studies of *Nod2* limited analyses of the contributions of specific cell populations in different tissues.

4.2.2 Immune cell NOD2 is not required for metabolic protection during HFD-induced obesity

In this thesis, we performed targeted *Nod2* deletions in different cell populations in mice. This prompted the investigation of the cell types and pathways that were engaged upon NOD2 activation. We first deleted *Nod2* from immune cells by lethally irradiating WT recipient mice, killing most immune stem cells derived from bone marrow. We then reconstituted their immune cell progenitors using bone marrow from donor WT and *Nod2*$^{-/-}$ mice. We replicated the experimental conditions described in Denou et al. in order to test if glycemic control was altered in mice that lack immune cell NOD2 (NOD2 chimera mice). We already knew that whole-body deletion of *Nod2* worsened dysglycemia in HFD-fed mice (316). Here, we found that HFD-fed immune cell *Nod2*-deleted mice had similar glycemic control compared to mice that were irradiated and repopulated with WT bone marrow (control counterparts). Thus, our results suggested that radio-sensitive immune cell NOD2 was dispensable for maintaining insulin sensitivity during diet-induced obesity. If immune cell NOD2 was important for metabolic protection, we would hypothesize that deleting it from the hematopoietic system would have resulted in increased insulin resistance. This result was interesting, as hematopoietic NOD1 has been demonstrated to contribute to metabolic inflammation and insulin resistance (348). Thus, the divergent effects of NOD1 versus NOD2 signaling appear to also

engage responses that are derived from different cellular sources during metabolic disease.

It should be noted that a small subset of original immune stem cells in recipient mice were resistant to the two rounds of irradiation. The presence of these "radio-resistant" cells is a common occurrence in the creation of chimeric mice. In addition, liver resident macrophages (Kupffer cells) with functional NOD2 were likely present in these NOD2 chimera mice. This is because Kupffer cells have a long turnover time before they are replenished from the hematopoietic compartment (349). To prevent this from occurring in future chimeric mouse studies, treatment of animals with clodronate liposomes has been shown to effectively deplete resident hepatic macrophages (350). Although it can be suggested that these persistent immune cell populations could mediate the protective effects of NOD2, experiments completed in parallel by collaborating investigators aid in explaining why this is unlikely. In addition to creating WT mice with *Nod2*$^{-/-}$ immune cells, as presented in this thesis, the Rémy Burcelin lab also generated "inverse" chimera mice (i.e. WT immune cells into *Nod2*$^{-/-}$ recipients). These *Nod2*$^{-/-}$ mice with an immune system derived from WT hematopoietic cells were more glucose intolerant and more insulin resistant than WT control mice. Thus, mice that lack NOD2 in non-hematopoietic cells have poorer glucose control during obesity. This result is similar to the response in obese mice that lack whole-body NOD2 (316). Together, these

studies indicated that the protective effects of NOD2 were mediated by non-immune cell populations during HFD-induced obesity.

We next tested if NOD2 activation with MDP required immune cells to promote improved glucose control. These experiments provided additional confirmation that NOD2 in immune cells was dispensable for the effects of NOD2 signaling on glycemia. Control diet-fed $NOD2^{-/-BMT}$ mice subjected to our acute low-level endotoxemia model responded to MDP treatment and had increased glucose tolerance, which mirrored the improved glycemic control in MDP-injected WT mice. Altogether, our data, and our collaborator's inverse chimera experiments, demonstrated that the consequences of both *Nod2* deletion and activation did not require NOD2 signaling within hematopoietic-derived immune cells. These findings were interesting because the purported function of NOD2 is to mediate an innate immune response to invading pathogens, where defense to external bacterial stimuli are commonly derived from immune cells (253,351). However, it should also be considered that there is a benefit, and possibly a requirement, for detection of bacterial danger signals within *all* cells of a host in order to limit infection and potentially modify other critical cell functions, including metabolism. Thus, our results here were in agreement with other studies showing that, while *Nod2* is expressed and can have direct effects within immune cells, hematopoietic NOD2 can be dispensable

for inflammatory disease pathology. These results were consistent with previous findings in colitis experiments (352).

4.2.3 Hepatocyte NOD2 is not required for metabolic protection during HFD-induced obesity

Both *Nod1* and *Nod2* are expressed in hepatocytes, but there is evidence that only NOD1 is capable of initiating direct inflammation in this cell type in the absence of other stimuli, such as LPS, highlighting a key difference between NOD1 and NOD2 signaling within the liver (353). Experiments from our lab demonstrated that HFD-feeding in mice increased expression of *Nod2* transcript in hepatocytes (versus non-hepatocyte liver cells) compared to control diet-fed animals. These findings highlighted a possible role for NOD2 in driving metabolic effects in a key metabolic tissue (316). Indeed, deletion of whole-body *Nod2* in obese mice revealed extensive liver phenotypes, including increased inflammation, lipid deposition, and insulin resistance (316), thus demonstrating a protective role for NOD2 signaling during metabolic disease. Not all experimental models are equivalent because there is evidence showing that hepatic NOD2 signaling has been implicated in exacerbating experimental hepatitis in mice (354). Therefore, clarifying the contribution of NOD2 in hepatocytes during the stress of diet-induced obesity in aspects of metabolic disease and metabolic inflammation was our next goal.

Based on available evidence, hepatocyte NOD2 was a logical next step to investigate to determine the cell type responsible for whole-body NOD2 metabolic phenotypes during obesity. Using a genetic approach, we deleted the *Nod2* gene from hepatocytes specifically by crossing an albumin-cre transgenic mouse with a mouse possessing *loxP* sequence-flanked *Nod2*. In this system, cre-lox recombination would occur only in hepatocytes due to the hepatocyte-specific expression of albumin-cre recombinase (321). The advantage of this approach (versus adenovirus-targeted deletion) was that the gene deletion is established within the germ cells of the offspring during development, thus preventing small populations of genetically unmodified (WT) cells from persisting and thus limiting experimental findings. After confirming the genetics of hepatocyte NOD2 knockout ($Nod2^{-/-HKO}$) and control mice, we replicated the experimental conditions described in Denou et al. that probed whole-body *Nod2* deletion (316). We found that HFD-fed hepatocyte NOD2 knockout mice were metabolically indistinguishable to littermate WT control mice. Therefore, our results showed that hepatocyte NOD2 was not required for maintaining insulin sensitivity during obesity.

We next tested if hepatocyte NOD2 was required for improvements in glycemia induced by NOD2 activation with MDP. Our results confirmed that NOD2 in hepatocytes was dispensable for the effects of MDP-induced activation of NOD2 signaling during acute low-level stress of a model of

metabolic endotoxemia. Control diet-fed NOD2$^{-/-HKO}$ mice subjected to acute low-level endotoxemia had increased glucose tolerance after MDP treatment, mirroring the improved glycemia caused by MDP in WT mice. Thus, our results with hepatocyte NOD2 knockout mice demonstrated that the consequences of both *Nod2* deletion and activation did not require NOD2 signaling within hepatocyte cells of the liver.

These findings were somewhat surprising because many liver-centric phenotypes were observed in whole-body *Nod2*$^{-/-}$ mice and NOD2 activation experiments using MDP. For example, whole-body deletion of *Nod2* caused increased immune cell infiltration, inflammation, and triglyceride deposition within the liver (316). Additionally, whole-body *Nod2* deletion caused increased HGO (from liver insulin insensitivity) and pyruvate intolerance. When NOD2 was *activated* in WT mice, liver-centric improvements in glucose control and inflammation were observed. Specifically, MDP treatment decreased hepatic inflammation, increased insulin-mediated suppression of HGO in obesity and endotoxemia models, and increased pyruvate tolerance. Therefore, whole-body deletion of *Nod2* facilitated effects within the liver despite both hepatocyte and immune cell (essentially the entire liver) NOD2 not being necessary for these phenotypes.

It is not yet clear how to reconcile these liver-centric effects of NOD2, despite *Nod2* being dispensable within hepatocytes. It was possible that the

effects on the liver were downstream of the primary NOD2 signaling event in another tissue, thus eliminating the need for functional NOD2 within hepatocytes. Although not directly supported by the evidence presented in this thesis, this speculation can be explained by the nature of recently described extracellular vesicles that can communicate between metabolic tissues. In particular, extracellular vesicles from adipose tissue have been shown to greatly expand the immunoregulatory crosstalk of adipose resident immune cells with distant tissues of the body including skeletal muscle and the liver (355–360). As the majority of NOD2 activation effects on inflammation occurred in mouse adipose tissue in our obesity model, it is possible that extracellular vesicles from adipose relayed signals such as cytokines, metabolites, or microRNAs to the liver, thus circumventing the need for intact hepatocyte *Nod2*. Regardless of the mechanism, the effects observed in this study and others from our lab contributed to the concept of compartmentalization of immune responses induced by NOD2, and also demonstrated the interconnectedness of metabolic tissues during obesity.

4.3 NOD activation and obesity

The previous sections in this thesis discussed various consequences associated with *Nod2* deletion in mice. The conclusions drawn from those studies aided the remainder of experiments that characterized the consequences of activating NOD2 in multiple inflammatory animal models.

The benefits of such experiments were twofold: understanding the mechanisms that link the innate immune system with metabolic health, and informing the potential development of novel therapeutics to combat metabolic disease. Activation of innate immune receptors that are known inflammatory factors, such as NOD1 or TLRs, is associated with increased inflammation and insulin resistance (95,235,237,244,276,280,282,348,361–364). However, NOD2 is uniquely positioned as a mediator of immune tolerance to inflammation in cell models and *in vivo* studies of inflammatory bowel disease (295,302–306,343–346,365–367). The contribution of chronic NOD2 activation to metabolic inflammation and glucose homeostasis during obesity, at this time, was not known.

4.3.1 Physiological effects of NOD2 activation during obesity

We built upon the known immune-regulating capabilities of NOD2 signaling and probed the inflammatory effects of chronic NOD2 activation during HFD-induced obesity in mice. Our initial experiments involved characterizing the physiological effects of intraperitoneal injections of MDP. When studying obesity-related metabolic disease characteristics in mice, it is important to consider potential changes in body mass that directly correlate with glucose control (368). Ligand activation of immune receptors such as TLR4 and NOD1 can cause weight loss in mice (369). Therefore, it

was important to first determine whether chronic NOD2 activation would induce changes in body weight or adiposity in mice that could confound interpretation of metabolic results. In contrast to other PRRs, activating NOD2 with MDP for 5 weeks had no significant impacts on body mass, metabolic and non-metabolic tissue mass, adiposity, or lipid deposition in liver or muscle. However, acute activation of NOD1 with its ligand FK565 induced significant weight loss and relative glucose intolerance in mice (Figure 4.1), which precluded us from assessing the chronic effects of NOD1 activation during HFD-induced obesity.

4.3.2 Metabolic effects of NOD2 activation during obesity

It was known that NOD1 ligands can induce acute insulin resistance in control diet-fed mice (237). Actually, NOD2 ligands, including certain MDP derivatives, can induce acute, transient insulin resistance in control diet-fed mice. This effect was observed to be much smaller compared to NOD1 activation, lasted for less than 24 hours, and was limited to reduced peripheral glucose disposal (237). The effect of chronic treatment with MDP on both glucose and insulin tolerance in HFD-fed mice was not known and was tested in this thesis. It was discovered that MDP improved glucose and insulin tolerance and improved hepatic insulin sensitivity during obesity in mice. The glucose-lowering effects of chronic MDP treatment were dependent on both NOD2 and RIPK2, confirming the receptor-ligand and

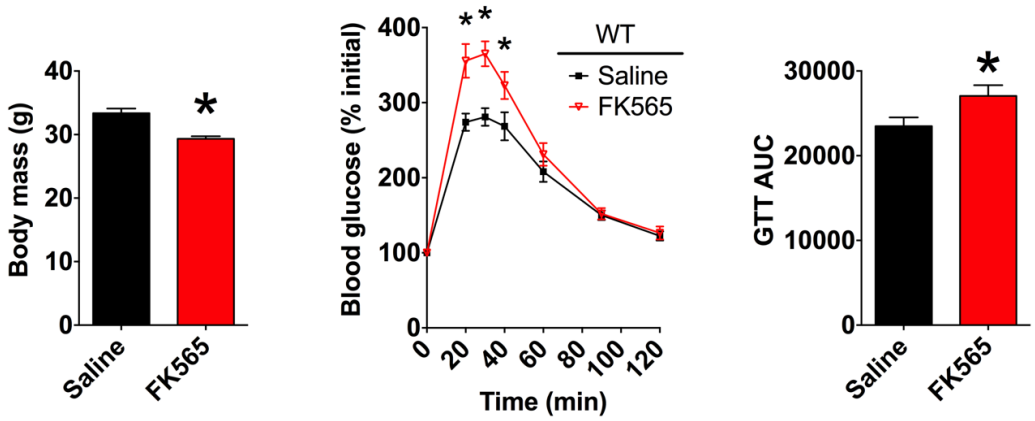

Figure 4.1 Glucose metabolism of WT mice treated with FK565.

Body mass and glucose tolerance test (2 g/kg) of control diet-fed WT mice that received saline or FK565 for 3 days. n = 10 mice for each group. Values are mean ± SEM. * indicates a significant difference between groups, as determined by two-way ANOVA (line graph) or unpaired two-tailed *t*-test (body mass and AUC graphs) on normally distributed data.

pathway specificity (327). Results using knockout mouse strains also demonstrated that the ligand solutions were not contaminated with other PRR activators, such as LPS.

The improved glycemic control and metabolic effects of MDP treatment were dependent on the stress of obesity (or low-level endotoxemia), but independent of dietary fat content. This is best evinced by the fact that control diet-fed leptin-deficient (*ob/ob*) mice that are obese due to hyperphagia were more glucose tolerant during MDP treatment. In contrast, glucose tolerance was unchanged in control diet-fed lean WT mice.

Experiments aimed at determining the key tissues responsible for mediating the metabolic effects of MDP revealed an important role for the liver in altered blood glucose control. Hyperinsulinemic-euglycemic clamp results demonstrated that MDP treatment increased the sensitivity of mouse livers to the suppressive effect of insulin on hepatic glucose production. In contrast, adipose-targeted experiments, such as insulin-mediated uptake of radioactive 2DG, showed that MDP did not have adipose-specific effects on insulin sensitivity in either model of murine obesity, including control diet-fed *ob/ob* mice or HFD-fed WT mice. This result was in agreement with data from the hyperinsulinemic-euglycemic clamp, which showed no change in tissue glucose disposal rate induced by MDP, also suggesting a limited role

for the contribution of MDP-induced effects on skeletal muscle to changes in glucose control.

The metabolic improvements of NOD2 activation were also effective in an acute setting despite the establishment of obesity. After obesity had manifested for 10 weeks by long-term HFD-feeding in untreated mice, 3 days of MDP ligand injections significantly increased glucose tolerance compared with control animals. Similar treatment with the minimal bioactive motif that activates NOD1, iE-DAP, had no effect on glucose tolerance in this acute model, reinforcing the fact that NOD1 and NOD2 have divergent effects on glucose metabolism. This protocol was a significant departure from the one used above, as it reduced the amount of treatments from 20 to 3. These results were interesting because they extended our findings with chronic MDP administration and demonstrated that similar results on glucose metabolism are possible when using a treatment model of obesity that is relatable to humans with established obesity (such as in an intervention approach to improve insulin action in obese individuals).

4.3.3 Inflammatory effects of NOD2 activation during obesity

Deletion of *Nod2* increases susceptibility to inflammatory pathologies including colorectal tumorigenesis in mice (299,300). Activation of NOD2 has well-established intestinal immunomodulatory effects in inflammatory bowel disease and experimental models of inflammation (305,306).

Expanding on these concepts, we next sought to assess whether chronic NOD2 activation could have similar inflammation-dampening effects during obesity.

In liver, chronic MDP treatment during HFD-feeding moderately decreased expression of classical pro-inflammatory genes, while not affecting expression of anti-inflammatory or immune cell genes. Hepatic *Tlr4* expression was significantly increased in MDP-treated mice. This finding was interesting because activation of hepatocyte TLR4 has been shown to contribute to obesity-induced inflammation and insulin resistance (243). However, our data was derived from whole-liver homogenates containing various cell types, therefore it could not be concluded that hepatocytes were responsible for this increased *Tlr4* expression. Additionally, despite this increased *Tlr4* expression, overall hepatic inflammation (both NF-κB activity and inflammatory transcript expression) was not increased, and the liver was also the main tissue in which MDP increased insulin sensitivity during the hyperinsulinemic-euglycemic clamp. Therefore, this increase in hepatic *Tlr4* expression appeared to have minimal consequences in terms of glucose control. It is also plausible that TLR4 signaling did indeed contribute to inflammation, and the effect was masking the true potential of NOD2 activation in liver. If this scenario were true, then inhibiting TLR4 signaling (already known to protect against HFD-

induced inflammation and insulin resistance (341,370,371)) in addition to activating NOD2 may lead to enhanced anti-inflammatory effects.

In white adipose tissue, chronic NOD2 activation had widespread anti-inflammatory effects. First, NF-κB activity was reduced by approximately 40% compared to control-treated animals. Expression of many pro-inflammatory cytokines and immune cell markers was significantly decreased by MDP treatment. Pattern recognition receptor gene expression of *Nod1*, *Nlrp3*, and *Tlr4* (but not *Nod2*) was also significantly, yet more moderately, decreased in adipose tissue after MDP treatment. We analyzed the whole adipose tissue in these experiments and changes in gene expression could have been derived from both adipocytes and the extent of pro-inflammatory polarization of adipose tissue resident immune or stromal cells. Interestingly, expression of some classical anti-inflammatory markers was also decreased by MDP, suggesting that chronic NOD2 activation was so potent in this tissue that immunomodulating cytokines such as IL4 and IL10 were unnecessary in this setting to combat the inflammation induced by HFD-feeding and obesity. Together these data suggested that the adipose tissue of NOD2-activated animals had fewer inflammatory immune cells and the overall inflammatory state in the adipose tissue was lower compared to vehicle-treated mice, which was consistent with NOD2 activation providing immune tolerance during an additional stress (302–304).

Interestingly, MDP did not have anti-inflammatory effects across different metabolic tissues. Analysis of tibialis anterior muscle revealed that MDP treatment moderately increased expression of pro-inflammatory genes and immune cell markers, indicating that muscle was in a heightened state of inflammation under NOD2-stimualted conditions. This result was in agreement with *in vitro* observations from our lab showing that MDP stimulation caused muscle cell-autonomous pro-inflammatory responses (332). This result also provides an additional example of the compartmentalization of innate immune responses: the immunomodulatory effects of NOD2 activation lead to decreased inflammation in adipose and liver, but increased inflammation in skeletal muscle. While the MDP-dependent increases in muscle inflammation could have conceivably impacted whole-body or muscle-specific glucose metabolism, as comparatively shown in cell culture models (332,372), there was no measurable change on peripheral tissue glucose disposal during hyperinsulinemic-euglycemic clamp experiments. This conclusion could be supported by further/direct testing of insulin action *in vivo* in mice treated chronically with MDP (e.g. 2DG-uptake).

Beyond the metabolic tissues discussed above, MDP treatment had only minor effects. The spleen is a major reservoir of monocytes that the body can use to regulate systemic inflammation, and therefore any large skewing of splenic immunity would have indicated a possible change in

systemic immunity (373). In the spleen, chronic NOD2 activation had only a minor impact on markers of inflammation.

Studies on the inflammatory effects of MDP have the potential to inform future human treatments using NOD2 activation therapy. Therefore, it was important to consider whether chronic NOD2 activation, given its known immunomodulatory capability and significant anti-inflammatory activity in adipose tissue (374), would have a quantifiable impact on host ability to resist infection. Therefore, we assessed the systemic effects of NOD2 activation on host immunity. Through analysis of serum cytokine levels, we observed that chronic MDP treatment did not induce changes in systemic cytokine levels in mice. Additionally, NOD2-activated mice were not more susceptible to death throughout all studies compared with saline-treated animals, and chronic MDP treatment has been demonstrated to be protective against infection (375).

The findings from this section described the inflammatory-modulating effects of NOD2 activation. Chronic MDP treatment was anti-inflammatory in adipose and liver, but pro-inflammatory in muscle. There was no whole-body inflammatory theme of NOD2 activation, but rather compartmentalized effects in different tissues. Despite the inflammatory variance in different tissues, MDP treatment was insulin-sensitizing during HFD-induced obesity.

4.4 NOD activation and endotoxemia

Certain models of obesity are associated with an increased quantity of circulating bacterial LPS that can contribute to metabolic inflammation and insulin resistance. Experimentally raising circulating LPS is sufficient to promote inflammation and insulin resistance (95). Obesity also upregulates adipose tissue TLR signaling in mice (333). NOD2 signaling negatively regulates inflammation from TLR ligands (302,304–306), therefore we hypothesized that mice deficient in the ability to sense LPS would not engage in the stress during endotoxemia that is required for MDP to potentiate its effects on blood glucose. Results from these experiments would help to decipher the mechanism of action of chronic NOD2 activation.

Chronic MDP treatment in LPS-receptor mutant C3H/HeJ mice fed a HFD caused *more* glucose intolerance, in contrast to the improved glucose tolerance during MDP treatment in WT mice. This result suggested that inhibition of TLR4 signaling was at least one mechanism of action of MDP treatment during obesity. Given the known contribution of TLR signaling to obesity, metabolism, and inflammation (95,333), we developed an *in vivo* model of acute endotoxemia in control diet-fed WT mice using a TLR4-specific ligand in order to directly and specifically investigate the interactions between NOD2 and TLR signaling.

4.4.1 Metabolic effects of NOD2 activation during acute endotoxemia

MDP treatment alone had no discernable effect on glucose metabolism when tested 24 hours after the last injection in control diet-fed mice. However, MDP treatment prior to an acute dose of endotoxin increased glucose tolerance. Thus, in the absence of any other stressor such as HFD or LPS, MDP alone did not affect glucose metabolism in our models. These results were consistent with studies demonstrating that acute MDP pre-stimulation alone, approximately 24 hours before experimental measurement, did not affect inflammatory cytokine production (302,304). However, acute treatment with MDP can also precipitate minor metabolic defects depending on the timing of treatment. For example, insulin-stimulated glucose disposal was decreased in mice 6 hours after MDP treatment but these effects were small compared to the more potent effects of NOD1 activation (237). Thus, there appears to be a priming period where NOD2 activation stimulates a small pro-inflammatory response characterized by inflammatory cytokines and anti-microbial peptides (271), but is followed by a tolerizing period where NOD2 signaling shifts to an immunomodulatory state to dampen the inflammatory response.

Acute endotoxemia creates a highly insulin resistant state (376). As a result, this model of insulin resistance was particularly useful in revealing the insulin-sensitizing capability of MDP treatment. For example, we

analyzed the insulin secretion of mice during a GTT. We found that MDP-treated and LPS-challenged mice, in addition to being significantly more glucose tolerant, secreted significantly less insulin during glucose challenge compared to LPS-challenged control mice. Together these data suggested that mice primed with MDP were so sensitive to insulin that they did not require additional insulin release to manage the glucose load. An additional metric of insulin resistance, HOMA-IR (325), was significantly lower in NOD2-activated animals acutely challenged with endotoxemia.

Hyperinsulinemic-euglycemic clamps revealed a hepatic insulin-sensitizing phenotype in MDP-treated mice challenged with LPS. Further testing of the liver by pyruvate challenge in this model confirmed an effect of MDP on hepatic glucose production. This phenotype was consistent with the effects of MDP observed in our model of diet-induced obesity, strongly supporting a role for NOD2 activation as an insulin-sensitizer in the liver. Interestingly, treatment of hepatocyte NOD2 knockout mice with MDP in our acute endotoxemia model increased glucose tolerance similar to WT mice. This finding was also consistent with effects in our diet-induced obesity model where just 3 injections of MDP was sufficient to improve glucose tolerance, identical to WT mice. Thus, in endotoxemia and obesity models, NOD2 activation sensitized the livers of mice to insulin in a hepatocyte-NOD2-independent manner.

The effects of MDP in this model were dependent on NOD2 and RIPK2, consistent with observations in our obesity model. Hematopoietic NOD2 was dispensable for improved glucose tolerance, supporting the conclusion that immune cells were not the primary location of NOD2 signaling effects. This result was interesting because studies comparing the roles of non-hematopoietic and hematopoietic NOD2 in the context of Crohn's disease pathogenesis have shown that non-hematopoietic cells were the key responsive population to the effects of MDP (377,378).

4.4.2 Metabolic effects of NOD1 activation during acute endotoxemia

As a comparison for the metabolic effects of pattern recognition receptor activation, we wanted to assess the metabolic consequences of NOD1 ligand injection *in vivo*. As mentioned above, testing NOD1 activation in our long-term obesity model was not feasible as this chronic treatment caused significant weight loss in mice. Activating NOD1 in an acute setting, such as in our endotoxemia model, would better allow for comparing the effects of NOD1 versus NOD2 signaling on glucose metabolism. Compared to mice treated with MDP prior to endotoxemia, mice treated with the NOD1-activating ligand FK565 were markedly glucose intolerant in a NOD1- and RIPK2-dependent manner. This result highlighted the striking difference between NOD1 and NOD2 signaling in the context of metabolism, and built

upon previous descriptions of the divergent functions of these PRRs (235,237,278,282,348).

4.5 Role of IRF4 in NOD-mediated metabolic and inflammatory changes during obesity and acute endotoxemia

The tolerance effect mediated by NOD2 in many studies has been reported to be a product of the transcription factor IRF4. IRF4 controls Th2 inflammation to limit aberrant immune responses (312,313,379,380), and controls TLR-induced inflammation (307,308,343). This transcription factor has also been implicated in obesity-induced inflammation and has a direct role in insulin sensitivity (310,311,381,382).

Our study with TLR4 (LPS receptor) mutant mice supported the role of IRF4 in regulating inflammation during obesity that can manifest in perturbed glucose metabolism. Mice lacking functional TLR4 treated with MDP displayed decreased glucose tolerance, suggesting that suppressing the LPS-sensing pathway in mice was at least one mechanism driving the metabolic effects of MDP during obesity. Expression of *Tlr4* in WAT was decreased by MDP treatment and this effect was found to be dependent on IRF4 (Figure 3.32 versus 3.64). Our finding was consistent with the known effects of IRF4 driving negative regulation of TLR-mediated inflammation (307,308). This result prompted further testing to determine whether IRF4

was involved in our obesity and acute endotoxemia phenotypes of NOD2 activation.

4.5.1 HFD-induced obesity: IRF4 and MDP

In our obesity model, WT mice treated with MDP had higher *Irf4* expression in liver and white adipose tissue, and this result was dependent on NOD2. This result was our first link connecting chronic NOD2 signaling during obesity with IRF4. Strikingly, MDP did not improve glucose tolerance in *Irf4*$^{-/-}$ mice. This result demonstrated that the glucose-tolerizing effects of MDP were wholly dependent on the transcription factor IRF4 during obesity. Our results on glucose control are in agreement with studies showing that the inflammatory effects of NOD2 during colitis and colorectal tumorigenesis were dependent on IRF4 (300,305,306).

We next sought to understand the NOD2/IRF4 signaling axis by investigating whether our NOD2-mediated effects on inflammation required IRF4. Consistent with other groups that established a direct link between NOD2, IRF4, and TLR-mediated NF-κB activity (300), chronic NOD2 activation with MDP decreased NF-κB activity in white adipose tissue of WT, but not *Irf4*$^{-/-}$ mice. We next assessed gene expression profiles of metabolic tissues from WT and *Irf4*$^{-/-}$ mice chronically treated with MDP during obesity. Consistent with the NF-κB results, the widespread anti-inflammatory effect of MDP treatment observed in adipose tissue of WT mice did not occur in

Irf4$^{-/-}$ mice. Inflammatory responses in the liver and muscle of *Irf4*$^{-/-}$ mice changed in the same direction as WT mice treated with MDP, suggesting that NOD2 effects on inflammation in these tissues did not require IRF4. Interestingly, while the changes were in the same direction, the magnitude of changes in muscle tissue was greatly increased in *Irf4*$^{-/-}$ mice. This result was consistent with the loss of IRF4 being linked with exaggerated inflammatory responses (383). The result in adipose tissue was consistent with findings reported previously, showing that IRF4 can alter adipose tissue inflammation during obesity (310).

4.5.2 Acute endotoxemia: IRF4 and MDP

In our endotoxemia model, WT mice treated with MDP had higher *Irf4* expression in the liver, but not white adipose tissue, throughout endotoxin challenge compared with saline-treated control mice. Similar to the results using knockout animals in our obesity model above, *Irf4*$^{-/-}$ mice treated with MDP prior to acute endotoxemia did not display increased glucose tolerance compared to controls, unlike what was observed in WT mice. *Irf4*$^{-/-}$ mice also did not show improved HOMA-IR in response to MDP during endotoxemia. Overall, these results showed that MDP engages a NOD2- and IRF4-dependent response to promote better glucose control during the stress of endotoxemia.

We next tested if the NOD2 and IRF4 response was separate from NOD1. We contrasted the effects of NOD1 versus NOD2 using specific NOD1 ligands and knockout mice for *Nod1*, *Nod2* and *Irf4*. Our results revealed that *Irf4*$^{-/-}$ mice were responsive to the NOD1 ligand, FK565, but not the NOD2 ligand, MDP. This finding was particularly interesting, as NOD1 or NOD2 can both synergize with multiple TLRs to increase inflammation (329,330,384–386). Our results reinforce the concept that only NOD2 engages IRF4 to tolerize and regulate TLR inflammation, which may have been part of the reason why NOD1 and NOD2 had such divergent effects on glucose metabolism.

In agreement with the results showing that NOD2 increased *Irf4* expression specifically in the liver in our endotoxemia model, NOD2 activation induced several hepatic changes in gene expression. We found that *Il10* was higher after LPS injection in MDP-treated WT mice compared to *Irf4*$^{-/-}$ mice, consistent with the fact that IRF4 binds to the promoter of *Il10* to regulate expression of this anti-inflammatory cytokine (312). Hepatic *Il1b* expression was significantly lower after LPS challenge in WT mice treated with MDP compared to *Irf4*$^{-/-}$ mice, which further suggested that MDP pre-treatment contributes to IRF4-dependent suppression of certain inflammatory responses in the liver during endotoxin challenge. However, injecting MDP prior to LPS equated to higher hepatic expression of some pro-inflammatory cytokines such as *Il6* and *Tnf* in WT compared to *Irf4*$^{-/-}$

mice. These data showed that IRF4 controlled an MDP-induced inflammatory gene program in the liver.

Comparatively, inflammatory changes induced by MDP were not observed in the adipose tissue of WT mice during endotoxemia and it was unclear why the endotoxemia model was different from the obesity model regarding adipose tissue inflammation. Given the widespread adipose tissue-specific IRF4-dependent effects observed in our obesity model, it is plausible that adipose-specific immunoregulation by NOD2/IRF4 is unique to a chronic, low-level inflammatory setting such as obesity as demonstrated by prior studies (310,311,381,382). In contrast with these obesity studies, acute inflammatory insults such as LPS challenge have been shown to be regulated by NOD2/IRF4 within the liver (343). Regardless of these compartmentalized inflammatory changes, NOD2 activation had whole-body insulin-sensitizing effects in WT, but not *Irf4*$^{-/-}$ mice.

4.6 Research limitations and future directions

4.6.1 Limitations

The data presented in this thesis was collected from living mice or their tissues, and thus a scrutiny of our animal models, especially potential health issues or known phenotypes of knockout strains, is warranted. For example, we had previously shown that *Nod2*$^{-/-}$ mice were insulin resistant

during obesity. A common control we utilized in studies to mitigate strain-specific phenotypes was the use of treatment and vehicle groups *within* a genotype. Some of the *Irf4*$^{-/-}$ mice developed health issues as they aged. The most obvious phenotype of this knockout strain was occasional rectal prolapse, which could be attributed to the lack of mature B and T cells (319). Mice that had this issue occur during a study were monitored, and incidences were distributed evenly between treatment groups. There appeared to be no metabolic or inflammatory effect of prolapse in the tissues we analyzed, and MDP treatment did not affect the occurrence of rectal prolapses.

Another issue in *Irf4*$^{-/-}$ mice was lower body mass compared to WT mice, which could have confounded obesity studies of NOD2 activation. However, this phenotype did not appear to have any effect on inflammation, as MDP-induced changes in liver and muscle inflammatory gene expression were similar to WT mice. It cannot be overlooked that the reduced body masses of *Irf4*$^{-/-}$ mice may have limited metabolic studies during HFD-feeding. However, NOD2 activation in *Irf4*$^{-/-}$ mice had no effect on glucose control in our endotoxemia model, which was not dependent on body mass for its phenotype. Therefore, it was unlikely that the lack of glucose tolerance changes by MDP treatment during obesity studies was due to lower weight gain in HFD-fed *Irf4*$^{-/-}$ mice. The more likely explanation for this phenotype was that NOD2 activation required IRF4 for metabolic effects.

To avoid whole-body health issues, such as those in *Irf4*$^{-/-}$ mice, cell and tissue-specific deletion strains are a good alternative. The downside of these studies is that they are time-consuming and often require prior knowledge about which cell or tissue type is likely mediating the phenotype of interest. Even with prior knowledge aiding their creation, our hematopoietic and hepatocyte NOD2 knockout strains did not solve which cell type mediated the known protective effects of NOD2 signaling. Regardless, these studies were still useful as the results obtained from these mice eliminated both the liver and all immune cells as possible primary targets of MDP. These results, and our data from WT mice treated with MDP, and the literature showing that IRF4 controls lipid handling within adipocytes (311), position white adipocytes as a good candidate cell for *Nod2*/*Irf4* deletion during MDP treatment during obesity.

Targeted knockout strains are also useful because they may inform future targeted therapies that take advantage of the now-characterized compartmentalization effects of potential drugs. For example, MDP had widespread anti-inflammatory effects in adipose tissue, moderate effects in liver and spleen, but pro-inflammatory effects in muscle. This tissue-dependent variability would be an undesirable side effect of a drug. Targeted activation of NOD2 within adipose could avoid the known problems associated with whole-body activation. Blocking NOD2 signaling within muscle could also achieve the intended effects of targeted delivery,

and may even improve the metabolic effects of MDP by preventing pro-inflammatory and insulin-desensitizing effects in muscle. Inhibiting NOD1 may also prove beneficial. While NOD1 and NOD2 inhibitors exist, targeted delivery of these inhibitors remains an unsolved parameter that would limit their effectiveness (283,387–391).

The majority of experiments in this thesis were performed in adult-aged male mice, which prevents the results from being generalized to a standard human population with insulin resistance. We attempted to address this limitation by showing that MDP also improved glucose tolerance in female mice in our endotoxemia model. We observed a significant increase in glucose tolerance in female mice treated with MDP, but the blood glucose response was qualitatively different compared to male mice. While this result is in line with literature showing that female mice exhibit a differential inflammatory response to LPS compared with male mice (392,393), further testing in female mice, especially in obesity models, is required to confirm that MDP is beneficial for glucose metabolism regardless of sex.

4.6.2 Future applications of this work

A possible outcome of the data presented in this thesis is the development of novel therapeutics based on NOD2 activation. With respect to drug design, two future directions based on our data may help to make

MDP a better drug for treating insulin resistance: a more optimal delivery method instead of intraperitoneal injection, and a more potent NOD2 activator that is longer lasting.

The beneficial metabolic and inflammatory effects of MDP treatment during obesity and acute endotoxemia were investigated by utilizing intraperitoneal delivery of the ligand to animals. To explore the potential of MDP as a practical agent to mitigate metabolic disease, we investigated the oral efficacy of this molecule in our models of obesity and acute endotoxemia. Chronic dosing for the obesity study was based on daily water consumption and designed to be equivalent to the total amount of MDP delivered i.p. over the course of the “prevention-style” HFD/MDP protocol described above. During obesity, chronic dosing of 25 μM MDP in drinking water provided *ad libitum* did not affect glucose tolerance after 5 weeks (Figure 4.2). Similarly, oral gavage of 100 μg MDP one day prior to acute endotoxin challenge did not improve glucose tolerance (Figure 4.3). Together these data suggest that oral delivery of NOD2-activating ligands is ineffective at improving glucose metabolism during obesity and acute endotoxemia. The results observed while testing oral delivery of MDP were not entirely surprising for multiple reasons. The intestinal environment is a barrier to the body, preventing bacteria and debris from escaping and multiplying in internal tissues. Additionally, the gut is already replete with MDP-producing bacteria (200 g bacteria in a 70-kg human; (192)). Thus,

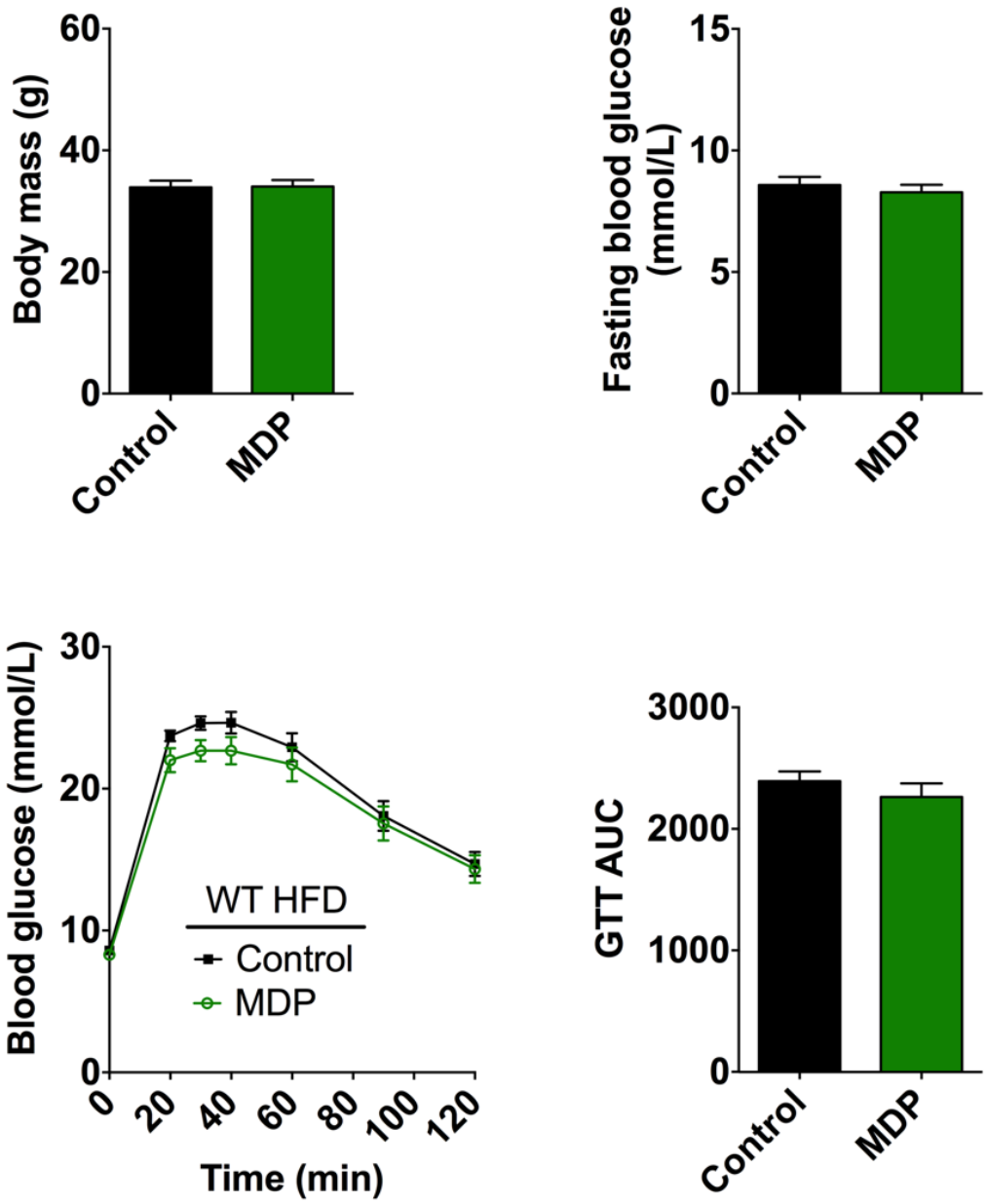

Figure 4.2 Glucose metabolism of WT mice chronically treated with MDP in drinking water.

Body mass, fasting blood glucose, and glucose tolerance test (1.5 g/kg) of HFD-fed WT mice that received water or water containing MDP daily for 5 weeks. n = 15 mice for each group. Values are mean ± SEM.

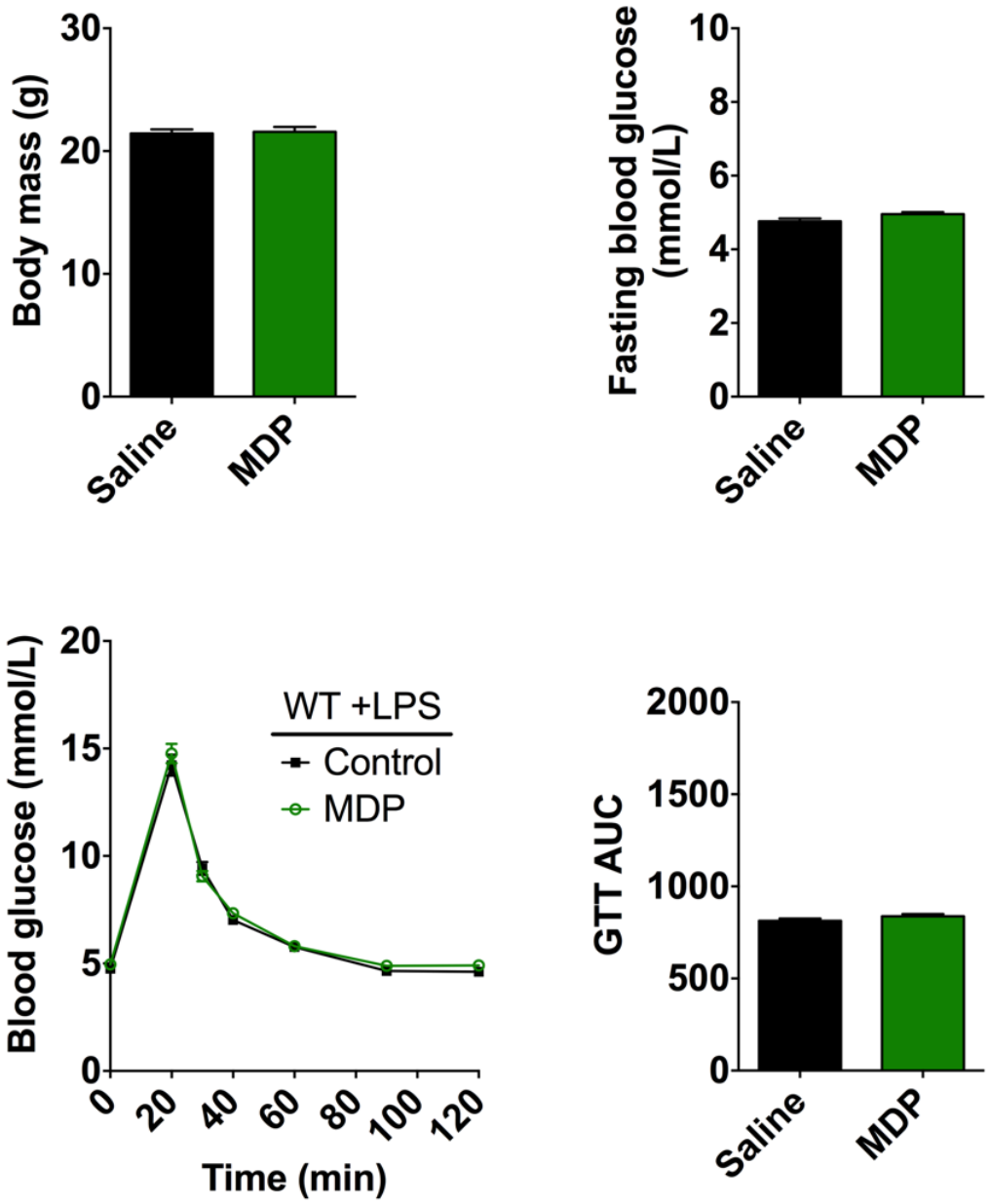

Figure 4.3 Glucose metabolism of WT mice treated with orally administered MDP prior to acute endotoxemia.

Body mass, fasting blood glucose, and glucose tolerance test (2 g/kg) of control diet-fed WT mice that received water or MDP via oral gavage for 3 days prior to acute endotoxemia. n = 15 mice for each group. Values are mean ± SEM.

successful oral delivery of NOD2-activating compounds would require a compound that can survive ingestion and be absorbed through the gut barrier. Bacterial vesicles have been shown to deliver microbial compounds and activate inflammatory pathways in host cells and tissues, and also translocate through the murine gut and have effects within metabolic tissues (394–399). Additionally, it has even been demonstrated that Gram-negative bacteria deliver peptidoglycan to NOD1 in epithelial cells via outer membrane vesicles (363,400). Endogenous host-derived vesicles are also a promising vehicle, as they can target metabolic tissues such as liver (356,359).

In our assessment of MDP as an insulin-sensitizer, we also tested the effects of other NOD2 agonists based on MDP that have been reported in the literature (365,401). Most of these ligands had similar effects as MDP in our models (data not shown). However, when we searched for pre-approved drugs derived from MDP, the orphan drug mifamurtide (muramyl tripeptide phosphatidylethanolamine) was identified as a more promising candidate. Mifamurtide is a synthetic NOD2-activating adjuvant used during chemotherapy of juvenile and adolescent osteosarcoma (402). The lipophilic nature of mifamurtide has been demonstrated to confer a more potent activity compared to MDP (403,404). We first tested mifamurtide at an equivalent dose of MDP (mifamurtide molecular weight: 1237.5 g/mol; MDP molecular weight: 492.5 g/mol) in our endotoxemia model. When

directly compared to a dose of MDP that did not alter glycemia (20 μg), an equimolar dose of mifamurtide (50 μg) improved glucose tolerance during acute endotoxemia in mice (Figure 4.4). Mifamurtide did not alter glucose tolerance in *Nod2*$^{-/-}$ mice, demonstrating the specificity of this orphan drug (Figure 4.5). In the "prevention-style" *in vivo* experimental HFD model, it was observed that injections of 50 μg of mifamurtide improved glucose tolerance during diet-induced obesity in WT mice (Figure 4.6). Mifamurtide was a more potent NOD2 activator compared with MDP in both of our models of insulin resistance, positioning this orphan drug as a tantalizing NOD2-activating drug candidate. Future studies that build upon the data presented in this thesis may lead to postbiotic drugs for improved glucose control during type 2 diabetes.

4.7 Summary

The advancing obesity pandemic has prompted novel approaches to combating metabolic disease and, in particular, the associated dysregulation of glucose control. In the current study, we found that the transcription factor IRF4 dictated divergent blood glucose effects of specific bacterial cell wall-derived peptidoglycan molecules in two independent models of inflammation and insulin resistance in mice. During both obesity and acute low-level endotoxemia we described a NOD2/MDP-based postbiotic phenotype that limited metabolic inflammation and increased

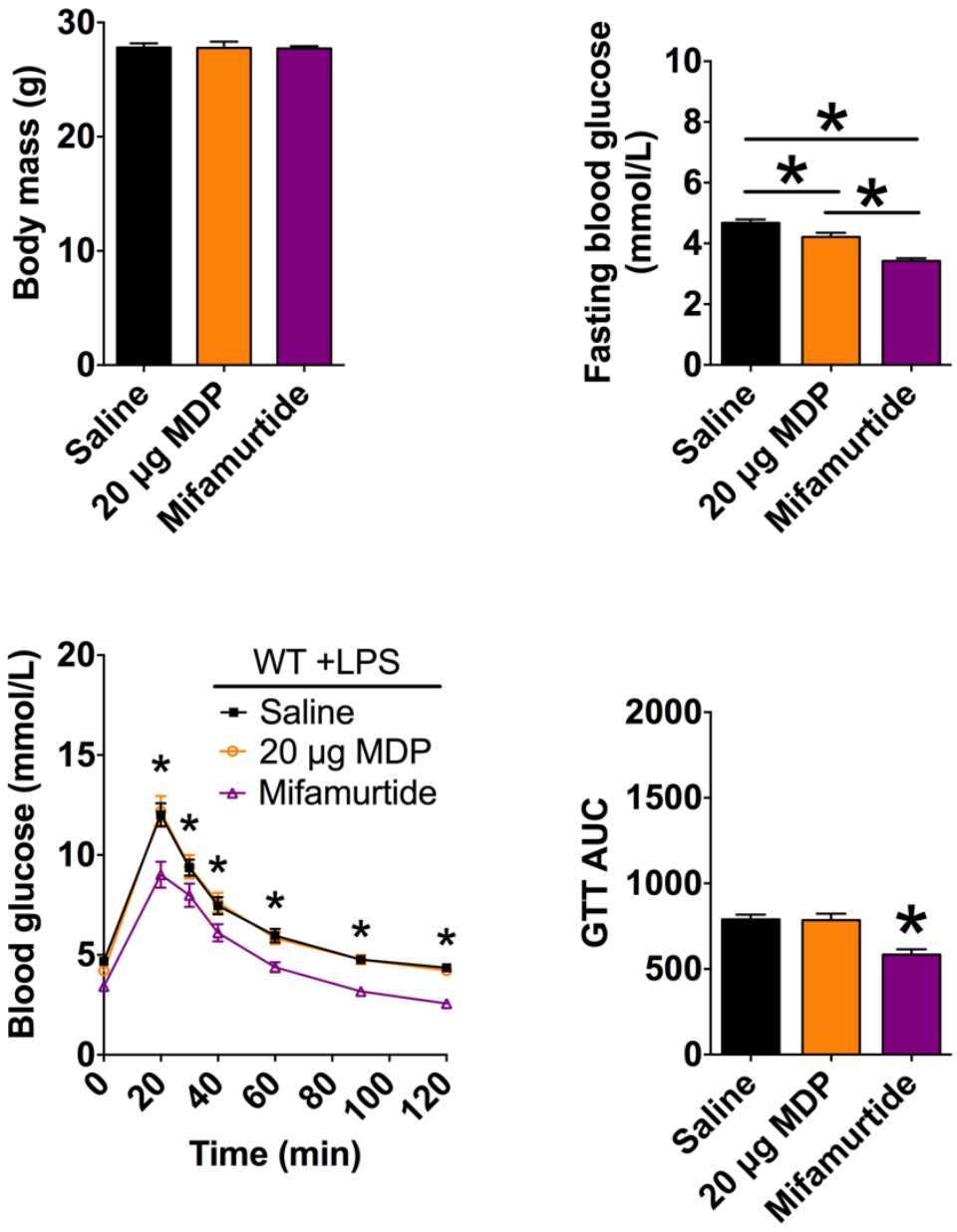

Figure 4.4 Glucose metabolism of WT mice treated with MDP or mifamurtide prior to acute endotoxemia.

Body mass, fasting blood glucose, and glucose tolerance test (2 g/kg) of control diet-fed WT mice that received saline, a low-dose of MDP, or an equimolar dose of mifamurtide for 3 days prior to acute endotoxemia. n = 9-10 mice for each group. Values are mean ± SEM. * indicates a significant difference between groups, as determined by two-way ANOVA (vs mifamurtide; line graph) or Kruskal-Wallis test (fasting blood glucose and AUC graphs) on non-normally distributed data.

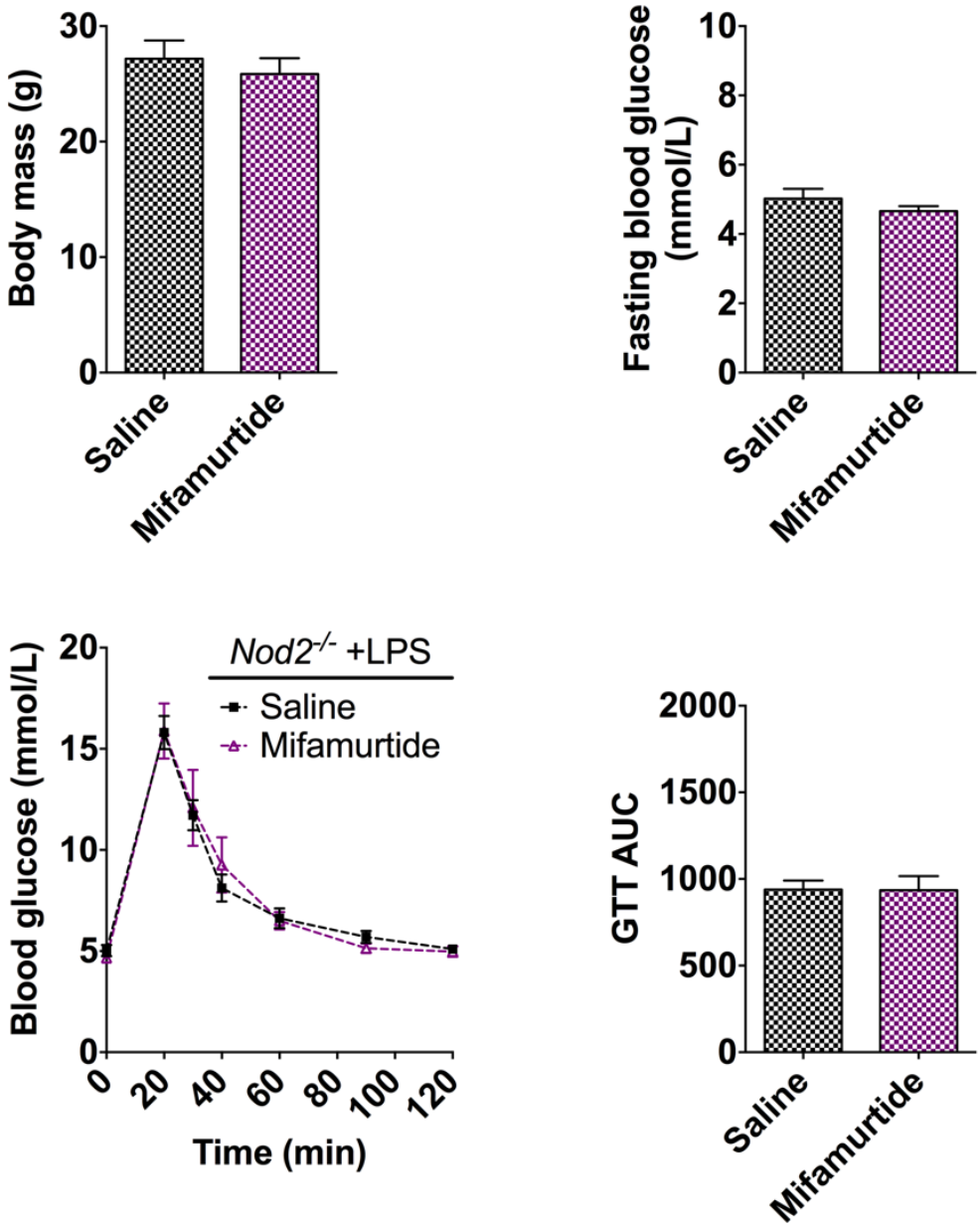

Figure 4.5 Glucose metabolism of *Nod2*$^{-/-}$ mice treated with mifamurtide prior to acute endotoxemia.

Body mass, fasting blood glucose, and glucose tolerance test (2 g/kg) of control diet-fed *Nod2*$^{-/-}$ mice that received saline or mifamurtide for 3 days prior to acute endotoxemia. n = 5 mice for each group. Values are mean ± SEM.

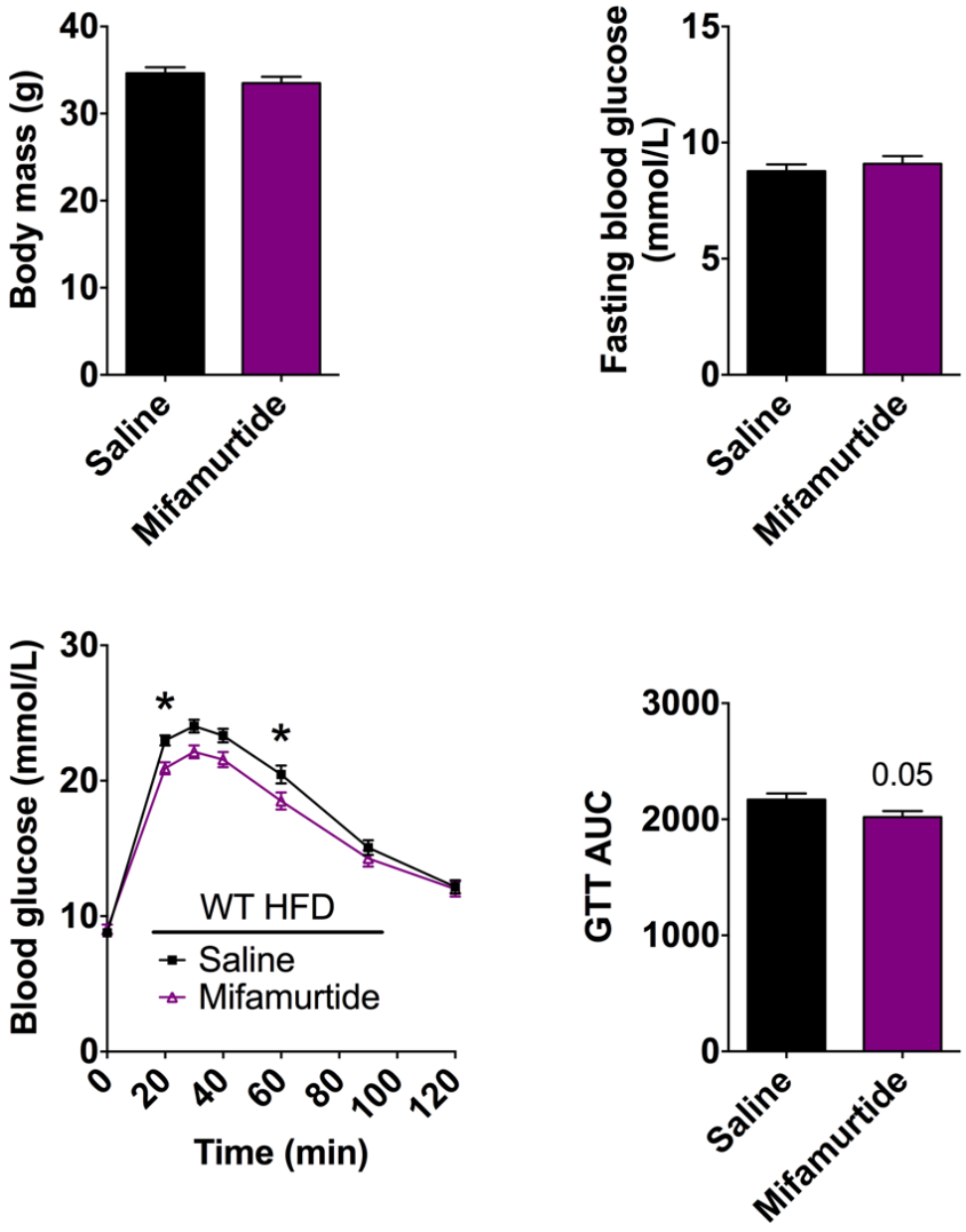

Figure 4.6 Glucose metabolism of WT mice chronically treated with mifamurtide.

Body mass, fasting blood glucose, and glucose tolerance test (1.5 g/kg) of HFD-fed WT mice that received saline or mifamurtide for 4 weeks. n = 12 mice for each group. Values are mean ± SEM. * indicates a significant difference between groups, as determined by two-way ANOVA.

insulin sensitivity (Figure 4.7) (405). Exploiting endogenous immunoregulatory programs via the repurposing of microbial-derived natural products should be considered in obesity-related metabolic disease. Postbiotics may represent an underutilized avenue of potential drug alternatives.

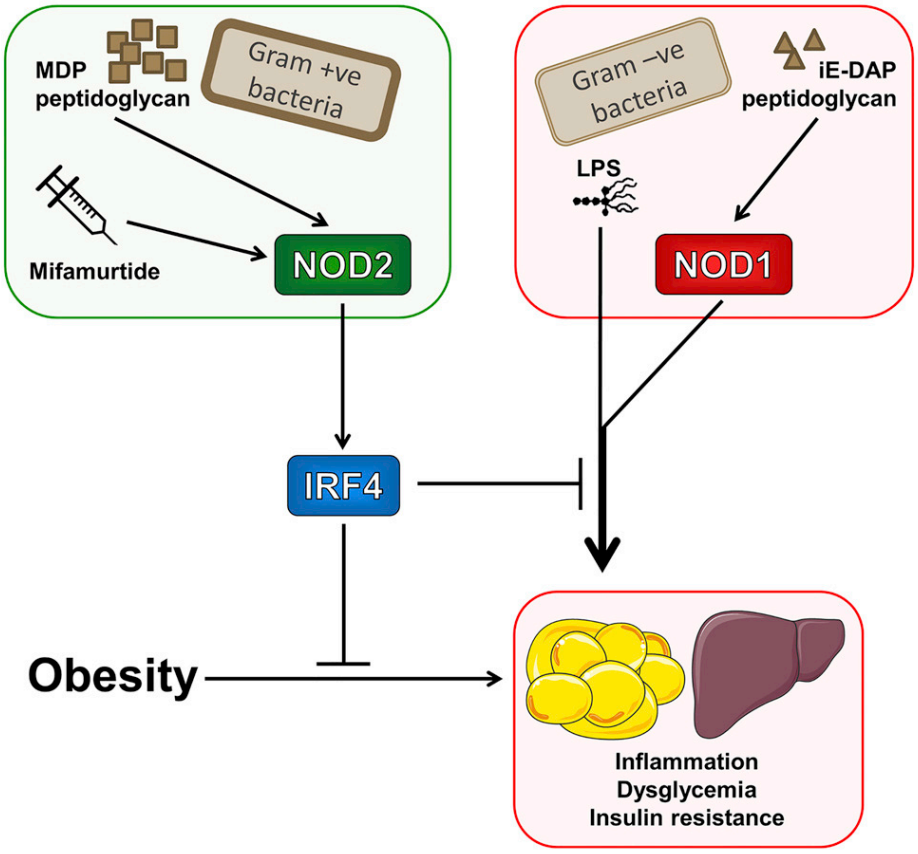

Figure 4.7 The immunometabolism of NOD protein signaling.

Muramyl dipeptide (and mifamurtide) reduces fat inflammation and liver insulin resistance via NOD2. NOD1-activating peptidoglycan ligands exacerbate glucose intolerance. IRF4 dictates insulin-sensitizing effects of NOD2, but not NOD1, peptidoglycan ligands. Adapted from Cavallari et al. 2017 (401).

CHAPTER FIVE: References

1. Haslam DW, James WPT. Obesity. Lancet (London, England). 2005 Oct 1;366(9492):1197–209.
2. Prentice AM. The emerging epidemic of obesity in developing countries. Int J Epidemiol. 2006 Feb;35(1):93–9.
3. Yoo HJ. Body Mass Index and Mortality. J Obes Metab Syndr. 2017 Mar 30;26(1):3–9.
4. Finkelstein EA, Khavjou OA, Thompson H, Trogdon JG, Pan L, Sherry B, et al. Obesity and severe obesity forecasts through 2030. Am J Prev Med. 2012 Jun;42(6):563–70.
5. Montague CT, Farooqi IS, Whitehead JP, Soos M a, Rau H, Wareham NJ, et al. Congenital leptin deficiency is associated with severe early-onset obesity in humans. Nature. 1997 Jun 26;387(6636):903–8.
6. Choquet H, Meyre D. Genetics of Obesity: What have we Learned? Curr Genomics. 2011 May;12(3):169–79.
7. Johnson F, Wardle J. Variety, palatability, and obesity. Adv Nutr. 2014 Nov;5(6):851–9.
8. Volkow ND, Wang G-J, Baler RD. Reward, dopamine and the control of food intake: implications for obesity. Trends Cogn Sci. 2011 Jan;15(1):37–46.
9. Martínez-González M a, Martínez J a, Hu FB, Gibney MJ, Kearney J. Physical inactivity, sedentary lifestyle and obesity in the European Union. Int J Obes Relat Metab Disord. 1999 Nov;23(11):1192–201.
10. Owen N, Sparling PB, Healy GN, Dunstan DW, Matthews CE. Sedentary behavior: emerging evidence for a new health risk. Mayo Clin Proc. 2010 Dec;85(12):1138–41.
11. Curhan GC, Chertow GM, Willett WC, Spiegelman D, Colditz GA, Manson JE, et al. Birth weight and adult hypertension and obesity in women. Circulation. 1996 Sep 15;94(6):1310–5.
12. Boney CM, Verma A, Tucker R, Vohr BR. Metabolic syndrome in childhood: association with birth weight, maternal obesity, and gestational diabetes mellitus. Pediatrics. 2005 Mar;115(3):e290-6.
13. O'Reilly JR, Reynolds RM. The risk of maternal obesity to the long-term health of the offspring. Clin Endocrinol (Oxf). 2013 Jan;78(1):9–16.
14. Cavallari JF, Schertzer JD. Intestinal Microbiota Contributes to Energy Balance, Metabolic Inflammation, and Insulin Resistance in Obesity. J Obes Metab Syndr. 2017 Sep 30;26(3):161–71.
15. Canadian Medical Association. CMA recognizes obesity as a disease [Internet]. 2015. Available from: https://www.cma.ca/En/Pages/cma-recognizes-obesity-as-a-disease.aspx
16. van Belle TL, Coppieters KT, von Herrath MG. Type 1 diabetes: etiology, immunology, and therapeutic strategies. Physiol Rev. 2011

Jan;91(1):79–118.
17. Olokoba AB, Obateru OA, Olokoba LB. Type 2 diabetes mellitus: a review of current trends. Oman Med J. 2012 Jul;27(4):269–73.
18. The Lancet. Life, death, and disability in 2016. Lancet. 2017;390(10100):1083.
19. Jellinger PS. Metabolic consequences of hyperglycemia and insulin resistance. Clin Cornerstone. 2007;8 Suppl 7(1):S30-42.
20. World Health Organization. Global Report on Diabetes. 2016;
21. Banting FG, Best CH, Collip JB, Campbell WR, Fletcher AA. Pancreatic Extracts in the Treatment of Diabetes Mellitus. Can Med Assoc J. 1922 Mar;12(3):141–6.
22. Wilcox G. Insulin and insulin resistance. Clin Biochem Rev. 2005 May;26(2):19–39.
23. Kiens B, Lithell H, Mikines KJ, Richter EA. Effects of insulin and exercise on muscle lipoprotein lipase activity in man and its relation to insulin action. J Clin Invest. 1989 Oct;84(4):1124–9.
24. Paulauskis JD, Sul HS. Hormonal regulation of mouse fatty acid synthase gene transcription in liver. J Biol Chem. 1989 Jan 5;264(1):574–7.
25. Sul HS, Latasa MJ, Moon Y, Kim KH. Regulation of the fatty acid synthase promoter by insulin. J Nutr. 2000 Feb;130(2S Suppl):315S–320S.
26. Griffin MJ, Sul HS. Insulin regulation of fatty acid synthase gene transcription: roles of USF and SREBP-1c. IUBMB Life. 2004 Oct;56(10):595–600.
27. Wong RHF, Sul HS. Insulin signaling in fatty acid and fat synthesis: a transcriptional perspective. Curr Opin Pharmacol. 2010 Dec;10(6):684–91.
28. Strålfors P, Honnor RC. Insulin-induced dephosphorylation of hormone-sensitive lipase. Correlation with lipolysis and cAMP-dependent protein kinase activity. Eur J Biochem. 1989 Jun 15;182(2):379–85.
29. Manchester KL. Effect of Insulin on Protein Synthesis. Diabetes. 1972 Jun 1;21(Supplement_2):447–52.
30. Fujita S, Rasmussen BB, Cadenas JG, Grady JJ, Volpi E. Effect of insulin on human skeletal muscle protein synthesis is modulated by insulin-induced changes in muscle blood flow and amino acid availability. Am J Physiol Endocrinol Metab. 2006 Oct;291(4):E745-54.
31. Bratanova-Tochkova TK, Cheng H, Daniel S, Gunawardana S, Liu Y-J, Mulvaney-Musa J, et al. Triggering and augmentation mechanisms, granule pools, and biphasic insulin secretion. Diabetes. 2002 Feb;51 Suppl 1:S83-90.
32. McCulloch LJ, van de Bunt M, Braun M, Frayn KN, Clark A, Gloyn

AL. GLUT2 (SLC2A2) is not the principal glucose transporter in human pancreatic beta cells: implications for understanding genetic association signals at this locus. Mol Genet Metab. 2011 Dec;104(4):648–53.
33. Seino S, Shibasaki T, Minami K. Dynamics of insulin secretion and the clinical implications for obesity and diabetes. J Clin Invest. 2011 Jun;121(6):2118–25.
34. Cerasi E, Luft R. The plasma insulin response to glucose infusion in healthy subjects and in diabetes mellitus. Acta Endocrinol (Copenh). 1967 Jun;55(2):278–304.
35. Curry DL, Bennett LL, Grodsky GM. Dynamics of insulin secretion by the perfused rat pancreas. Endocrinology. 1968 Sep;83(3):572–84.
36. Ganda OP, Srikanta S, Brink SJ, Morris MA, Gleason RE, Soeldner JS, et al. Differential sensitivity to beta-cell secretagogues in “early,” type I diabetes mellitus. Diabetes. 1984 Jun;33(6):516–21.
37. Ward WK, Bolgiano DC, McKnight B, Halter JB, Porte D. Diminished B cell secretory capacity in patients with noninsulin-dependent diabetes mellitus. J Clin Invest. 1984 Oct;74(4):1318–28.
38. Opara EC, Hubbard VS, Burch WM, Akwari OE. Characterization of the insulinotropic potency of polyunsaturated fatty acids. Endocrinology. 1992 Feb;130(2):657–62.
39. Itoh Y, Kawamata Y, Harada M, Kobayashi M, Fujii R, Fukusumi S, et al. Free fatty acids regulate insulin secretion from pancreatic beta cells through GPR40. Nature. 2003 Mar 13;422(6928):173–6.
40. Cases JA, Gabriely I, Ma XH, Yang XM, Michaeli T, Fleischer N, et al. Physiological increase in plasma leptin markedly inhibits insulin secretion in vivo. Diabetes. 2001 Feb;50(2):348–52.
41. Gromada J, Brock B, Schmitz O, Rorsman P. Glucagon-like peptide-1: regulation of insulin secretion and therapeutic potential. Basic Clin Pharmacol Toxicol. 2004 Dec;95(6):252–62.
42. Holst JJ. The physiology of glucagon-like peptide 1. Physiol Rev. 2007 Oct;87(4):1409–39.
43. Peschke E. Melatonin, endocrine pancreas and diabetes. J Pineal Res. 2008 Jan;44(1):26–40.
44. Sharma G, Prossnitz ER. Mechanisms of estradiol-induced insulin secretion by the G protein-coupled estrogen receptor GPR30/GPER in pancreatic beta-cells. Endocrinology. 2011 Aug;152(8):3030–9.
45. Fu Z, Gilbert ER, Liu D. Regulation of insulin synthesis and secretion and pancreatic Beta-cell dysfunction in diabetes. Curr Diabetes Rev. 2013 Jan 1;9(1):25–53.
46. Raptis SA, Dimitriadis GD. Oral hypoglycemic agents: insulin secretagogues, alpha-glucosidase inhibitors and insulin sensitizers. Exp Clin Endocrinol Diabetes. 2001;109 Suppl(SUPPL. 2):S265-87.

47. Taniguchi CM, Emanuelli B, Kahn CR. Critical nodes in signalling pathways: insights into insulin action. Nat Rev Mol Cell Biol. 2006 Feb;7(2):85–96.
48. Boucher J, Kleinridders A, Kahn CR. Insulin receptor signaling in normal and insulin-resistant states. Cold Spring Harb Perspect Biol. 2014 Jan 1;6(1):1–25.
49. Guo S. Insulin signaling, resistance, and the metabolic syndrome: insights from mouse models into disease mechanisms. J Endocrinol. 2014 Feb 8;220(2):T1–23.
50. Sano H, Kane S, Sano E, Mîinea CP, Asara JM, Lane WS, et al. Insulin-stimulated phosphorylation of a Rab GTPase-activating protein regulates GLUT4 translocation. J Biol Chem. 2003 Apr 25;278(17):14599–602.
51. Zhang W, Patil S, Chauhan B, Guo S, Powell DR, Le J, et al. FoxO1 regulates multiple metabolic pathways in the liver: effects on gluconeogenic, glycolytic, and lipogenic gene expression. J Biol Chem. 2006 Apr 14;281(15):10105–17.
52. Tzivion G, Dobson M, Ramakrishnan G. FoxO transcription factors; Regulation by AKT and 14-3-3 proteins. Biochim Biophys Acta. 2011 Nov;1813(11):1938–45.
53. Duckworth WC, Bennett RG, Hamel FG. Insulin degradation: progress and potential. Endocr Rev. 1998 Oct;19(5):608–24.
54. Rabkin R, Ryan MP, Duckworth WC. The renal metabolism of insulin. Diabetologia. 1984 Sep;27(3):351–7.
55. Duckworth WC, Hamel FG, Peavy DE. Hepatic metabolism of insulin. Am J Med. 1988 Nov 28;85(5A):71–6.
56. Affholter JA, Fried VA, Roth RA. Human insulin-degrading enzyme shares structural and functional homologies with E. coli protease III. Science. 1988 Dec 9;242(4884):1415–8.
57. Akiyama H, Yokono K, Shii K, Ogawa W, Taniguchi H, Baba S, et al. Natural regulatory mechanisms of insulin degradation by insulin degrading enzyme. Biochem Biophys Res Commun. 1990 Aug 16;170(3):1325–30.
58. Valera Mora ME, Scarfone A, Calvani M, Greco A V., Mingrone G. Insulin clearance in obesity. J Am Coll Nutr. 2003 Dec;22(6):487–93.
59. Lee CC, Haffner SM, Wagenknecht LE, Lorenzo C, Norris JM, Bergman RN, et al. Insulin clearance and the incidence of type 2 diabetes in Hispanics and African Americans: the IRAS Family Study. Diabetes Care. 2013 Apr;36(4):901–7.
60. Kim SH, Reaven GM. Insulin clearance: an underappreciated modulator of plasma insulin concentration. J Investig Med. 2016 Oct;64(7):1162–5.
61. Takahashi M, Eto M, Makino I. Peripheral insulin resistance precedes the onset of hyperglycemia in spontaneously diabetic

Chinese hamsters of Asahikawa colony. Diabetes Res Clin Pract. 1993 May;20(2):101–9.
62. Davis RC, Castellani LW, Hosseini M, Ben-Zeev O, Mao HZ, Weinstein MM, et al. Early hepatic insulin resistance precedes the onset of diabetes in obese C57BLKS-db/db mice. Diabetes. 2010 Jul;59(7):1616–25.
63. Mehran AE, Templeman NM, Brigidi GS, Lim GE, Chu K-Y, Hu X, et al. Hyperinsulinemia drives diet-induced obesity independently of brain insulin production. Cell Metab. 2012 Dec 5;16(6):723–37.
64. Templeman NM, Flibotte S, Chik JHL, Sinha S, Lim GE, Foster LJ, et al. Reduced Circulating Insulin Enhances Insulin Sensitivity in Old Mice and Extends Lifespan. Cell Rep. 2017 Jul 11;20(2):451–63.
65. Fonseca VA. Defining and characterizing the progression of type 2 diabetes. Diabetes Care. 2009 Nov;32 Suppl 2:S151-6.
66. Powell DJ, Hajduch E, Kular G, Hundal HS. Ceramide disables 3-phosphoinositide binding to the pleckstrin homology domain of protein kinase B (PKB)/Akt by a PKCzeta-dependent mechanism. Mol Cell Biol. 2003 Nov;23(21):7794–808.
67. Copps KD, White MF. Regulation of insulin sensitivity by serine/threonine phosphorylation of insulin receptor substrate proteins IRS1 and IRS2. Diabetologia. 2012 Oct;55(10):2565–82.
68. Tanti JF, Grémeaux T, van Obberghen E, Le Marchand-Brustel Y. Serine/threonine phosphorylation of insulin receptor substrate 1 modulates insulin receptor signaling. J Biol Chem. 1994 Feb 25;269(8):6051–7.
69. Aguirre V, Werner ED, Giraud J, Lee YH, Shoelson SE, White MF. Phosphorylation of Ser307 in insulin receptor substrate-1 blocks interactions with the insulin receptor and inhibits insulin action. J Biol Chem. 2002 Jan 11;277(2):1531–7.
70. Gao Z, Hwang D, Bataille F, Lefevre M, York D, Quon MJ, et al. Serine phosphorylation of insulin receptor substrate 1 by inhibitor kappa B kinase complex. J Biol Chem. 2002 Dec 13;277(50):48115–21.
71. Gual P, Gonzalez T, Grémeaux T, Barres R, Le Marchand-Brustel Y, Tanti J-F. Hyperosmotic stress inhibits insulin receptor substrate-1 function by distinct mechanisms in 3T3-L1 adipocytes. J Biol Chem. 2003 Jul 18;278(29):26550–7.
72. Powell DJ, Turban S, Gray A, Hajduch E, Hundal HS. Intracellular ceramide synthesis and protein kinase Czeta activation play an essential role in palmitate-induced insulin resistance in rat L6 skeletal muscle cells. Biochem J. 2004 Sep 1;382(Pt 2):619–29.
73. Schenk S, Saberi M, Olefsky JM. Insulin sensitivity: modulation by nutrients and inflammation. J Clin Invest. 2008 Sep;118(9):2992–3002.

74. Zhang J, Gao Z, Yin J, Quon MJ, Ye J. S6K directly phosphorylates IRS-1 on Ser-270 to promote insulin resistance in response to TNF-(alpha) signaling through IKK2. J Biol Chem. 2008 Dec 19;283(51):35375–82.
75. Boura-Halfon S, Zick Y. Phosphorylation of IRS proteins, insulin action, and insulin resistance. Am J Physiol Endocrinol Metab. 2009 Apr;296(4):E581-91.
76. Karasik A, Rothenberg PL, Yamada K, White MF, Kahn CR. Increased Protein Kinase-C Activity Is Linked To Reduced Insulin-Receptor Autophosphorylation in Liver of Starved Rats. J Biol Chem. 1990;265(18):10226–31.
77. Dunaif A, Xia J, Book CB, Schenker E, Tang Z. Excessive insulin receptor serine phosphorylation in cultured fibroblasts and in skeletal muscle. A potential mechanism for insulin resistance in the polycystic ovary syndrome. J Clin Invest. 1995 Aug;96(2):801–10.
78. Shao J, Catalano PM, Yamashita H, Ruyter I, Smith S, Youngren J, et al. Decreased insulin receptor tyrosine kinase activity and plasma cell membrane glycoprotein-1 overexpression in skeletal muscle from obese women with gestational diabetes mellitus (GDM): evidence for increased serine/threonine phosphorylation in pregnancy a. Diabetes. 2000 Apr;49(4):603–10.
79. Draznin B. Molecular mechanisms of insulin resistance: serine phosphorylation of insulin receptor substrate-1 and increased expression of p85alpha: the two sides of a coin. Diabetes. 2006 Aug;55(8):2392–7.
80. Hirosumi J, Tuncman G, Chang L, Görgün CZ, Uysal KT, Maeda K, et al. A central role for JNK in obesity and insulin resistance. Nature. 2002 Nov 21;420(6913):333–6.
81. Um SH, Frigerio F, Watanabe M, Picard F, Joaquin M, Sticker M, et al. Absence of S6K1 protects against age- and diet-induced obesity while enhancing insulin sensitivity. Nature. 2004 Sep 9;431(7005):200–5.
82. Werner ED, Lee J, Hansen L, Yuan M, Shoelson SE. Insulin resistance due to phosphorylation of insulin receptor substrate-1 at serine 302. J Biol Chem. 2004 Aug 20;279(34):35298–305.
83. Taylor SI, Kadowaki T, Kadowaki H, Accili D, Cama A, McKeon C. Mutations in insulin-receptor gene in insulin-resistant patients. Diabetes Care. 1990 Mar;13(3):257–79.
84. Haruta T, Imamura T, Iwanishi M, Egawa K, Goji K, Kobayashi M. Amplification and analysis of promoter region of insulin receptor gene in a patient with leprechaunism associated with severe insulin resistance. Metabolism. 1995 Apr;44(4):430–7.
85. Almind K, Inoue G, Pedersen O, Kahn CR. A common amino acid polymorphism in insulin receptor substrate-1 causes impaired insulin

signaling. Evidence from transfection studies. J Clin Invest. 1996 Jun 1;97(11):2569–75.
86. Barroso I, Luan J, Middelberg RPS, Harding A, Franks PW, Jakes RW, et al. Candidate gene association study in type 2 diabetes indicates a role for genes involved in beta-cell function as well as insulin action. PLoS Biol. 2003 Oct;1(1):E20.
87. George S, Rochford JJ, Wolfrum C, Gray SL, Schinner S, Wilson JC, et al. A family with severe insulin resistance and diabetes due to a mutation in AKT2. Science. 2004 May 28;304(5675):1325–8.
88. Cnop M, Vidal J, Hull RL, Utzschneider KM, Carr DB, Schraw T, et al. Progressive loss of beta-cell function leads to worsening glucose tolerance in first-degree relatives of subjects with type 2 diabetes. Diabetes Care. 2007 Mar;30(3):677–82.
89. Yuan M, Konstantopoulos N, Lee J, Hansen L, Li ZW, Karin M, et al. Reversal of obesity- and diet-induced insulin resistance with salicylates or targeted disruption of Ikkbeta. Science. 2001 Aug 31;293(5535):1673–7.
90. Hotamisligil GS. Inflammation and metabolic disorders. Nature. 2006 Dec 14;444(7121):860–7.
91. Gregor MF, Hotamisligil GS. Inflammatory mechanisms in obesity. Annu Rev Immunol. 2011 Jan;29:415–45.
92. Johnson AMF, Olefsky JM. The origins and drivers of insulin resistance. Cell. 2013 Feb 14;152(4):673–84.
93. Hotamisligil GS. Inflammation, metaflammation and immunometabolic disorders. Nature. 2017 Feb 8;542(7640):177–85.
94. Boden G. Obesity, insulin resistance and free fatty acids. Curr Opin Endocrinol Diabetes Obes. 2011 Apr;18(2):139–43.
95. Cani PD, Amar J, Iglesias MA, Poggi M, Knauf C, Bastelica D, et al. Metabolic endotoxemia initiates obesity and insulin resistance. Diabetes. 2007 Jul;56(7):1761–72.
96. Lukens JR, Dixit VD, Kanneganti T-D. Inflammasome activation in obesity-related inflammatory diseases and autoimmunity. Discov Med. 2011 Jul;12(62):65–74.
97. Aroor AR, DeMarco VG. Oxidative stress and obesity: the chicken or the egg? Diabetes. 2014 Jul;63(7):2216–8.
98. Lang CH, Dobrescu C, Bagby GJ. Tumor necrosis factor impairs insulin action on peripheral glucose disposal and hepatic glucose output. Endocrinology. 1992 Jan;130(1):43–52.
99. Hotamisligil GS, Spiegelman BM. Tumor necrosis factor alpha: a key component of the obesity-diabetes link. Diabetes. 1994 Nov;43(11):1271–8.
100. Hotamisligil GS, Budavari A, Murray D, Spiegelman BM. Reduced tyrosine kinase activity of the insulin receptor in obesity-diabetes. Central role of tumor necrosis factor-alpha. J Clin Invest. 1994

Oct;94(4):1543–9.
101. Zick Y. Ser/Thr phosphorylation of IRS proteins: a molecular basis for insulin resistance. Sci STKE. 2005 Jan 25;2005(268):pe4.
102. Hotamisligil GS, Shargill NS, Spiegelman BM. Adipose expression of tumor necrosis factor-alpha: direct role in obesity-linked insulin resistance. Science. 1993 Jan 1;259(5091):87–91.
103. Ofei F, Hurel S, Newkirk J, Sopwith M, Taylor R. Effects of an engineered human anti-TNF-alpha antibody (CDP571) on insulin sensitivity and glycemic control in patients with NIDDM. Diabetes. 1996 Jul;45(7):881–5.
104. Kim H-J, Higashimori T, Park S, Choi H, Dong J, Kim Y-J, et al. Differential effects of interleukin-6 and -10 on skeletal muscle and liver insulin action in vivo. Diabetes. 2004 Apr;53(4):1060–7.
105. Weiss R, Dziura J, Burgert TS, Tamborlane W V, Taksali SE, Yeckel CW, et al. Obesity and the metabolic syndrome in children and adolescents. N Engl J Med. 2004 Jun 3;350(23):2362–74.
106. Eder K, Baffy N, Falus A, Fulop AK. The major inflammatory mediator interleukin-6 and obesity. Inflamm Res. 2009 Nov;58(11):727–36.
107. Goyal R, Faizy AF, Siddiqui SS, Singhai M. Evaluation of TNF-α and IL-6 Levels in Obese and Non-obese Diabetics: Pre- and Postinsulin Effects. N Am J Med Sci. 2012 Apr;4(4):180–4.
108. Pedersen BK, Febbraio MA, Mooney RA. Interleukin-6 does/does not have a beneficial role in insulin sensitivity and glucose homeostasis. J Appl Physiol. 2006 Oct 26;102(2):814–6.
109. Wallenius V, Wallenius K, Ahrén B, Rudling M, Carlsten H, Dickson SL, et al. Interleukin-6-deficient mice develop mature-onset obesity. Nat Med. 2002 Jan;8(1):75–9.
110. Wunderlich FT, Ströhle P, Könner AC, Gruber S, Tovar S, Brönneke HS, et al. Interleukin-6 signaling in liver-parenchymal cells suppresses hepatic inflammation and improves systemic insulin action. Cell Metab. 2010 Sep 8;12(3):237–49.
111. Mauer J, Chaurasia B, Goldau J, Vogt MC, Ruud J, Nguyen KD, et al. Signaling by IL-6 promotes alternative activation of macrophages to limit endotoxemia and obesity-associated resistance to insulin. Nat Immunol. 2014 May;15(5):423–30.
112. de Carvalho Vidigal F, Guedes Cocate P, Gonçalves Pereira L, de Cássia Gonçalves Alfenas R. The role of hyperglycemia in the induction of oxidative stress and inflammatory process. Nutr Hosp. 2012;27(5):1391–8.
113. Riboulet-Chavey A, Pierron A, Durand I, Murdaca J, Giudicelli J, Van Obberghen E. Methylglyoxal impairs the insulin signaling pathways independently of the formation of intracellular reactive oxygen species. Diabetes. 2006 May;55(5):1289–99.

114. Harte AL, Varma MC, Tripathi G, McGee KC, Al-Daghri NM, Al-Attas OS, et al. High fat intake leads to acute postprandial exposure to circulating endotoxin in type 2 diabetic subjects. Diabetes Care. 2012 Feb;35(2):375–82.
115. Caro JF, Sinha MK, Kolaczynski JW, Zhang PL, Considine R V. Leptin: the tale of an obesity gene. Diabetes. 1996 Nov;45(11):1455–62.
116. Lönnqvist F, Arner P, Nordfors L, Schalling M. Overexpression of the obese (ob) gene in adipose tissue of human obese subjects. Nat Med. 1995 Sep;1(9):950–3.
117. Masuo K, Straznicky NE, Lambert GW, Katsuya T, Sugimoto K, Rakugi H, et al. Leptin-receptor polymorphisms relate to obesity through blunted leptin-mediated sympathetic nerve activation in a Caucasian male population. Hypertens Res. 2008 Jun;31(6):1093–100.
118. Iikuni N, Kwan Lam Q, Lu L, Matarese G, Cava A. Leptin and Inflammation. Curr Immunol Rev. 2008 May 1;4(2):70–9.
119. Li L, Messina JL. Acute insulin resistance following injury. Trends Endocrinol Metab. 2009 Nov;20(9):429–35.
120. Van Cromphaut S, Vanhorebeek I, Berghe G. Glucose Metabolism and Insulin Resistance in Sepsis. Curr Pharm Des. 2008 Jul 1;14(19):1887–99.
121. Gornik I, Vujaklija A, Lukić E, Madzarac G, Gasparović V. Hyperglycemia in sepsis is a risk factor for development of type II diabetes. J Crit Care. 2010 Jun;25(2):263–9.
122. McPhee JB, Schertzer JD. Immunometabolism of obesity and diabetes: microbiota link compartmentalized immunity in the gut to metabolic tissue inflammation. Clin Sci (Lond). 2015 Dec;129(12):1083–96.
123. Cavallari JF, Denou E, Foley KP, Khan WI, Schertzer JD. Different Th17 immunity in gut, liver, and adipose tissues during obesity: the role of diet, genetics, and microbes. Gut Microbes. 2016;7(1):82–9.
124. Trayhurn P, Beattie JH. Physiological role of adipose tissue: white adipose tissue as an endocrine and secretory organ. Proc Nutr Soc. 2001 Aug;60(3):329–39.
125. Sun S, Ji Y, Kersten S, Qi L. Mechanisms of inflammatory responses in obese adipose tissue. Annu Rev Nutr. 2012 Aug 21;32(1):261–86.
126. Turner N, Kowalski GM, Leslie SJ, Risis S, Yang C, Lee-Young RS, et al. Distinct patterns of tissue-specific lipid accumulation during the induction of insulin resistance in mice by high-fat feeding. Diabetologia. 2013 Jul;56(7):1638–48.
127. Kawasaki N, Asada R, Saito A, Kanemoto S, Imaizumi K. Obesity-induced endoplasmic reticulum stress causes chronic inflammation

in adipose tissue. Sci Rep. 2012;2:799.
128. Bogdanovic E, Kraus N, Patsouris D, Diao L, Wang V, Abdullahi A, et al. Endoplasmic reticulum stress in adipose tissue augments lipolysis. J Cell Mol Med. 2015 Jan;19(1):82–91.
129. Xu H, Barnes GT, Yang Q, Tan G, Yang D, Chou CJ, et al. Chronic inflammation in fat plays a crucial role in the development of obesity-related insulin resistance. J Clin Invest. 2003 Dec 15;112(12):1821–30.
130. Weisberg SP, McCann D, Desai M, Rosenbaum M, Leibel RL, Ferrante AW. Obesity is associated with macrophage accumulation in adipose tissue. J Clin Invest. 2003 Dec 15;112(12):1796–808.
131. Stefanovic-Racic M, Yang X, Turner MS, Mantell BS, Stolz DB, Sumpter TL, et al. Dendritic cells promote macrophage infiltration and comprise a substantial proportion of obesity-associated increases in CD11c+ cells in adipose tissue and liver. Diabetes. 2012 Sep;61(9):2330–9.
132. Han MS, Jung DY, Morel C, Lakhani SA, Kim JK, Flavell RA, et al. JNK expression by macrophages promotes obesity-induced insulin resistance and inflammation. Science. 2013 Jan 11;339(6116):218–22.
133. Hotamisligil GS, Arner P, Caro JF, Atkinson RL, Spiegelman BM. Increased adipose tissue expression of tumor necrosis factor-alpha in human obesity and insulin resistance. J Clin Invest. 1995 May;95(5):2409–15.
134. Wicovsky A, Müller N, Daryab N, Marienfeld R, Kneitz C, Kavuri S, et al. Sustained JNK activation in response to tumor necrosis factor is mediated by caspases in a cell type-specific manner. J Biol Chem. 2007 Jan 26;282(4):2174–83.
135. Kern PA, Ranganathan S, Li C, Wood L, Ranganathan G. Adipose tissue tumor necrosis factor and interleukin-6 expression in human obesity and insulin resistance. Am J Physiol Endocrinol Metab. 2001 May;280(5):E745-51.
136. Ozes ON, Akca H, Mayo LD, Gustin JA, Maehama T, Dixon JE, et al. A phosphatidylinositol 3-kinase/Akt/mTOR pathway mediates and PTEN antagonizes tumor necrosis factor inhibition of insulin signaling through insulin receptor substrate-1. Proc Natl Acad Sci U S A. 2001 Apr 10;98(8):4640–5.
137. Kanda H, Tateya S, Tamori Y, Kotani K, Hiasa K, Kitazawa R, et al. MCP-1 contributes to macrophage infiltration into adipose tissue, insulin resistance, and hepatic steatosis in obesity. J Clin Invest. 2006 Jun;116(6):1494–505.
138. Weisberg SP, Hunter D, Huber R, Lemieux J, Slaymaker S, Vaddi K, et al. CCR2 modulates inflammatory and metabolic effects of high-fat feeding. J Clin Invest. 2006 Jan;116(1):115–24.

139. Zhang X, Goncalves R, Mosser DM. The isolation and characterization of murine macrophages. Curr Protoc Immunol. 2008 Nov;Chapter 14:Unit 14.1.
140. Nov O, Shapiro H, Ovadia H, Tarnovscki T, Dvir I, Shemesh E, et al. Interleukin-1β regulates fat-liver crosstalk in obesity by auto-paracrine modulation of adipose tissue inflammation and expandability. PLoS One. 2013;8(1):e53626.
141. DeFronzo RA, Jacot E, Jequier E, Maeder E, Wahren J, Felber JP. The effect of insulin on the disposal of intravenous glucose. Results from indirect calorimetry and hepatic and femoral venous catheterization. Diabetes. 1981 Dec;30(12):1000–7.
142. DeFronzo RA, Gunnarsson R, Björkman O, Olsson M, Wahren J. Effects of insulin on peripheral and splanchnic glucose metabolism in noninsulin-dependent (type II) diabetes mellitus. J Clin Invest. 1985 Jul;76(1):149–55.
143. Blaak EE, Wagenmakers AJ, Glatz JF, Wolffenbuttel BH, Kemerink GJ, Langenberg CJ, et al. Plasma FFA utilization and fatty acid-binding protein content are diminished in type 2 diabetic muscle. Am J Physiol Endocrinol Metab. 2000 Jul;279(1):E146-54.
144. Abdul-Ghani MA, DeFronzo RA. Pathogenesis of insulin resistance in skeletal muscle. J Biomed Biotechnol. 2010;2010:476279.
145. Kelley DE, Simoneau JA. Impaired free fatty acid utilization by skeletal muscle in non-insulin-dependent diabetes mellitus. J Clin Invest. 1994 Dec;94(6):2349–56.
146. Krssak M, Falk Petersen K, Dresner A, DiPietro L, Vogel SM, Rothman DL, et al. Intramyocellular lipid concentrations are correlated with insulin sensitivity in humans: a 1H NMR spectroscopy study. Diabetologia. 1999 Jan;42(1):113–6.
147. Richter EA, Garetto LP, Goodman MN, Ruderman NB. Muscle glucose metabolism following exercise in the rat: increased sensitivity to insulin. J Clin Invest. 1982 Apr;69(4):785–93.
148. Goodpaster BH, He J, Watkins S, Kelley DE. Skeletal muscle lipid content and insulin resistance: evidence for a paradox in endurance-trained athletes. J Clin Endocrinol Metab. 2001 Dec;86(12):5755–61.
149. Stump CS, Henriksen EJ, Wei Y, Sowers JR. The metabolic syndrome: role of skeletal muscle metabolism. Ann Med. 2006;38(6):389–402.
150. Itani SI, Ruderman NB, Schmieder F, Boden G. Lipid-induced insulin resistance in human muscle is associated with changes in diacylglycerol, protein kinase C, and IkappaB-alpha. Diabetes. 2002 Jul;51(7):2005–11.
151. Szendroedi J, Yoshimura T, Phielix E, Koliaki C, Marcucci M, Zhang D, et al. Role of diacylglycerol activation of PKCθ in lipid-induced

muscle insulin resistance in humans. Proc Natl Acad Sci U S A. 2014 Jul 1;111(26):9597–602.
152. Schubert KM, Scheid MP, Duronio V. Ceramide inhibits protein kinase B/Akt by promoting dephosphorylation of serine 473. J Biol Chem. 2000 May 5;275(18):13330–5.
153. Stratford S, DeWald DB, Summers SA. Ceramide dissociates 3'-phosphoinositide production from pleckstrin homology domain translocation. Biochem J. 2001 Mar 1;354(Pt 2):359–68.
154. Ghosh N, Patel N, Jiang K, Watson JE, Cheng J, Chalfant CE, et al. Ceramide-activated protein phosphatase involvement in insulin resistance via Akt, serine/arginine-rich protein 40, and ribonucleic acid splicing in L6 skeletal muscle cells. Endocrinology. 2007 Mar;148(3):1359–66.
155. Chavez JA, Siddique MM, Wang ST, Ching J, Shayman JA, Summers SA. Ceramides and glucosylceramides are independent antagonists of insulin signaling. J Biol Chem. 2014 Jan 10;289(2):723–34.
156. Wei Y, Chen K, Whaley-Connell AT, Stump CS, Ibdah J a, Sowers JR. Skeletal muscle insulin resistance: role of inflammatory cytokines and reactive oxygen species. Am J Physiol Regul Integr Comp Physiol. 2008 Mar;294(3):R673-80.
157. Fink LN, Costford SR, Lee YS, Jensen TE, Bilan PJ, Oberbach A, et al. Pro-inflammatory macrophages increase in skeletal muscle of high fat-fed mice and correlate with metabolic risk markers in humans. Obesity (Silver Spring). 2014 Mar;22(3):747–57.
158. Khan IM, Perrard XY, Brunner G, Lui H, Sparks LM, Smith SR, et al. Intermuscular and perimuscular fat expansion in obesity correlates with skeletal muscle T cell and macrophage infiltration and insulin resistance. Int J Obes (Lond). 2015 Nov;39(11):1607–18.
159. Samokhvalov V, Bilan PJ, Schertzer JD, Antonescu CN, Klip A. Palmitate- and lipopolysaccharide-activated macrophages evoke contrasting insulin responses in muscle cells. Am J Physiol Endocrinol Metab. 2009 Jan;296(1):E37-46.
160. Eckardt K, Görgens SW, Raschke S, Eckel J. Myokines in insulin resistance and type 2 diabetes. Diabetologia. 2014 Jun;57(6):1087–99.
161. Wu H, Ballantyne CM. Skeletal muscle inflammation and insulin resistance in obesity. J Clin Invest. 2017 Jan 3;127(1):43–54.
162. del Aguila LF, Claffey KP, Kirwan JP. TNF-alpha impairs insulin signaling and insulin stimulation of glucose uptake in C2C12 muscle cells. Am J Physiol. 1999 May;276(5 Pt 1):E849-55.
163. Plomgaard P, Bouzakri K, Krogh-Madsen R, Mittendorfer B, Zierath JR, Pedersen BK. Tumor necrosis factor-alpha induces skeletal muscle insulin resistance in healthy human subjects via inhibition of

Akt substrate 160 phosphorylation. Diabetes. 2005 Oct;54(10):2939–45.
164. Roytblat L, Rachinsky M, Fisher A, Greemberg L, Shapira Y, Douvdevani A, et al. Raised interleukin-6 levels in obese patients. Obes Res. 2000 Dec;8(9):673–5.
165. Park EJ, Lee JH, Yu G, He G, Ali SR, Holzer RG, et al. Dietary and genetic obesity promote liver inflammation and tumorigenesis by enhancing IL-6 and TNF expression. Cell. 2010 Jan 22;140(2):197–208.
166. Sindhu S, Thomas R, Shihab P, Sriraman D, Behbehani K, Ahmad R. Obesity Is a Positive Modulator of IL-6R and IL-6 Expression in the Subcutaneous Adipose Tissue: Significance for Metabolic Inflammation. PLoS One. 2015;10(7):e0133494.
167. Fischer CP. Interleukin-6 in acute exercise and training: what is the biological relevance? Exerc Immunol Rev. 2006;12(115):6–33.
168. Pedersen BK, Febbraio MA. Muscles, exercise and obesity: skeletal muscle as a secretory organ. Nat Rev Endocrinol. 2012 Aug;8(8):457–65.
169. Dixon LJ, Barnes M, Tang H, Pritchard MT, Nagy LE. Kupffer Cells in the Liver. In: Comprehensive Physiology. Hoboken, NJ, USA: John Wiley & Sons, Inc.; 2013. p. 303–9.
170. Tencerova M, Aouadi M, Vangala P, Nicoloro SM, Yawe JC, Cohen JL, et al. Activated Kupffer cells inhibit insulin sensitivity in obese mice. FASEB J. 2015 Jul;29(7):2959–69.
171. Clementi AH, Gaudy AM, van Rooijen N, Pierce RH, Mooney RA. Loss of Kupffer cells in diet-induced obesity is associated with increased hepatic steatosis, STAT3 signaling, and further decreases in insulin signaling. Biochim Biophys Acta. 2009 Nov;1792(11):1062–72.
172. Odegaard JI, Ricardo-Gonzalez RR, Red Eagle A, Vats D, Morel CR, Goforth MH, et al. Alternative M2 activation of Kupffer cells by PPARdelta ameliorates obesity-induced insulin resistance. Cell Metab. 2008 Jun;7(6):496–507.
173. Krssak M, Roden M. The Role of Lipid Accumulation in Liver and Muscle for Insulin Resistance and Type 2 Diabetes Mellitus in Humans. Rev Endocr Metab Disord. 2004 May;5(2):127–34.
174. Magkos F, Su X, Bradley D, Fabbrini E, Conte C, Eagon JC, et al. Intrahepatic diacylglycerol content is associated with hepatic insulin resistance in obese subjects. Gastroenterology. 2012 Jun;142(7):1444–6.e2.
175. Galbo T, Perry RJ, Jurczak MJ, Camporez J-PG, Alves TC, Kahn M, et al. Saturated and unsaturated fat induce hepatic insulin resistance independently of TLR-4 signaling and ceramide synthesis in vivo. Proc Natl Acad Sci U S A. 2013 Jul 30;110(31):12780–5.

176. Konstantynowicz-Nowicka K, Harasim E, Baranowski M, Chabowski A. New evidence for the role of ceramide in the development of hepatic insulin resistance. PLoS One. 2015;10(1):e0116858.
177. Petersen MC, Shulman GI. Roles of Diacylglycerols and Ceramides in Hepatic Insulin Resistance. Trends Pharmacol Sci. 2017 Jul;38(7):649–65.
178. Samuel VT, Liu Z-X, Wang A, Beddow SA, Geisler JG, Kahn M, et al. Inhibition of protein kinase Cepsilon prevents hepatic insulin resistance in nonalcoholic fatty liver disease. J Clin Invest. 2007 Mar;117(3):739–45.
179. Bettelli E, Korn T, Oukka M, Kuchroo VK. Induction and effector functions of T(H)17 cells. Nature. 2008 Jun 19;453(7198):1051–7.
180. Ouyang W, Kolls JK, Zheng Y. The biological functions of T helper 17 cell effector cytokines in inflammation. Immunity. 2008 Apr;28(4):454–67.
181. Geddes K, Rubino SJ, Magalhaes JG, Streutker C, Le Bourhis L, Cho JH, et al. Identification of an innate T helper type 17 response to intestinal bacterial pathogens. Nat Med. 2011 Jun 12;17(7):837–44.
182. Winer S, Paltser G, Chan Y, Tsui H, Engleman E, Winer D, et al. Obesity predisposes to Th17 bias. Eur J Immunol. 2009 Sep;39(9):2629–35.
183. Sumarac-Dumanovic M, Stevanovic D, Ljubic A, Jorga J, Simic M, Stamenkovic-Pejkovic D, et al. Increased activity of interleukin-23/interleukin-17 proinflammatory axis in obese women. Int J Obes (Lond). 2009 Jan;33(1):151–6.
184. Garidou L, Pomié C, Klopp P, Waget A, Charpentier J, Aloulou M, et al. The Gut Microbiota Regulates Intestinal CD4 T Cells Expressing RORγt and Controls Metabolic Disease. Cell Metab. 2015 Jul 7;22(1):100–12.
185. Johnson AMF, Costanzo A, Gareau MG, Armando AM, Quehenberger O, Jameson JM, et al. High fat diet causes depletion of intestinal eosinophils associated with intestinal permeability. PLoS One. 2015;10(4):e0122195.
186. Cani PD, Bibiloni R, Knauf C, Waget A, Neyrinck AM, Delzenne NM, et al. Changes in gut microbiota control metabolic endotoxemia-induced inflammation in high-fat diet-induced obesity and diabetes in mice. Diabetes. 2008 Jun;57(6):1470–81.
187. Cani PD, Possemiers S, Van de Wiele T, Guiot Y, Everard A, Rottier O, et al. Changes in gut microbiota control inflammation in obese mice through a mechanism involving GLP-2-driven improvement of gut permeability. Gut. 2009 Aug;58(8):1091–103.
188. Cani PD, Delzenne NM. The role of the gut microbiota in energy metabolism and metabolic disease. Curr Pharm Des. 2009

Jan;15(13):1546–58.
189. Ding S, Chi MM, Scull BP, Rigby R, Schwerbrock NMJ, Magness S, et al. High-fat diet: bacteria interactions promote intestinal inflammation which precedes and correlates with obesity and insulin resistance in mouse. PLoS One. 2010 Aug 16;5(8):e12191.
190. Ding S, Lund PK. Role of intestinal inflammation as an early event in obesity and insulin resistance. Curr Opin Clin Nutr Metab Care. 2011 Jul;14(4):328–33.
191. Luck H, Tsai S, Chung J, Clemente-Casares X, Ghazarian M, Revelo XS, et al. Regulation of obesity-related insulin resistance with gut anti-inflammatory agents. Cell Metab. 2015 Apr 7;21(4):527–42.
192. Sender R, Fuchs S, Milo R. Revised Estimates for the Number of Human and Bacteria Cells in the Body. PLoS Biol. 2016 Aug;14(8):e1002533.
193. Round JL, Mazmanian SK. The gut microbiota shapes intestinal immune responses during health and disease. Nat Rev Immunol. 2009 May;9(5):313–23.
194. Bäckhed F, Ding H, Wang T, Hooper L V, Koh GY, Nagy A, et al. The gut microbiota as an environmental factor that regulates fat storage. Proc Natl Acad Sci U S A. 2004 Nov 2;101(44):15718–23.
195. Bäckhed F, Manchester JK, Semenkovich CF, Gordon JI. Mechanisms underlying the resistance to diet-induced obesity in germ-free mice. Proc Natl Acad Sci U S A. 2007 Jan 16;104(3):979–84.
196. Rabot S, Membrez M, Bruneau A, Gérard P, Harach T, Moser M, et al. Germ-free C57BL/6J mice are resistant to high-fat-diet-induced insulin resistance and have altered cholesterol metabolism. FASEB J. 2010 Dec;24(12):4948–59.
197. Turnbaugh PJ, Ley RE, Mahowald M a, Magrini V, Mardis ER, Gordon JI. An obesity-associated gut microbiome with increased capacity for energy harvest. Nature. 2006 Dec 21;444(7122):1027–31.
198. Turnbaugh PJ, Ridaura VK, Faith JJ, Rey FE, Knight R, Gordon JI. The effect of diet on the human gut microbiome: a metagenomic analysis in humanized gnotobiotic mice. Sci Transl Med. 2009 Nov 11;1(6):6ra14.
199. Ridaura VK, Faith JJ, Rey FE, Cheng J, Duncan AE, Kau AL, et al. Gut microbiota from twins discordant for obesity modulate metabolism in mice. Science. 2013 Sep 6;341(6150):1241214.
200. Krajmalnik-Brown R, Ilhan Z-E, Kang D-W, DiBaise JK. Effects of gut microbes on nutrient absorption and energy regulation. Nutr Clin Pract. 2012 Apr;27(2):201–14.
201. Nelson FE, Jensen LS, McGinnis J. Studies on the Stimulation of

Growth by Dietary Antibiotics: 2. Effect of Antibiotics on Metabolizable Energy of the Diet. Poult Sci. 1963 Jul 1;42(4):909–12.
202. Cho I, Yamanishi S, Cox L, Methé BA, Zavadil J, Li K, et al. Antibiotics in early life alter the murine colonic microbiome and adiposity. Nature. 2012 Aug 30;488(7413):621–6.
203. Mahana D, Trent CM, Kurtz ZD, Bokulich N a, Battaglia T, Chung J, et al. Antibiotic perturbation of the murine gut microbiome enhances the adiposity, insulin resistance, and liver disease associated with high-fat diet. Genome Med. 2016 Apr 27;8(1):48.
204. Mikkelsen KH, Frost M, Bahl MI, Licht TR, Jensen US, Rosenberg J, et al. Effect of Antibiotics on Gut Microbiota, Gut Hormones and Glucose Metabolism. PLoS One. 2015;10(11):e0142352.
205. Reijnders D, Goossens GH, Hermes GDA, Neis EPJG, van der Beek CM, Most J, et al. Effects of Gut Microbiota Manipulation by Antibiotics on Host Metabolism in Obese Humans: A Randomized Double-Blind Placebo-Controlled Trial. Cell Metab. 2016 Jul 12;24(1):63–74.
206. Kekkonen R-A, Lummela N, Karjalainen H, Latvala S, Tynkkynen S, Jarvenpaa S, et al. Probiotic intervention has strain-specific anti-inflammatory effects in healthy adults. World J Gastroenterol. 2008 Apr 7;14(13):2029–36.
207. Osterberg KL, Boutagy NE, McMillan RP, Stevens JR, Frisard MI, Kavanaugh JW, et al. Probiotic supplementation attenuates increases in body mass and fat mass during high-fat diet in healthy young adults. Obesity (Silver Spring). 2015 Dec;23(12):2364–70.
208. Hulston CJ, Churnside AA, Venables MC. Probiotic supplementation prevents high-fat, overfeeding-induced insulin resistance in human subjects. Br J Nutr. 2015 Feb 28;113(4):596–602.
209. Simon M-C, Strassburger K, Nowotny B, Kolb H, Nowotny P, Burkart V, et al. Intake of Lactobacillus reuteri improves incretin and insulin secretion in glucose-tolerant humans: a proof of concept. Diabetes Care. 2015 Oct;38(10):1827–34.
210. Dao MC, Everard A, Aron-Wisnewsky J, Sokolovska N, Prifti E, Verger EO, et al. Akkermansia muciniphila and improved metabolic health during a dietary intervention in obesity: relationship with gut microbiome richness and ecology. Gut. 2016 Mar;65(3):426–36.
211. Everard A, Belzer C, Geurts L, Ouwerkerk JP, Druart C, Bindels LB, et al. Cross-talk between Akkermansia muciniphila and intestinal epithelium controls diet-induced obesity. Proc Natl Acad Sci. 2013 May 28;110(22):9066–71.
212. Everard A, Lazarevic V, Derrien M, Girard M, Muccioli GG, Muccioli GM, et al. Responses of gut microbiota and glucose and lipid metabolism to prebiotics in genetic obese and diet-induced leptin-

resistant mice. Diabetes. 2011 Nov;60(11):2775–86.
213. Cani PD, Joly E, Horsmans Y, Delzenne NM. Oligofructose promotes satiety in healthy human: a pilot study. Eur J Clin Nutr. 2006 May;60(5):567–72.
214. Cani PD, Neyrinck AM, Maton N, Delzenne NM. Oligofructose promotes satiety in rats fed a high-fat diet: involvement of glucagon-like Peptide-1. Obes Res. 2005 Jun;13(6):1000–7.
215. Schneeberger M, Everard A, Gómez-Valadés AG, Matamoros S, Ramírez S, Delzenne NM, et al. Akkermansia muciniphila inversely correlates with the onset of inflammation, altered adipose tissue metabolism and metabolic disorders during obesity in mice. Sci Rep. 2015 Nov 13;5(October):16643.
216. Roopchand DE, Carmody RN, Kuhn P, Moskal K, Rojas-Silva P, Turnbaugh PJ, et al. Dietary Polyphenols Promote Growth of the Gut Bacterium Akkermansia muciniphila and Attenuate High-Fat Diet-Induced Metabolic Syndrome. Diabetes. 2015 Aug;64(8):2847–58.
217. Chang C-J, Lin C-S, Lu C-C, Martel J, Ko Y-F, Ojcius DM, et al. Ganoderma lucidum reduces obesity in mice by modulating the composition of the gut microbiota. Nat Commun. 2015 Jun 23;6(May):7489.
218. David L a., Maurice CF, Carmody RN, Gootenberg DB, Button JE, Wolfe BE, et al. Diet rapidly and reproducibly alters the human gut microbiome. Nature. 2014 Jan 23;505(7484):559–63.
219. Kristensen NB, Bryrup T, Allin KH, Nielsen T, Hansen TH, Pedersen O. Alterations in fecal microbiota composition by probiotic supplementation in healthy adults: a systematic review of randomized controlled trials. Genome Med. 2016;8(1):52.
220. Charteris WP, Kelly PM, Morelli L, Collins JK. Development and application of an in vitro methodology to determine the transit tolerance of potentially probiotic Lactobacillus and Bifidobacterium species in the upper human gastrointestinal tract. J Appl Microbiol. 1998 May;84(5):759–68.
221. Champomier Vergès MC, Zuñiga M, Morel-Deville F, Pérez-Martínez G, Zagorec M, Ehrlich SD. Relationships between arginine degradation, pH and survival in Lactobacillus sakei. FEMS Microbiol Lett. 1999 Nov 15;180(2):297–304.
222. Van Loo J. The specificity of the interaction with intestinal bacterial fermentation by prebiotics determines their physiological efficacy. Nutr Res Rev. 2004 Jun;17(1):89–98.
223. Anhê FF, Marette A. A microbial protein that alleviates metabolic syndrome. Nat Med. 2017 Jan 6;23(1):11–2.
224. Plovier H, Everard A, Druart C, Depommier C, Van Hul M, Geurts L, et al. A purified membrane protein from Akkermansia muciniphila or

the pasteurized bacterium improves metabolism in obese and diabetic mice. Nat Med. 2017 Jan 28;23(1):107–13.
225. Cicenia A, Scirocco A, Carabotti M, Pallotta L, Marignani M, Severi C. Postbiotic activities of lactobacilli-derived factors. J Clin Gastroenterol. 2014;48 Suppl 1(Supplement 1):S18-22.
226. Patel RM, Denning PW. Therapeutic use of prebiotics, probiotics, and postbiotics to prevent necrotizing enterocolitis: what is the current evidence? Clin Perinatol. 2013 Mar;40(1):11–25.
227. Canfora EE, Jocken JW, Blaak EE. Short-chain fatty acids in control of body weight and insulin sensitivity. Nat Rev Endocrinol. 2015 Oct;11(10):577–91.
228. Kimura I, Ozawa K, Inoue D, Imamura T, Kimura K, Maeda T, et al. The gut microbiota suppresses insulin-mediated fat accumulation via the short-chain fatty acid receptor GPR43. Nat Commun. 2013;4(May):1829.
229. Perry RJ, Peng L, Barry NA, Cline GW, Zhang D, Cardone RL, et al. Acetate mediates a microbiome-brain-β-cell axis to promote metabolic syndrome. Nature. 2016;534(7606):213–7.
230. Thaiss CA, Itav S, Rothschild D, Meijer M, Levy M, Moresi C, et al. Persistent microbiome alterations modulate the rate of post-dieting weight regain. Nature. 2016 Nov 24;540(7634):1–27.
231. Remely M, Aumueller E, Jahn D, Hippe B, Brath H, Haslberger AG. Microbiota and epigenetic regulation of inflammatory mediators in type 2 diabetes and obesity. Benef Microbes. 2014 Mar;5(1):33–43.
232. Remely M, Tesar I, Hippe B, Gnauer S, Rust P, Haslberger AG. Gut microbiota composition correlates with changes in body fat content due to weight loss. Benef Microbes. 2015;6(4):431–9.
233. Krautkramer KA, Kreznar JH, Romano KA, Vivas EI, Barrett-Wilt GA, Rabaglia ME, et al. Diet-Microbiota Interactions Mediate Global Epigenetic Programming in Multiple Host Tissues. Mol Cell. 2016 Dec 1;64(5):982–92.
234. Khan MT, Nieuwdorp M, Bäckhed F. Microbial modulation of insulin sensitivity. Cell Metab. 2014 Nov 4;20(5):753–60.
235. Chi W, Dao D, Lau TC, Henriksbo BD, Cavallari JF, Foley KP, et al. Bacterial peptidoglycan stimulates adipocyte lipolysis via NOD1. PLoS One. 2014 May 14;9(5):e97675.
236. Fritz JH, Le Bourhis L, Sellge G, Magalhaes JG, Fsihi H, Kufer TA, et al. Nod1-mediated innate immune recognition of peptidoglycan contributes to the onset of adaptive immunity. Immunity. 2007 Apr;26(4):445–59.
237. Schertzer JD, Tamrakar AK, Magalhães JG, Pereira S, Bilan PJ, Fullerton MD, et al. NOD1 activators link innate immunity to insulin resistance. Diabetes. 2011 Sep;60(9):2206–15.
238. Wolf AJ, Reyes CN, Liang W, Becker C, Shimada K, Wheeler ML, et

al. Hexokinase Is an Innate Immune Receptor for the Detection of Bacterial Peptidoglycan. Cell. 2016 Jul 28;166(3):624–36.
239. Pomié C, Blasco-Baque V, Klopp P, Nicolas S, Waget A, Loubières P, et al. Triggering the adaptive immune system with commensal gut bacteria protects against insulin resistance and dysglycemia. Mol Metab. 2016 Jun;5(6):392–403.
240. Amar J, Burcelin R, Ruidavets JB, Cani PD, Fauvel J, Alessi MC, et al. Energy intake is associated with endotoxemia in apparently healthy men. Am J Clin Nutr. 2008 May;87(5):1219–23.
241. Serino M, Luche E, Gres S, Baylac A, Bergé M, Cenac C, et al. Metabolic adaptation to a high-fat diet is associated with a change in the gut microbiota. Gut. 2012 Apr;61(4):543–53.
242. Fernández-Real JM, Pérez del Pulgar S, Luche E, Moreno-Navarrete JM, Waget A, Serino M, et al. CD14 modulates inflammation-driven insulin resistance. Diabetes. 2011 Aug 1;60(8):2179–86.
243. Jia L, Vianna CR, Fukuda M, Berglund ED, Liu C, Tao C, et al. Hepatocyte Toll-like receptor 4 regulates obesity-induced inflammation and insulin resistance. Nat Commun. 2014 May 12;5(May):3878.
244. Shi H, Kokoeva M V, Inouye K, Tzameli I, Yin H, Flier JS. TLR4 links innate immunity and fatty acid-induced insulin resistance. J Clin Invest. 2006 Nov;116(11):3015–25.
245. Reyna SM, Ghosh S, Tantiwong P, Meka CSR, Eagan P, Jenkinson CP, et al. Elevated toll-like receptor 4 expression and signaling in muscle from insulin-resistant subjects. Diabetes. 2008 Oct;57(10):2595–602.
246. Lee JY, Sohn KH, Rhee SH, Hwang D. Saturated fatty acids, but not unsaturated fatty acids, induce the expression of cyclooxygenase-2 mediated through Toll-like receptor 4. J Biol Chem. 2001 May 18;276(20):16683–9.
247. Nguyen MTA, Favelyukis S, Nguyen A-K, Reichart D, Scott PA, Jenn A, et al. A subpopulation of macrophages infiltrates hypertrophic adipose tissue and is activated by free fatty acids via Toll-like receptors 2 and 4 and JNK-dependent pathways. J Biol Chem. 2007 Nov 30;282(48):35279–92.
248. Suganami T, Tanimoto-Koyama K, Nishida J, Itoh M, Yuan X, Mizuarai S, et al. Role of the Toll-like receptor 4/NF-kappaB pathway in saturated fatty acid-induced inflammatory changes in the interaction between adipocytes and macrophages. Arterioscler Thromb Vasc Biol. 2007 Jan;27(1):84–91.
249. Fessler MB, Rudel LL, Brown JM. Toll-like receptor signaling links dietary fatty acids to the metabolic syndrome. Curr Opin Lipidol. 2009 Oct;20(5):379–85.

250. Pal D, Dasgupta S, Kundu R, Maitra S, Das G, Mukhopadhyay S, et al. Fetuin-A acts as an endogenous ligand of TLR4 to promote lipid-induced insulin resistance. Nat Med. 2012 Aug 29;18(8):1279–85.
251. Piccinini AM, Midwood KS. DAMPening inflammation by modulating TLR signalling. Mediators Inflamm. 2010;2010.
252. Watanabe Y, Nagai Y, Takatsu K. Activation and regulation of the pattern recognition receptors in obesity-induced adipose tissue inflammation and insulin resistance. Nutrients. 2013 Sep 23;5(9):3757–78.
253. Carneiro L a M, Travassos LH, Philpott DJ. Innate immune recognition of microbes through Nod1 and Nod2: implications for disease. Microbes Infect. 2004 May;6(6):609–16.
254. Inohara N, Koseki T, del Peso L, Hu Y, Yee C, Chen S, et al. Nod1, an Apaf-1-like activator of caspase-9 and nuclear factor-kappaB. J Biol Chem. 1999 May 21;274(21):14560–7.
255. Ogura Y, Inohara N, Benito A, Chen FF, Yamaoka S, Nunez G. Nod2, a Nod1/Apaf-1 family member that is restricted to monocytes and activates NF-kappaB. J Biol Chem. 2001 Feb 16;276(7):4812–8.
256. Philpott DJ, Sorbara MT, Robertson SJ, Croitoru K, Girardin SE. NOD proteins: regulators of inflammation in health and disease. Nat Rev Immunol. 2014 Jan 13;14(1):9–23.
257. Lauro ML, D'Ambrosio EA, Bahnson BJ, Grimes CL. Molecular Recognition of Muramyl Dipeptide Occurs in the Leucine-rich Repeat Domain of Nod2. ACS Infect Dis. 2017 Apr 14;3(4):264–70.
258. Vijayrajratnam S, Pushkaran AC, Balakrishnan A, Vasudevan AK, Biswas R, Mohan CG. Understanding the molecular differential recognition of muramyl peptide ligands by LRR domains of human NOD receptors. Biochem J. 2017 Jul 27;474(16):2691–711.
259. Mavrogiorgos N, Mekasha S, Yang Y, Kelliher M a, Ingalls RR. Activation of NOD receptors by Neisseria gonorrhoeae modulates the innate immune response. Innate Immun. 2014 May 24;20(4):377–89.
260. Girardin SE, Travassos LH, Hervé M, Blanot D, Boneca IG, Philpott DJ, et al. Peptidoglycan molecular requirements allowing detection by Nod1 and Nod2. J Biol Chem. 2003 Oct 24;278(43):41702–8.
261. Girardin SE, Boneca IG, Carneiro L a M, Antignac A, Jéhanno M, Viala J, et al. Nod1 detects a unique muropeptide from gram-negative bacterial peptidoglycan. Science. 2003 Jun 6;300(5625):1584–7.
262. Chamaillard M, Hashimoto M, Horie Y, Masumoto J, Qiu S, Saab L, et al. An essential role for NOD1 in host recognition of bacterial peptidoglycan containing diaminopimelic acid. Nat Immunol. 2003 Jul;4(7):702–7.

263. Antosz H, Osiak M. NOD1 and NOD2 receptors: integral members of the innate and adaptive immunity system. Acta Biochim Pol. 2013;60(3):351–60.
264. Vollmer W, Blanot D, de Pedro MA. Peptidoglycan structure and architecture. FEMS Microbiol Rev. 2008 Mar;32(2):149–67.
265. Girardin SE, Boneca IG, Viala J, Chamaillard M, Labigne A, Thomas G, et al. Nod2 is a general sensor of peptidoglycan through muramyl dipeptide (MDP) detection. J Biol Chem. 2003 Mar 14;278(11):8869–72.
266. Inohara N, Koseki T, Lin J, del Peso L, Lucas PC, Chen FF, et al. An induced proximity model for NF-kappa B activation in the Nod1/RICK and RIP signaling pathways. J Biol Chem. 2000 Sep 8;275(36):27823–31.
267. Kobayashi K, Inohara N, Hernandez LD, Galán JE, Núñez G, Janeway CA, et al. RICK/Rip2/CARDIAK mediates signalling for receptors of the innate and adaptive immune systems. Nature. 2002 Mar 14;416(6877):194–9.
268. Inohara, Chamaillard, McDonald C, Nuñez G. NOD-LRR proteins: role in host-microbial interactions and inflammatory disease. Annu Rev Biochem. 2005;74(1):355–83.
269. Kobayashi KS, Chamaillard M, Ogura Y, Henegariu O, Inohara N, Nuñez G, et al. Nod2-dependent regulation of innate and adaptive immunity in the intestinal tract. Science. 2005 Mar 4;307(5710):731–4.
270. Correa RG, Milutinovic S, Reed JC. Roles of NOD1 (NLRC1) and NOD2 (NLRC2) in innate immunity and inflammatory diseases. Biosci Rep. 2012 Dec;32(6):597–608.
271. Caruso R, Warner N, Inohara N, Núñez G. NOD1 and NOD2: signaling, host defense, and inflammatory disease. Immunity. 2014 Dec 18;41(6):898–908.
272. Hu YW, Wu XM, Ren SS, Cao L, Nie P, Chang MX. NOD1 deficiency impairs CD44a/Lck as well as PI3K/Akt pathway. Sci Rep. 2017 Jun 7;7(1):2979.
273. Kasimsetty SG, Shigeoka AA, Scheinok AA, Gavin AL, Ulevitch RJ, McKay DB. Lack of Both Nucleotide-Binding Oligomerization Domain-Containing Proteins 1 and 2 Primes T Cells for Activation-Induced Cell Death. J Immunol. 2017 Aug 1;199(3):1196–205.
274. Mine Y, Yokota Y, Wakai Y, Fukada S, Nishida M, Goto S, et al. Immunoactive peptides, FK-156 and FK-565. I. Enhancement of host resistance to microbial infection in mice. J Antibiot (Tokyo). 1983 Aug;36(8):1045–50.
275. Lysenko ES, Clarke TB, Shchepetov M, Ratner AJ, Roper DI, Dowson CG, et al. Nod1 signaling overcomes resistance of S. pneumoniae to opsonophagocytic killing. PLoS Pathog. 2007 Aug

24;3(8):e118.
276. Clarke TB, Davis KM, Lysenko ES, Zhou AY, Yu Y, Weiser JN. Recognition of peptidoglycan from the microbiota by Nod1 enhances systemic innate immunity. Nat Med. 2010 Feb;16(2):228–31.
277. Hergott CB, Roche AM, Tamashiro E, Clarke TB, Bailey AG, Laughlin A, et al. Peptidoglycan from the gut microbiota governs the lifespan of circulating phagocytes at homeostasis. Blood. 2016 May 19;127(20):2460–71.
278. Amar J, Chabo C, Waget A, Klopp P, Vachoux C, Bermúdez-Humarán LG, et al. Intestinal mucosal adherence and translocation of commensal bacteria at the early onset of type 2 diabetes: molecular mechanisms and probiotic treatment. EMBO Mol Med. 2011 Sep;3(9):559–72.
279. Zhou Y-J, Liu C, Li C-L, Song Y-L, Tang Y-S, Zhou H, et al. Increased NOD1, but not NOD2, activity in subcutaneous adipose tissue from patients with metabolic syndrome. Obesity (Silver Spring). 2015 Jul;23(7):1394–400.
280. Nishio H, Kanno S, Onoyama S, Ikeda K, Tanaka T, Kusuhara K, et al. Nod1 ligands induce site-specific vascular inflammation. Arterioscler Thromb Vasc Biol. 2011 May;31(5):1093–9.
281. Kanno S, Nishio H, Tanaka T, Motomura Y, Murata K, Ihara K, et al. Activation of an innate immune receptor, Nod1, accelerates atherogenesis in Apoe-/- mice. J Immunol. 2015 Jan 15;194(2):773–80.
282. Purohit JS, Hu P, Chen G, Whelan J, Moustaid-Moussa N, Zhao L. Activation of nucleotide oligomerization domain containing protein 1 induces lipolysis through NF-κB and the lipolytic PKA activation in 3T3-L1 adipocytes. Biochem Cell Biol. 2013 Dec;91(6):428–34.
283. Khan PM, Correa RG, Divlianska DB, Peddibhotla S, Sessions EH, Magnuson G, et al. Identification of Inhibitors of NOD1-Induced Nuclear Factor-κB Activation. ACS Med Chem Lett. 2011 Oct 13;2(10):780–5.
284. Petnicki-Ocwieja T, Hrncir T, Liu Y-J, Biswas A, Hudcovic T, Tlaskalova-Hogenova H, et al. Nod2 is required for the regulation of commensal microbiota in the intestine. Proc Natl Acad Sci U S A. 2009 Sep 15;106(37):15813–8.
285. Rehman A, Sina C, Gavrilova O, Häsler R, Ott S, Baines JF, et al. Nod2 is essential for temporal development of intestinal microbial communities. Gut. 2011 Oct;60(10):1354–62.
286. Jiang W, Wang X, Zeng B, Liu L, Tardivel A, Wei H, et al. Recognition of gut microbiota by NOD2 is essential for the homeostasis of intestinal intraepithelial lymphocytes. J Exp Med. 2013 Oct 21;210(11):2465–76.
287. Jeong Y-J, Kang M-J, Lee S-J, Kim C-H, Kim J-C, Kim T-H, et al.

Nod2 and Rip2 contribute to innate immune responses in mouse neutrophils. Immunology. 2014 Oct 25;143(2):269–76.
288. Ramanan D, Tang MS, Bowcutt R, Loke P, Cadwell K. Bacterial sensor Nod2 prevents inflammation of the small intestine by restricting the expansion of the commensal Bacteroides vulgatus. Immunity. 2014 Aug 21;41(2):311–24.
289. Stronati L, Negroni A, Merola P, Pannone V, Borrelli O, Cirulli M, et al. Mucosal NOD2 expression and NF-kappaB activation in pediatric Crohn's disease. Inflamm Bowel Dis. 2008 Mar;14(3):295–302.
290. Hugot JP, Chamaillard M, Zouali H, Lesage S, Cézard JP, Belaiche J, et al. Association of NOD2 leucine-rich repeat variants with susceptibility to Crohn's disease. Nature. 2001 May 31;411(6837):599–603.
291. Ogura Y, Bonen DK, Inohara N, Nicolae DL, Chen FF, Ramos R, et al. A frameshift mutation in NOD2 associated with susceptibility to Crohn's disease. Nature. 2001 May 31;411(6837):603–6.
292. Yang S, Wang B, Humphries F, Jackson R, Healy ME, Bergin R, et al. Pellino3 ubiquitinates RIP2 and mediates Nod2-induced signaling and protective effects in colitis. Nat Immunol. 2013 Sep;14(9):927–36.
293. Jing X, Zulfiqar F, Park SY, Núñez G, Dziarski R, Gupta D. Peptidoglycan recognition protein 3 and Nod2 synergistically protect mice from dextran sodium sulfate-induced colitis. J Immunol. 2014 Sep 15;193(6):3055–69.
294. Barreau F, Madre C, Meinzer U, Berrebi D, Dussaillant M, Merlin F, et al. Nod2 regulates the host response towards microflora by modulating T cell function and epithelial permeability in mouse Peyer's patches. Gut. 2010 Feb 1;59(2):207–17.
295. Watanabe T, Kitani A, Murray PJ, Strober W. NOD2 is a negative regulator of Toll-like receptor 2-mediated T helper type 1 responses. Nat Immunol. 2004 Aug;5(8):800–8.
296. Richardson WM, Sodhi CP, Russo A, Siggers RH, Afrazi A, Gribar SC, et al. Nucleotide-binding oligomerization domain-2 inhibits toll-like receptor-4 signaling in the intestinal epithelium. Gastroenterology. 2010;139(3):904–917.e6.
297. Netea MG, Kullberg BJ, de Jong DJ, Franke B, Sprong T, Naber THJ, et al. NOD2 mediates anti-inflammatory signals induced by TLR2 ligands: implications for Crohn's disease. Eur J Immunol. 2004 Jul;34(7):2052–9.
298. Matsui K, Ikeda R. Peptidoglycan in combination with muramyldipeptide synergistically induces an interleukin-10-dependent T helper 2-dominant immune response. Microbiol Immunol. 2014 Apr;58(4):260–5.
299. Couturier-Maillard A, Secher T, Rehman A, Normand S, De

Arcangelis A, Haesler R, et al. NOD2-mediated dysbiosis predisposes mice to transmissible colitis and colorectal cancer. J Clin Invest. 2013 Feb 2;123(2):700–11.
300. Udden SMN, Peng L, Gan J-L, Shelton JM, Malter JS, Hooper L V., et al. NOD2 Suppresses Colorectal Tumorigenesis via Downregulation of the TLR Pathways. Cell Rep. 2017 Jun 27;19(13):2756–70.
301. Afonina IS, Zhong Z, Karin M, Beyaert R. Limiting inflammation-the negative regulation of NF-κB and the NLRP3 inflammasome. Nat Immunol. 2017 Jul 19;18(8):861–9.
302. Hedl M, Li J, Cho JH, Abraham C. Chronic stimulation of Nod2 mediates tolerance to bacterial products. Proc Natl Acad Sci U S A. 2007 Dec 4;104(49):19440–5.
303. Hedl M, Abraham C. Distinct roles for Nod2 protein and autocrine interleukin-1beta in muramyl dipeptide-induced mitogen-activated protein kinase activation and cytokine secretion in human macrophages. J Biol Chem. 2011 Jul 29;286(30):26440–9.
304. Hedl M, Abraham C. Secretory mediators regulate Nod2-induced tolerance in human macrophages. Gastroenterology. 2011 Jan;140(1):231–41.
305. Watanabe T, Asano N, Murray PJ, Ozato K, Tailor P, Fuss IJ, et al. Muramyl dipeptide activation of nucleotide-binding oligomerization domain 2 protects mice from experimental colitis. J Clin Invest. 2008 Feb;118(2):545–59.
306. Watanabe T, Asano N, Meng G, Yamashita K, Arai Y, Sakurai T, et al. NOD2 downregulates colonic inflammation by IRF4-mediated inhibition of K63-linked polyubiquitination of RICK and TRAF6. Mucosal Immunol. 2014 Nov 26;7(6):1312–25.
307. Negishi H, Ohba Y, Yanai H, Takaoka A, Honma K, Yui K, et al. Negative regulation of Toll-like-receptor signaling by IRF-4. Proc Natl Acad Sci U S A. 2005 Nov 1;102(44):15989–94.
308. Honma K, Udono H, Kohno T, Yamamoto K, Ogawa A, Takemori T, et al. Interferon regulatory factor 4 negatively regulates the production of proinflammatory cytokines by macrophages in response to LPS. Proc Natl Acad Sci U S A. 2005 Nov 1;102(44):16001–6.
309. Shaffer AL, Emre NCT, Romesser PB, Staudt LM. IRF4: Immunity. Malignancy! Therapy? Clin Cancer Res. 2009 May 1;15(9):2954–61.
310. Eguchi J, Kong X, Tenta M, Wang X, Kang S, Rosen ED. Interferon regulatory factor 4 regulates obesity-induced inflammation through regulation of adipose tissue macrophage polarization. Diabetes. 2013 Oct;62(10):3394–403.
311. Eguchi J, Wang X, Yu S, Kershaw EE, Chiu PC, Dushay J, et al. Transcriptional control of adipose lipid handling by IRF4. Cell Metab.

2011 Mar 2;13(3):249–59.
312. Ahyi A-NN, Chang H-C, Dent AL, Nutt SL, Kaplan MH. IFN regulatory factor 4 regulates the expression of a subset of Th2 cytokines. J Immunol. 2009 Aug 1;183(3):1598–606.
313. Lee C-G, Hwang W, Maeng K-E, Kwon H-K, So J-S, Sahoo A, et al. IRF4 regulates IL-10 gene expression in CD4(+) T cells through differential nuclear translocation. Cell Immunol. 2011 Jan;268(2):97–104.
314. Wu D, Molofsky AB, Liang H-E, Ricardo-Gonzalez RR, Jouihan HA, Bando JK, et al. Eosinophils sustain adipose alternatively activated macrophages associated with glucose homeostasis. Science. 2011 Apr 8;332(6026):243–7.
315. Fujisaka S, Usui I, Bukhari A, Ikutani M, Oya T, Kanatani Y, et al. Regulatory mechanisms for adipose tissue M1 and M2 macrophages in diet-induced obese mice. Diabetes. 2009 Nov;58(11):2574–82.
316. Denou E, Lolmède K, Garidou L, Pomie C, Chabo C, Lau TC, et al. Defective NOD2 peptidoglycan sensing promotes diet-induced inflammation, dysbiosis, and insulin resistance. EMBO Mol Med. 2015 Mar 1;7(3):259–74.
317. Rodriguez-Nunez I, Caluag T, Kirby K, Rudick CN, Dziarski R, Gupta D. Nod2 and Nod2-regulated microbiota protect BALB/c mice from diet-induced obesity and metabolic dysfunction. Sci Rep. 2017 Apr 3;7(1):548.
318. Henriksbo BD, Lau TC, Cavallari JF, Denou E, Chi W, Lally JS, et al. Fluvastatin causes NLRP3 inflammasome-mediated adipose insulin resistance. Diabetes. 2014 Nov;63(11):3742–7.
319. Mittrücker HW, Matsuyama T, Grossman A, Kündig TM, Potter J, Shahinian A, et al. Requirement for the transcription factor LSIRF/IRF4 for mature B and T lymphocyte function. Science. 1997 Jan 24;275(5299):540–3.
320. Lee AJ, Chen B, Chew M V., Barra NG, Shenouda MM, Nham T, et al. Inflammatory monocytes require type I interferon receptor signaling to activate NK cells via IL-18 during a mucosal viral infection. J Exp Med. 2017 Apr 3;214(4):1153–67.
321. Postic C, Shiota M, Niswender KD, Jetton TL, Chen Y, Moates JM, et al. Dual roles for glucokinase in glucose homeostasis as determined by liver and pancreatic beta cell-specific gene knock-outs using Cre recombinase. J Biol Chem. 1999 Jan 1;274(1):305–15.
322. Postic C, Magnuson M a. DNA excision in liver by an albumin-Cre transgene occurs progressively with age. Genesis. 2000 Feb;26(2):149–50.
323. Kim JK. Hyperinsulinemic-euglycemic clamp to assess insulin

sensitivity in vivo. Stocker C, editor. Methods Mol Biol. 2009 Jan;560:221–38.
324. Galic S, Fullerton MD, Schertzer JD, Sikkema S, Marcinko K, Walkley CR, et al. Hematopoietic AMPK β1 reduces mouse adipose tissue macrophage inflammation and insulin resistance in obesity. J Clin Invest. 2011 Dec;121(12):4903–15.
325. Matthews DR, Hosker JP, Rudenski AS, Naylor BA, Treacher DF, Turner RC. Homeostasis model assessment: insulin resistance and beta-cell function from fasting plasma glucose and insulin concentrations in man. Diabetologia. 1985 Jul;28(7):412–9.
326. Okafuji I, Nishikomori R, Kanazawa N, Kambe N, Fujisawa A, Yamazaki S, et al. Role of the NOD2 genotype in the clinical phenotype of Blau syndrome and early-onset sarcoidosis. Arthritis Rheum. 2009 Jan;60(1):242–50.
327. Boyle JP, Parkhouse R, Monie TP. Insights into the molecular basis of the NOD2 signalling pathway. Open Biol. 2014 Dec 17;4(12):140178–140178.
328. Lee K-H, Biswas A, Liu Y-J, Kobayashi KS. Proteasomal degradation of Nod2 protein mediates tolerance to bacterial cell wall components. J Biol Chem. 2012 Nov 16;287(47):39800–11.
329. Tukhvatulin AI, Dzharullaeva AS, Tukhvatulina NM, Shcheblyakov D V., Shmarov MM, Dolzhikova I V., et al. Powerful Complex Immunoadjuvant Based on Synergistic Effect of Combined TLR4 and NOD2 Activation Significantly Enhances Magnitude of Humoral and Cellular Adaptive Immune Responses. PLoS One. 2016;11(5):e0155650.
330. Tukhvatulin AI, Gitlin II, Shcheblyakov D V, Artemicheva NM, Burdelya LG, Shmarov MM, et al. Combined stimulation of Toll-like receptor 5 and NOD1 strongly potentiates activity of NF-κB, resulting in enhanced innate immune reactions and resistance to Salmonella enterica serovar Typhimurium infection. Infect Immun. 2013 Oct;81(10):3855–64.
331. Solovjov DA, Pluskota E, Plow EF. Distinct roles for the alpha and beta subunits in the functions of integrin alphaMbeta2. J Biol Chem. 2005 Jan 14;280(2):1336–45.
332. Tamrakar AK, Schertzer JD, Chiu TT, Foley KP, Bilan PJ, Philpott DJ, et al. NOD2 activation induces muscle cell-autonomous innate immune responses and insulin resistance. Endocrinology. 2010 Dec;151(12):5624–37.
333. Kim S, Choi Y, Choi Y, Park T. Obesity activates toll-like receptor-mediated proinflammatory signaling cascades in the adipose tissue of mice. J Nutr Biochem. 2012 Feb;23(2):113–22.
334. Miller SI, Wallace RJ, Musher DM, Septimus EJ, Kohl S, Baughn RE. Hypoglycemia as a manifestation of sepsis. Am J Med. 1980

May;68(5):649–54.
335. Raetzsch CF, Brooks NL, Alderman JM, Moore KS, Hosick P a, Klebanov S, et al. Lipopolysaccharide inhibition of glucose production through the Toll-like receptor-4, myeloid differentiation factor 88, and nuclear factor kappa b pathway. Hepatology. 2009 Aug;50(2):592–600.
336. Vijay-Kumar M, Aitken JD, Carvalho F a, Cullender TC, Mwangi S, Srinivasan S, et al. Metabolic syndrome and altered gut microbiota in mice lacking Toll-like receptor 5. Science. 2010 Apr 9;328(5975):228–31.
337. Nackiewicz D, Dan M, He W, Kim R, Salmi A, Rütti S, et al. TLR2/6 and TLR4-activated macrophages contribute to islet inflammation and impair beta cell insulin gene expression via IL-1 and IL-6. Diabetologia. 2014 Aug;57(8):1645–54.
338. Hong C-P, Yun CH, Lee G-W, Park A, Kim Y-M, Jang MH. TLR9 regulates adipose tissue inflammation and obesity-related metabolic disorders. Obesity (Silver Spring). 2015 Nov;23(11):2199–206.
339. Jackson EE, Rendina-Ruedy E, Smith BJ, Lacombe VA. Loss of Toll-Like Receptor 4 Function Partially Protects against Peripheral and Cardiac Glucose Metabolic Derangements During a Long-Term High-Fat Diet. PLoS One. 2015;10(11):e0142077.
340. Wu S-C, Rau C-S, Lu T-H, Tzeng S-L, Wu Y-C, Wu C-J, et al. Effect of Weight-Reduction in Obese Mice Lacking Toll-Like Receptor 5 and C57BL/6 Mice Fed a Low-Fat Diet. Mediators Inflamm. 2015;2015:852126.
341. Zhang N, Liang H, Farese R V., Li J, Musi N, Hussey SE. Pharmacological TLR4 Inhibition Protects against Acute and Chronic Fat-Induced Insulin Resistance in Rats. PLoS One. 2015;10(7):e0132575.
342. Sepehri Z, Kiani Z, Nasiri AA, Kohan F. Toll-like receptor 2 and type 2 diabetes. Cell Mol Biol Lett. 2016;21(1):2.
343. Castellaneta A, Sumpter TL, Chen L, Tokita D, Thomson AW. NOD2 ligation subverts IFN-alpha production by liver plasmacytoid dendritic cells and inhibits their T cell allostimulatory activity via B7-H1 up-regulation. J Immunol. 2009 Dec 1;183(11):6922–32.
344. Rahman MK, Midtling EH, Svingen P a, Xiong Y, Bell MP, Tung J, et al. The pathogen recognition receptor NOD2 regulates human FOXP3+ T cell survival. J Immunol. 2010 Jun 15;184(12):7247–56.
345. Zheng S, Hedl M, Abraham C. TAM receptor-dependent regulation of SOCS3 and MAPKs contributes to proinflammatory cytokine downregulation following chronic NOD2 stimulation of human macrophages. J Immunol. 2015 Feb 15;194(4):1928–37.
346. Zheng S, Hedl M, Abraham C. Twist1 and Twist2 Contribute to Cytokine Downregulation following Chronic NOD2 Stimulation of

Human Macrophages through the Coordinated Regulation of Transcriptional Repressors and Activators. J Immunol. 2015 Jul 1;195(1):217–26.
347. Bist P, Cheong WS, Ng A, Dikshit N, Kim B-H, Pulloor NK, et al. E3 Ubiquitin ligase ZNRF4 negatively regulates NOD2 signalling and induces tolerance to MDP. Nat Commun. 2017 Jun 28;8(May):15865.
348. Chan KL, Tam TH, Boroumand P, Prescott D, Costford SR, Escalante NK, et al. Circulating NOD1 Activators and Hematopoietic NOD1 Contribute to Metabolic Inflammation and Insulin Resistance. Cell Rep. 2017 Mar 7;18(10):2415–26.
349. Klein I, Cornejo JC, Polakos NK, John B, Wuensch S a, Topham DJ, et al. Kupffer cell heterogeneity: functional properties of bone marrow derived and sessile hepatic macrophages. Blood. 2007 Dec 1;110(12):4077–85.
350. Van Rooijen N, Sanders A. Kupffer cell depletion by liposome-delivered drugs: comparative activity of intracellular clodronate, propamidine, and ethylenediaminetetraacetic acid. Hepatology. 1996 May;23(5):1239–43.
351. Basset C, Holton J, O'Mahony R, Roitt I. Innate immunity and pathogen-host interaction. Vaccine. 2003 Jun 1;21 Suppl 2(SUPPL. 2):S12-23.
352. Zanello G, Goethel A, Forster K, Geddes K, Philpott DJ, Croitoru K. Nod2 activates NF-kB in CD4+ T cells but its expression is dispensable for T cell-induced colitis. PLoS One. 2013 Jan;8(12):e82623.
353. Scott MJ, Chen C, Sun Q, Billiar TR. Hepatocytes express functional NOD1 and NOD2 receptors: a role for NOD1 in hepatocyte CC and CXC chemokine production. J Hepatol. 2010 Oct;53(4):693–701.
354. Body-Malapel M, Dharancy S, Berrebi D, Louvet A, Hugot J-P, Philpott DJ, et al. NOD2: a potential target for regulating liver injury. Lab Invest. 2008 Mar;88(3):318–27.
355. EL Andaloussi S, Mäger I, Breakefield XO, Wood MJ a. Extracellular vesicles: biology and emerging therapeutic opportunities. Nat Rev Drug Discov. 2013 May;12(5):347–57.
356. Hirsova P, Ibrahim SH, Verma VK, Morton LA, Shah VH, LaRusso NF, et al. Extracellular vesicles in liver pathobiology: Small particles with big impact. Hepatology. 2016 Dec;64(6):2219–33.
357. de Candia P, De Rosa V, Gigantino V, Botti G, Ceriello A, Matarese G. Immunometabolism of human autoimmune diseases: from metabolites to extracellular vesicles. FEBS Lett. 2017 Jun 26;1–16.
358. Nguyen M-A, Karunakaran D, Geoffrion M, Cheng HS, Tandoc K, Perisic Matic L, et al. Extracellular Vesicles Secreted by Atherogenic Macrophages Transfer MicroRNA to Inhibit Cell Migration.

Arterioscler Thromb Vasc Biol. 2017 Sep 7;ATVBAHA.117.309795.
359. Szabo G, Momen-Heravi F. Extracellular vesicles in liver disease and potential as biomarkers and therapeutic targets. Nat Rev Gastroenterol Hepatol. 2017 Aug;14(8):455–66.
360. Ying W, Riopel M, Bandyopadhyay G, Dong Y, Birmingham A, Seo JB, et al. Adipose Tissue Macrophage-Derived Exosomal miRNAs Can Modulate In Vivo and In Vitro Insulin Sensitivity. Cell. 2017 Sep 19;1–13.
361. Caesar R, Reigstad CS, Bäckhed HK, Reinhardt C, Ketonen M, Lundén GÖ, et al. Gut-derived lipopolysaccharide augments adipose macrophage accumulation but is not essential for impaired glucose or insulin tolerance in mice. Gut. 2012 Dec;61(12):1701–7.
362. Purohit J, Hu P, Burke SJ, Collier JJ, Chen J, Zhao L. The Effects of NOD Activation on Adipocyte Differentiation. Obesity (Silver Spring). 2012 Jun 20;21(4):737–47.
363. Irving AT, Mimuro H, Kufer T a, Lo C, Wheeler R, Turner LJ, et al. The immune receptor NOD1 and kinase RIP2 interact with bacterial peptidoglycan on early endosomes to promote autophagy and inflammatory signaling. Cell Host Microbe. 2014 May 14;15(5):623–35.
364. Yang H, Li N, Song L-N, Wang L, Tian C, Tang C-S, et al. Activation of NOD1 by DAP contributes to myocardial ischemia/reperfusion injury via multiple signaling pathways. Apoptosis. 2015 Apr 22;20(4):512–22.
365. Rubino SJ, Magalhaes JG, Philpott D, Bahr GM, Blanot D, Girardin SE. Identification of a synthetic muramyl peptide derivative with enhanced Nod2 stimulatory capacity. Innate Immun. 2013 Oct 22;19(5):493–503.
366. Zheng S, Abraham C. NF-κB1 inhibits NOD2-induced cytokine secretion through ATF3-dependent mechanisms. Mol Cell Biol. 2013 Dec;33(24):4857–71.
367. Chen X, Xiao Z, Xie X, Liu X, Jiang M, Yuan C, et al. TNF-α-induced NOD2 and RIP2 contribute to the up-regulation of cytokines induced by MDP in monocytic THP-1 cells. J Cell Biochem. 2017 Jun 21;(June).
368. Ayala JE, Samuel VT, Morton GJ, Obici S, Croniger CM, Shulman GI, et al. Standard operating procedures for describing and performing metabolic tests of glucose homeostasis in mice. Dis Model Mech. 2010;3(9–10):525–34.
369. Okla M, Wang W, Kang I, Pashaj A, Carr T, Chung S. Activation of Toll-like receptor 4 (TLR4) attenuates adaptive thermogenesis via endoplasmic reticulum stress. J Biol Chem. 2015 Oct 30;290(44):26476–90.
370. Poggi M, Bastelica D, Gual P, Iglesias M a., Gremeaux T, Knauf C,

et al. C3H/HeJ mice carrying a toll-like receptor 4 mutation are protected against the development of insulin resistance in white adipose tissue in response to a high-fat diet. Diabetologia. 2007 Jun;50(6):1267–76.
371. Santos SHS, Andrade JMO, Fernandes LR, Sinisterra RDM, Sousa FB, Feltenberger JD, et al. Oral Angiotensin-(1-7) prevented obesity and hepatic inflammation by inhibition of resistin/TLR4/MAPK/NF-κB in rats fed with high-fat diet. Peptides. 2013 Aug;46:47–52.
372. Maurya CK, Arha D, Rai AK, Kumar SK, Pandey J, Avisetti DR, et al. NOD2 activation induces oxidative stress contributing to mitochondrial dysfunction and insulin resistance in skeletal muscle cells. Free Radic Biol Med. 2015 Dec;89:158–69.
373. Swirski FK, Nahrendorf M, Etzrodt M, Wildgruber M, Cortez-Retamozo V, Panizzi P, et al. Identification of splenic reservoir monocytes and their deployment to inflammatory sites. Science. 2009 Jul 31;325(5940):612–6.
374. Lessard A-J, LeBel M, Egarnes B, Préfontaine P, Thériault P, Droit A, et al. Triggering of NOD2 Receptor Converts Inflammatory Ly6C(high) into Ly6C(low) Monocytes with Patrolling Properties. Cell Rep. 2017 Aug 22;20(8):1830–43.
375. Chedid LA, Parant MA, Audibert FM, Riveau GJ, Parant FJ, Lederer E, et al. Biological activity of a new synthetic muramyl peptide adjuvant devoid of pyrogenicity. Infect Immun. 1982 Feb;35(2):417–24.
376. Virkamäki A, Yki-Järvinen H. Mechanisms of insulin resistance during acute endotoxemia. Endocrinology. 1994 May;134(5):2072–8.
377. Al Nabhani Z, Montcuquet N, Roy M, Dussaillant M, Hugot J-P, Barreau F. Complementary Roles of Nod2 in Hematopoietic and Nonhematopoietic Cells in Preventing Gut Barrier Dysfunction Dependent on MLCK Activity. Inflamm Bowel Dis. 2017 Jul;23(7):1109–19.
378. Al Nabhani Z, Dietrich G, Hugot J-P, Barreau F. Nod2: The intestinal gate keeper. PLoS Pathog. 2017 Mar;13(3):e1006177.
379. Williams JW, Tjota MY, Clay BS, Vander Lugt B, Bandukwala HS, Hrusch CL, et al. Transcription factor IRF4 drives dendritic cells to promote Th2 differentiation. Nat Commun. 2013 Dec 20;4(May):2990.
380. Gao Y, Nish SA, Jiang R, Hou L, Licona-Limón P, Weinstein JS, et al. Control of T helper 2 responses by transcription factor IRF4-dependent dendritic cells. Immunity. 2013 Oct 17;39(4):722–32.
381. Fabrizi M, Marchetti V, Mavilio M, Marino A, Casagrande V, Cavalera M, et al. IL-21 is a major negative regulator of IRF4-dependent lipolysis affecting Tregs in adipose tissue and systemic

insulin sensitivity. Diabetes. 2014 Jun;63(6):2086–96.
382. Vasanthakumar A, Moro K, Xin A, Liao Y, Gloury R, Kawamoto S, et al. The transcriptional regulators IRF4, BATF and IL-33 orchestrate development and maintenance of adipose tissue-resident regulatory T cells. Nat Immunol. 2015 Mar 19;16(3):276–85.
383. Akbari M, Honma K, Kimura D, Miyakoda M, Kimura K, Matsuyama T, et al. IRF4 in dendritic cells inhibits IL-12 production and controls Th1 immune responses against Leishmania major. J Immunol. 2014 Mar 1;192(5):2271–9.
384. Tada H, Aiba S, Shibata K-I, Ohteki T, Takada H. Synergistic effect of Nod1 and Nod2 agonists with toll-like receptor agonists on human dendritic cells to generate interleukin-12 and T helper type 1 cells. Infect Immun. 2005 Dec;73(12):7967–76.
385. Farzi A, Reichmann F, Meinitzer A, Mayerhofer R, Jain P, Hassan AM, et al. Synergistic effects of NOD1 or NOD2 and TLR4 activation on mouse sickness behavior in relation to immune and brain activity markers. Brain Behav Immun. 2015 Feb;44:106–20.
386. Khan N, Pahari S, Vidyarthi A, Aqdas M, Agrewala JN. NOD-2 and TLR-4 Signaling Reinforces the Efficacy of Dendritic Cells and Reduces the Dose of TB Drugs against Mycobacterium tuberculosis. J Innate Immun. 2016;8(3):228–42.
387. Jakopin Ž. Nucleotide-binding oligomerization domain (NOD) inhibitors: a rational approach toward inhibition of NOD signaling pathway. J Med Chem. 2014 Aug 28;57(16):6897–918.
388. Rickard DJ, Sehon C a, Kasparcova V, Kallal L a, Zeng X, Montoute MN, et al. Identification of benzimidazole diamides as selective inhibitors of the nucleotide-binding oligomerization domain 2 (NOD2) signaling pathway. PLoS One. 2013 Jan;8(8):e69619.
389. Rickard DJ, Sehon C a, Kasparcova V, Kallal L a, Haile P a, Zeng X, et al. Identification of selective small molecule inhibitors of the nucleotide-binding oligomerization domain 1 (NOD1) signaling pathway. PLoS One. 2014 Jan;9(5):e96737.
390. Tigno-Aranjuez JT, Benderitter P, Rombouts F, Deroose F, Bai X, Mattioli B, et al. In vivo inhibition of RIPK2 kinase alleviates inflammatory disease. J Biol Chem. 2014 Oct 24;289(43):29651–64.
391. Keček Plešec K, Urbančič D, Gobec M, Pekošak A, Tomašič T, Anderluh M, et al. Identification of indole scaffold-based dual inhibitors of NOD1 and NOD2. Bioorg Med Chem. 2016 Nov 1;24(21):5221–34.
392. Cai KC, van Mil S, Murray E, Mallet J-F, Matar C, Ismail N. Age and sex differences in immune response following LPS treatment in mice. Brain Behav Immun. 2016 Nov;58:327–37.
393. Everhardt Queen A, Moerdyk-Schauwecker M, McKee LM, Leamy LJ, Huet YM. Differential Expression of Inflammatory Cytokines and

Stress Genes in Male and Female Mice in Response to a Lipopolysaccharide Challenge. PLoS One. 2016;11(4):e0152289.
394. Kuehn MJ, Kesty NC. Bacterial outer membrane vesicles and the host-pathogen interaction. Genes Dev. 2005 Nov 15;19(22):2645–55.
395. Lee E-Y, Choi D-Y, Kim D-K, Kim J-W, Park JO, Kim S, et al. Gram-positive bacteria produce membrane vesicles: proteomics-based characterization of Staphylococcus aureus-derived membrane vesicles. Proteomics. 2009 Dec;9(24):5425–36.
396. Choi Y, Kwon Y, Kim D-K, Jeon J, Jang SC, Wang T, et al. Gut microbe-derived extracellular vesicles induce insulin resistance, thereby impairing glucose metabolism in skeletal muscle. Sci Rep. 2015 Oct 29;5(December 2014):15878.
397. Cecil JD, O'Brien-Simpson NM, Lenzo JC, Holden JA, Chen Y-Y, Singleton W, et al. Differential Responses of Pattern Recognition Receptors to Outer Membrane Vesicles of Three Periodontal Pathogens. PLoS One. 2016;11(4):e0151967.
398. Vanaja SK, Russo AJ, Behl B, Banerjee I, Yankova M, Deshmukh SD, et al. Bacterial Outer Membrane Vesicles Mediate Cytosolic Localization of LPS and Caspase-11 Activation. Cell. 2016 May 19;165(5):1106–19.
399. Cecil JD, O'Brien-Simpson NM, Lenzo JC, Holden JA, Singleton W, Perez-Gonzalez A, et al. Outer Membrane Vesicles Prime and Activate Macrophage Inflammasomes and Cytokine Secretion In Vitro and In Vivo. Front Immunol. 2017;8(AUG):1017.
400. Kaparakis M, Turnbull L, Carneiro L, Firth S, Coleman H a., Parkington HC, et al. Bacterial membrane vesicles deliver peptidoglycan to NOD1 in epithelial cells. Cell Microbiol. 2010 Mar;12(3):372–85.
401. Macho Fernandez E, Fernandez EM, Valenti V, Rockel C, Hermann C, Pot B, et al. Anti-inflammatory capacity of selected lactobacilli in experimental colitis is driven by NOD2-mediated recognition of a specific peptidoglycan-derived muropeptide. Gut. 2011 Aug;60(8):1050–9.
402. Nardin A, Lefebvre M-L, Labroquère K, Faure O, Abastado J-P. Liposomal muramyl tripeptide phosphatidylethanolamine: Targeting and activating macrophages for adjuvant treatment of osteosarcoma. Curr Cancer Drug Targets. 2006 Mar;6(2):123–33.
403. Fogler WE, Wade R, Brundish DE, Fidler IJ. Distribution and fate of free and liposome-encapsulated [3H]nor-muramyl dipeptide and [3H]muramyl tripeptide phosphatidylethanolamine in mice. J Immunol. 1985 Aug;135(2):1372–7.
404. Fogler WE, Fidler IJ. Comparative interaction of free and liposome-encapsulated nor-muramyl dipeptide or muramyl tripeptide

phosphatidylethanolamine (3H-labelled) with human blood monocytes. Int J Immunopharmacol. 1987;9(2):141–50.
405. Cavallari JF, Fullerton MD, Duggan BM, Foley KP, Denou E, Smith BK, et al. Muramyl Dipeptide-Based Postbiotics Mitigate Obesity-Induced Insulin Resistance via IRF4. Cell Metab. 2017 May 2;25(5):1063–1074.e3.